VISCOSITY AND THERMODYNAMICS OF
MACROMOLECULAR SOLUTIONS

Dissertation for the Degree of Ph. D.
MICHIGAN STATE UNIVERSITY
BAKULESH NAVARANGLAL SHAH
1975

This is to certify that the

thesis entitled

VISCOSITY AND THERMODYNAMICS OF
MACROMOLECULAR SOLUTIONS

presented by

Bakulesh Navaranglal Shah

has been accepted towards fulfillment
of the requirements for

Ph.D. degree in Chemical Engr.

Robert F. Blanks
Major professor

Date April 29, 1975

O-7639

F006

ABSTRACT

VISCOSITY AND THERMODYNAMICS OF
MACROMOLECULAR SOLUTIONS

By

Bakulesh Navaranglal Shah

In this work, viscosity and its shear dependence were measured for the solutions of polystyrene (PS) and styrene (ST)-acrylonitrile (ACN) copolymers (SAN) in the solvents benzene, methyl ethyl ketone (MEK), dioxane and dimethylformamide (DMF). The low shear viscosity data indicate that for a polymer, the chemical structure of the solvent has a significant influence on viscosity in both dilute and moderately concentrated solutions. This finding is contrary to the widely held view that the nature of the solvent is unimportant when considering viscosities of moderately concentrated solutions.

In a dilute solution the relative viscosity, η_r, in a poor solvent is lower than that in a good solvent. The reverse is the case at higher concentrations, η_r in a poor solvent being several orders of magnitude larger than that in a good solvent. Plots of solution viscosity against concentration in thermodynamically good and poor solvents, therefore, have different slopes and the curves for different solvents cross over each other at a particular concentration. As the proportion of ACN in a

copolymer increases, the "cross-over" concentration--the concentration at which relative viscosities in good and poor solvents are the same--decreases.

In dilute solution a polymer molecule exists as an isolated chain. In more concentrated solutions the polymer molecules overlap and are entangled. Solution viscosity depends upon the first power of concentration in dilute solutions and upon the fifth power in concentrated solutions. This has led to the concept of a critical value of concentration called the entanglement concentration where the slope of a viscosity concentration plot is supposed to change dramatically from one to five. The estimate of onset-of-entanglement concentration, c_{ent}, for PS of 501,000 weight average molecular weight in only good solvents is correlated by a characteristic value of the product cM. The data of this work indicate that c_{ent} of a polymer depends on the thermodynamic interaction between the polymer and the solvent and the solvent effects cannot be neglected. Thus the concept of a "universal" critical entanglement concentration for a particular polymer is invalid. The value of c_{ent} is lower in poor solvents than that in good solvents; e.g., for high molecular weight azeotropic SAN copolymer, c_{ent} is equal to 6 gm/dl in DMF (good solvent) while in benzene (poor solvent) it is equal to 3 gm/dl.

Polymer solution viscosities are often correlated with concentration and molecular weight using a power law correlation of viscosity with the product cM^b. The value of b has often been considered in the past to be a universal value of 0.68. This value

was found to be inadequate in this work for correlating the data in poor solvents. The value of b depends on the thermodynamic quality of the solvent and it seems to be related to the Mark-Houwink exponent a in the intrinsic viscosity-molecular weight relation, $[\eta] = KM^a$, which is known to be dependent on the nature of the solvent; a being 0.5 for Θ-solvents and 0.8 for good solvents. The Simha correlation was found to unify the same data quite well up to high concentrations.

M. C. Williams has developed a thermodynamic-hydrodynamic molecular rheological model for prediction of polymer solution viscosity in moderately concentrated solutions. It was found that Williams' model for predicting low shear viscosity, when used with a modified Frankel and Acrivos friction coefficient, gave a better prediction in good solvents than in poor solvents. This model gave order of magnitude estimates of viscosity of moderately concentrated polymer solutions but failed at higher concentrations where entanglements of polymer chains are of significant density.

In most polymer solutions of the type studied in this investigation, the solution viscosity depends upon shear rate; i.e., the solutions are pseudoplastic. It was found that the slope of the non-Newtonian decrease in viscosity with increasing shear rate is a function of mechanical formation and break-up of entanglements and the polymer-solvent thermodynamic forces are unimportant. Of the many suggested forms of the relaxation parameter, τ_0, the Graessley form

$$\tau_0 \propto \eta_0 M/cT \ (1 + \beta cM)$$

for dependence on c was observed to be adequate for the systems considered.

For the study of the influence of polymer-solvent thermodynamics on the viscosity of polymer solutions, two samples of PS and four samples of SAN copolymers were synthesized by free radical bulk polymerization at 60°C using α-α'-azo-bis-isobutyronitrile initiator. The PS homopolymers, PS-1 and PS-2, were of 185,000 and 501,000, respectively, weight average molecular weight, M_w. The SAN copolymers were SAN C-1 of 15 weight per cent ACN content and of 290,000 M_w, SAN C-2 of 24 weight per cent ACN content and of 180,000 M_w, SAN C-2' of 23 weight per cent ACN content and of 666,000 M_w, and SAN C-3 of 38 weight per cent ACN content and of 332,000 M_w.

The kinetics of SAN copolymerization could not be described by either the chemical-controlled or the diffusion-controlled termination mechanism. Both the mechanisms appear to be acting simultaneously and a single parameter--ϕ in the first and $k_{t(12)}$ in the second--kinetic expression appears inadequate to describe the rate of SAN bulk copolymerizations.

The stiffness factor, σ, which is a measure of short-range interaction in polymer chains was found to be higher for each of the SAN copolymers than those for the individual homopolymers, PS and polyacrylonitrile. This indicates that in the unperturbed state the copolymers are more extended than the constituent homopolymers.

The viscosity measurements were made by using capillary viscometers and a cone-and-plate viscometer at 30°C. The solvents that were selected covered a range of polymer-solvent thermodynamic interactions. A light scattering photometer was used to measure weight average molecular weights of the polymers. From the above measurements, the expansion factor, α, and the Flory thermodynamic parameter, χ_1, were calculated for each of the polymer-solvent systems. The influence of ACN content on thermodynamic interaction can be clearly seen from the values of intrinsic viscosity, $[\eta]$, α, second virial coefficient, A_2, and χ_1. The better a solvent, the higher are the values of $[\eta]$, α, A_2 and c_{ent} and the lower is the value of χ_1 for a polymer in that solvent.

VISCOSITY AND THERMODYNAMICS OF MACROMOLECULAR SOLUTIONS

By

Bakulesh Navaranglal Shah

A DISSERTATION

Submitted to
Michigan State University
in partial fulfillment of the requirements
for the degree of

DOCTOR OF PHILOSOPHY

Department of Chemical Engineering

1975

To my parents

NAVARANG and JASHVANTI

and my brother

NIRAD

ACKNOWLEDGMENTS

I would like to express my deep appreciation to my major professor, Dr. R. F. Blanks, for providing constant guidance, assitance and encouragement throughout the course of this investigation, and also for his painstaking review of the manuscript. Gratitude is expressed and thanks extended to Dr. J. B. Kinsinger for his generous assistance and guidance during the course of this work. Many hours of fruitful discussion with him have furthered my understanding of macromolecules.

Sincere appreciation is extended to Drs. M. H. Chetrick, D. K. Anderson and C. M. Cooper for their review of the manuscript.

Thanks are also due to Dr. J. Goddard and Bill Talbot of the University of Michigan for providing unlimited use of the Weissenberg Rheogoniometer, to Dr. W. Deal and Dr. J. Trujillo of Michigan State University for their assistance in the use of the light scattering apparatus, to Mr. Donald Childs of the machine shop and Mr. Robert Rose of the electronic shop for their willingness to assist when an apparatus did not cooperate, and to Dow Chemical Company for gel permeation chromatography results.

I am indebted to the Division of Engineering Research and the Petroleum Research Fund administered by the American Chemical Society for providing financial support during the course of my graduate work.

Sincere gratitude is due to my parents for their constant moral support and encouragement. Special thanks are expressed to my brother Nirad for providing thoughtful guidance, encouragement and genuine wisdom throughout my graduate studies.

TABLE OF CONTENTS

LIST OF TABLES

LIST OF FIGURES

Figure

Page

LIST OF APPENDICES

CHAPTER I

INTRODUCTION

A. Motivation

Engineers must frequently deal with systems for processing, handling, transporting, storage and characterizing of liquids. In many cases it has been assumed commonly that the liquids are Newtonian. Today the engineer must deal with an increasing variety of "rheologically complex" liquids. These include process streams in the plastics, chemical, pharmaceutical, paper and pulp, food and fermentation and many other industries. Complex fluids such as polymer solutions and melts, emulsions, suspensions, and colloids are generally non-Newtonian in their flow behavior.

In dealing with flow systems, viscosity is a very important design parameter and the viscosity studies of these materials have resulted in renewed and increased interest in the science of rheology. Rheology is a study of the response of a material to external forces. The variety of viscous behavior observed has led to numerous empirical formulations of rheological equations of state. Unfortunately, these empirical equations, although adequate for curve fitting, are often not reliable for extrapolation and prediction.

The above problem has led to more fundamental studies of flow phenomena. The ultimate objective is to formulate a

relationship between the molecular structure of a fluid and its flow behavior and to apply this to problems of interest, namely, mixing, pumping, extrusion, molding, filtration, viscometry, heat transfer and many other engineering operations. Through increased understanding of the relationship between the physical properties and the flow characteristics of polymeric materials, engineers will be better equipped to deal with these materials and to perform the design of equipment needed for engineering of flow systems.

Polymer solutions and melts display the viscous nature of liquids, but also show elastic properties of solids. Thus, for describing the rheology of these systems, Newton's and Hooke's laws are of limited use in their original form. Researchers have developed various molecular and phenomenological models to predict or describe the flow behavior of these materials. These models may be classified as empirical, continuum and molecular. The various viewpoints from different disciplines have been expressed in numerous excellent books and articles (F-1, M-1, engineering; F-2, F-3, F-14, Y-1, M-2, chemistry; L-2, mathematics; and E-1, continuum mechanics).

In order to put the rheological and thermodynamic studies in the proper perspective with respect to the process flow problem, a chart is shown in Fig. 1.1. The concept pictured in the chart is the following. The aim of rheological studies and molecular modeling of polymer solutions is to provide sufficient information with which to solve process flow problems. This aim is represented by the arrow pointing to the upper box in the chart. The equations of

Figure 1.1.--Chart Showing Rheological and Thermodynamic Studies in Relation to Process Flow Problems.

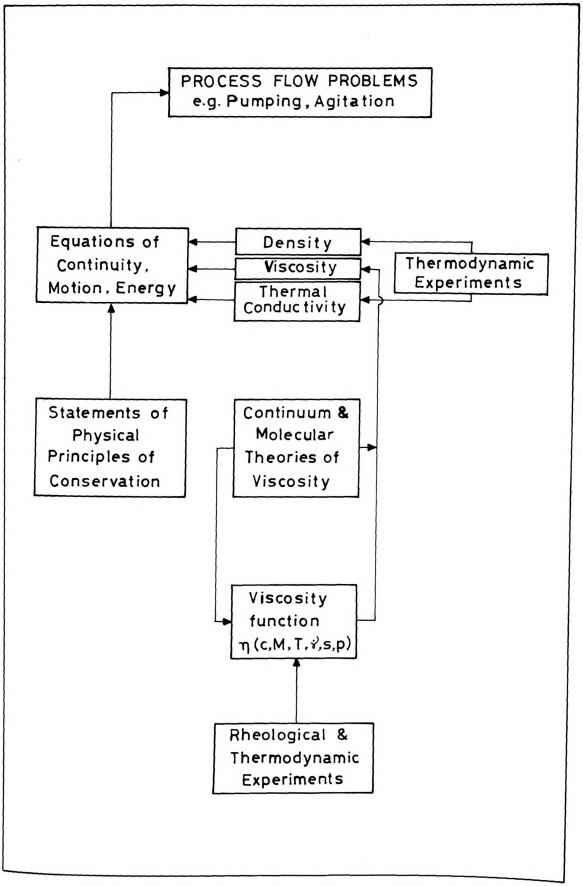
PROCESS FLOW PROBLEMS
e.g. Pumping, Agitation
Equations of Continuity, Motion, Energy
Density
Viscosity
Thermal Conductivity
Thermodynamic Experiments
Statements of Physical Principles of Conservation
Continuum & Molecular Theories of Viscosity
Viscosity function
$\eta(c, M, T, \dot{\gamma}, s, p)$
Rheological & Thermodynamic Experiments

continuity, motion, and energy are required for this purpose. They are obtained by input-out balances which are statements of the laws of conservation of mass, momentum, and energy. The conservation equations are not sufficient in themselves to solve the flow problems. In addition, a knowledge is required of the behavior and properties of the material in question, such as viscosity, density and thermal conductivity. The boxes at the right of the chart represent experimental, empirical and theoretical efforts required to obtain the needed material functions.

To be useful, the equation of motion requires a knowledge of the relationship between the stress exerted on a material in a flow field and the resulting rate of strain, or material response. For Newtonian fluids the stress, τ, is proportional to the strain rate, $\dot{\gamma}$, and the proportionality constant is the viscosity, μ, Eq. 1.1:

$$\tau = \mu\dot{\gamma}. \tag{1.1}$$

For solving many flow problems and when dealing with a large class of polymer solutions and melts, a generalization of Eq. 1.1 has proven useful. This generalization replaces the Newtonian viscosity, μ, in Eq. 1.1 with a viscosity function, η, but maintains the proportionality between stress and strain rate.

$$\tau = \eta\dot{\gamma} \tag{1.2}$$

This equation is adequate for the solution of many engineering flow problems, although it does not account for the elastic behavior of

polymer solutions (B-2a). In the case of polymer solutions, the viscosity, η, is a function of concentration of polymer, c, molecular weight of polymer, M, temperature of solution, T, shear rate, $\dot{\gamma}$, and chemical nature of the solvent and the polymer, s and p, respectively. The symbols s and p are used in the sense that intermolecular free energies of interaction between solvent and polymer are variables influencing rheological response and these depend on the particular polymer, p, solvent, s, pair being studied. A discussion of the nature of the solvent in terms of thermodynamics is given later in the chapter. Two of the least studied parameters are s and p. The parameter s describes the thermodynamic interaction between polymer and solvent and the parameter p describes the skeletal structure of the polymer such as linear or branched. Furthermore, both of these parameters, s and p, depend upon the chemical composition of the solvent and that of the polymer, and also the resulting intermolecular forces present in any particular polymer solution.

In deriving quantitative representations of the viscosity function, η, continuum mechanics provides a mathematical framework, molecular modeling attempts to relate observed behavior to molecular structural variables and intermolecular forces, and experimental data is needed to test the validity of the models and for curve fitting. As mentioned earlier, these concepts are descriped in Ref. (F-1, F-2, F-3, F-14, Y-1, L-2, E-1, M-1, and M-2). In this work the adequacy of several molecular models for the viscosity

function is to be tested with respect to experimental information with particular reference to the variables s and p.

B. Goals

The investigation reported here was carried out with the following goals in mind:

(1) To investigate the effects of polymer-solvent thermodynamic interaction on viscosities of dilute to moderately concentrated polymer solutions.

(2) To investigate techniques of correlating viscosity of polymer solutions with concentration and molecular weight of polymer and to evaluate these techniques.

(3) To test the applicability of a model (W-1) that includes polymer-solvent thermodynamic interaction, s and p, for predicting viscosity of moderately concentrated polymer solutions and to ascertain the parameters involved for further investigation.

(4) To study the effect of solvent character on the non-Newtonian viscosity function, η.

Along with the above goals, the following was also of interest with respect to the copolymers investigated:

(5) To investigate the effect of acrylonitrile content on the configuration of polymer chains in terms of both short-range and long-range effects (long-range effects in different solvent environments). Configuration refers to the spatial configuration of the molecules in various solvent environments.

(6) To investigate the kinetic models for the rate of copolymerization and their applicability to styrene-acrylonitrile

copolymerization. (Copolymer samples used in this study were prepared by laboratory, free radical, polymerizations.)

C. Polymers and Solvents

It was necessary to choose systems having a wide range of polymer-solvent thermodynamic interactions in order to study their effect on viscosity. In principle this can be accomplished by using "good" and "poor" solvents for a given polymer. A good solvent is one in which polymer segments prefer contacts with the solvent molecules and the polymer expands or swells in solution as opposed to a poor solvent in which the polymer segments prefer contacts with their own kind and thereby the polymer molecule tends to coil-up in solution.

The configuration of a polymer molecule in solution depends on its environment, i.e., the quality of the solvent. In a good solvent, where the energy of interaction between a polymer element and a solvent molecule adjacent to it exceeds or is about the same as the mean of the energies of interaction between the polymer-polymer and solvent-solvent pair, the molecule will tend to expand so as to reduce the frequency of contacts between pairs of polymer elements. In a poor solvent, on the other hand, where the energy of interaction between polymer segment and solvent molecule is unfavorable, smaller configurations in which polymer-polymer contacts occur, will be favored.

Any theoretical considerations of the solubility of a polymer in a solvent must necessarily consider the free energy of

mixing of the two phases. By a statistical mechanical treatment, Flory (F-3a) derived analytical expressions for the free energy of mixing based on a lattice model of the liquid. This model considers that both solvent molecules and polymer segments occupy equivalent sites in the lattice. The formation of a solution is considered to occur in two steps: disorientation of the polymer molecules and mixing of the disoriented polymers with solvent. The latter is more important. The entropy of mixing disoriented polymer and solvent is given as

$$\Delta S_m^{conf} = -k(n_1 \ln V_{1s} + n_2 \ln v_p) \tag{1.3}$$

where V_{1s} and v_p are the volume fractions of solvent and solute, respectively; n_1 and n_2 are the number of solvent and polymer molecules, respectively, in a solution; and k is Boltzmann's constant. There may also be an entropy change owing to orienting influences on the components in the solution which differ from those existing in the pure component. This entropy change associated with first neighbor interactions must be proportional to the number of pair contacts developed in the solution. Flory (F-3a) obtains this as

$$\Delta S_m = -k[\partial(\chi_1 T)/\partial T]n_1 v_p \tag{1.4}$$

where χ_1 is a reduced residual chemical potential. It consists of enthalpy and entropy terms. This is discussed later in the chapter.

Since ΔS_m^{total} is positive, it is the heat of mixing term that is more important in determining the sign of the free energy change of mixing, ΔF_m. Two substances will mix whenever ΔF_m is negative.

$$\Delta F_m = \Delta H_m - T\Delta S_m^{total} \tag{1.5}$$

The heat of mixing results from replacement of solvent-solvent and polymer-polymer contacts. The magnitude of this contribution to the free energy depends upon the degree of interaction of the unlike species in solution. The solvent is good when heat of mixing is exothermic which is the case when polymer-solvent specific interactions are large, i.e., when hydrogen bonding takes place. The total excess entropy term is usually positive and good solvents have $\Delta H_m < 0$.

Since there are two different monomer species present in a copolymer, the expression for the interaction energy must be amended to include the additional interactions. Stockmayer et al. (S-4) represented χ_1 for a copolymer solvent system as

$$\chi_1 = \bar{x}_A\chi_A + \bar{x}_B\chi_B - \bar{x}_A\bar{x}_B\chi_{AB} \tag{1.6}$$

where $\bar{x}_A$ and $\bar{x}_B$ are mole fractions of monomers A and B in the copolymer, χ_A and χ_B are the interaction parameters for the homopolymers A and B with pure solvent, and χ_{AB} is a parameter expressing A-B interactions.

The definition of "good" and "poor" solvents may be given thermodynamically. The change in chemical potential of the solvent, $\Delta\mu_1$, may be split into an ideal and an excess term:

$$\Delta\mu_1 \equiv \Delta\mu_1^{id} + \Delta\mu_1^{ex}. \tag{1.7}$$

Flory (F-3a) obtains with complete generality excess (i.e., nonideal) chemical potential of the solvent in terms of partial molar heat of dilution, $\Delta\bar{H}_1$, and partial molar entropy, $\Delta\bar{S}_1$. According to his derivation,

$$\Delta\mu_1^{ex} = RT(\kappa_1 - \psi_1)v_p^2 \tag{1.8}$$

where κ_1 and ψ_1 are heat and entropy parameters such that

$$\Delta\bar{H}_1 = RT\kappa_1 v_p^2, \tag{1.9}$$

and

$$\Delta\bar{S}_1 = R\psi_1 v_p^2. \tag{1.10}$$

Within the limits and validity of his theory and simplifying assumptions, he relates parameters κ_1, ψ_1 and χ_1 by

$$\kappa_1 - \psi_1 = \chi_1 - 1/2. \tag{1.11}$$

He also defines an "ideal" temperature Θ as

$$\Theta = \kappa_1 T/\psi_1 \tag{1.12}$$

such that

$$\chi_1 = 1/2 - \psi_1(1 - \Theta/T). \tag{1.13}$$

Hence the excess chemical potential may be written as

$$\Delta\mu_1^{ex} = -RT\psi_1(1 - \Theta/T)v_p^2. \tag{1.14}$$

In a poor solvent, κ_1 and ψ_1 are generally positive. According to the above equation, at the temperature T equal to Θ, the chemical potential due to segment-solvent interaction is zero. Hence at the Θ-temperature deviations from ideality vanish. From the above equations it can be seen that in poor solvents ψ_1 is nearly equal to κ_1 and χ_1 is close to 1/2. These quantities or equivalent ones may be experimentally determined by light scattering or intrinsic viscosity measurements and these methods were used in this work to quantify the thermodynamic "goodness" or "poorness" of solvents.

In the past most of the rheological work reported in the literature has been done in good solvents. In many of these studies, in spite of a variety of solvents used for a polymer, the solvents were all good and thus distinct thermodynamic effects were not observed. In this work a different approach was considered. Copolymers from two very different monomers were synthesized and studied in different solvents. Each of the selected solvents had a different degree of goodness toward the homopolymers of the two monomers. Some of the solvents were very highly compatible with one of the homopolymers while others were non-solvents.

Thus the copolymers helped in providing distinctly different polymer-solvent thermodynamic interactions in different solvents.

Styrene* and acrylonitrile* monomers were selected to synthesize linear polystyrene* homopolymers and styrene-acrylonitrile copolymers.* The two vinyl monomers are very different in character; styrene has a bulky benzene ring while ACN has a polar C≡N group. Styrene is non-polar while ACN is polar. The copolymers that were synthesized had different ACN contents, thereby providing different degrees of localized polarity in different copolymers. Excellent references to ST and ACN polymerization can be found in Ref. (B-1, M-1) and (A-4), respectively, and of polymerization in general in Ref. (O-1).

Four solvents were selected for this work: (1) Benzene, (2) Dioxane, (3) Methyl ethyl ketone,* and (4) Dimethylformamide.* Benzene is non-polar and is an excellent solvent for PS while it is a non-solvent for polyacrylonitrile.* Dioxane has two symmetric oxygen atoms and hence its dipole moment is zero but it has localized charge separation. Dioxane is a good solvent for PS but is a non-solvent for PAN. The two polar solvents, MEK and DMF, are relatively poor solvents for PS while for PAN, MEK is a non-solvent and DMF is an excellent solvent. Thus this choice of solvents gives a wide range of polymer-solvent interaction in terms of a variety of polymer-solvent intermolecular forces.

---

*Henceforth styrene is referred to as ST, acrylonitrile as ACN, polystyrene as PS, styrene-acrylonitrile copolymers as SAN copolymers, methyl ethyl ketone as MEK, dimethylformamide as DMF and polyacrylonitrile as PAN.

It may be mentioned here that copolymers are often manufactured or tailored for specific physical and chemical properties which are often unobtainable from simple homopolymers. The properties of a particular linear homopolymer are determined primarily by two factors: (1) average molecular weight and (2) molecular weight distribution. In copolymers, along with the above two factors, third and fourth important factors are the average chemical composition and the distribution of composition about this average. The polymers that were synthesized in this work were similar to industrial PS and SAN copolymers with respect to their molecular weights and molecular weight distribution.

D. Experimental Method

To achieve the goals of this research, a rather wide range of experimental work was involved. This consisted of polymerization of monomers, characterization of polymers, viscosity measurements of dilute and moderately concentrated solutions and experimental determination of polymer-solvent thermodynamic interactions. This required the use of the following equipment:

1. Glass reactor with baffles and stirrer for polymerization (Chemical Engineering Department).
2. Capillary viscometers for dilute solution viscometry (Chemical Engineering Department).
3. Cone-and-plate viscometer for moderately concentrated solution viscometry (Chemical Engineering Department, University of Michigan).
4. Light scattering photometer and differential refractometer for thermodynamic parameters and molecular weights of polymers (Biochemistry Department).

The laboratories of Dow Chemical Company in Midland, Michigan, performed the measurements of molecular weights and molecular weight distributions of the polymers by gel permeation chromatography (GPC). Spang Microanalytical Laboratory, Ann Arbor, Michigan, did the nitrogen analysis of the copolymers.

CHAPTER II

POLYMERIZATION AND PREPARATION OF SAMPLE MATERIALS

Polystyrene homopolymers and styrene-acrylonitrile copolymers used in this work were synthesized by free radical polymerization in bulk. The reasons for this were (1) to avoid contamination from solvents used in solution polymerization; (2) to obtain a maximum quantity of each polymer with a restricted size reactor and restricted conversion of monomers to copolymers, low conversion being necessary to obtain uniform composition of copolymers (this is discussed in detail later in the chapter); and (3) because of low conversions, mixing and heat-transfer would not present difficulties in these bulk polymerizations.

This chapter presents methods for the selection and purification of materials, the theory of vinyl homo and copolymerization, and a description of the sample homo and copolymers which were synthesized to use in the viscosity and thermodynamic studies.

A. Initiator

The rate of vinyl, free radical copolymerization in a binary system depends not only on the rates of the four propagation steps but also on the rates of initiation and termination reactions. To simplify the matter, the rate of initiation may be made independent of the monomer composition by choosing an initiator which releases

primary radicals that combine efficiently with either monomer. The spontaneous decomposition rate of the initiator should be substantially independent of the reaction medium, as otherwise the rate of initiation may vary with composition. The initiator α-α'-Azo-bis-isobutyronitrile* (AIBN) meets these requirements satisfactorily (W-2). Also, AIBN offers an advantage in that, unlike benzoyl peroxide, it is not susceptible to induced decomposition (F-3b).

B. Purification

1. Initiator

The AIBN obtained from Eastman Kodak Co.† was purified by recrystallization from acetone. A large quantity was dissolved in acetone at room temperature till saturation. The solution was filtered through a funnel under vacuum. The filtered solution was cooled in an ice-water bath until a crop of crystals precipitated. This procedure was repeated twice and the crystals were dried in a vacuum oven at room temperature. After drying, the purified, crystalline AIBN was stored in a refrigerator.

2. Monomers

High purity ST and ACN were obtained from Eastman Kodak Co.† The containers were stored in a refrigerator and only the approximate amount needed for each run was withdrawn at one time. The liquid monomers, for an experiment, were withdrawn and separated

---

*Henceforth referred to as AIBN.

†Eastman Kodak Co., Rochester, New York 14650.

from the dissolved inhibitor by passing through columns of activated alumina (B-3, F-4). The monomers were then distilled at reduced pressure. Only the middle fractions were collected and used.

C. Homopolymerization

The kinetic scheme for homopolymerization in the presence of an initiator may be written as

$$\sim\sim M_x^* + M \xrightarrow{k_p} \sim\sim M_{x+1}^* \qquad (2.1)$$

where superscript * indicates a radical at the end of a growing chain.

1. Rate of Reaction

As shown by Flory (F-3b), the rate of propagation in free radical polymerization is given by

$$R_p = \frac{-d[m]}{dt} = k_p (fk_d [I]/k_t)^{1/2}[M] \qquad (2.2)$$

where k_d, k_p and k_t are the reaction rate constants for initiator decomposition, chain propagation, and chain termination, respectively; f is the fraction of primary radicals available for initiation of polymerization (efficiency of initiation); [I] is the initiator concentration; and [M] is the monomer concentration.

Equation 2.2 can be integrated and solved for the time of reaction necessary for the required conversion with a known amount of initiator. It was found that for 10 per cent conversion with

0.1 per cent initiator concentration, the total reaction time was about four hours at 60°C for ST homopolymerization. Hamielec et al. (H-2) have derived an expression relating conversion with the time of reaction and the amount of initiator. This is given by

$$x = 1 - \exp\left[\left(\frac{2k_p}{k_d}\right)\left(\frac{2fk_d[I]}{k_{td}+k_{tc}}\right)^{1/2}\left(\exp\left(\frac{-k_t t}{2}\right) - 1\right)\right] \qquad (2.3)$$

where x is the fractional conversion of monomer to polymer, k_{td} and k_{tc} are the reaction rate constants for termination by disproportionation and termination by combination, respectively. In bulk polymerization of ST, k_{td} can be neglected (F-3b). The calculated time for 10 per cent conversion with 0.1 per cent initiator concentration was also about 4 hours. This should not be very surprising since Eq. 2.3 is an integrated form of the rate expression and the origin of Eqs. 2.2 and 2.3 is the same.

2. Molecular Weight

The expected molecular weight can be calculated from the knowledge of the kinetic chain length which is given by

$$\nu = (k_p^2/2k_t)[M]^2/R_p \qquad (2.4)$$

where R_p is given by Eq. 2.2. The kinetic chain length, ν, of PS obtained after 10 per cent conversion of ST at 60°C with 0.1 per cent concentration of initiator is about 460. Then the number average molecular weight is given by

$$M_n = 2\nu M_0 \qquad (2.5)$$

where M_0 is the molecular weight of the monomer unit and the factor 2 is due to the fact that termination is by coupling whereby two chains are joined to each other. This gives M_n equal to 95,600. Assuming that a low conversion, stirred, bulk polymerization will give the most probable distribution of weights, i.e., M_w/M_n equal to 2 (F-3c), the weight average molecular weight M_w is about 191,000. Thus, in homopolymerization, with a given amount of initiator, one can readily synthesize a polymer of any desired molecular weight and determine the time of reaction for the desired conversion. The theory and experiment agree quite well for homopolymerization of PS.

D. Copolymerization

1. Copolymer-Monomer Composition Equation

In the copolymerization of two monomers, M_1 and M_2, the four different chain growth steps may be indicated by the scheme shown in Eqs. 2.6 to 2.9 (A-1),

$$\sim\sim M_1^* + M_1 \xrightarrow{k_{11}} \sim\sim M_1M_1^* \qquad (2.6)$$

$$\sim\sim M_1^* + M_2 \xrightarrow{k_{12}} \sim\sim M_1M_2^* \qquad (2.7)$$

$$\sim\sim M_2^* + M_1 \xrightarrow{k_{21}} \sim\sim M_2M_1^* \qquad (2.8)$$

$$\sim\sim M_2^* + M_2 \xrightarrow{k_{22}} \sim\sim M_2M_2^* \qquad (2.9)$$

where superscript * indicates a radical at the end of a growing chain, subscripts 1 and 2 denote two types of monomers and k_{ij}'s are the propagation rate constants.

On assuming that the reactivity depends only on the terminal unit and making the steady state assumption (F-3d, O-1) for the free radical species, an expression may be obtained which relates the instantaneous mole fraction, F_1, of monomer M_1 in the copolymer formed from a binary monomer mixture, to f_1, the mole fraction of monomer M_1 in the monomer mixture. This expression is

$$F_1 = \frac{r_1 f_1^2 + f_1 f_2}{r_1 f_1^2 + 2 f_1 f_2 + r_2 f_2^2} \tag{2.10}$$

where

$$r_1 = k_{11}/k_{12}, \qquad r_2 = k_{22}/k_{21}, \tag{2.11}$$

$$F_1 = 1 - F_2 = \frac{d[M_1]}{d[M_1] + d[M_2]}, \tag{2.12}$$

and

$$f_1 = 1 - f_2 = \frac{[M_1]}{[M_1] + [M_2]}. \tag{2.13}$$

For ST and ACN at 60°C, r_1 is equal to 0.41 and r_2 is equal to 0.04 (B-4).

Figure 2.1 shows the dependence of instantaneous copolymer composition, F_1, on the comonomer feed composition, f_1, for ST-ACN

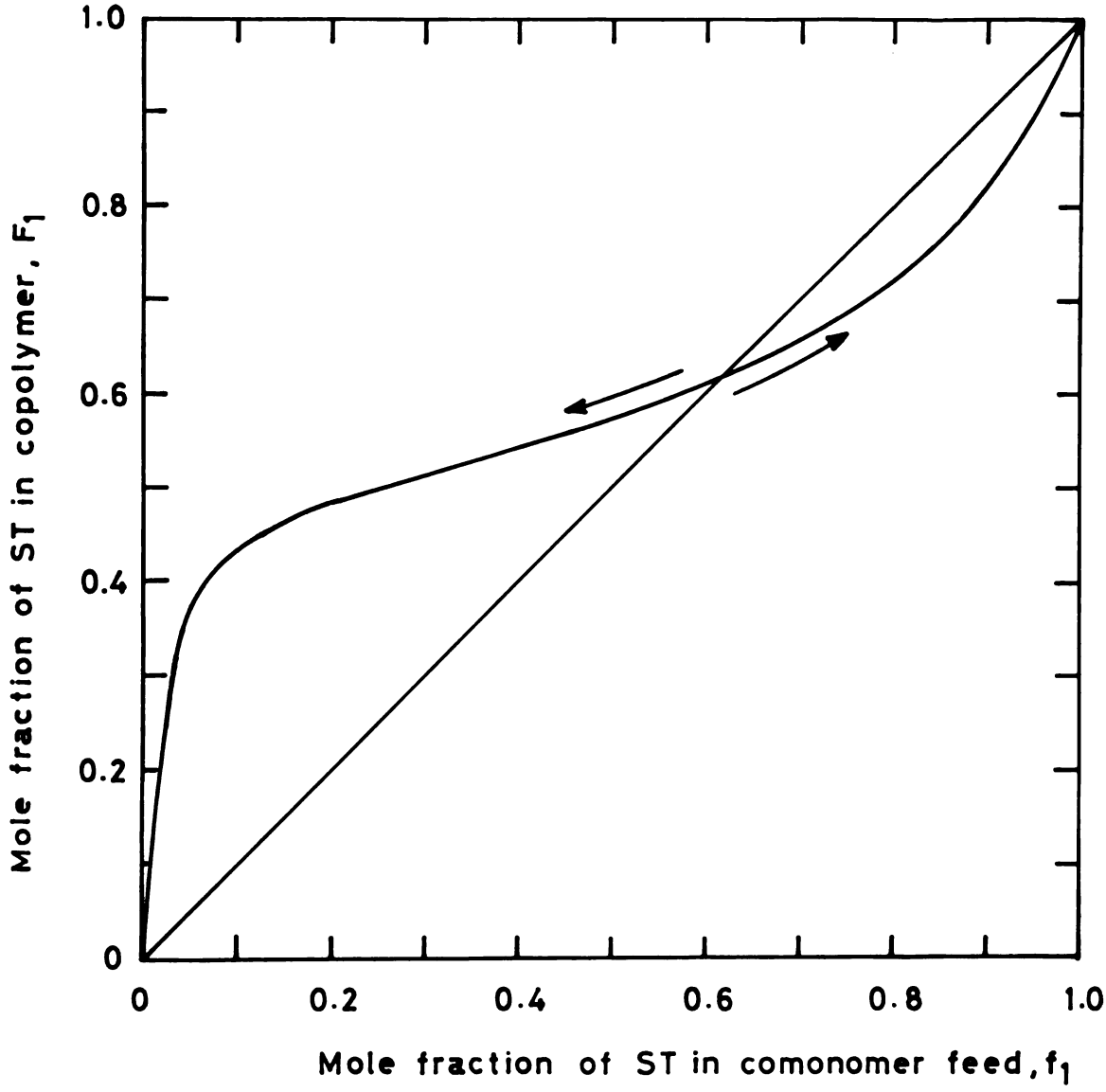

Figure 2.1a.--Dependence of Instantaneous Copolymer Composition, F_1, on Comonomer Feed Composition, f_1, for SAN in Free Radical Copolymerization at 60°C, Mole Basis.

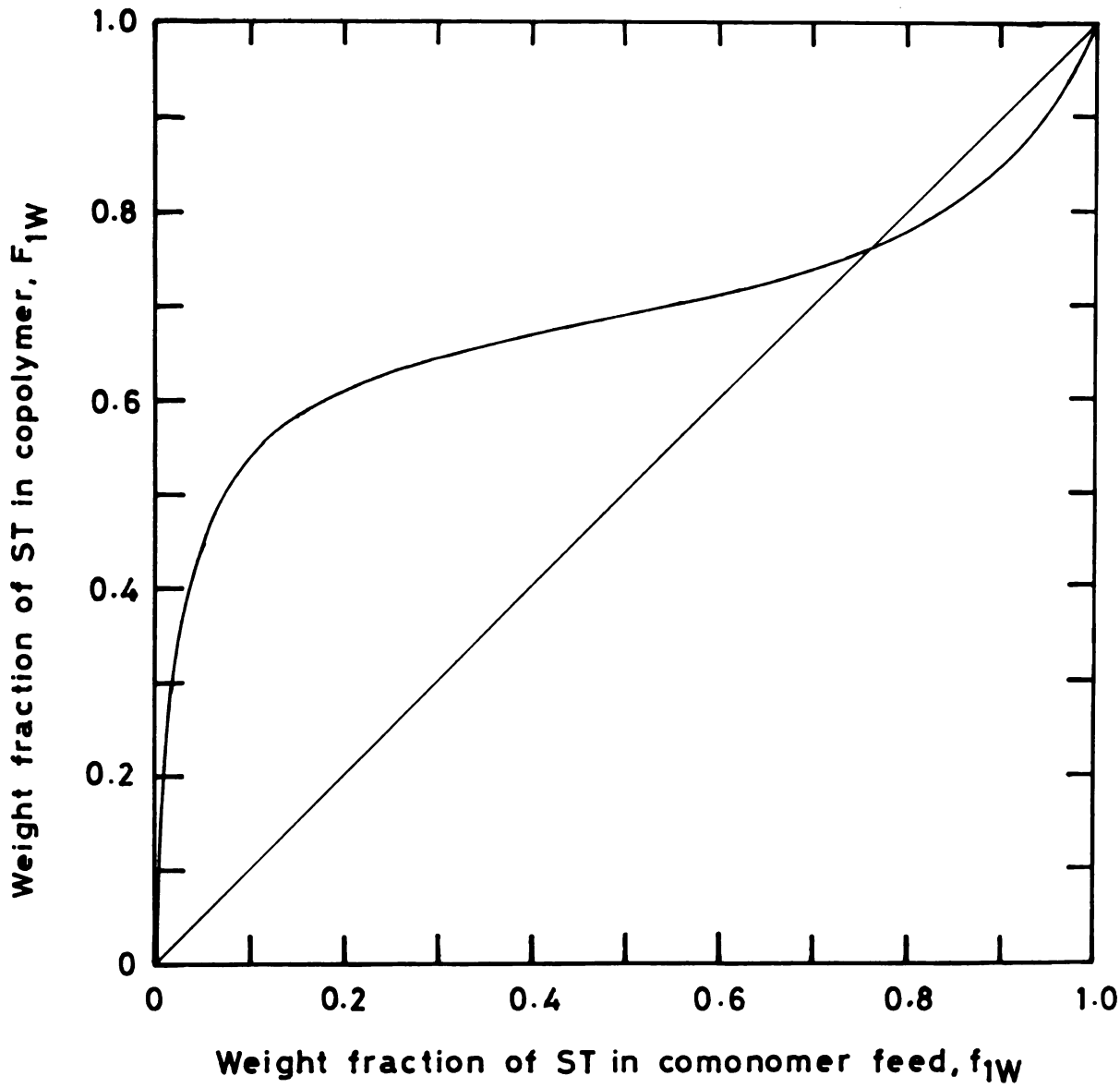

Figure 2.1b.--Dependence of Instantaneous Copolymer Composition, F_{1W}, on Comonomer Feed Composition, f_{1W}, for SAN in Free Radical Copolymerization at 60°C, Weight Basis.

monomers in radical copolymerization. Subscripts 1 and 2 refer to ST and ACN, respectively. Actually Fig. 2.1a is the representation of equilibrium between the copolymer and monomer compositions expressed by Eq. 2.10 in molar units while Fig. 2.1b shows the same equilibrium relationship in weight units.

Since, except at the cross-over point (with the 45° line), the instantaneous copolymer composition, F_1, is different from the composition of the monomer mixture, f_1, from which it is being formed, a drift in both copolymer and monomer mixture compositions occurs during the course of a batch-type copolymerization. The direction of drift has been indicated by arrows in Fig. 2.1a. It is also to be noted that the drift is in opposite directions on either side of the cross-over point. Thus monomer mixtures having compositions f_1 greater than the cross-over point composition become depleted in ACN with polymerization. Monomer mixtures having compositions f_1 less than the cross-over point composition become depleted in ST with polymerization. This occurs because of the different values of reactivity ratios, r_1 and r_2, which in turn indicate the difference in the reactivity of the two monomers involved. The composition at the cross-over point is called the azeotropic composition since at this composition, the composition of the copolymer formed is the same as that of the monomer mixture composition and it remains constant with polymerization. At the cross-over point F_1 is equal to f_1, and hence, from Eq. 2.10,

$$F_1 = f_1 = (1 - r_2)/(2 - r_1 - r_2). \qquad (2.14)$$

For SAN, the azeotropic composition from Eq. 2.14 occurs at F_1 equal to f_1 equal to 0.6194 mole fraction or at 0.7615 weight fraction of ST.

2. Variation of Copolymer Composition With Conversion

The copolymerization equation (Eq. 2.10) gives the instantaneous copolymer composition, i.e., the composition of the copolymer formed at a particular monomer composition. For all copolymerizations except azeotropic, the comonomer and copolymer compositions (copolymer formed out of that comonomer) are different from each other. This results in a variation of copolymer composition with conversion since the feed comonomer composition changes at each instant with copolymerization. In order to determine the instantaneous copolymer composition as a function of conversion for any given comonomer feed, one must resort to an integrated form of the copolymerization equation. The most general, useful method is that derived by Skiest (S-1). From a material balance one can obtain

$$\int_{M^0}^{M} \frac{dM}{M} = \ln \frac{M}{M^0} = \int_{f_1^0}^{f_1} \frac{df_1}{(F_1 - f_1)} , \qquad (2.15)$$

where M denotes the total moles of the two monomers, and superscript 0 denotes initial values. Equation 2.10 allows the calculation of F_1 as a function of f_1 for a given set of r_1 and r_2 values which can then be used in Eq. 2.15 to obtain variations in monomer and copolymer compositions with the degree of conversion defined as $1 - M/M^0$.

Equation 2.15 has been integrated (M-3, M-4) to the useful closed form

$$1 - \frac{M}{M^0} = 1 - \left[\frac{f_1}{f_1^0}\right]^{\alpha}\left[\frac{1 - f_1}{1 - f_1^0}\right]^{\beta}\left[\frac{f_1^0 - \delta}{f_1 - \delta}\right]^{\gamma} \tag{2.16}$$

which relates the degree of conversion to changes in monomer composition and where

$$\alpha = \frac{r_2}{(1 - r_2)}, \qquad \beta = \frac{r_1}{(1 - r_1)},$$

$$\gamma = \frac{1 - r_1 r_2}{(1 - r_1)(1 - r_2)}, \text{ and} \qquad \delta = \frac{1 - r_2}{(2 - r_1 - r_2)}. \tag{2.17}$$

Equation 2.16 was used to calculate the drift in the monomer and copolymer compositions with conversion. The calculations can be conveniently performed by means of a simple computer program with an appropriate computer. The essential feature of the computer program (in FORTRAN IV for CDC 6500 computer) is that f_1 is decreased or increased (depending on whether the initial composition, f_1, is less than or greater than the azeotropic composition) in step increments of 0.005 from f_1 to 0 or 1.0, respectively. For each value of f_1, the corresponding mole conversion is calculated from Eq. 2.16 and the corresponding instantaneous copolymer composition from Eq. 2.10. With the monomer mixture composition, f_1, and mole conversion $(1 - M/M^0)$ known, the cumulative average composition can be easily calculated. The output of these calculations can also be easily

converted from molar into weight units. Figure 2.2a shows variations in instantaneous compositions of copolymer, F_1, and monomer mixture, f_1, with conversion in molar units, and Fig. 2.2b shows the same in weight units for two particular SAN copolymerizations. As can be seen in these figures (and also in Fig. 2.1), a copolymer formed from the monomer feed composition greater than the azeotropic composition is less rich in ST than the feed composition, and vice versa for the monomer feed composition less than the azeotropic composition. Again, Figs. 2.2a and 2.2b clearly show the drift in composition with respect to conversion. The straight horizontal lines indicate azeotropic composition. For any feed composition other than azeotropic, as the polymerization proceeds, ultimately at some conversion the feed mixture will become depleted in one of the two monomers depending on the initial feed composition. After this happens, simple homopolymerization takes place and this is shown by horizontal lines at fractions 1 and 0, for PS and PAN, respectively. Figures 2.2a and 2.2b show the instantaneous composition of copolymers. The average composition at each fractional conversion can be easily calculated and plotted on the same figures but it is not shown for the sake of clarity. The line representing average composition will be more horizontal. Again, it is amply clear from the figures that at low conversion (less than 10 per cent), the composition of copolymer formed is practically uniform; i.e., the composition drift is very small. The farther away the initial composition of monomer mixture from the azeotropic composition, the greater is the drift in composition with increasing conversion.

Figure 2.2.--Variations in Feed and Copolymer Compositions with Conversion for SAN in Free Radical Copolymerization at 60°C.

Figure 2.2a.--Mole Basis.

	1	2
Initial feed composition in mole fraction of ST	0.821	0.193
Initial copolymer composition in mole fraction of ST	0.741	0.485

Figure 2.2b.--Weight Basis.

	1	2
Initial feed composition in weight fraction of ST	0.900	0.320
Initial copolymer composition in weight fraction of ST	0.846	0.649

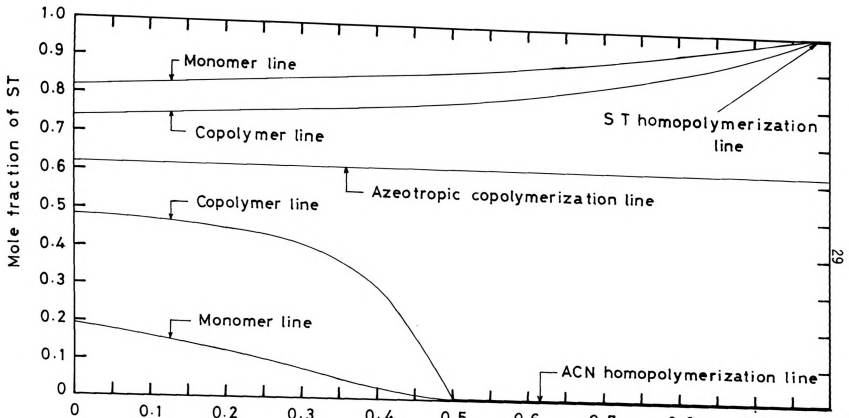

Figure 2.2a.--Variations in Feed and Copolymer Compositions with Conversion for SAN, Mole Basis.

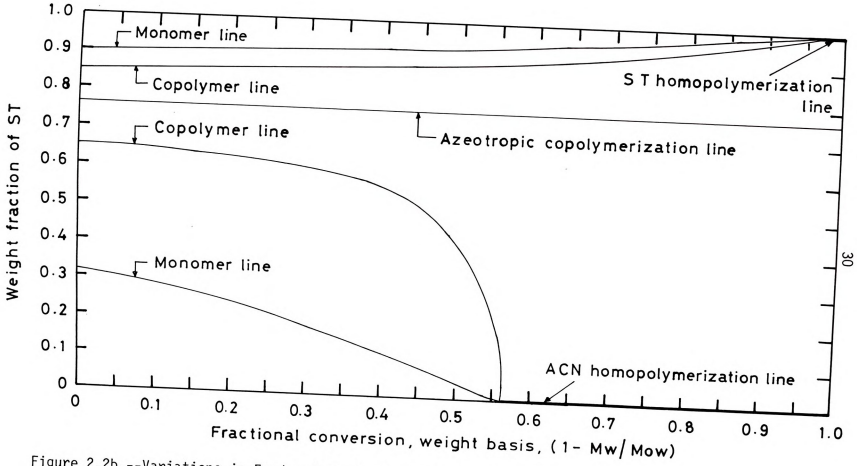

Figure 2.2b.--Variations in Feed and Copolymer Compositions with Conversion for SAN, Weight Basis.

3. Rate of Copolymerization

It was hoped to be able to determine the rate of radical copolymerization so as to be able to predict the total reaction time necessary for the required conversion at a given composition of monomer mixture with a given concentration of initiator. Two different approaches are proposed on the basis of two kinetic mechanisms of termination of the reaction.

a. Chemical-controlled termination.--This approach found in standard texts (F-3b, O-1, W-3a) assumes the termination reaction to be chemically controlled. Copolymerization is assumed to consist of four propagation reactions, Eqs. 2.6 to 2.9, and three termination steps as

$$\sim\sim M_1^* + \sim\sim M_1^* \xrightarrow{k_{t11}} \left.\begin{matrix} \\ \\ \end{matrix}\right\} \quad (2.18)$$

$$\sim\sim M_2^* + \sim\sim M_2^* \xrightarrow{k_{t22}} \longrightarrow \begin{matrix}\text{Dead}\\ \text{Polymer}\end{matrix} \quad (2.19)$$

$$\sim\sim M_1^* + \sim\sim M_2^* \xrightarrow{k_{t12}} \left.\begin{matrix} \\ \\ \end{matrix}\right\} \quad (2.20)$$

orresponding to termination between like radicals, Eqs. 2.18 and .19, and cross-termination between unlike radicals, Eq. 2.20. The te of copolymerization is then

$$R_p = \frac{(r_1[M_1]^2 + 2[M_1][M_2] + r_2[M_2]^2)R_i^{1/2}}{\{r_1^2\delta_1^2[M_1]^2 + 2\phi r_1 r_2 \delta_1\delta_2[M_1][M_2] + r_2^2\delta_2^2[M_2]^2\}^{1/2}} \quad (2.21)$$

where R_i is the rate of initiation of chain radicals of both types, M_1^* and M_2^*, and it is given by

$$R_i = 2fk_d[I] \tag{2.22}$$

and where

$$\delta_1 = (2k_{t11}/k_{11}^2)^{1/2} , \tag{2.23a}$$

$$\delta_2 = (2k_{t22}/k_{22}^2)^{1/2} , \tag{2.23b}$$

and

$$\phi = k_{t12}/2(k_{t11}K_{t22})^{1/2} . \tag{2.23c}$$

The δ terms are simply the reciprocals of $k_p/(2k_t)^{1/2}$ ratios for the homopolymerizations of the individual monomers. The ϕ term represents the ratio of half the cross-termination rate constant to the geometric mean of the rate constants for self-termination of like radicals. A value of $\phi < 1$ means that cross-termination is not favored, while $\phi > 1$ means that cross-termination is favored (F-3d).

Table 2.1 lists kinetic parameters for radical chain copolymerization at 60°C.

TABLE 2.1.--Kinetic Parameters,* k_p and k_t, of ST and ACN at 60°C.

Monomer	$k_p \times 10^{-3}$, l/mole/sec	$k_t \times 10^{-7}$, l/mole/sec
Styrene	0.145	2.9
Acrylonitrile	1.96	78.2

*From Ref. (B-4) and (W-3b).

For AIBN from Ref. (V-1),

$$k_d = 1.58 \times 10^{15} \exp(-30{,}800/RT) \text{ sec}^{-1} \tag{2.24}$$

where R is the gas constant and T is the absolute temperature. The δ_1 and δ_2 values in Eqs. 2.23a and 2.23b are obtained from homopolymerization. Experimental determination of the rate of copolymerization then allows calculation of ϕ from Eq. 2.21.

b. Diffusion-controlled termination.--A kinetic expression for the rate of diffusion-controlled copolymerization was obtained by Atherton and North (A-2) by considering the termination reaction as

$$\left.\begin{array}{l} \sim\sim M_1^* + \sim\sim M_1^* \\ \sim\sim M_1^* + \sim\sim M_2^* \\ \sim\sim M_2^* + \sim\sim M_2^* \end{array}\right\} \xrightarrow{k_{t(12)}} \begin{array}{l}\text{Dead} \\ \text{Polymer}\end{array} \tag{2.25}$$

where the termination rate constant $k_{t(12)}$ is a function of copolymer composition. The expression for the rate of copolymerization, R_p, was found to be

$$R_p = \frac{(r_1[M_1]^2 + 2[M_1][M_2] + r_2[M_2]^2) R_i^{1/2}}{k_{t(12)}^{1/2} \left(\frac{r_1[M_1]}{k_{11}} + \frac{r_2[M_2]}{k_{22}} \right)} . \tag{2.26}$$

This equation was used to calculate the value of $k_{t(12)}$ for each copolymer composition from the knowledge of experimental values of R_p for two concentrations of initiator.

c. Conversion as a function of time.--For diffusion-controlled termination O'Driscoll and Knorr (0-3) have derived an expression which gives conversion as a function of time. Their expression is

$$\ln\left(\left[\frac{\bar{f}_1}{f_1^0}\right]^a\left[\frac{1-\bar{f}_1}{1-f_1^0}\right]^b\left[\frac{f_1^0-\delta}{\bar{f}_1-\delta}\right]^c\right) = 2(k_{21}-Xk_{22})\left(\frac{f[I]^{1/2}}{k_d k_{t(12)}}\right)\left(\exp\left(\frac{-k_d t}{2}\right)-1\right) \qquad (2.27)$$

here

$$X = (k_{11}-k_{21})/(k_{12}-k_{22}), \qquad (2.28)$$

$$a = \alpha(1-X)+1, \qquad (2.29a)$$

$$b = \beta(1-X)-X, \qquad (2.29b)$$

$$c = \gamma(1-X), \qquad (2.29c)$$

t is the time of reaction in sec.

ation 2.27 should permit the calculation of f_1 as a function of e. The resulting values of f_1 may be used in Eq. 2.16 to obtain version as a function of time and in Eq. 2.10 to obtain F_1 as a

function of time. Equation 2.27 is therefore a complete description of time dependency of free radical copolymerization.

d. Small scale experiments.--In order to determine which of these two kinetic mechanisms is useful for the purpose of predicting rates of SAN copolymerizations, several small scale experiments were performed.

Free radical chain polymerization was carried out with pure ST monomer to PS and with SAN comonomers in different proportions to SAN copolymers of different compositions. Polymerization was carried out in sealed pyrex ampules after bubbling nitrogen through the monomers to displace oxygen. The nitrogen was first passed through a column of drierite to remove moisture and then into the monomers. Pure ST and four different mixtures of the two monomers in the ST:ACN ratios of 90:10, 76.2:23.8, 32:68 and 7.3:92.7 by weight were used so as to obtain PS and the SAN copolymers in the ST:ACN ratios of 84.6:15.4, 76.1:23.9, 64.9:35.1 and 50:50 by weight, respectively. Five monomer mixtures of each ratio were polymerized for different lengths of time at 60° ± 1°C. For PS, concentration of initiator was 0.008 moles/l and for all copolymers, 0.032 and 0.016 moles/l concentrations were used. The overall rate of polymerization in each case was determined from the yield of polymer. The polymers were obtained by precipitation in chilled methanol. The volume of methanol used for each precipitation was four times the volume of reaction mixture. The polymers were then redissolved in MEK, filtered and reprecipitated in

methanol. The polymers were then dried in a vacuum oven at 55°C to constant weight. The drying time was about 24 hours.

e. Discussion.--For all the polymers, plots of moles of monomers, M, remaining versus time, t, of reaction were made and fit by computer and then extrapolated to zero time, from which the initial rate of polymerization, $R_p = -d[M]/dt$, could easily be found. Table 2.2 shows these values.

TABLE 2.2.--Initial Rate of Polymerization, R_p, at 60°C for Different Initial Ratios of ST:ACN in Monomer Mixture.

Mole Fraction of ST in Monomer	Mole Fraction of ACN in Monomer	Concentration of AIBN, [I], moles/l	Initial Rate of Polymerization, $R_p \times 10^5$, mole/l/sec
1.0	0.0	0.008	5.6
0.821	0.179	0.032	26.7
0.821	0.179	0.016	18.0
0.620	0.380	0.032	44.9
0.620	0.380	0.016	27.8
0.193	0.807	0.032	63.3
0.193	0.807	0.016	35.5
0.0386	0.9614	0.032	56.9
0.0386	0.9614	0.016	31.3
1.0*	0.0	0.032	13.2
1.0*	0.0	0.016	9.2

*From Ref. (B-5).

Figure 2.3 shows plots of R_p versus mole fraction of ST in the initial monomer mixture for both [I] equal to 0.032 moles/l and 0.016 moles/l. Using these experimental rates of copolymerization, R_p, in Eq. 2.21, values of ϕ for both concentrations of initiator were determined by using a computer. The procedure was the same as that followed by Walling (W-2) in his study of the dependence of the rate of radical copolymerization on the comonomer feed composition for the system styrene-methyl methacrylate at 60°C with AIBN. The value of ϕ is determined by a curve-fitting technique such that for a particular value of ϕ the "best" curve is obtained. Table 2.3 shows these values.

TABLE 2.3.--Values of ϕ With Different Initiator Concentrations for Free Radical SAN Copolymerization at 60°C.

Concentration of AIBN, [I], moles/l	ϕ
0.032	2.09
0.016	4.42

The above result is rather baffling in light of the fact that ϕ is supposed to be a constant for a system regardless of the initiator concentration. Das et al. (D-1) determined the values of ϕ for the SAN system in a slightly different manner. They used different concentrations of the initiator for one monomer ratio and determined ϕ. This was then repeated for different values of monomer ratio. The values of ϕ thus obtained were nearly constant. The average value of ϕ was 7.5.

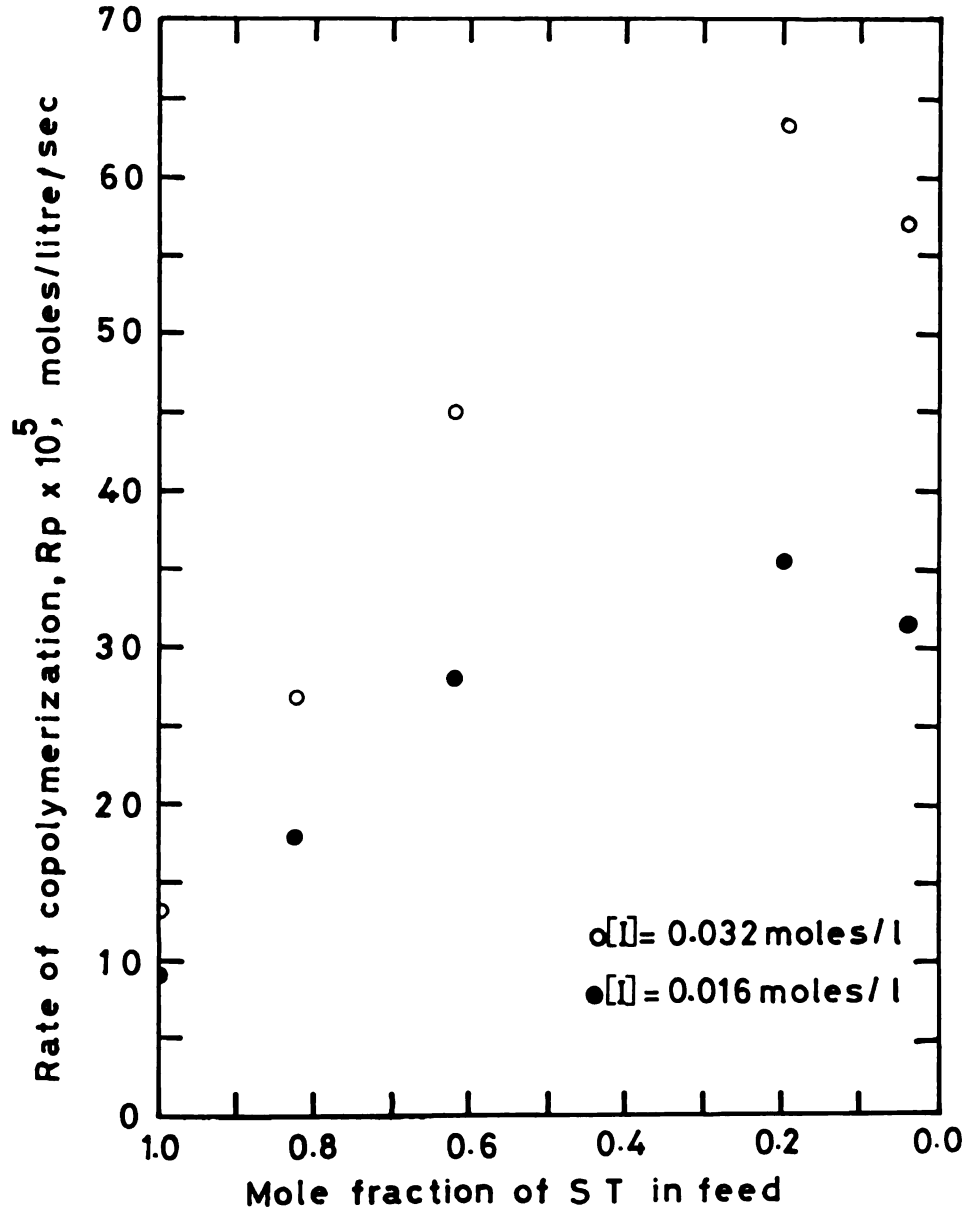

Figure 2.3.--Variations in Initial Rate of Copolymerization with Mole Fraction of ST in Feed at Different Initiator Concentrations at 60°C.

It was found in this work, however, that the value of ϕ in his system varies with copolymer composition and hence the use of q. 2.21 to predict the initial rate of copolymerization with a ingle value of ϕ is of dubious value for this system. North and oworkers (N-1, A-2) have also pointed out the variation of ϕ with opolymer composition in several systems. They pointed out that he termination in radical polymerization could be diffusion-ontrolled. Thus, the interpretation of ϕ primarily in terms of ne chemical effects of the radical ends appears questionable.

Table 2.4 shows the values of $k_{t(12)}$ obtained from the iffusion-controlled equation, Eq. 2.26.

BLE 2.4.--Values of $k_{t(12)}$ for Different Copolymer Compositions for Free Radical SAN Copolymerization at 60°C.

le Fraction of in Copolymer	$k_{t(12)} \times 10^{-7}$ moles/liter/sec	
	[I] = 0.032 moles/liter	[I] = 0.016 moles/liter
742	3.74	4.12
52	3.4	4.49
68	8.6	13.7
37	25.5	41.9

e 2.4 indicates that $k_{t(12)}$ is not constant for any particular lymer composition irrespective of initiator concentration. rton and North (N-1, A-2) and O'Driscoll et al. (O-2) have d to demonstrate the utility of the above method in a few s. Although their work was not extensive, none have studied

the effect of rate of reaction on the termination rate constant, $k_{t(12)}$, as demonstrated here. Thus neither mechanism alone appears to satisfactorily explain instantaneous SAN copolymerization reaction rates.

Figure 2.4 shows experimental and theoretical conversion from Eq. 2.27 as a function of time for three different monomer mixtures. As can be seen, there is no agreement between the calculated time-conversion plots and the experimental data even at small conversions where any effects due to drift are small. The value of $k_{t(12)}$ used for each monomer mixture was that found from Eq. 2.26 where it is assumed that $k_{t(12)}$ is totally diffusion-controlled. As discussed above, this may not be true and the complete disregard of chemical-controlled termination is open to question. Secondly, $k_{t(12)}$ was assumed to be time independent. Actually, $k_{t(12)}$ is dependent on the composition of the polymer chain, and this could be dependent on time of polymerization. O'Driscoll and Knorr (O-3) compared experimental and theoretical conversion predicted by Eq. 2.27 for a mixture of methyl methacrylate and vinyl acetate and found an agreement only up to about 3 per cent conversion. Equation 2.27 has not been tested extensively yet, and the result obtained here indicates that it must be used with caution since the assumptions made during its derivation may not hold for many systems.

It may be concluded that the ϕ-factor singly may not be suitable for describing the behavior of systems where ϕ varies with composition. At any rate, the value of $\phi > 1$ emphasizes the fact

0.18
0.16
0.14
0.12
0.10
0.08

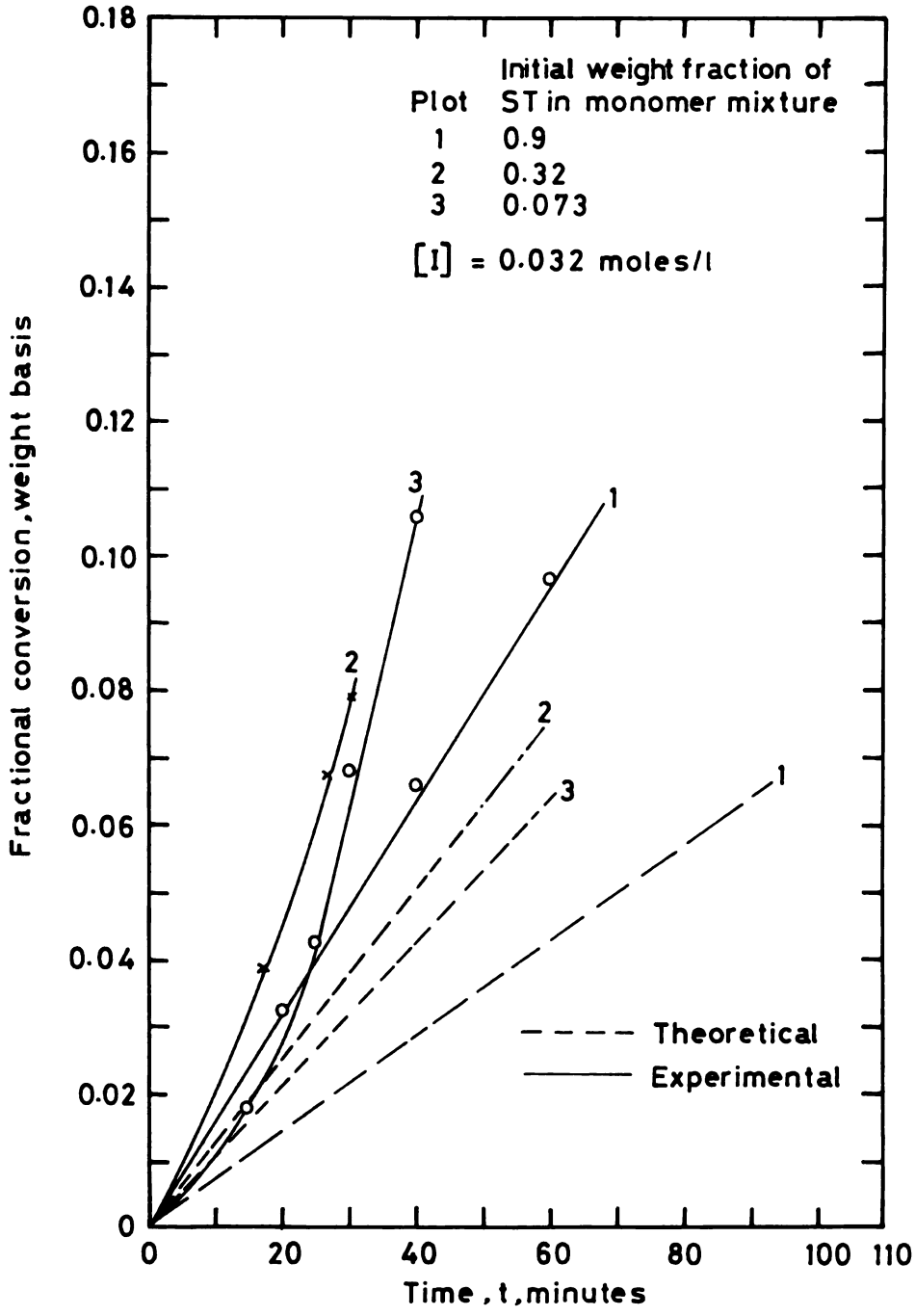

Figure 2.4.--Fractional Conversion as a Function of Time for SAN Monomer Mixtures of Different Compositions.

observed repeatedly in high polymer chemistry that a free radical has a decided preference for combining with an unlike radical. The rate of termination should differ if the last units are the same or different because of polar repulsion effects. If such a repulsion exists, the rate k_t for the reaction $\sim\sim M_1M_2^*$ + $M_1^*\sim\sim$ should be less than that for $\sim\sim M_2M_2^*$ + $\sim\sim M_1^*$ and the value of ϕ will change since

$$\phi = k_{t12}/(k_{t11}k_{t22})^{1/2}. \tag{2.30}$$

Also, in the copolymerization of ST with ACN, it may be postulated that the interaction between the phenyl rings on adjacent ST units will tend to make the segmental motion slower because of hindered rotation about the chain axis. Barb (B-6) has suggested that the effect of the penultimate unit in a radical chain must be considered.

It has been recognized that the increased viscosity during the free radical polymerization of some vinyl monomers causes a decrease in the termination rate constant. This may cause the onset of diffusion-controlled termination. The termination reaction in free radical polymerization is <u>at least</u> partially diffusion-controlled even in an environment of low viscosity. Thus it seems that characterization by simple ϕ or $k_{t(12)}$ factors is inadequate.

Further effort to correlate the rate of copolymerization, R_p, with the monomer composition was not made since this was not the main goal of this research, although it can be seen that the

correlation of R_p with monomer composition would help immensely in predicting the time required for a reaction for the required low conversion using a specified initiator concentration. It is very important to know the required time for a reaction to be able to produce a copolymer reasonably uniform in compositional distribution. In this work it was deemed of vital importance that copolymers of uniform composition distribution be produced for the viscometric and thermodynamic studies, and therefore empirical reaction time information generated by the small scale experiments was used.

E. Large Scale Polymerization

It was found that the theoretical rate expressions for polymerization could not be relied upon to determine the time of action for a required conversion. It was therefore decided to produce large amounts of PS homopolymers and SAN copolymers for viscosity and other measurements on the basis of small scale experiments with corresponding amounts of initiator, and the reactions were carried out for corresponding lengths of time.

Each reaction was carried out in a two-liter, round-bottomed flask at 60°C under nitrogen atmosphere. Cold monomer mixture was heated up to 58°C as quickly as possible, dumped in the reactor and the AIBN was added. After the completion of the reaction, the contents of the flask were poured into chilled methanol (four times the volume of the flask contents) in a Waring blender to precipitate the polymer. The precipitated polymer was

redissolved in MEK, filtered and reprecipitated by addition of methanol. The polymer was dried at 55°C in a vacuum oven. Table 2.5 gives the details of large scale polymerization at 60°C using AIBN.

F. Chemical Analysis of Copolymers

The copolymers were analyzed for nitrogen content (and hence for acrylonitrile content) by Spang Microanalytical Laboratory.* Also, a sample of polyacrylonitrile (PAN) was analyzed as a reference. It was synthesized in bulk at 60°C using AIBN. Table 2.6 gives the results of nitrogen analysis.

It can be seen that the copolymerization reactions were carried out successfully in obtaining the desired compositions. Again the conversion by weight per cent was small in each case, giving a practically uniform copolymer composition.

G. Monomer Reactivity Ratios From Composition of Copolymers

Equation 2.10 can be rearranged into the form

$$\frac{f_1(1 - 2F_1)}{F_1(1 - f_1)} = r_2 + \left[\frac{f_1^2(F_1 - 1)}{F_1(1 - f_1)^2}\right] r_1 \qquad (2.31)$$

as suggested by Fineman and Ross (F-5). The left side of this equation when plotted against the coefficient of r_1 should yield a straight line with slope r_1 and intercept r_2. This plot is called

---

*P.O. Box 1107, Ann Arbor, Michigan 48106.

TABLE 2.5.--Details of Large Scale Polymerization at 60°C With AIBN Initiator.

Polymer	Monomer Mixture Composition, ST		Amount of Monomer Mixture, gms	Initiator Concentration, moles/l	Amount of Initiator, gms	Reaction Time, minutes	Amount of Polymer, gms	Conversion, weight, %
	weight %	mole %						
PS-1	100.0	100.0	1,000	0.008	1.462	240	99	9.9
PS-2	100.0	100.0	1,100	0.00048	0.0955	630	85	7.7
SAN C-1	90.0	82.1	1,100	0.0169	3.146	75	100	9.1
SAN C-2	76.2	62.0	879	0.032	5.279	50	90	10.2
SAN C-2'	76.2	62.0	879	0.00191	0.314	120	53	6
SAN C-3	32.0	19.3	1,000	0.0161	3.150	45	80	8

TABLE 2.6.--Nitrogen Ana

ber	We F
NB-1	
AN 1-1	
AN 1-2	
AN 1-2'	
AN 1-3	

the Ross-Fineman plot.

ect on F, of ST in the

ts: The least squ

4, and 1.3429, respect

The iterature value

ts: good agreemen

ts: of the copol

Molecul
Distr

ions of all th

ta sent to

ing" for det

ta on gas distribu

Set 2 7 shows t

ng end, Mayo-Lewi

TABLE 2.6.--Nitrogen Analysis of Polymers.

Polymer	Weight % of ACN From Nitrogen Analysis	Calculated Weight % of ACN
PAN-1	99.7	100
SAN C-1	14.2	15.4
SAN C-2	24	23.9
SAN C-2'	23	23.9
SAN C-3	38	35.1

the Ross-Fineman plot. Figure 2.5 is such a plot where the mole fraction F_1 of ST in the copolymers is obtained from the nitrogen analysis. The least square values of r_1 and r_2 from Fig. 2.5 are 0.463 and 0.0429, respectively. These values compare quite well with the literature values of 0.41 and 0.04 that were used in this work. This good agreement reinforces the confidence in the chemical analysis of the copolymers.

H. Molecular Weights and Molecular Weight Distribution of Polymer Samples

Samples of all the polymers that were synthesized on a large scale were sent to the analytical laboratories of the Dow Chemical Company* for determination of molecular weights and molecular weight distribution by gel permeation chromatography (GPC). Table 2.7 shows the GPC results.

*Midland, Michigan 48640.

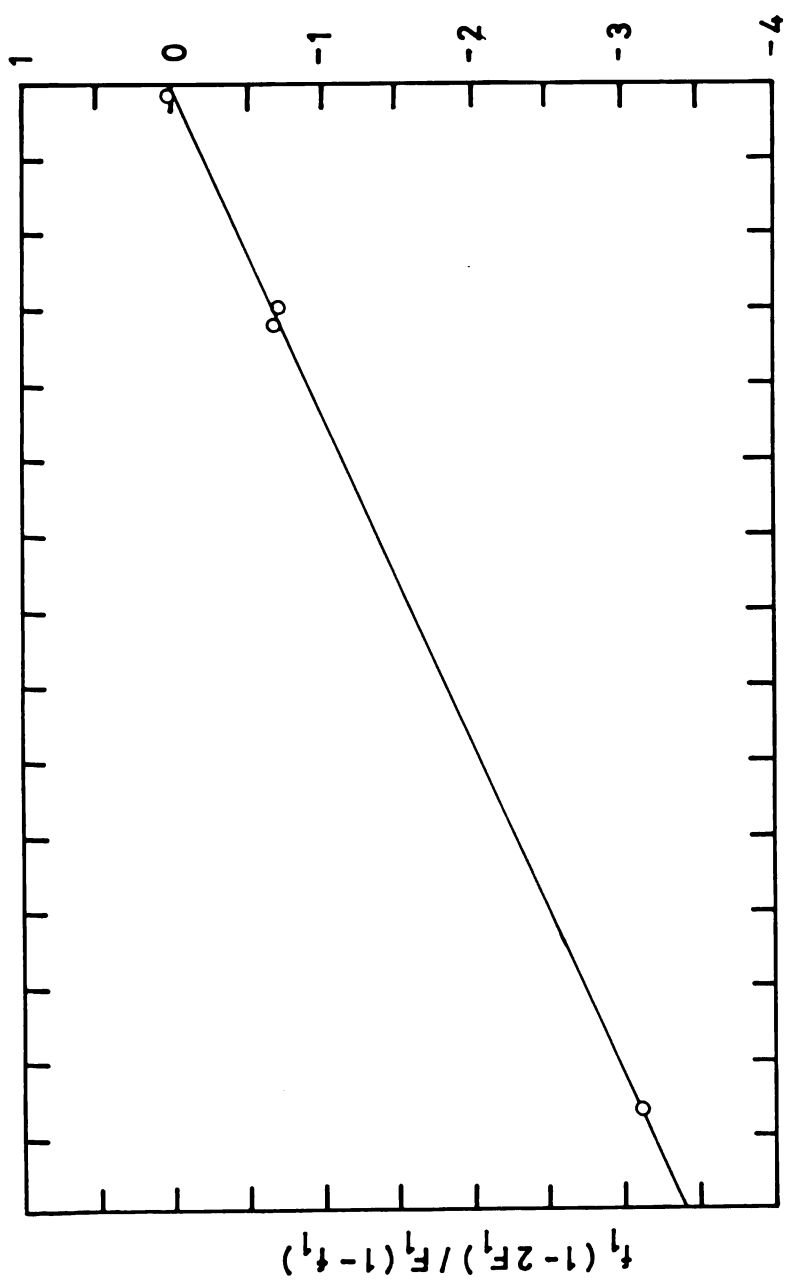

Figure 2.5.--Ross-Fineman Plot for Determination of Monomer Reactivity Ratios, r_1 and r_2, from Nitrogen Analysis of Copolymers.

TABLE 2.7.--Molecular W
Polymers by

Polymer	Composition, Weight % ST
[illegible]	100.0
[illegible]	100.0
[illegible]	85.8
[illegible]	76.0
[illegible]	77.0
[illegible]	62.0

[illegible] result is reliab
[illegible] composition b
[illegible] weights, M_w, o
[illegible] light scatte
[illegible] to note th
[illegible] close to
[illegible], as expected
[illegible] 5%.

[illegible] are give

TABLE 2.7.--Molecular Weights and Molecular Weight Distribution of Polymers by GPC.

Polymer	Composition, Weight % ST	M_w	M_n	M_w/M_n	M_w by Light Scattering*
PS-1	100.0	185,000	103,000	1.79	191,000
PS-2	100.0	501,000	241,000	2.08	504,000
SAN C-1	85.8	275,000	141,000	1.95	290,000
SAN C-2	76.0	203,000	120,000	1.69	180,000
SAN C-2'	77.0	634,000	339,000	1.87	666,000
SAN C-3	62.0	332,000	205,000	1.62	332,000

The GPC result is reliable since the copolymers are practically uniform in composition because of low conversions. Again the molecular weights, M_w, obtained by GPC compare very well with those obtained by light scattering in this work (Chapters III and V). It is interesting to note that the molecular weight distribution, M_w/M_n, is quite close to the most probable molecular weight distribution of 2, as expected from kinetic models of polymerization for random polymers (F-3c).

*Details are given in Chapters III and V.

A. Intrin

In this section

ation is discussed.

a macromolecule in solut

square end-to-end distan

figuration, $\langle s^2 \rangle^{1/2}$. T

how the measurements of

ications. The size of

ormed upon short-range

range or vert environmen

e may in solution depe

on the molecular weig

rom hydrodynamic, therm

he results of this sect

hermodynamic sense, o

from intrinsic visc

measurements may be used

on in solution and to

or in some molecular we

The generation of

tion of some or a fe

CHAPTER III

BACKGROUND AND THEORY

A. Intrinsic Viscosity and Expansion Factor

In this section, the configuration of a macromolecule in solution is discussed. Parameters describing the effective size of a macromolecule in solution are defined. They are the root-mean-square end-to-end distance, $\langle L^2 \rangle^{1/2}$, and the root-mean-square radius of gyration, $\langle S^2 \rangle^{1/2}$. These parameters may be found experimentally from the measurements of the intrinsic viscosities of the polymer solutions. The size of a polymer chain in solution is shown to depend upon short-range polymer structural parameters and long-range solvent environment factors. The intrinsic viscosity of a polymer in solution depends upon the molecular weight of the polymer. The molecular weight dependence is discussed in this section from hydrodynamic, thermodynamic, and empirical points of view. The results of this section are used to show how the goodness, in a thermodynamic sense, of a solvent for a polymer may be determined from intrinsic viscosity measurements, how the viscosity measurements may be used to estimate the dimensions of macromolecules in solution and to develop the relationship between viscosity and polymer molecular weight in dilute solutions.

The generation of the structure of a macromolecule through repetition of one or a few elementary units is the basic

characteristic of polym

polymer (i.e., "many me

whose fully stretched l

Thus, a polymer molecul

solution, or in bulk, t

not lengthwise, but, du

configurations which ch

between the ends of the

of its many configuratio

solution, is also often

segments whose density

The dimension of

characterize its spatial

some distance, L, the

those for a long, flex

number of configurations

for it impossible to de

of a dual conformat

set by the chain i

sometimes regarded, the

root-mean-square end-to-

measure of the effective

the square distance of t

Here, this quantity

method of integration, ge

whose Gaussian statisti

characteristic of polymeric substances as is implied by the term polymer (i.e., "many member"). A polymer molecule is a molecule whose fully stretched length is much greater than its diameter. Thus, a polymer molecule may be considered as a long chain. In solution, or in bulk, the chain molecule is in general not stretched out lengthwise, but, due to Brownian motion assumes many spatial configurations which change randomly with time. The distance between the ends of the polymer chain is time dependent. Because of its many configurations, a polymer molecule, in bulk or in solution, is also often considered as a spherical cloud of polymer segments whose density varies radially about a center of gravity.

The dimension of a polymer molecule most widely used to characterize its spatial or configurational character is the end-to-end distance, L, the distance from one chain-end group to the other. For a long, flexible chain, the number of distinguishable shapes or configurations will obviously be very large. It is clearly impossible to describe such a chain molecule in terms of the individual conformations in which the position of each atom constituting the chain is specified. A time average value of L is therefore required, the usually appropriate average being the root-mean-square end-to-end distance, $\langle L^2 \rangle^{1/2}$. Another important measure of the effective size of a polymer molecule is the root-mean-square distance of the elements of the chain from its center of gravity. This quantity, designated as $\langle s^2 \rangle^{1/2}$, is often called the radius of gyration of the molecule. For linear chain polymers obeying Gaussian statistics, Flory (F-3e) has shown that

$$\langle L^2 \rangle = 6\langle S^2 \rangle.$$

The configurati

epends on its environm

ous solvent, where the

r mer and a solvent m

he same as the mean of

n mer-polymer and sol

s expand so as to redu

r mer elements. I

he energy of interacti

r : unfavorable, sma

r mer contacts occur,

It must be emph

r is twofold. It c

ers and angles of

ers are the short-rang

n of the chai

ers. Secondly, the

ers interactions b

. The latter

ences in the polyme

r ers affect dependi

r the

r the coils more

ers and less

$$\langle L^2 \rangle = 6\langle S^2 \rangle. \tag{3.1}$$

The configuration of the polymer molecule in solution depends on its environment, i.e., the quality of solvent. In a good solvent, where the energy of interaction between a polymer element and a solvent molecule adjacent to it exceeds or is about the same as the mean of the energies of interaction between the polymer-polymer and solvent-solvent pairs, the molecule will tend to expand so as to reduce the frequency of contacts between pairs of polymer elements. In a poor solvent, on the other hand, where the energy of interaction between polymer segment and solvent molecule is unfavorable, smaller configurations in which polymer-polymer contacts occur, will be favored.

It must be emphasized that the problem of polymer configuration is twofold. It depends in the first place on the bond dimensions and angles of the atoms along the chain backbone. These are the short-range effects depending on the characteristics of the units of the chain which are very near one another in sequence. Secondly, the configuration is influenced also by thermodynamic interactions between the polymer elements and their environment. The latter is referred to as the long-range effect. It depends on the polymer molecule and its environment, whereas the first effect depends on the parameters of the polymer molecule alone.

If the solvent medium is sufficiently poor, i.e., a Θ-solvent defined later in the chapter, the overall dimensions

'l be determined sole

his state will prevail

s a unique temperature

nections will reflect

nperturbed by environm

s vent condition a θ-c

en designated as $\cdot L_0^2$,1

urbed dimensions, $\cdot L^2$,

ange effects in solven

om the unperturbed di

e as scale arising fr

$$\cdot L^{2\ 1/2} = \cdot L_0^2$$

$$\cdot L^{2\ 1/2} = \cdot L_0^2$$

e of is often

(Baumgart [5-2]

measurements on d

characterization of poly

e temperature is great

s are discovered

the term is

randomly coiled

of an ideal gr

will be determined solely by polymer unit bond lengths and angles. This state will prevail in a poor solvent for the given polymer at a unique temperature. Physical measurements made under these conditions will reflect the characteristics of the polymer molecule unperturbed by environment. Flory (F-3a) calls this state of solvent condition a Θ-condition. The unperturbed dimensions are designated as $\langle L_0^2 \rangle^{1/2}$ or $\langle S_0^2 \rangle^{1/2}$ to distinguish them from perturbed dimensions, $\langle L^2 \rangle^{1/2}$ or $\langle S^2 \rangle^{1/2}$, arising due to the long-range effects in solvents. The perturbed dimensions will differ from the unperturbed dimensions by the average expansion, α, of the molecule arising from the long-range effects. Then one may write

$$\langle L^2 \rangle^{1/2} = \alpha \langle L_0^2 \rangle^{1/2} \tag{3.2}$$

and

$$\langle S^2 \rangle^{1/2} = \alpha \langle S_0^2 \rangle^{1/2}. \tag{3.3}$$

The value of α is often appreciably greater than unity.

Staudinger (S-2) called attention to the utility of viscosity measurements on dilute polymer solutions as a means of characterization of polymers. High polymer molecules possess the unique capacity to greatly increase the viscosity of the liquid in which they are dissolved, even when present at concentrations which are quite low. This is the manifestation of the voluminous character of randomly coiled long chain molecules. The higher the molecular weight, the greater is the increase in viscosity produced

by a given weight conce

olution when divided b

elative viscosity, η_r.

$_{sp}$ by

$$\eta_{sp} = \eta_r - 1$$

where η_{sp} expresses the

a meric solute. The

f dissolved polymer, i

r mer to increase the

ic ratio at infinite

e.,

$$[\eta] = (\eta_{sp}/c)_{c\to}$$

n concentration, c, i

ion of sp, the intrin

ecular size of each unit

ecular size is usually

n can be read out 'M.

ion of macromolecule

n as a viscosity.

ion usually rep

$$\eta_{sp} = [\eta]c + k$$

by a given weight concentration of polymer. The viscosity of the solution when divided by the viscosity of the solvent gives the relative viscosity, η_r. Also, η_r is related to specific viscosity, η_{sp}, by

$$\eta_{sp} = \eta_r - 1 \tag{3.4}$$

here η_{sp} expresses the incremental viscosity attributable to the olymeric solute. The ratio, η_{sp}/c, where c is the concentration dissolved polymer, is a measure of the specific capacity of the lymer to increase the relative viscosity. The limiting value of is ratio at infinite dilution is called the intrinsic viscosity,]; i.e.,

$$[\eta] = (\eta_{sp}/c)_{c\to 0} = [(\eta_r - 1)/c]_{c\to 0}. \tag{3.5}$$

concentration, c, is customarily expressed in grams per 100 cc solution, the intrinsic viscosity, [η], then being given in the iprocal of this unit. i.e., in deciliters per gram. Plots of c against c usually are very nearly linear for $\eta_r < 2$, and it been pointed out (M-5, H-3) that the slopes of these plots for ven polymer-solvent system vary approximately as the square of intrinsic viscosity. Thus the equation proposed by Huggins to empirically represent data of this type is

$$\eta_{sp}/c = [\eta] + k_1[\eta]^2 c \tag{3.6}$$

where k_1 is called the

$[\eta]$ is thus the interc

against c.

When the logari

series of fractionated

the logarithms of their

linear within experimen

relationships may be ex

$$[\eta] = KM^a$$

where K and a are empir

the intercept and the s

with both the polymer a

ure. It should be empl

of the convenience of

become using intrins

One of the earl

connecting the visco

linear approach of Debj

where K is a simple che

called Rouse. This mod

the hydrodynamic re

consists of a sequenc

the polymer by spring

and the corresponding

which is the drawb

where k_1 is called the Huggins constant. The intrinsic viscosity, $[\eta]$, is thus the intercept on the ordinate of the plot of η_{sp}/c against c.

When the logarithms of the intrinsic viscosities of a series of fractionated linear polymer homologs are plotted against the logarithms of their molecular weights, relationships which are linear within experimental error are usually obtained. The linear relationships may be expressed by a simple equation of the form

$$[\eta] = KM^a \tag{3.7}$$

where K and a are empirical constants determined, respectively, by the intercept and the slope of the plot. Values of K and a vary with both the polymer and the solvent and are dependent on temperature. It should be emphasized that Eq. 3.7 is empirical in origin but its convenience of application has maintained its continued use for correlating intrinsic viscosities and molecular weights.

One of the earliest quantitative approaches to the problem of predicting the viscosity of dilute polymer solutions is a hydrodynamic approach of Debye (D-2). He considered an isolated polymer molecule in a simple shear field and developed the so-called "bead-spring" model. This model is convenient for the purpose of discussing the hydrodynamic resistance to the flow of surrounding medium. It consists of a sequence of beads. Each of the beads, connected to one another by springs, offers hydrodynamic resistance to the flow of the surrounding medium. The springs do not offer any resistance to the flow. In the bead-spring model of a polymer

molecule, the total m monomer units in the chain are subdivided into N subgroups, each subgroup containing m/N monomer units (m > N). The special property of the subgroup is that it contains enough monomer units so that at equilibrium its dimensions obey Gaussian statistics. The subgroup is referred to as "bead" or "segment." In dynamic calculations employing the bead-spring model, it is assumed that all the mass of the subgroup is concentrated in a bead such that the total frictional resistance offered by the solvent to all the monomers of the subgroup is accounted for by the frictional forces on the fictitious bead. The segment distribution function is Gaussian also. The beads are assumed to be connected by linear springs. These concepts are discussed in detail by Zimm (Z-1) and Rouse (R-1).

Debye assumed the frictional effects to be so small that the motion of the surrounding fluid is only very slightly disturbed by the movement of the polymer molecule relative to the medium. This means that the velocity of the medium everywhere is the same as though the polymer molecule were not present. The solvent streams through the molecule almost unperturbed by it. This is called the free-draining coil model of a polymer molecule. Figure 3.1a illustrates this case. According to the Debye theory,

$$[\eta] = N_{AV}\zeta R_e^2/100\ \eta_s M_0 \tag{3.8}$$

where N_{AV} is the Avogadro's number, η_s is the viscosity of solvent, M_0 is the molecular weight of monomer, ζ is the frictional

Figure 3.1a.-
through Solvent.*

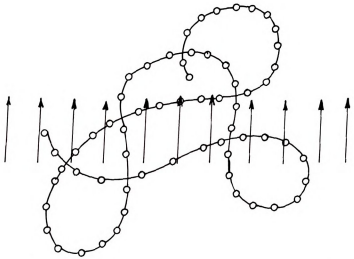

Figure 3.1a.--A Free-Draining Molecule During Translation Through Solvent.*

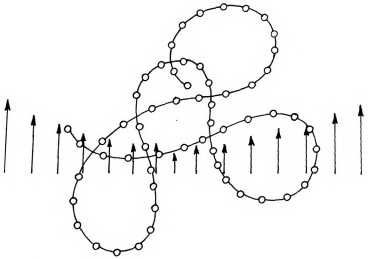

Figure 3.1b.--Translation of a Chain Molecule with Perturbation f Solvent Flow Relative to the Molecule.*

*Arrows indicate flow vectors of the solvent relative to the lymer chain.

coefficient for a bead

radius of the polymer

macroscopic measure of

i.e. 3.8 has been introd

to the usual units, gm/

linear polymers, R_e^2 is

hence, from Eq. 3.8,

$$[\eta] = K_m M$$

where K_m is a constant

the solvent, and the fr

actual observations of

described by Eq. 3.7 wh

$$[\eta] = \nu R^3.$$

these units from Eq. 3.9

molecule is not freely

solvent's viscosity tak

is introduced by the

'drag effect' is

rods are imagined to be

the flow external flow

the linear rods have

the treatments are sim

of a macromolecule. Each

perpendicular to the flow

molecule. Figure 3.1b

coefficient for a bead of the polymer chain and R_e is the effective radius of the polymer chain. The parameter R_e is a convenient macroscopic measure of a polymer chain size. The factor 100 in Eq. 3.8 has been introduced in the denominator in order to convert to the usual units, gm/100 cm^3, for the intrinsic viscosity. For linear polymers, R_e^2 is proportional to molecular weight M, and hence, from Eq. 3.8,

$$[\eta] = K_m M \quad . \tag{3.9}$$

where K_m is a constant peculiar to the monomer, the viscosity of the solvent, and the frictional coefficient. As mentioned before, actual observations of $[\eta]$ as a function of M in a solvent are described by Eq. 3.7 which is

$$[\eta] = KM^a. \tag{3.7}$$

Deviations from Eq. 3.9 are attributed to the fact that a polymer molecule is not freely drained. More sophisticated treatments of intrinsic viscosity take a more detailed view of the flow perturbation introduced by the monomer units. In particular, the idea of a "shielding effect" is introduced, whereby peripheral monomer units are imagined to be able to shield interior monomer units from the external flow (F-3f). Debye and Bueche (D-3) and Kirkwood and Riseman (K-1) have carried out analyses with the above model. Their treatments are similar in philosophy but different in mathematical technique. Each presents a mathematical treatment of perturbation to the flow field interior and exterior to a polymer molecule. Figure 3.1b illustrates this situation. From their

esults, the intrinsic

arameter varying from

or no shielding, respe

Flory (F-3f),

ig 3.3b) and thermo

ow the more quantita

ory : theory predict

he mean-square end-to-

$$[\eta] = \Phi \langle L^2 \rangle^{3/2} /$$

where Φ is a universal

he macromolecule (provided

ain flexible, and f

ding to this treat

s of the effective

he molecular weight

represented as being pro

he randomly coiled

to obtain the fa

denotes the quantity $\langle L$

see Fig. 3.2,.

$\ldots = \Phi \langle \ldots^2 \rangle^{3/2} / M$

mean square number of

$\ldots = \ldots^2$

where r, i

$= 0$.

results, the intrinsic viscosity follows Eq. 3.7 in which a is a parameter varying from 0.5 to 1.0 for the case of maximum shielding or no shielding, respectively.

Flory (F-3f), in considering hydrodynamic shielding (see Fig. 3.1b) and thermodynamic expansion of the polymer coil, follows the more quantitative treatment of Debye and Bueche (D-3). Flory's theory predicts that the intrinsic viscosity is related to the mean-square end-to-end distance and is given as

$$[\eta] = \Phi \langle L^2 \rangle^{3/2} / M \tag{3.10}$$

where Φ is a universal constant independent of the nature of the macromolecule (provided only that the molecular chain is sufficiently flexible) and is also independent of the solvent medium. According to this treatment, $[\eta]$ is considered proportional to the ratio of the effective volume of the molecule in solution divided by its molecular weight. In particular, this effective volume is represented as being proportional to the cube of a linear dimension of the randomly coiled polymer chain.

To obtain the factors influencing $[\eta]$, it is desirable to separate the quantity $\langle L^2 \rangle^{3/2}$ into its component factors, α^3 and $\langle L_0^2 \rangle^{3/2}$ (see Eq. 3.2). Equation 3.10 may then be written as

$$[\eta] = \Phi (\langle L_0^2 \rangle / M)^{3/2} M^{1/2} \alpha^3. \tag{3.11}$$

For a linear polymer of a given unit structure, $\langle L^2 \rangle^{1/2}$ is proportional to $n^{1/2}$ where n is the number of links in the polymer chain (F-3e), i.e.,

$$\langle L^2 \rangle^{1/2} = C n^{1/2}$$

where C is a constant ch

or a polymer chain con

ional to the length, l

independent of M for

ow, from Eq. 3.11,

$$[\eta] = \Phi \langle r_0^2 \rangle^{3/2} / M$$

where

$$\Phi = \Phi_0 [1 - L_0^2 / M)$$

ds to the preced

ic polymer independen

on the nature of th

Incidentally, $[\eta]$

ation, Φ as in Eq. 3.

ce of the exp

can be eliminate

theory (Φ_0

ic conditio

ation and Eq.

$$[\eta] = K M^{1/2}$$

ence of interme

ion to random coiled

$$\langle L^2 \rangle^{1/2} = Cn^{1/2} \tag{3.12}$$

where C is a constant characteristic of the given chain structure. For a polymer chain composed of identical bonds, C will be proportional to the length, l, of the bond. It then follows that $\langle L_0^2 \rangle / M$ is independent of M for a linear polymer of a given unit structure. Then, from Eq. 3.11,

$$[\eta] = KM^{1/2}\alpha^3 \tag{3.13}$$

where

$$K = \Phi(\langle L_0^2 \rangle / M)^{3/2}. \tag{3.14}$$

According to the preceding hydrodynamic analysis, K is a constant for a polymer independent of both the molecular weight of the polymer and the nature of the solvent.

Ordinarily, $[\eta]$ should depend on M not only owing to the factor $n^{1/2}$ as in Eq. 3.12 but also on the expansion factor, α. The influence of the expansion resulting from intermolecular interactions may be eliminated by suitable choice of the solvent and temperature. Flory (F-3f) calls this choice of solvent and temperature a Θ-condition or ideal condition. At the Θ-condition, α is equal to 1 and Eq. 3.13 reduces to

$$[\eta]_\Theta = KM^{1/2}. \tag{3.15}$$

The influence of intermolecular interactions on the configuration can thus be neutralized by this choice of solvent medium. The

mensions at the Θ-co

mensions, $\langle L_0^2 \rangle^{1/2}$ and

follows that

$$[\cdot]/[\cdot]_\Theta = \alpha^3.$$

from the measuren

vents, the expansi

α^3, α is then a m

vent for a polymer.

vent for that po

rises experimentally

rises at this time (

B Light Sca

Rayleigh

ght scattering

ter at a distance

the reduced

the intensity

incident

ter and

we index

Debye

new measurement

dimensions at the Θ-condition are the same as the unperturbed dimensions, $\langle L_0^2 \rangle^{1/2}$ and $\langle S_0^2 \rangle^{1/2}$ (F-3f). From Eqs. 3.12 and 3.14 it follows that

$$[\eta]/[\eta]_\Theta = \alpha^3. \tag{3.16}$$

Thus, from the measurements of intrinsic viscosities in good and Θ-solvents, the expansion factor, α, can be calculated by using Eq. 3.16; α is then a measure of the "degree of goodness" of the solvent for a polymer. The higher the value of α, the better is the solvent for that polymer. These concepts have been amply demonstrated experimentally and Eq. 3.15 for Θ-conditions is universally accepted at this time (K-2).

B. Light Scattering and Second Virial Coefficient

Lord Rayleigh (L-1) first correctly explained the phenomenon of light scattering and expressed the intensity of light as observed at a distance r from a scattering center as

$$R_\theta = i_\theta r^2/I_0 = 8\pi^4 \varepsilon \alpha^2 n_0^4 (1 + \cos^2\theta)/\lambda^4 \tag{3.17}$$

where R_θ is the reduced intensity (often called Rayleigh ratio), i_θ is the intensity of light scattered at an angle θ, I_0 is the unpolarized incident intensity, ε is the number of isotropic scattering particles per unit volume having polarizability α, and n_0 is the refractive index at wave length λ.

Following Debye's application of Rayleigh theory of scattering to the measurement of scattering from polymer solutions (D-4),

the turbidity, τ, whic

of light per unit of s

thus.

$$\tau = 2\pi \int_0^{\pi} \frac{i_\theta r^2}{I_0}$$

or

$$\tau = \left(\frac{16\pi}{3}\right) R_\theta / (1$$

the Rayleigh scattering

of homogeneous molecul

homogeneous by adding

it were by Rayleig

the structure of solute

the angular distribu

Considering the

the concentration d

from (2-3), as

$$\frac{K_c}{R_\theta} = \frac{}{M_w}$$

$$\frac{1}{M_w} = 2A_2 c$$

where A_2 is the second virial

the weight average

where A_2

the turbidity, τ, which is the reduction of the incident intensity of light per unit of scattering volume, has been commonly used, thus,

$$\tau = 2\pi \int_0^{\pi} \frac{i_\theta r^2 \sin\theta}{I_0} d\theta \tag{3.18}$$

or

$$\tau = (\frac{16\pi}{3})R_\theta/(1 + \cos^2\theta). \tag{3.19}$$

The Rayleigh scattering from gases and liquids arises from their non-homogeneous molecular structure. Making a solvent even more inhomogeneous by adding a solute increases scattering. From this initial work by Rayleigh and Debye, knowledge of the number, size and structure of solute particles can be obtained from observations on the angular distribution of the scattered light.

Considering the non-ideality of the system, the expression for the concentration dependence of the scattering can be given in virial form (S-3) as

$$\frac{KC}{R_{90}} = \frac{2\pi^2 n_0^2 (dn/dc)^2 c}{N_{AV}\lambda^4 \quad R_{90}} = \frac{1}{M_w} + 2A_2c + 3Bc^2 + \cdots \tag{3.20}$$

or

$$\frac{Hc}{\tau} = \frac{1}{M_w} + 2A_2c + \cdots \tag{3.21}$$

neglecting higher virial terms. The concentration, c, is in gm/cm^3, M_w is the weight average molecular weight and the optical constant H is given by

$H = 16\pi/K$

and depends only upon

ive index of the solv

refractive index incre

ely only to solute p

ength of the incident

anger than $\lambda/20$, inter

resulting in an unsymme

ation, Eq. 3.21 is multi

the observed scattering

of the interference. T

particle sizes and shap

the form

$$\frac{Kc}{R_\theta} = \frac{1}{M_w P(\theta)}$$

ence of the major

ng at low the scatteri

for ... ing chain molec

ange ... segment ... ration,

ger ... ... than $\lambda/(2-2)$ a

a certain ang..., which is

... angle ... mmer molecu

... ... and ... Th

...

$$H = 16\pi/K \tag{3.22}$$

and depends only upon the wave length of radiation, λ, the refractive index of the solvent, n_0, at wave length, λ, and the specific refractive index increment, (dn/dc), at λ. Equations 3.20 and 3.21 apply only to solute particles which are small compared to the wave length of the incident radiation (less than $\lambda/20$). For particles larger than $\lambda/20$, interference occurs in the scattered radiation resulting in an unsymmetrical angular scattering pattern. In this case, Eq. 3.21 is multiplied by a factor $P(\theta)$ (D-4), which corrects the observed scattering to the value it would have in the absence of the interference. This function has been tabulated for various particle sizes and shapes (D-5, B-7). Equation 3.21 then assumes the form

$$\frac{Hc}{\tau} = \frac{Kc}{R_\theta} = \frac{1}{M_w P(\theta)} + 2A_2c + \cdots \tag{3.21a}$$

One of the major problems in light scattering has been that of relating the scattering intensity to the dimensions of a randomly coiling chain molecule in solution. Owing to its continuous change in configuration, the dimension obtained is a time-average dimension. Zimm (Z-2) approached the problem by recognizing that the scattering, which is a function of both angle and concentration for large polymer molecules, could be plotted simultaneously as a function of θ and c. The limiting value of $1/P(\theta)$ is expressed as

$$\lim_{c\to 0} 1/P(\theta) = 1 + \frac{16\pi^2}{3\lambda^2}\langle S^2\rangle \sin^2\frac{\theta}{2} + \cdots \tag{3.23}$$

where $\langle S^2 \rangle$ is the mean

molecules. For a rand

$\langle S^2 \rangle_\theta$ where $\langle L^2 \rangle$ is t

zero. Substituting E

$$\lim_{c \to 0} \frac{Kc}{R_\theta} = \frac{1}{M_w P(\theta)}$$

A general meth

data is as to eliminat

obtaining the correct

are obtained by Zimm (

for a number of solute

zero angles, θ. The

$\sin^2(\theta/2) + qc$, whe

data is spread out the

the scattering angle

data points obtained fo

these lines to equal

a plot of

are a measure

concentration

molecular, ar

q is where the

these lines should meet

the y axis, W_w^{-1}

where $\langle S^2 \rangle$ is the mean-square radius of gyration of the polymer molecules. For a random coil configuration $\langle S^2 \rangle$ is equal to $\langle L^2 \rangle/6$ where $\langle L^2 \rangle$ is the mean-square end-to-end distance of the chain. Substituting Eq. 3.23 into Eq. 3.21a, we have

$$\lim_{c \to 0} \frac{Kc}{R_\theta} = \frac{1}{M_w P(\theta)} = \frac{1}{M_w} \left(1 + \frac{8\pi^2}{9\lambda^2} \langle L^2 \rangle \sin^2 \frac{\theta}{2} + \cdots \right) \quad (3.24)$$

A general method for treating experimental light scattering data so as to eliminate the effects of destructive interference and obtaining the correct values for the molecular weight of the solute was outlined by Zimm (Z-2). In this procedure data are obtained for a number of solute concentrations, c, each at a number of scattering angles, θ. The ratio Kc/R_θ is then plotted as a function f $\sin^2 (\theta/2)$ + qc, where q is an arbitrary constant selected to uitably spread out the data. Experimental points obtained at any iven scattering angle may then be extrapolated to c equal to 0 and ta points obtained for any concentration at different angles trapolated to θ equal to 0. Thus the limiting slope of the zero gle line in a plot of Kc/R_θ against $\sin^2 (\theta/2)$ + qc yields the cond virial coefficient, A_2. The ratio of the limiting slope of e zero concentration line to the intercept gives the mean-square l-to-end dimension, and the reciprocal of the intercept on the R_θ axis (where the θ equal to 0 and c equal to 0 lines when rapolated should meet at a point) gives the weight average ecular weight, M_w.

In a homopolym

ner and the only diffe

eight heterogeneity.

ymers with a unifor

ormed by dilute soluti

apply only if the

uniform throughout

he copolymers produce

sult of the drift in

he azeotropic copolym

aying the reacti

for copolymers

ecurse, the equation

Skeist and cowor

$$F_{n_1} = \frac{Z_1}{Z_1 + Z_2} M_1$$

$$F_{w_1} = \frac{Z_1 Z_2 (r_1 r_2 + 1)}{(Z_1 + Z_2)^2} M_{AV}$$

where M_1 and M_2 ar

concentration and

components 1

$$F_{z_1} = \frac{Z_1 M_1}{Z_1 M_1 + Z_2 M_2}$$

where F_{z_1} is the average

the average weight

In a homopolymer all the elements scatter in the same manner and the only difference within the sample is due to molecular weight heterogeneity. The preceding treatment applies only to polymers with a uniform composition. In measuring the light scattered by dilute solutions of copolymers, the preceding treatment will apply only if the distribution of the two monomer components is uniform throughout the copolymer. As mentioned in Chapter II, the copolymers produced could be heterogeneous in composition as a result of the drift in composition at high conversion, except for the azeotropic copolymer. In this work this effect was minimized by carrying the reactions only to low conversions.

For copolymers where considerable dispersity in composition may occur, the equation for Rayleigh scattering has been expressed by Stockmayer and coworkers (S-4) and Bushuk and Benoit (B-8) as

$$R_\theta = K' \sum \nu_i^2 c_i M_i \tag{3.26}$$

and

$$K' = 2\pi^2 n_0^2 / N_{AV} \lambda^4 \tag{3.27}$$

where ν_i, c_i, and M_i are the specific refractive index increment, weight concentration and molecular weight, respectively, of the scattering component i. For such a system, the actual measured quantity is

$$R_\theta = K' \nu_0^2 c M_{app} \tag{3.28}$$

where ν_0 is the average refractive index increment and M_{app} is the apparent molecular weight obtained from the data.

The specific r

copolymer in a solvent

index increments of th

solvent weighted by th

independent of molecul

have long been establ

Huglin and Benoit (B-8

copolymer, as determined

yet of that obtained

have also establi

ermination over a wi

ham et al. (K-4) and

The negative nature

the average c

measurements of dn/dc v

the inherent copolymer

dn dc... copolymer

where [illegible] is the

the concentration of

where: A and B are the

Huglin and Benoit

dn/dc = W_B * 25

The specific refractive index increment, dn/dc, of a copolymer in a solvent is a simple sum of the specific refractive index increments of the two component homopolymers in the same solvent weighted by their weight fractions in the copolymer and independent of molecular weight. The dn/dc of homopolymers has since long been established to be independent of molecular weight. Bushuk and Benoit (B-8) showed that the mole fraction of each monomer, as determined from measurements of dn/dc is within 2 per cent of that obtained through chemical analysis. Kinsinger et al. (K-4) have also established the colligative nature of dn/dc after investigation over a wide range of copolymer composition. Kinsinger et al. (K-4) and Klimisch (K-5) have shown in their study of the colligative nature of this increment that it is possible to calculate the average composition of a copolymer based on the measurements of dn/dc of the whole copolymer and that of the individual parent homopolymers (A and B) in the same solvent. Hence,

$$(dn/dc)_{copolymer} = \nu_0 = x_A\nu_A + (1 - x_A)\nu_B \qquad (3.29)$$

where $x_A = c_A/(c_A + c_B)$ is the weight fraction of species A having weight concentration c_A in the copolymer. The refractive index increments, ν_A and ν_B, are the dn/dc values for the two homopolymers A and B in the same solvent.

Bushuk and Benoit (B-8) through their derivation obtained

$$M_{app} = M_w + 2P[(\nu_A - \nu_B)/\nu_0] + Q[(\nu_A - \nu_B)/\nu_0]^2 \qquad (3.30)$$

where M_w is the true m

represent the heteroge

compositional skewness

$$F = \sum_i Y_i M_i(x_i$$

$$J = \sum_i Y_i M_i(x_i$$

where Y_i is the weight

weight M_i and the co

$$\bar{x} = \sum_i Y_i x_i$$

The average composit

where

"The osmotic pre

the pressure which h

to the partial molar

at 0° K. i.e., Thi

$$\bar{G} - \bar{G}_w = \sum_i x_i$$

where $\bar{G}$ is the partial

ambient state, $\bar{G}_w$ is

x_i is the mole and

$\bar{G} - \bar{G}_w = RT \ln$

$\bar{G} - \bar{G}^0 = RT \ln$

where M_w is the true molecular weight. The parameters P and Q represent the heterogeneity in composition; P relates to the compositional skewness about the average x_A and Q to its broadness.

$$P = \sum_i \gamma_i M_i (x_i - x) \tag{3.31}$$

$$Q = \sum_i \gamma_i M_i (x_i - x)^2 \tag{3.32}$$

where γ_i is the weight fraction of component i whose molecular weight is M_i and the composition is x_i, and x, given as

$$x = \sum_i \gamma_i x_i, \tag{3.33}$$

is the average composition of the sample in weight fraction of component 1.

The osmotic pressure of a polymer solution, π, is defined as the pressure which has to be applied to a solution so as to raise the partial molar free energy of the solvent to the standard state value (F-3a). Thus,

$$\bar{G}_1^0 = \bar{G}_1 + \int_0^{\pi} (\partial \bar{G}_1 / \partial P)_{T,x_1} dP \tag{3.34}$$

where $\bar{G}_1^0$ is the partial molar Gibbs free energy of the solvent in the standard state, T is the absolute temperature, x_1 is the mole fraction of solvent and P is the pressure. The variation of $(\partial \bar{G}_1 / \partial P)_{T,x_1} = \bar{V}_1$ with pressure may be neglected, so that

$$\bar{G}_1 - \bar{G}_1^0 = RT \ln a_1 = -\pi \bar{V}_1 \tag{3.35}$$

where $\bar{V}_1$ is the partia

in which Raoult's law

$$\ln a_1 = \ln (1$$

where x_2 is the mole

By combining E

osmotic pressure of a

a use of the solvent,

e use, v_s) in the con

$$= (RT/v_s)x_2$$

Since x_2/v_s is

expressed in gm/

$$= (RT/M_n)c.$$

the concentration

the particles hav

$$= RT[c/M_n + $$

where A_2, A_3, etc. are

and so on. The coef

$A_2 = 0$ is a thermodyn

Viscosity

In this section,

the use of polymer

where $\bar{V}_1$ is the partial molar volume of the solvent. In the range in which Raoult's law applies, one may write

$$\ln a_1 = \ln (1 - x_2) \simeq -x_2 \tag{3.36}$$

where x_2 is the mole fraction of the solute.

By combining Eqs. 3.35 and 3.36 one may write for the osmotic pressure of a dilute solution (for which the partial molar volume of the solvent, $\bar{V}_1$, is indistinguishable from its molar volume, v_s) in the concentration range satisfying Raoult's law

$$\pi = (RT/v_s)x_2. \tag{3.37}$$

Since x_2/v_s is equal to c/M where the solute concentration, c, is expressed in gm/ml,

$$\pi = (RT/M)c. \tag{3.38}$$

At higher concentrations, where binary and higher order interactions of solute particles have to be taken into account,

$$\pi = RT[(c/m) + A_2c^2 + A_3c^3 + \ldots .] \tag{3.39}$$

where A_2, A_3, etc. are the second, third, and higher order virial coefficients. The coefficients A_2, A_3, etc. have the same value as in Eq. 3.21a. Thus A_2 is related to Gibbs free energy through π and so it is a thermodynamic quantity.

C. Viscosity Correlation Techniques

In this section two empirical correlations for correlating viscosities of polymer solutions are described.

Power Law Correla

As the concen

he polymer "spheres"

become "entangled" as

ery dilute solutions.

. depends much more

r weight than it doe

$$\eta_r = 1 + KcM^a$$

ere c is the concent

ere the solvent depe

concentrated soluti

$$\eta_r \propto (cM^b)^E$$

ere K and E are corre

ow found to have a v

e some aspects of th

n E.

The value of th

ecome the low shear

t particles a reas

ter-segment points or "e

n" entanglements

ore of the polymer spheres

. As we approach the "cri

erties of the solutio

1. Power Law Correlation

As the concentration of polymer in solution is increased, the polymer "spheres" begin to overlap and finally polymer chains become "entangled" as opposed to existing as isolated chains in very dilute solutions. When this happens, the low-shear viscosity, η_r, depends much more strongly on polymer concentration and molecular weight than it does in dilute solution. In dilute solutions,

$$\eta_r = 1 + KcM^a \tag{3.40}$$

where c is the concentration, M is the molecular weight and a and K are the solvent dependent constants for a polymer-solvent system. In concentrated solutions,

$$\eta_r \sim (cM^b)^\beta \tag{3.41}$$

where b and β are correlation parameters. Experimentally, β is often found to have a value near 5, and b, a value near 0.68, so that correlations of the type $\eta_r \sim c^5M^{3.4}$ are frequently successful (M-1a, P-1).

The value of the product cM, where Eq. 3.40 ceases to describe the low shear viscosity of a polymer solution and where Eq. 3.41 provides a reasonable fit, is termed the "critical" entanglement point or "critical" entanglement density. Below the "critical" entanglement point, the size and concentration of the effective polymer spheres dominate the flow phenomena and Eq. 3.40 applies. Above the "critical" entanglement point, the network structure of the solution is usually presumed to dominate the flow

nenomena and Eq. 3.4

concentration and mol

he flow entanglement

nenomena in concentr

hermodynamic parame

' entanglement poi

A log-log plo

aster curve for a pol

olecular weights of t

bove the "critical" v

. e., ferry (f-2a) a

ets of this type f

mple : Correlatio

"he power law

arameters from the expe

"his correl

this a good above. A

mpirical way of correl

mple : Polymer Mol

"his spheres:

Average ro: to Ei

s spheres w

ameter is the Hydrodi

Hydrodynamic Properties of

phenomena and Eq. 3.41 is used to describe the dependence of η_r on concentration and molecular weight. Since the physical nature of the flow entanglements is usually thought to dominate the flow phenomena in concentrated polymer solutions, polymer-solvent thermodynamic parameters are most often neglected above the "critical" entanglement point (B-9).

A log-log plot of η_r against $cM^{0.68}$ usually yields a single master curve for a polymer-solvent system covering a wide range of molecular weights of the polymer. This plot is a straight line above the "critical" value of $cM^{0.68}$ with a slope of 5. Middleman (M-1a), Ferry (F-2a) and Fox et al. (F-6) summarize available results of this type for a few polymer solvent systems.*

2. Simha's Correlation

The power law correlation is based on determination of a parameter from the experimental observation of the dependence of η_r on cM^b. This correlation has been used for correlating the data as explained above. As an alternative, Simha (S-6) suggested a different way of correlating the data. This correlation is based on Einstein's model for the treatment of viscosity of a suspension of rigid spheres.

According to Einstein's (M-2a) original hydrodynamic treatment of rigid spheres with interparticle distances very large compared to the particle diameters,

---

*Williams Model (W-1) predicts $\eta_r \sim cM^{0.625}$. This model is discussed in Section D of this chapter.

$$\eta_{sp} = \frac{\eta - \eta_s}{\eta_s}$$

where η is the viscos

the solvent and ϕ is

In this treatment the

which preserve their

$$\eta_{sp} = \eta_r - 1$$

where k is a pure numb

The actual vis

increased by an order of

Eq. 3.42 and

interaction effects.

In extremely d

The sum of the effe

arises. The perturb

macromolecules are t

The concentration, i

macromolecules are no l

arises from interacti

which are less than

macromolecular particles

The ratio of the visc

are, respectively,

where η is the viscosity

$$\eta_{sp} = \frac{\eta - \eta_s}{\eta_s} = 5/2\ \phi \tag{3.42}$$

where η is the viscosity of the suspension, η_s is the viscosity of the solvent and ϕ is the volume fraction occupied by the spheres. In this treatment the particles are treated as rigid structures which preserve their shape in the course of flow. In general,

$$\eta_{sp} = \eta_r - 1 = a\phi \tag{3.43}$$

where a is a pure number depending on particle shape.

The actual viscosity of dilute colloidal suspension often exceeds by an order of magnitude the value predicted from Einstein's relation (Eq. 3.42 and 3.43). This is most probably due to concentration effects.

In extremely dilute suspensions, the total viscosity effect is the sum of the effects caused by each of the individual suspended particles. The perturbations of solvent flow produced by the suspended particles are therefore independent of each other. However, as the concentration is increased from infinite dilution, flow perturbations are no longer independent. For moderately dilute solutions the interaction of perturbations of the solvent flow can be classified into those caused by two, three, and higher number of suspended particles. The strength of these effects is directly proportional to the second, third, and higher power of concentration of particles, respectively. This indicates that η_{sp} can be presented as a polynomial in the concentration of the particles. As

...ne concentration inc...

...ncrease to obtain a ...

...oncentration behavio...

Simha (S-5) h...

...herical particles a...

$$\eta_{sp} = (5/2)\phi$$

...e concentration depe...

...ther may be written

$$\frac{\eta_{sp}}{c} = [\eta] + a_2$$

$$\frac{\eta_{sp}}{c} = [\eta] + k_1$$

...where ... is equal to ...

...s independent of di...

...ers. Frisch and ...

...mperature dependen...

...ers and non-spherical ...

...ers + concentration ...

$$\frac{\eta_{sp}}{c} = \dots + k$$

...Simha and Utrac...

...the value of our corr...

...we would be obtai...

the concentration increases, the degree of the polynomial must increase to obtain a reasonable description of the experimental concentration behavior.

Simha (S-5) has calculated the coefficient of ϕ^2 for spherical particles and obtained

$$\eta_{sp} = (5/2)\phi + 12.6\ \phi^2 + \cdots \tag{3.46}$$

The concentration dependence of spherical particles to terms ϕ^3 and higher may be written as (F-7)

$$\frac{\eta_{sp}}{\phi} = [\eta] + a_2\phi + a_3\phi^2 + \cdots \tag{3.47}$$

or

$$\frac{\eta_{sp}}{\phi} = [\eta] + \bar{k}_1[\eta]^2 + \bar{k}_2[\eta]^3\phi^2 + \cdots \tag{3.48}$$

where $[\eta]$ is equal to 2.5 for spheres and $\bar{k}_1$, $\bar{k}_2$, etc. are pure numbers independent of dimensions or molecular weight of the suspended particles. Frisch and Simha (F-7) have presented details of the concentration dependence of the viscosity of suspensions of spherical and non-spherical particles. Rearranging Eq. 3.48, a power series in concentration may be written as

$$\frac{\eta_{sp}}{c} = [\eta]\{1 + k_1[\eta]c + k_2[\eta]^2c^2 + k_3[\eta]^3c^3 + \cdots\} \tag{3.49}$$

Simha and Utracki (S-6) have proposed to make use of the above equation for correlating viscosity-concentration data for a range of molecular weights of a particular polymer in a particular

olvent. The linear

suspended spheres. T

dependence of the rel

near. Different cu

superposed to produce

$[\eta^{*}]$ against c a

a given so

fact that these plots

ever observed (S-6) t

3.1.

D. Will

This section c

has been developed to

real polymer solutio

Continuum rheo

ical response cont

interpretation and yet

any model that g

ons that contain tw

ular reference t

molecular theory exist

with reference to recen

theories of rheological

molecular theory

ories or models for

solvent. The linear macromolecules in solutions are modeled as suspended spheres. The experimentally observed concentration dependence of the relative viscosity in the very dilute region is linear. Different curves for different molecular weights can be superposed to produce a master curve. Log-log plots of $\eta_{sp}/c[\eta]$ against c are made for different molecular weights of a polymer in a given solvent. Then $\gamma(M)$ is chosen as a shift factor such that these plots merge into a single master plot. It has been observed (S-6) that γ is proportional to $M^{-\varepsilon}$ where, usually, $0.5 \leq \varepsilon \leq 1.1$.

D. Williams Model for Zero Shear Viscosity

This section describes a molecular theory of Williams which has been developed to describe the viscosity of moderately concentrated polymer solutions.

Continuum rheological models for the treatment of rheological response contain parameters that frequently lack molecular interpretation and yet they are used because of their simplicity. Middleman (M-1b) has given an excellent review of many of these models that contain two, three, or four parameters. These models contain no reference to the structure of a material, but contain empirical "curve fit" parameters that may or may not have molecular significance. In recent years developments have been made in the treatment of rheological response of a material based on its molecular structure. Ferry (F-2) and Middleman (M-1) deal extensively with molecular models. For polymer solutions these models are of the form

$$\frac{\eta - \eta_s}{\eta_0 - \eta_s} = f(\dot{\gamma}$$

where η, η_0 and η_s ar
ero shear or low sh
ic vent, respectively
constant for a system
and $\dot{\gamma}$ are material pa
ner solutions, log-lo
shape of the one shown

Several funct
have been proposed (M
the one shown in Fig.
ately for describing
ner systems. In all
these parameters ar
ls of the test curve.
η_0 describes the
ity or viscosi
r shear rate. The m
es the value of the
r shear rate at whic
ion and $\dot{\gamma}_c$ is relate
ameter α and $n-1$,
ameter α is suggested
e of more solutions

$$\frac{\eta - \eta_s}{\eta_0 - \eta_s} = f(\lambda\dot{\gamma}) \tag{3.50}$$

where η, η_0 and η_s are the viscosity of solution at shear rate $\dot{\gamma}$, zero shear or low shear viscosity of solution and the viscosity of solvent, respectively. The parameter λ is a characteristic time constant for a system and $\dot{\gamma}$ is the shear rate. In Eq. 3.50, η_0 and λ are material parameters of the system. For many typical polymer solutions, log-log viscosity-shear rate (η-$\dot{\gamma}$) plots have the shape of the one shown in Fig. 3.2.

Several functional forms of continuum models and Eq. 3.50 have been proposed (M-1c) to describe a typical η-$\dot{\gamma}$ curve such as the one shown in Fig. 3.2. These equations have been quite successful in describing the experimentally observed η-$\dot{\gamma}$ behavior of many systems. In all these equations experimental values of the material parameters are required in order to be able to fit the data of the η-$\dot{\gamma}$ curve. The horizontal portion of the curve in Fig. 3.2 describes the Newtonian-like, low shear rate behavior. In this region viscosity is constant irrespective of the value of the shear rate. The horizontal curve extended to zero shear rate gives the value of the upper Newtonian viscosity, η_0, for a system. The shear rate at which non-Newtonian behavior, or the falling cruve begins, is related to the parameter λ.

Williams (W-1) has suggested a model for predicting the curve and has also suggested a molecular model for predicting the η_0 value of a polymer solution from a knowledge of its molecular weight,

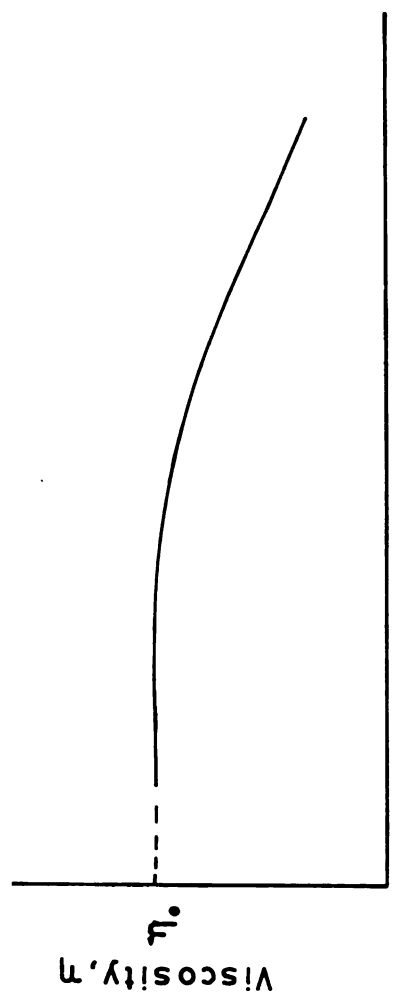

Figure 3.2.--Illustration of Experimentally Observed Viscosity-Shear Rate, η - $\dot{\gamma}$, Behavior of a Polymer Solution on a log-log Plot.

thermodynamic behavio

rected his effort t

ntrated solutions.

xtremes of isolated

ite solutions and

ge"

The problem w

nswer distinct poly

ctions, intramolecul

surrounded by an i

ctions both intra

ording to Williams

nolecules in sol

ctions most commonly

of stresses in so

ng for "G"

ble model

model. Each

of identica

and the chain.

ed volum

ts with th

represented

of segmenta

ains because a

thermodynamic behavior, theta dimensions, and friction factor. He directed his effort toward describing the flow of moderately concentrated solutions. These solutions lie between the conceptual extremes of isolated polymer molecules in a sea of solvent in very dilute solutions and the rubber-like network of polymer chains in a gel.

The problem was to find a method of treating the forces between distinct polymer chains in a flowing medium. In dilute systems, intramolecular forces are important since a macromolecule is surrounded by an infinite sea of solvent while in concentrated solutions both intra and intermolecular forces are important. According to Williams, the latter interactions (between different macromolecules in solution) are probably more dominant in polymer systems most commonly encountered. He used Fixman's (F-8) description of stresses in solutions of linear polymers to develop his relationship for η_0. The model for a polymer molecule is the pearl necklace chain model (see Section A in this chapter for description of this model). Each polymeric solute molecule is represented by a series of N identical segments which interact with adjacent segments along the chain through spring forces and with other segments through excluded volume forces and hydrodynamic forces. Each segment interacts with the solvent through frictional resistance. The solvent is represented as a continuum phase creating frictional resistance to segmental motion. Fixman's equation describes the total stress tensor $\underline{\underline{\tau}}$ as

$$\bar{\bar{\pi}} = \bar{\bar{\pi}}_0 + n \sum_{i}^{N}$$

where $\bar{\bar{\pi}}_0$ represents s

sotropic pressures,

n use, R_i^j is the pos

ar molecule relative

the interaction po

between that segment

or between two molec

between those tw

n m_i whose cente

e coordinates illus

$$r_{(n_j} + b$$

$$r_{m_j} = r_{(n_j}$$

where j the positi

the brackets

the conformations

ber of the segments

ber of the coordi

the ave

integrating over t

ibution of a sol

ence and interact

$$\underline{\underline{\tau}} = \underline{\underline{\tau}}_0 + n \sum_i^N \langle \underline{R}_i^1 \nabla_i U \rangle + \frac{1}{2} n^2 \langle \underline{r} \nabla_r V \rangle \tag{3.51}$$

where $\underline{\underline{\tau}}_0$ represents stresses due to solvent and externally imposed isotropic pressures, n is the number of polymer molecules in a unit volume, $\underline{R}_i^1$ is the position vector of i^{th} segment of the first polymer molecule relative to the center of mass of its own molecule, U is the interaction potential (or intersegmental potential energy) between that segment and all other segments, $\underline{r}$ is the position vector between two molecular centers and V is the interaction potential between those two molecules and i runs over the segments of molecule 1 whose center is fixed at $\underline{r}_1$. The relation between position coordinates illustrated in Fig. 3.3 is

$$\underline{x}_i = \underline{r}_{(m)} + \underline{R}_i^{(m)} \tag{3.52a}$$

$$\underline{r}_{(m)} - \underline{r}_{(n)} = \underline{r}_{(mn)} \quad [= \underline{r}] \tag{3.52b}$$

where $\underline{x}_i$ is the position of i^{th} segment referring to an arbitrary origin. The brackets < > are used to signify the averaging over all possible conformations. The term $\langle \underline{R}_i^1 \nabla_i U \rangle$ is a function of coordinates of the segments of a single molecule. If Ψ is a distribution function in the coordinate space of all S segments, then the term $\langle \underline{R}_i^1 \nabla_i U \rangle$ (i.e., the average) is obtained by multiplying $\underline{R}_i^1 \nabla_i U$ by Ψ and integrating over the complete space (H-4). The term $\langle \underline{r} \nabla_r V \rangle$ is a function of $\underline{r}$ only. If $g(\underline{r})$is a pair correlation function for intermolecular interaction, then the term $\langle \underline{r} \nabla_r V \rangle$ (i.e., the average)

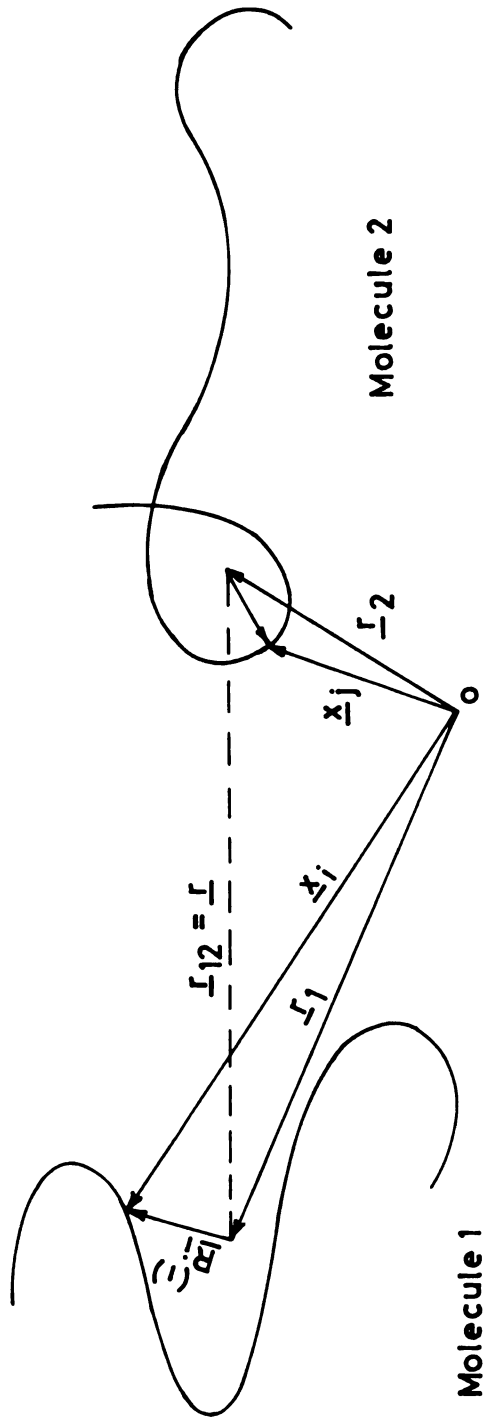

Figure 3.3.--Illustration of Position Coordinates Referring to Polymer Molecules and Segments in Derivation of Williams Model.

s obtained by multi

omplete space (H-4)

ermined by the stater

which are separated b

s the number of mole

It should be

ngly an arbitrary s

ave soped directly fr

ate. From the exa

he ber potential (F

ss stable for polyme

ss of the polymer m

ns concentrated so

e ose additive pote

In the case o

ss because χ_{ij} is u

ns becomes negli

ngement is not a

ns separated molec

In the case o

χ_{ij} is 3.51

ange be muse add

ranges taken over th

ervse temperatures.

ter segments and the

ne set is of some

is obtained by multiplying $\underline{r}\nabla_r V$ by $g(\underline{r})$ and integrating over the complete space (H-4). The pair correlation function, $g(\underline{r})$, is defined by the statement that the number of pairs of molecules which are separated by a distance r is $(N^2/2V)g(r)\ 4\pi r^2 dr$ where N is the number of molecules in volume V (H-5a).

It should be pointed out that Eq. 3.51 does not represent simply an arbitrary series expansion of $\underline{\underline{\tau}}$ in powers of n but is developed directly from the equation of motion of solvent and solute. From the examination of the concentration dependence of the pair potential (F-9, F-10), Fixman expects the model to be applicable for polymer volume fraction less than one-tenth regardless of the polymer molecular weight. He assumed that in moderately concentrated solution (volume fraction ≤ 0.1) U must be a pairwise additive potential.

In the case of very dilute solutions, Eq. 3.51 is simplified because $\nabla_r V$ is unimportant for two reasons: n^2 is very small and $V(\underline{r})$ becomes negligible as $\underline{r}$ increases. Thus the force on the i^{th} segment is not a function of the positions of segments belonging to separated molecules.

In the case of higher polymer concentrations (volume fraction ≥ 0.1), Eq. 3.51 may be inadequate. The parameter, U, is then no longer pairwise additive. This would necessitate the use of averages taken over three-body interactions, with terms in n^3 becoming important. This would correspond to the presence of entanglements and the form of Eq. 3.51 would change considerably. On the basis of some experimental investigation, Williams proposed

that Eq. 3.51 would

solutions. He then

mer in solution,

the term with n^2 wou

result, the term wit

some intermediate ra

$$= \frac{1}{2} n^2$$

$$= \frac{1}{2} n^2$$

For estimatin

made use of Fixman's

ion of a single po

described by a pro

another molecule at p

the segment of the f

is obtained by

we ex

from

$$\frac{d^2}{d}$$

where ζ is the mo

a time average of n_i

that Eq. 3.51 would be satisfactory for moderately concentrated solutions. He then argued that with higher concentration of polymer in solution, the intermolecular forces become dominant and the term with n^2 would be much greater than the term with n. As a result, the term with n^2 would suffice to describe the behavior in some intermediate range of concentration. This reduces Eq. 3.51 to

$$\underline{\underline{\tau}} - \underline{\underline{\tau}}_0 \doteq \frac{1}{2} n^2 \langle \underline{r} \nabla_r V \rangle \tag{3.53a}$$

$$\doteq \frac{1}{2} n^2 \int r \nabla_r V(\underline{r}) g(\underline{r}) d\underline{r}. \tag{3.53b}$$

For estimating intermolecular potential, $V(\underline{r})$, Williams made use of Fixman's equilbrium theory (F-8). The segment distribution of a single polymer molecule about its center of mass can be described by a probability density, $\nu(\underline{R})$. The presence of another molecule at position $\underline{r}$ will lead to a repulsive force on each segment of the first molecule. The net force on this molecule is obtained by integrating over the segments at all $\underline{R}$ and is given as

$$V(\underline{r}) = A \int \nu(\underline{R}) \nu(\underline{r} + \underline{R}) d\underline{R} \tag{3.54}$$

where

$$A = V_p^2 \frac{d^2 \varepsilon}{dv_p^2} \tag{3.55}$$

in which V_p is the molecular volume of polymer in solution, ε is the free energy of mixing segments with solvent and v_p is the

me fraction of p

is known as

iams expressed t

unction (F-3e) but

te

Williams use

mbers (K-3) for

te the stresses in

herical molecules.

ere $\dot{\gamma}$ is a shear ra

he zero shear rat

n function, K is

perature. The she

where $\dot{\gamma}$ is the magnit

volume fraction of polymer in solution. Equation 3.54 can be used if $\nu(\underline{R})$ is known as a function of concentration and shear rate. Williams expressed the function $\nu(\underline{R})$ as a Gaussian distribution function (F-3e) but expressed it in terms of a dimensionless shear rate.

Williams used the technique adopted by Kirkwood and coworkers (K-3) for estimating $g(\underline{r})$ which has been used to calculate the stresses in single component systems composed of simple spherical molecules. He obtained a steady state equation for g as

$$\nabla \cdot \{\nabla g - g\nabla \ln g_0\} = \left(\frac{\xi}{2kT}\right)\underline{r} \cdot \underline{G} \cdot \nabla g \qquad (3.56)$$

where $\underline{G}$ is a shear rate tensor, ξ is the friction coefficient, g_0 is the zero shear rate form of g usually called the radial distribution function, k is the Boltzmann constant and T is the absolute temperature. The shear dependence of $g(\underline{r})$ was expressed as

$$g \doteq g_0[1 + \frac{\xi}{kT}(\underline{e}_r \cdot \underline{G} \cdot \underline{e}_r)\psi(r) + \cdots] \qquad (3.57a)$$

$$\doteq g_0[1 + \left(\frac{\xi\dot{\gamma}}{kT}\right)(\sin\theta\cos\theta\cos\phi)\psi(r) + O(\xi^2\dot{\gamma}^2)] \qquad (3.57b)$$

where $\dot{\gamma}$ is the magnitude of shear rate in simple shear flow. Williams truncated the series after the linear term in $\dot{\gamma}$ because of the smallness of $\xi\dot{\gamma}$. Combination of Eqs. 3.56 and 3.57b yields an equation for $\psi(r)$ whose solution is necessary in the evaluation of Eq. 3.53b rewritten as

$$\bar{a} - \bar{a}_0 = \frac{1}{2} n$$

$$+ \frac{1}{2}$$

...ams argued that
...cent or more) th
...s ... Then each s
...er of segmental fo
...sequently, $g_0(r)$ ...

$$g_0(r) = 1.$$

...s is ..., this mea
... of polymer molec
...he equation for ...
... and = 57%.

...he intermole
... = 54 where
... terms of dimer
... terms four
... and the rem

...
...
... the ...

$$\underline{\underline{\tau}} - \underline{\underline{\tau}}_0 \doteq \frac{1}{2} n^2 \int [\underline{r}\nabla V] g_0 d\underline{r}$$

$$+ \frac{1}{2} n^2 \left(\frac{\xi\dot{\gamma}}{kT}\right) \int [\underline{r}\nabla v] g_0 \psi \sin\theta \cos\theta \cos\phi \, d\underline{r} \qquad (3.58)$$

illiams argued that at high concentration (for high polymers, one er cent or more) the segments of separate molecules begin to inter- ingle. Then each segment is subject to a nearly random distribu- ion of segmental forces which tend to cancel each other; onsequently, $g_0(r)$ approaches unity.

$$g_0(r) \doteq 1. \qquad (3.59)$$

hysically, this means that such a solution contains a uniform den- ity of polymer molecules. This results in a great simplification n the equation for ψ which is obtained by the combination of Eqs. .56 and 3.57b.

The intermolecular potential $V(\underline{r})$ was obtained from $\nu(\underline{R})$ ing Eq. 3.54 where $\nu(\underline{R})$ is shear dependent and Williams expressed in terms of dimensionless shear rate. Finally, to compute vis- sity, Williams found the symmetrized shear component of $\underline{\underline{\tau}}$ from . 3.58 and the result obtained was

$$\frac{\eta - \eta_s}{\eta_0 - \eta_s} = f(\lambda\dot{\gamma}) = 1 - \frac{9}{14} \lambda^2 \dot{\gamma}^2 \ldots . \qquad (3.60)$$

re λ is the unspecified time constant for polymer chain response,

$$\eta_0 = \eta_s + \left[\frac{c}{} \right.$$

where c is the conce
number, M is the mol
constant and T is th

$$B = 3/2 \cdot [^2,$$

where $[^2,$ is the me
molecule,

$$[= \frac{1}{3\sqrt{2}}$$

η_0 is the friction
used to predict [an
ween and Acrivos
In this model
particles due to the
of its weight
are not
be not correct
can be measu
the model
that

$$\eta_0 = \eta_s + \left[\frac{cN_{AV}}{M}\right]^2 \frac{A}{kT} B^{3/2} C\xi \tag{3.61}$$

where c is the concentration of polymer, N_{AV} is the Avogadro's number, M is the molecular weight of polymer, k is the Boltzmann's constant and T is the absolute temperature. In the above equation,

$$B = 3/2 \langle L^2 \rangle \tag{3.62}$$

where $\langle L^2 \rangle$ is the mean-sequare end-to-end distance of a polymer molecule,

$$C = \frac{1}{30\sqrt{2\pi}} \left[\frac{3.53}{\sqrt{2B \ln\left[\frac{cN_{AV}}{M} \frac{A}{kT}\right]}}\right]^5 \tag{3.63}$$

and ξ is the friction coefficient. Several models have been proposed to predict ξ and two of them are by Williams (W-1) and Frankel and Acrivos (F-11).

In this model for η_0, thermodynamic solvent effects are accounted for by the term A/kT, obtained from the measurement of activity of solvent in solution, and related to the second virial coefficient A_2. Equation 3.61 can be tested rigorously since it does not contain any unknown constants and all the parameters involved can be measured or estimated. An interesting feature is that the model predicts $\eta_r \sim cM^{0.625}$. A common experimental observation is that $\eta_r \sim cM^{0.68}$ (see Section C of this chapter).

EXPE

The rheologi
ers shear viscositi
ear rates. Capill
ons of low conce
scometer was emplo
er solutions.
the capillary visc
s were measured b
ary viscometer.
ues obtained
er each other.
surements with a c
ere measured by the
ymers are extensiv
ere measured at 30°C

CHAPTER IV

EXPERIMENTAL APPARATUS AND MEASUREMENTS

A. Viscometry

The rheological behavior of solutions was characterized by zero shear viscosities as well as by viscosities over a range of shear rates. Capillary viscometers were used for measuring viscosities of low concentration solutions. A cone-and-plate viscometer was employed for measuring viscosities of high concentration solutions. Viscosities less than 0.1 poise were measured by the capillary viscometers. Viscosities between 0.1 and 0.5 poise were measured by both the capillary viscometers and the cone-and-plate viscometer. In this latter case, the experimental viscosities obtained by each of the two methods were within 5 per cent of each other. This is within the error bounds of rheological measurements with a cone-and-plate viscometer. Higher viscosities were measured by the cone-and-plate viscometer. Both types of viscometers are extensively described in Ref. (V-2). All viscosities were measured at 30°C.

1. Capillary Viscometer

a. Practice.--Cannon-Ubbelohde* suspended level U-tube capillary viscometers with four bulbs (for four different shear

*Cannon Instrument Company, State College, Pennsylvania 16801.

ntes) were used for

ations. The basi

viscometer, (2)

Ostwald viscometer

the end of the capil

the fluid in the cap

It is a great impr

ber 1-2 A lower,

rder to make dilut

ds to stopping the ca

ation by providing d

ibration is avail

measurements were ma

ven easily in an ins

mmercial. The tim

e was measured at

he average value wa

ver 200 seconds so

e to 0.1 s.

Before introd

ons by Dre

e used. The

measurement was 5 ml

The measurements

ere predetermined

rates) were used for measuring viscosities of low concentration solutions. The basic components for capillary viscometry are (1) viscometer, (2) thermostat, and (3) timer. In the Cannon-Ubbelohde viscometers used here, a side arm provided just below the end of the capillary established the same external pressure on the fluid in the capillary above and below the flowing column. This is a great improvement over the very simple Ostwald viscometer (V-2). A lower, larger bulb acts as a solution reservoir in order to make dilution directly in the viscometer. The multiple bulbs topping the capillary are used to provide several shear rates by providing different hydrostatic heads. A complete description is available in the instrument bulletin (V-3). The measurements were made at 30° ± 0.01°C by clamping the viscometer vertically in an insulated water bath equipped with a precision thermostat. The time required for a solution to flow through a bulb was measured at least three times to within 0.1 seconds and the average value was taken. The flow times were always greater than 200 seconds so that kinetic energy corrections were found to be negligible.

Before introducing the solutions into the viscometers, they were clarified by pressure filtration through ultrafine sintered glass filters. The minimum volume necessary for making the measurements was 5 ml. Solutions were diluted in the reservoir bulb for measurements of viscosity at different concentrations by adding predetermined quantities of clarified solvent.

b. Calibrat

cometers were provid

ecked by measuring

. The measured

ues reported in T

struments that wer

Cone-and-Plate V

a. Practice

scometer are (1) v

torsion bar (to

ne-plate viscometer

was used for m

. The visc

Figure

viscometer was bei

ual description

A brief desc

through a ra

plate diameter

three different

ge of accuracy.

Manufactured

Military, Inc. an

number of viscosi

ge of Newtonian

b. Calibration.--The calibration constants of the viscometers were provided by the Cannon Instrument Company. They were checked by measuring viscosities of distilled water and benzene at 30°C. The measured viscosities were within 0.1 per cent of the values reported in literature. Appendix A gives constants of the instruments that were used in this work.

2. Cone-and-Plate Viscometer

a. Practice.--The basic components of a cone-and-plate viscometer are (1) variable speed motor, (2) cone and plate, (3) torsion bar (to measure torque), and (4) recorder. A cone-and-plate viscometer called a Weissenberg Rheogoniometer,* model R-16, was used for measuring viscosities of high concentration solutions. The viscometer was used in the constant shear configuration. Figure 4.1 shows the main body of the viscometer. The apparatus has been sufficiently documented in Ref. (P-2). An exhaustive description is available in the instruction manual (I-1). A brief description of the minor modification will be given here.

Although a range of sizes are available with the instrument, a platen diameter of 7.5 cms, and a cone angle of 1°-37' were used. Three different torsion bars were available for different ranges of viscosity. Depending on the expected viscosity, the

*Manufactured by Farol Research Engineers, Ltd., Bognor Regis, Sussex, England, and made available for this work by the Department of Chemical Engineering and G. G. Brown Laboratory, University of Michigan, Ann Arbor, Michigan 48105.

A. To

B. To

C. Sh

D. Ou

E. Up

F. Ai

G. Ra

H. Ro

I. Co

J. Pi

K. He

L. He

M Ur

N Ea

Legend for Figure 4.1

A. Torsion Bar Clamp

B. Torsion Bar

C. Shear Stress Quartz Load Cell

D. Output of Load Cell to Charge Amplifier

E. Upper Air Bearing

F. Air Input to Air Bearing

G. Radius Arm

H. Rotor

I. Cone

J. Plate

K. Heating Chamber

L. Heat Transfer Fluid

M. Drive Shaft from Motor and Gear Box

N. Base

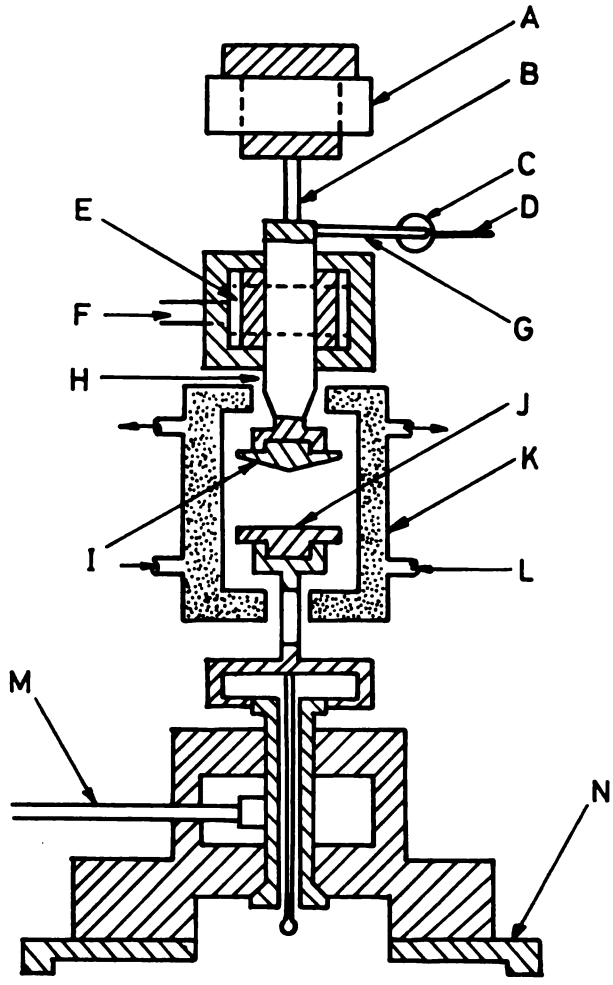

Figure 4.1.--Rheogoniometer (Constant Shear Rate Configuration).

corresponding torsi

and to record the

Setting the

the temperature of

results. Theoretica

touching the center

practice this is not

flattened at the ape

the experimental err

the tac during the

projection of the co

rate. Before takin

the items and the

the manual

Prior to eve

turned on, allowing

clamp and reservoi

to the desired te

valve is completed by

valve - the top

the temperature bat

the components be attac

Before prepar

valve through an

is were not

fabric reservoir

corresponding torsion bar was used. An ultraviolet recorder was used to record the output signal.

Setting the correct gap between the cone and the plate at the temperature of measurements is extremely important for accurate results. Theoretically, the cone should have a perfect point touching the center of the flat plate during the measurements. In practice this is not possible to achieve. The cone is therefore flattened at the apex (tip) but the viscometer is designed so that the experimental error which results is negligible. The gap between the two during the measurements should be such that an imaginary projection of the cone to a point should touch the center of the plate. Before taking the data, the squareness and concentricity of the platens and the gap were adjusted according to the procedure given in the manual (I-1).

Prior to every run, the constant temperature bath was turned on, allowing the temperature chamber which enclosed the platens and reservoir (described later in the chapter) to heat up to the desired temperature of 30°C. The temperature was continuously sampled by a thermocouple placed in the thermocouple well located in the top platen. The test solutions were kept in a constant temperature bath at 30° ± 0.1°C for several hours prior to measurements to attain the desired temperature.

Before preparing the test solutions, the solvents were filtered through an ultra fine sintered glass filter. The test solutions were not filtered because of high viscosities. It was felt, in fact, necessary to filter the solutions for cone-and-plate

viscosity measureme

bubble-free sample

and then the top pl

setting.

The steady

highest shear rates

available range of

[possible] of the

and then increasing

repeated back to the

effect. The viscos

of speed to low sp

Reservoi

with evaporation w

of gas at the lip

flow of the platens.

tremendous increase

were used to minimize

it was inside the

to the "pool" o

as it may be have

that it was no

a drum was cover

between the

and to obtain

where the gas and

viscosity measurements (I-1). With a hypodermic syringe, 3 ml of bubble-free sample were placed on the lower platen in the center and then the top platen was lowered slowly to the required gap setting.

The steady state data were taken from the lowest to the highest shear rates attainable. Whenever possible, the widest available range of speeds (to cover as wide a range of shear rates as possible) of the gear box was used, starting with a low speed and then increasing to higher values. Occasionally, readings were repeated back to the lowest value of shear rate starting with the highest. The viscosity curves could be essentially retraced from high speed to low speed.

b. Reservoir chamber.--With the solvents used in this study, evaporation was severe. This caused gelling of polymer solutions at the lips of the platens and then skinning around the edge of the platens. This could be immediately observed by a tremendous increase in the output reading for the viscosity. It was tried to minimze the evaporation by creating an atmosphere of a solvent inside the temperature box enclosing the platens by leaving small pools of solvent in the temperature box. Williams (W-4) claims to have avoided evaporation by this method but in this study it was not very helpful. Finally, a reservoir chamber of aluminum was constructed to fit around the platens. Along with the gap between the platens, this chamber was also filled up with the test solution. This helped in preventing gelling and skinning around the gap and the viscosity measurements could easily be made.

igure 4.2 shows th

as also completely

c. Calibra

nstrument (mainly

ents on a series o

he Cannon Instrume

he ASTM oil standa

brations were w

he constants of th

Many differe

he performing light

ral for molecular

ht scattering sho

Photometer

e. Practice

ht source,

photon, photo-

ments were perfo

number of the ca

measures "PZ" -

ht beam are gi

Wyatt's Pro

Figure 4.2 shows the design of the chamber. The reservoir chamber was also completely surrounded by the temperature box.

c. Calibration.--Machine calibrations furnished with the instrument (mainly torsion bar constants) were tested by measurements on a series of Newtonian viscosity standards obtained from the Cannon Instrument Company (V-4). These standards conform to the ASTM oil standard. The viscosities obtained with the supplied calibrations were within the experimental error of 6 per cent. The constants of the instrument are given in Appendix A.

B. Light Scattering

Many different commercial instruments have been developed for performing light scattering measurements. The complete apparatus for molecular weight and other measurements consists of light scattering photometer and differential refractometer.

1. Photometer

a. Practice.--The photometer has four major components: (1) optical source, (2) scattering cell, (3) collection optics, and (4) photomultiplier-electronic recording equipment. All the measurements were performed with a Brice-Phoenix* light scattering photometer of the series 2000 located in a low humidity constant temperature (25° ± 1°C) room. Complete details of the instrument and operation are given in the Brice-Phoenix manual (B-10).

---

*Phoenix Precision Instrument Co., Vir Tis, Gardiner, New York 12525.

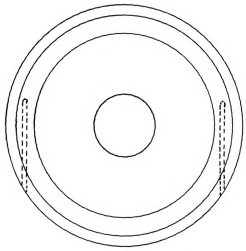

a

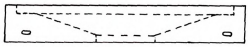

b

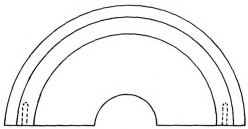

c

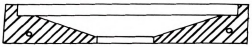

d

a. Plan.
b. Front elevation.
c. Plan of one-half of chamber.
d. Sectional elevation.

Figure 4.2.--Reservoir Chamber for Rheogoniometer.

No solvent

ight (4358 Å) was

ed using blue ligh

e pressure filtrat

The solutions were

thicknesses of 0.5

ter filters had

ere attacked filte

ers, a pore size s

imum volume neces

the measurements

portion of each s

rement, dr/dc, m

ed or to the abov

the external surface

of particles, smud

ring cell. If opt

ed is removed by w

ng is brushing

d as described

ed but for d

ing a gel remov

ving a sand remov

ed as possible

ore

No solvent was found to fluoresce appreciably when blue light (4358 Å) was used and hence all the measurements were carried out using blue light. The dry, distilled solvents were clarified by pressure filtration through ultra fine sintered glass filters. The solutions were clarified by double filtration through three thicknesses of 0.5 mircon Millipore* filters made up of Teflon. Teflon filters had to be used because some of the solvents used here attacked filters made up of other materials. In Teflon filters, a pore size smaller than 0.5 micron was not available. The minimum volume necessary for making the measurements was 30 ml. All the measurements were made in a cylindrical cell, C-101 (B-10). A portion of each solution was set aside for refractive index increment, dn/dc, measurements by a differential refractometer. In addition to the above precautions on the clarity of the solutions, the external surface of the cell was checked for the presence of dust particles, smudges, etc. by shining white light on the surface of the cell. If optically not clear, the surface was most effectively cleaned by wiping with an acetone-soaked, lint-free tissue, followed by brushing with an anti-static brush.

A brief description of the scattering measurements will be given here but for details, the manual (B-10) must be consulted. A full scale galvanometer deflection was obtained at 90° with all neutral filters removed. Then the shutter was closed and "dark current" zeroed if necessary. Then the highest galvonometer deflection possible was obtained at 0°, 45°, 50°, and then at 10°

---

*Millipore Corporation, Bedford, Massachusetts.

intervals up to 130

he beam as require

reverse order endin

readings at each of

measurements the ra

rometer reading a

rtance of the neu

ach non-zero angle

ated. The above

nd solvents.

When using

ent is different fr

is used. A

ment was according

n equation for obta

ent data is given

In principle

d the scattere

ment, while us

ment of is consid

ments is no more t

or less time...

In calibrat

ber of the amount

ments at an examp

the ments are amo

intervals up to 130° and finally at 135° with neutral filters in the beam as required. The measurements were then repeated in the reverse order ending at 0°. Thus, a total of two galvonometer readings at each of the 12 angles were obtained. For each of the measurements the ratio, G_θ/F_θ was calculated where G_θ is the galvanometer reading at angle θ and F_θ is the product of the transmittance of the neutral filters used for that angle. Finally, for each non-zero angle, an average value of $(G_\theta/F_\theta)/(G_0/F_0)$ was calculated. The above procedure was carried out for all the solutions and solvents.

When using the cylindrical cell the beam geometry to be used is different from that when the standard rectangular cell, T-104, is used. A calibration factor for the new geometry was determined according to the procedure given in the manual (B-10). An equation for obtaining Rayleigh ratio, R_θ, from the light scattering data is given in Appendix D.

In principle the data should be corrected for depolarization of the scattered light induced by the anisotropically polarized molecules. While usually appreciable with small molecules, this correction is considered to be negligible for high polymers and amounts to no more than one per cent for molecular weights greater than 10,000 (0-4).

b. Calibration.--Most calibration procedures consist of measuring the amount of light scattered by a known pure liquid. Benzene, as an example, has most frequently been used as a result of the intensive amount of study on the absolute scattering of this

'ould (P-3, B-11,

'ormatsu and Palme

ervation of light sc

In this wor

eriodically calibr

ade by using benze

:: ..on Carbide Co

ported the validi

anual (B-10) also

'andard method. S

ers Oil Corporation

e molecular weights ar

ers within 6 per ce

benzene, P_{95}, was

e value was obtained

measured values comp

ntrifugally and

Thus, the P_{95}

ompared with the

Experimental Ref

Experime

ers were obtained

ecimens a specimen

the same sa

ers of Certi

liquid (P-3, B-11, C-1). Kratohvil et al. (K-6, K-7) and Tomimatsu and Palmer (T-1) have reported extensive work on calibration of light scattering instruments.

In this work the opal glass method (B-10) was used to periodically calibrate the instrument and then frequent checks were made by using benzene and fresh solutions of standard PS supplied by Union Carbide Corporation.* Tomimatsu and Palmer (T-1) have reported the validity of this method after a careful study. The manual (B-10) also strongly recommends the opal glass-working standard method. Standard polystyrene samples supplied by Union Carbide Corporation were used in benzene and MEK to measure the molecular weights and in repeated measurements the values obtained were within 8 per cent of the supplied values. The Rayleigh ratio of benzene, R_{90}, was measured periodically using the blue light and the values obtained were between 48.5×10^{-6} to 49.2×10^{-6}. The reported values compiled in (K-6) are 48.5×10^{-6} by Brice et al. and Trossareli and Saini, and 48.2×10^{-6} by Doty and Steiner at 25°C. Thus, the R_{90} values obtained in this study are in excellent agreement with the literature values.

2. Differential Refractometer

a. Review.--In order to determine reliable values of the molecular weights of polymers by light scattering, it is necessary to accurately measure the specific refractive index increment, dn/dc, since this quantity appears as a squared term in the optical

*Union Carbide Corporation, Bound Brook, New Jersey 08805.

onstant in Debye's

θ dc value be as l

ered by a polymer

his value. The si

ng on whether the

ower than that of

he results. For p

θ dc encountered i

ow or above this

Since solut

ver or less, this

ecause the refract

the third or hig

ver capable of det

ent is far less t

measure absolute

ers measure only

ion or and that

ch we a different

Fract

parameters are

microscope, and

ay to be

e that above

ering a limi

constant in Debye's equation, Eq. 3.20. It is desirable that the dn/dc value be as large as possible since the amount of light scattered by a polymer solution is also proportional to the square of this value. The sign of dn/dc may be positive or negative depending on whether the refractive index of the polymer is higher or lower than that of the solvent; however, the sign is unimportant to the results. For polymer solutions, the usual range of values of dn/dc encountered is 0.08 to 0.22 dl/gm, though occasionally values below or above this range may be observed.

Since solutions are usually at concentrations of one per cent or less, this means that one is dealing with the difference between the refractive index of a solution and that of a solvent in the third or higher decimal place and this requires a measurement capable of detecting changes of the order of 5×10^{-6} units, which is far less than can be obtained with the instruments designed to measure absolute refractive indices. Consequently, instruments which measure only the difference between the refractive index of a solution and that of a solvent are necessary. These instruments are called differential refractometers.

b. Practice.--The five basic components of a differential refractometer are (1) optical source, (2) adjustable slit, (3) cell, (4) microscope, and (5) micrometer. For the measurements in this work, a Brice Phoenix Differential Refractometer Model BP-2000-V was used. When carefully calibrated, this instrument is capable of achieving a limiting sensitivity of about three units in the

sixth decimal place

detailed descriptio

operation procedure

for ordinar

still having a rem

In the case of more

ever, a means to pr

the two compartment

the solvent will re

ator, and unless

from the solution,

ve was encountered

e removable cover

ch is produced

ion of the direct c

ring a solution of

ne rate tests p

ake out, or

ssed unless wa

ly a

the compartments

ing test ce

compartments

ompartments.

The cell charg

ers as we descri

sixth decimal place of refractive index difference (B-12). A detailed description of the instrument and the calibration and operation procedures are given in the manual (B-13).

For ordinary liquids having relatively low vapor pressures, a cell having a removable cover plate may be used with confidence. In the case of more volatile liquids like the ones used here, however, a means to prevent mixing of solvent and solution kept in the two compartments of the cell must be assured. With such liquids, the solvent will readily creep up the edges of the cell by capillary action, and unless an impenetrable barrier separates the solvent from the solution, dilution of the solution will occur. This problem was encountered when using benzene and MEK in the cell with the removable cover plate. Contact between the cover glass and cell-rim produced immediate "wetting" around the entire rim, thereby furnishing direct contact between the solvent and the solution and causing dilution of the latter. Various cells have been devised to eliminate this problem, with most of them having either a mercury seal (O-5) or a permanent top. One of the latter types with all-fused joints was used. This type of cell has a quarter-inch thick permanently fused top having a tapered hole opening into each of the compartments. The holes can be stoppered with small penny-head round glass stoppers. The capacity of the cells is 2 ml per compartment with 1-1.5 ml being sufficient for performing the measurements.

The calibration constants are principally dependent upon the relative positions of the various optical components,

particularly that

the telescope. For

and should not be

necessary. If the

necessary.

c. Calibra

rence to standard

m sucrose or sodi

ensive tables of

found in the litera

oride solutions

made at 25° ± 1°C u

of potassium chlori

es

Reagent gra

ware. Yours and

ion before weighi

ermentation and

in U.S. Bolt, w

as necessary to mi

fermentation ve

t least or register

ar value to ver

required before and

in the same settings

particularly that of the cell and projection lens with respect to the telescope. For this reason the cell, once calibrated, was not and should not be removed from the cell block unless absolutely necessary. If the cell is removed for any reason, recalibration is necessary.

c. Calibration.--The instrument may be calibrated by reference to standard solutions. References most frequently employed are sucrose or sodium chloride or potassium chloride solutions. Extensive tables of refractive index data for these solutions are found in the literature (B-14, K-8). In this study potassium chloride solutions were used. All calibration measurements were made at 25° ± 1°C using the blue (4358 Å) light. Tabulated data of potassium chloride solutions given in the manual (B-13) were used.

Reagent grade potassium chloride was dried at 100°C for several hours and cooled over magnesium perchlorate in a desiccator before weighing. Four solutions covering a broad range in concentration and having values of concentration close to those of Kruis (K-8, B-13) were prepared using conductivity water. This was necessary to minimize errors in the interpolation of the graph of concentration versus refractive index difference, Δn. The calibration constant, k, obtained with 4358 Å was 1.0246×10^{-3} for k equal to $\Delta n/\Delta d$ where Δd is the difference in the deviations produced before and after the rotation of the cell and corrected for the deviations produced by the solvent alone. Thus,

$$dn/dc = k$$

where the subscript

cate and the super

[illegible] The results

the calibration val

polystyrene samples

period of several m

measurements was (c

of agreement with t

C. Measure

[illegible] const

[illegible] photomet

[illegible] prepared for

[illegible] Gate for ear

[illegible] refractometer

[illegible] filtered

[illegible] water

[illegible] DC vert

[illegible] read [illegible] was re

[illegible] of a solut

[illegible] 2244

[illegible] from the

[illegible] or DC, wa

$$dn/dc = k\,\frac{\Delta d}{c} = \frac{1.0246 \times 10^{-3}}{c}\,[(d_2 - d_1) - (d_2^0 - d_1^0)] \quad (4.1)$$

where the subscripts refer to the positions of the lever on the cell table and the superscripts refer to pure solvent (see manual, Ref. B-13). The results are also shown in Appendix C. As a check on the calibration value, solutions of two different Union Carbide polystyrene samples in benzene were used for measurements over a period of several months. The average value obtained from the measurements was (dn/dc) equal to 0.116 for 4358 Å light showing an agreement with the I.U.P.A.C. value (F-12).

d. Measurements.--The refractometer was kept in the same low humidity, constant temperature (25° ± 1°C) room as the light scattering photometer. The measurements were made on the solutions prepared for light scattering measurements after the scattering data for each solution were collected. The solution side of the refractometer cell was rinsed thoroughly with the solution to be used, filled and allowed to reach temperature equilibrium by circulating water at 25° ± 0.1°C in the temperature box surrounding the cell. Solvent was kept in the other half of the cell. At least three readings were taken for each position of the cell. From the Δd value of a solution, Δn could be calculated from

$$\Delta n = 1.0246 \times 10^{-3}\ \Delta d. \quad (4.2)$$

inally, from the plots of Δn versus c, specific refractive index ncrement, dn/dc, was calculated for each polymer-solvent system.

A. Int

Relative vi

ity of the solut

w shear rates

ented solvents.

ental ons at 30°

e Huggins equatio

$$\eta_{sp}/c = [\eta]$$

Figures 5.1

CAN 5-7, 5

ues. Intrin

ases with

from the

from the

CHAPTER V

PRESENTATION OF EXPERIMENTAL DATA

A. Intrinsic Viscosities and Huggins Constants

Relative viscosity, η_r, is defined as the ratio of the viscosity of the solution to that of the solvent. Relative viscosities at low shear rates were measured for all of the polymers in the selected solvents. Measurements were made for different low concentrations at 30° ± 0.01°C. The data were treated according to the Huggins equation,

$$\eta_{sp}/c = [\eta] + k_1[\eta]^2 c. \qquad (5.1)$$

Figures 5.1 to 5.6 show the Huggins plots for PS-1, PS-2, SAN C-1, SAN C-2, SAN C-2' and SAN C-3, respectively, in the solvents used. Intrinsic viscosity, $[\eta]$, in each case was determined by extrapolation to zero concentration and the Huggins constant, k_1, from the slope. The results are presented in Table 5.1. The diagrams show that all the data lie on straight lines, as expected at low concentrations.

From the values of $[\eta]$, the trend of the "degree of goodness" of solvents for different polymers can be seen clearly; the best solvents yielding the highest intrinsic viscosity and vice versa.

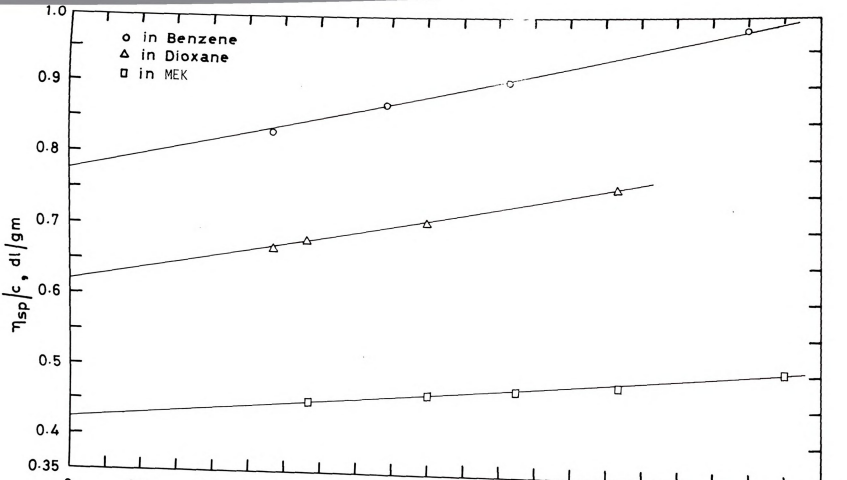

Figure 5.1.--Ratio of Specific Viscosity to Concentration, η_{sp}/c, vs. c for PS-1 in Benzene, Dioxane and MEK at 30°C.

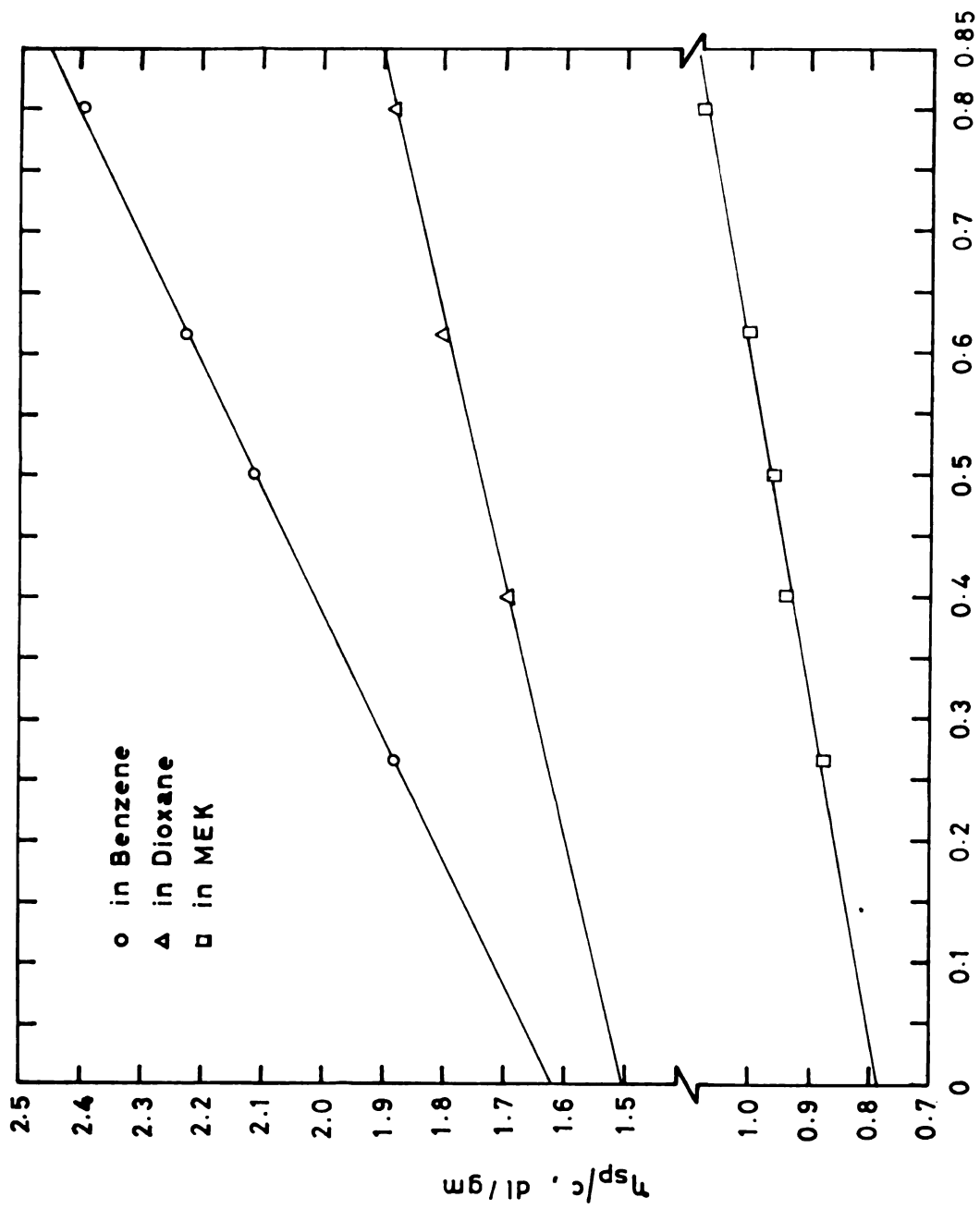

Figure 5.2.--Ratio of Specific Viscosity to Concentration, η_{sp}/c, vs. c for PS-2 in Benzene, Dioxane and MEK at 30°C.

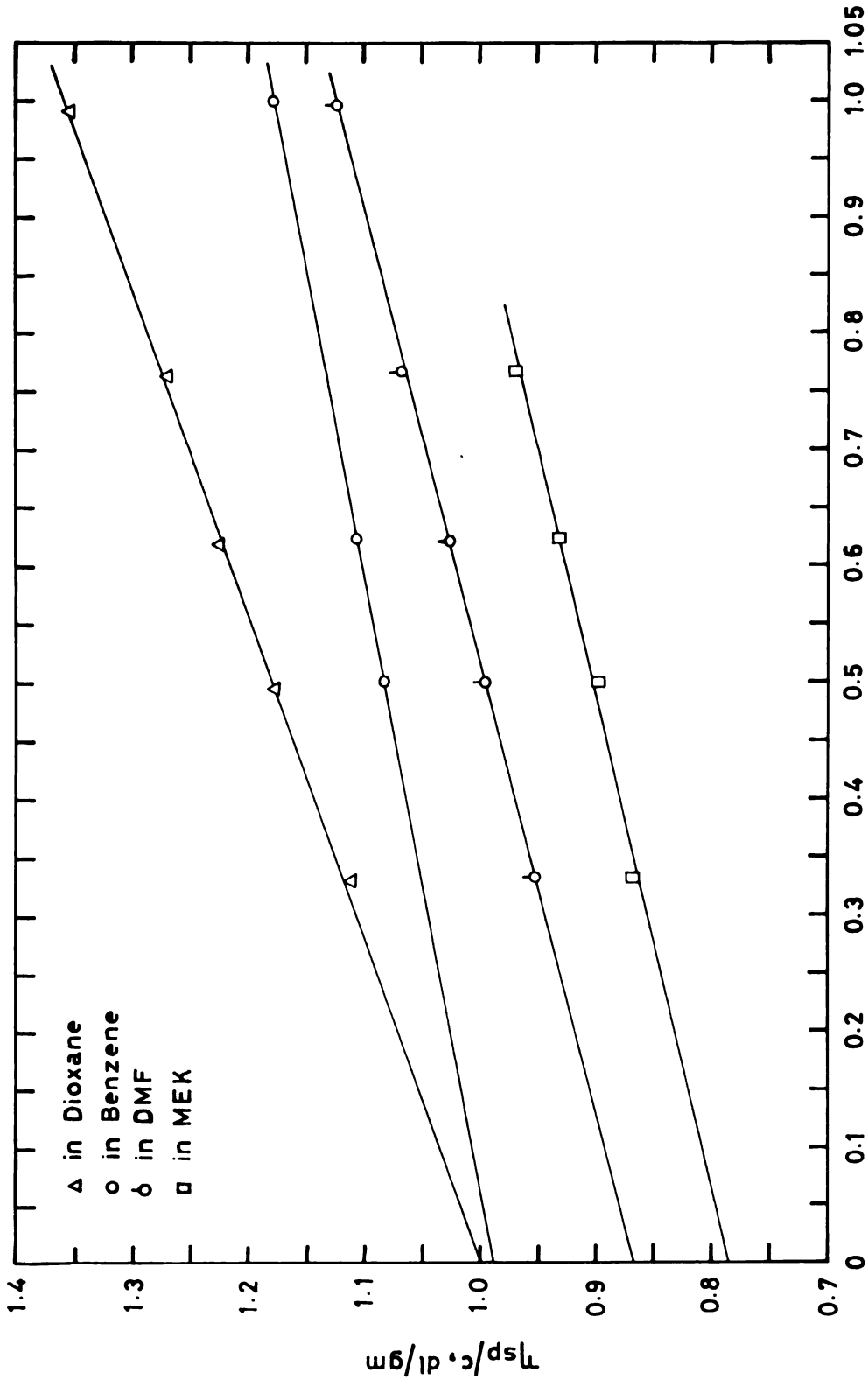

Figure 5.3.--Ratio of Specific Viscosity to Concentration, η_{sp}/c, vs. c for SAN C-1 in Dioxane, Benzene, DMF and MEK at 30°C.

Figure 5.4.--Ratio of Specific Viscosity to Concentration, η_{sp}/c, vs. c for SAN C-2 in DMF, Dioxane, MEK and Benzene at 30°C.

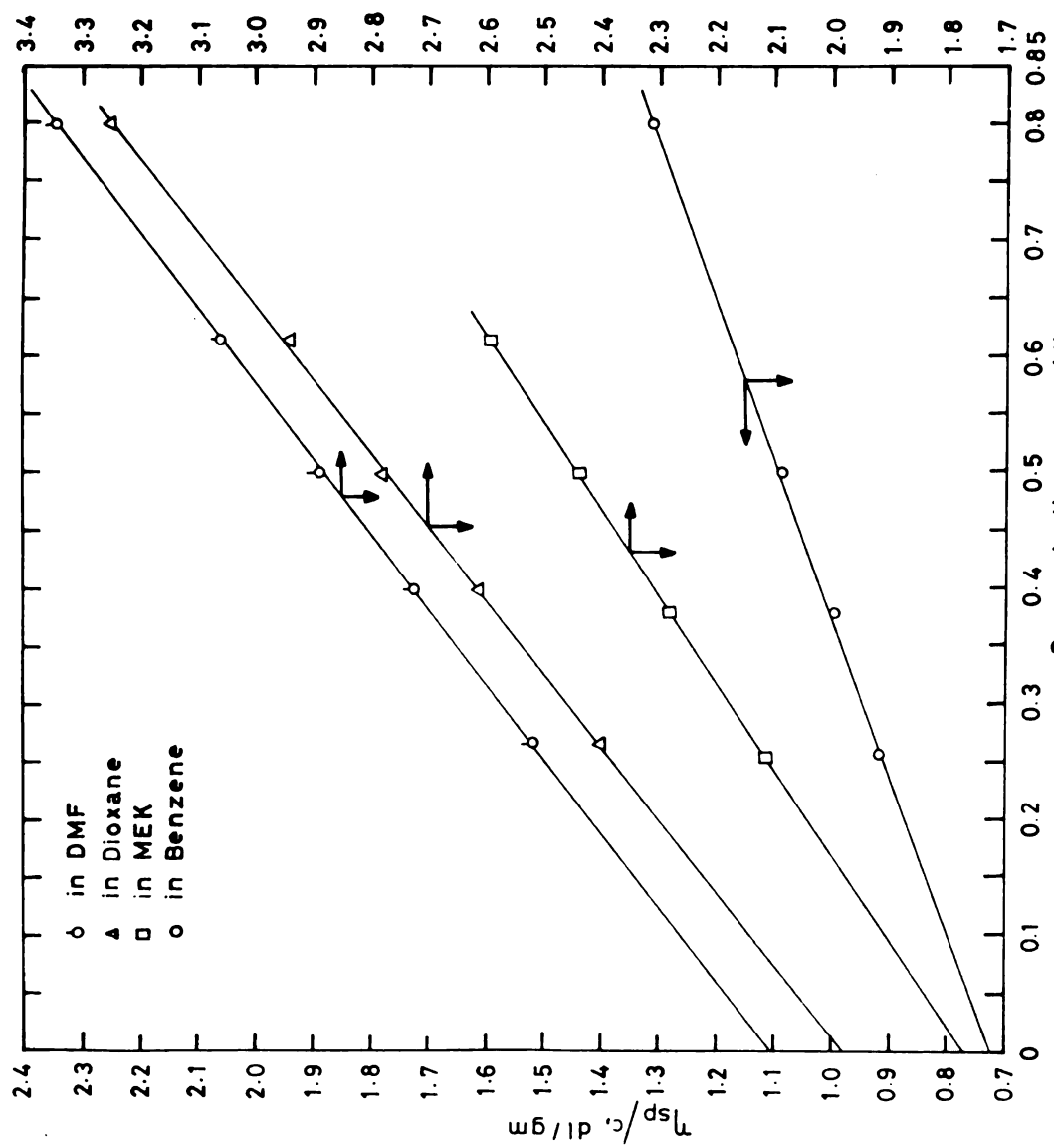

Figure 5.5.--Ratio of Specific Viscosity to Concentration, η_{sp}/c, vs. c for SAN C-2 in DMF, Dioxane, MEK and Benzene at 30°C.


2.8
2.7
2.6
2.5

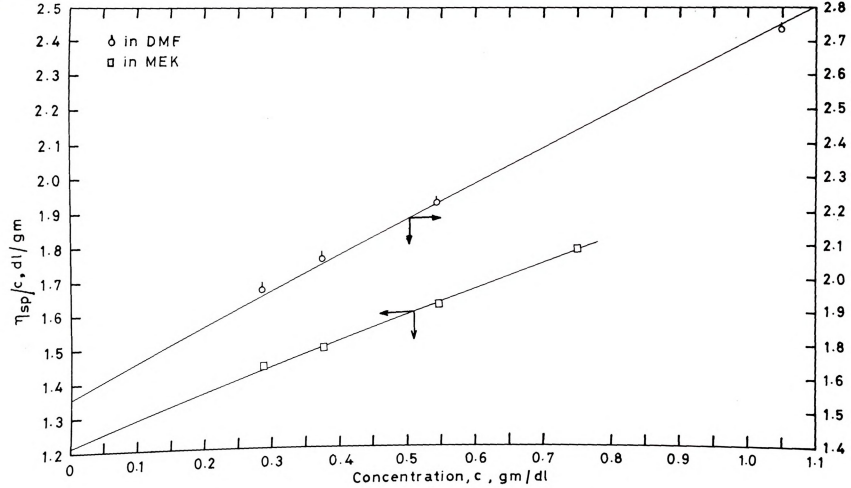

Figure 5.6.--Ratio of Specific Viscosity to Concentration, η_{sp}/c, vs. c for SAN C-3 in DMF and MEK at 30°C.

TABLE 5.1.--Intrin
of Pol

Polymer

TABLE 5.1.--Intrinsic Viscosities, $[\eta]$, and Huggins Constants, k_1, of Polymers in Various Solvents at 30°C.

Polymer	Solvent	$[\eta]$, dl/gm	k_1
PS-1	Benzene	0.782	0.33
	Dioxane	0.622	0.47
	MEK	0.433	0.34
PS-2	Benzene	1.619	0.38
	Dioxane	1.503	0.21
	MEK	0.785	0.58
SAN C-1	Dioxane	1.007	0.34
	Benzene	0.988	0.20
	DMF	0.867	0.34
	MEK	0.783	0.40
SAN C-2	DMF	0.862	0.34
	Dioxane	0.816	0.37
	MEK	0.742	0.38
	Benzene	0.446	0.86
SAN C-2'	DMF	2.110	0.35
	Dioxane	1.987	0.40
	MEK	1.776	0.42
	Benzene	0.725	1.40
SAN C-3	DMF	1.653	0.40
	MEK	1.219	0.51

A peculiar but interesting behavior was observed in the case of PS-DMF solutions. When a film of PS-DMF solution of any concentration came in contact with air, it immediately formed a dry, powdery, non-sticky film of PS. This presented problems in the measurements of viscosities. Because of this strange behavior, no viscosity measurements were made with the PS-DMF solutions.

B. Cone-and-Plate Viscosities

Steady state cone-and-plate viscosity data, $\eta(\dot{\gamma})$, are presented in Appendix B. The viscometric curves, viscosity, η, versus

shear rate, $\dot{\gamma}$, are

ions, for several

concentrations. F

ar weight polymer

e extended very f

f the machine lim

ear instability.

meter. The visc

meter used in

the subscribed value

ers have a prec

ed a wobble in t

measurements on st

without heating wa

been stopped oper

of ers. It was

s (i.e. and had n

or rock i ase sw

e an essential

the steady

e appears

ers on addressi

s rich, the atte

ermore, a commo

...ability that
...ments (Ref.

shear rate, $\dot{\gamma}$, are presented in Figures 5.7 to 5.9, as illustrations, for several polymers in different solvents at several concentrations. For many systems, particularly for lower molecular weight polymers and lower concentrations, the data could not be extended very far into the non-Newtonian region either because of the machine limit on available shear rates or because of the flow instability. The flow instability is discussed later in the chapter. The viscosities of standard oils* measured with the viscometer used in this work were found to be within 6 per cent of the supplied values. This means that the viscometric curves should have a precision of about 6 per cent. There was no appreciable wobble in the rotating cone at higher speeds. From the measurements on standard oils, it could be concluded that viscous heating was not a problem except for a slight heating during prolonged operation at high shear rates and for high viscosity solutions. It was easy to avoid, however, by recording the data rapidly, and had no influence on the results. No shear degradation took place over the time of testing and the viscosity curves could be essentially retraced from high speed to low speed.

One difficulty was experienced with the measurements on polymer solutions. A flow instability developed at higher shear rates which effectively placed an upper limit on the shear rates that could be attained with a given sample. This problem is apparently a common one for viscoelastic fluids in cone-and-plate

---

*Supplied by Cannon Instrument Company, State College, Pennsylvania 16801.

10^2
10
Intensity, n. doses

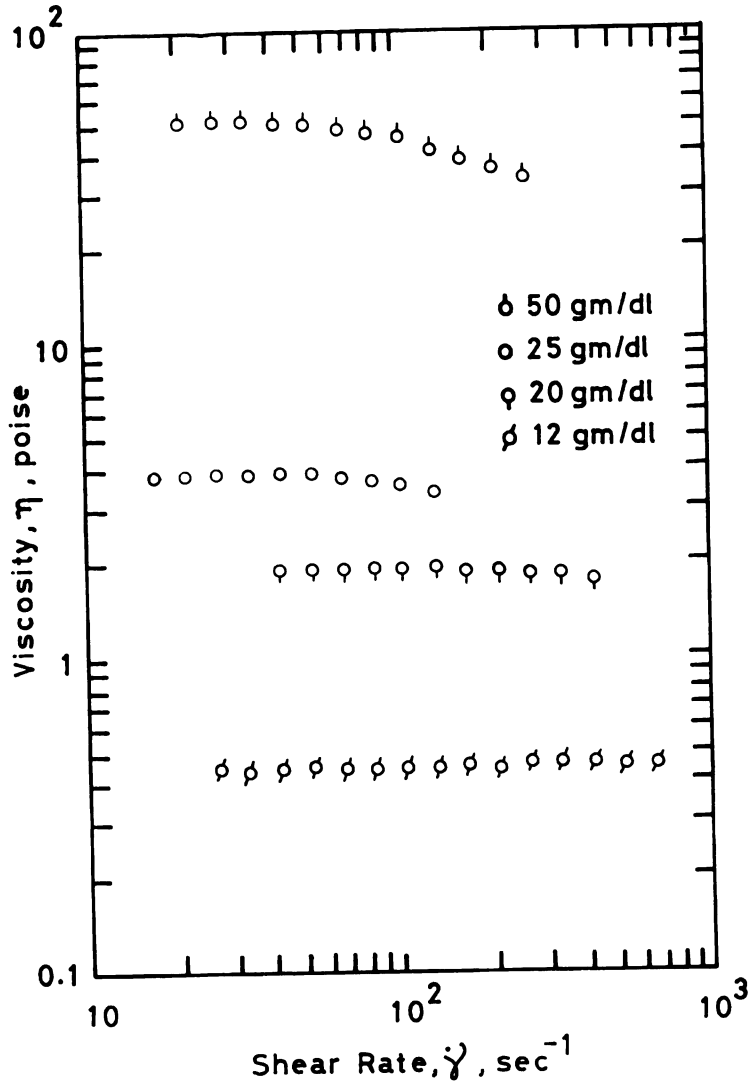

Figure 5.7.--Viscosity, η, vs. Shear Rate, $\dot{\gamma}$, for PS-1 in Dioxane at 30°C.

0.4
10^2
10
3
4
0.2
40
10
4
2

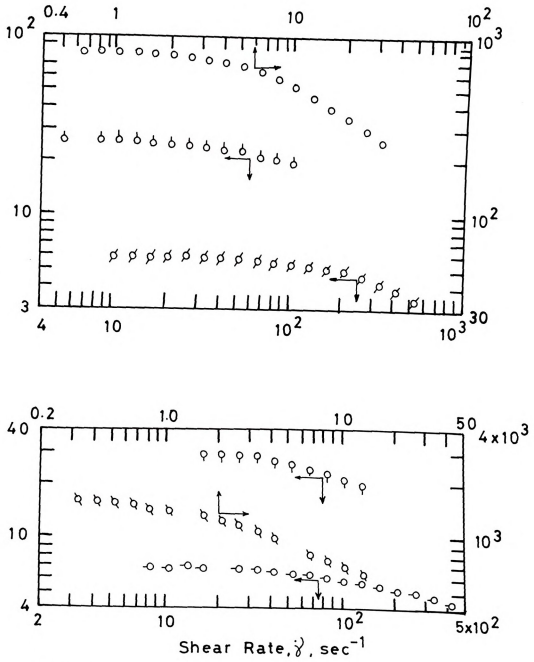

Figure 5.8.--Viscosity, η, vs. Shear Rate, $\dot{\gamma}$, for SAN C-2' in Benzene and Dioxane at 30°C.

Fig
for SAN C-3

Figure 5.9.--Viscosity, η, vs. Shear Rate, $\dot{\gamma}$, for SAN C-3 in MEK and DMF at 30°C.

In MEK	In DMF
○ 35 gm/dl	⌀ 50 gm/dl
⌀ 20 gm/dl	⌀ 35 gm/dl
	⊖ 20 gm/dl
	⊖ 10 gm/dl

Viscosity, η, poise
2x10²
10²
10
4
0.4
6

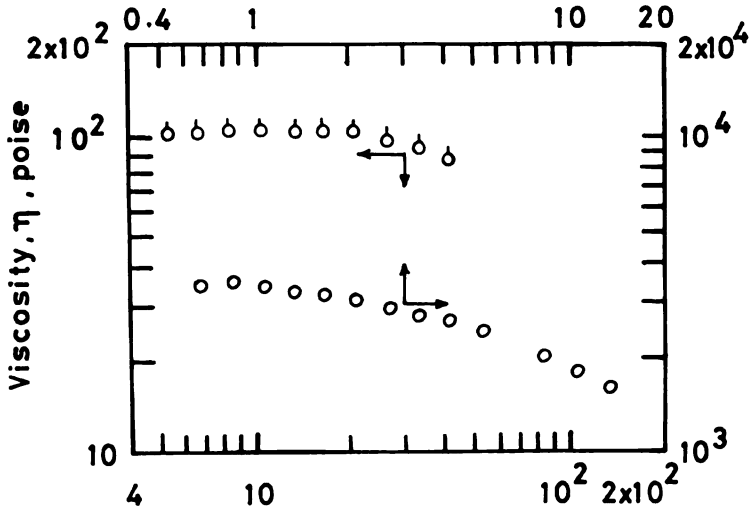
0.4
1
10
20
2x10^2
10^2
10
4
10
2x10^4
10^4
10^3
10^2
2x10^2
Viscosity, η, poise

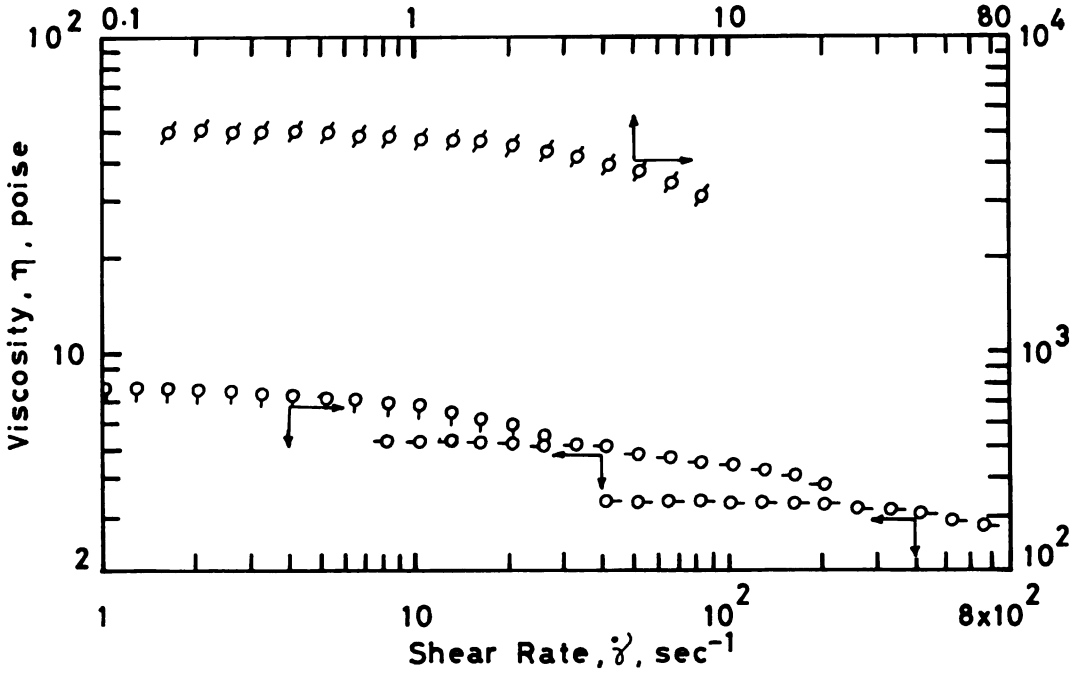
10^2
0.1
1
10
80
10^4
10
2
10^3
10^2
1
10
10^2
8x10^2
Viscosity, η, poise
Shear Rate, γ̇, sec^-1

nstruments (G-1,

ld erratically

ate at some loc

thers. The inst

ted by the pres

general, it wa

lowerian region

ther concentrat

rder by a sud

ce it seemed t

the rim, the b

ties as th

le to cast

rotational sp

meter used i

ere it n

rates sustai

s use a gra

meter w th

instruments (G-1, H-6, K-9, B-15). In the instability region the fluid erratically exuded from the gap between the cone and the plate at some locations on the rim and pulled back from the rim at others. The instability was probably deferred to higher shear rates by the presence of the reservoir filled with sample solution. In general, it was possible to penetrate deeper into the non-Newtonian region for higher molecular weight polymers and also for higher concentrations. The flow instability was indicated on the recorder by a sudden and erratic movement of the output signal. Since it seemed that this behavior was related to centrifugal forces at the rim, the behavior of Newtonian oils with the same range of viscosities as that of polymer solutions was examined. It was not possible to cast any of these fluids from the gap even at the highest rotational speed. The highest rotational speed for the viscometer used in this work corresponded to $\dot{\gamma}$ equal to 1674.3 sec^{-1}. This is not a very high shear rate in comparison to the shear rates obtainable in capillary viscometers for concentrated solutions. This implies that for high shear measurements one should use a different type of viscometer where, without encountering such problems, high shear rates are obtainable. A capillary viscometer with pumps is one example.

C. Refractive Index Increments

Table 5.2 presents the values of refractive indices, n_0, of the solvents used, at 25°C for the wave length of 4358 Å.

TABLE 5.2.--Refra
and 4

Sol
Ben
Dio
MEK
DMF
Ace
Dim

*From Ref

Hencefor

Table 5.3

TABLE 5.2.--Refractive Indices,* n_0, of Various Solvents at 25°C and 4358 Å.

Solvent	n_0
Benzene	1.5194
Dioxane	1.4297
MEK	1.3863
DMF	1.4406
Acetic anhydride	1.3970
Dimethylsulfoxide†	1.4903

*From Ref. (R-3) and n_0 of DMSO from Ref. (T-2).

†Henceforth referred to as DMSO.

Table 5.3 lists the refractive index increments, dn/dc, of the polymers in the above solvents at 25°C and 4358 Å.

Copolymer SAN C-3 was not soluble in benzene and dioxane and so acetic anhydride and DMSO were used for the light scattering measurements.

As indicated in Eq. 3.30 in Chapter III, for obtaining the true value of molecular weight of a copolymer, light scattering measurements must be done in at least three solvents. The values of dn/dc (i.e., ν_A and ν_B) must be known for the two homopolymers and for the copolymer (ν_0) in the same solvents. Of the solvents used in this work, PAN is soluble only in DMF, DMSO and acetic anhydride and hence the values of ν_B in benzene, dioxane, and MEK could not be obtained by direct experimentation. These values were

TABLE 5.3.--Refra
Vario

Polymer	Benzen
PS	0.114
AA C-1	0.096
AA C-2	0.085
AA C-2'	0.086
AA C-3	--
PAA	-0.008

*Values
*Values
Values
Values of
Values

TABLE 5.3.--Refractive Index Increments, dn/dc, of Polymers in Various Solvents at 25°C and 4358 Å.

Polymer	Benzene	Dioxane	MEK	DMF	Acetic Anhydride	DMSO
PS*	0.114	0.185	0.223	0.176	0.212	0.137
SAN C-1	0.0966	0.174	0.212	0.163	--	--
SAN C-2	0.0856	0.166	0.206	0.154	--	--
SAN C-2'	0.0866	0.167	0.207	0.155	--	--
AN C-3	--	--	0.196	0.140	0.184	0.0967
AN†	-0.0089	0.104	0.152	0.0809	0.138	0.030

*Values in acetic anhydride and DMSO were obtained from
q. 5.3.

†Values in benzene, dioxane and MEK were obtained from
q. 5.2.
Values in DMF, acetic anhydride and DMSO were calculated
om ν_0 values of SAN C-3 and using ν_A values of PS in Eq. 3.29,
ich is $\nu_0 = x_A\nu_A + (1 - x_A)\nu_B$.
Values in DMSO and DMF were obtained experimentally.

tained indirectly by an extrapolation procedure. From Eq. 3.29
Chapter III, we can show that

$$\nu_0 = bx_B + d \qquad (5.2)$$

re $x_B = 1 - x_A$ is the weight fraction of ACN in a copolymer and
nd d are constants characteristic of each solvent. Thus,
ording to Eq. 5.2, ν_0 values of different copolymers (contain-
different weight fractions of ACN) in a particular solvent
plotted against x_B should give a straight line. Figure 5.10


0.25

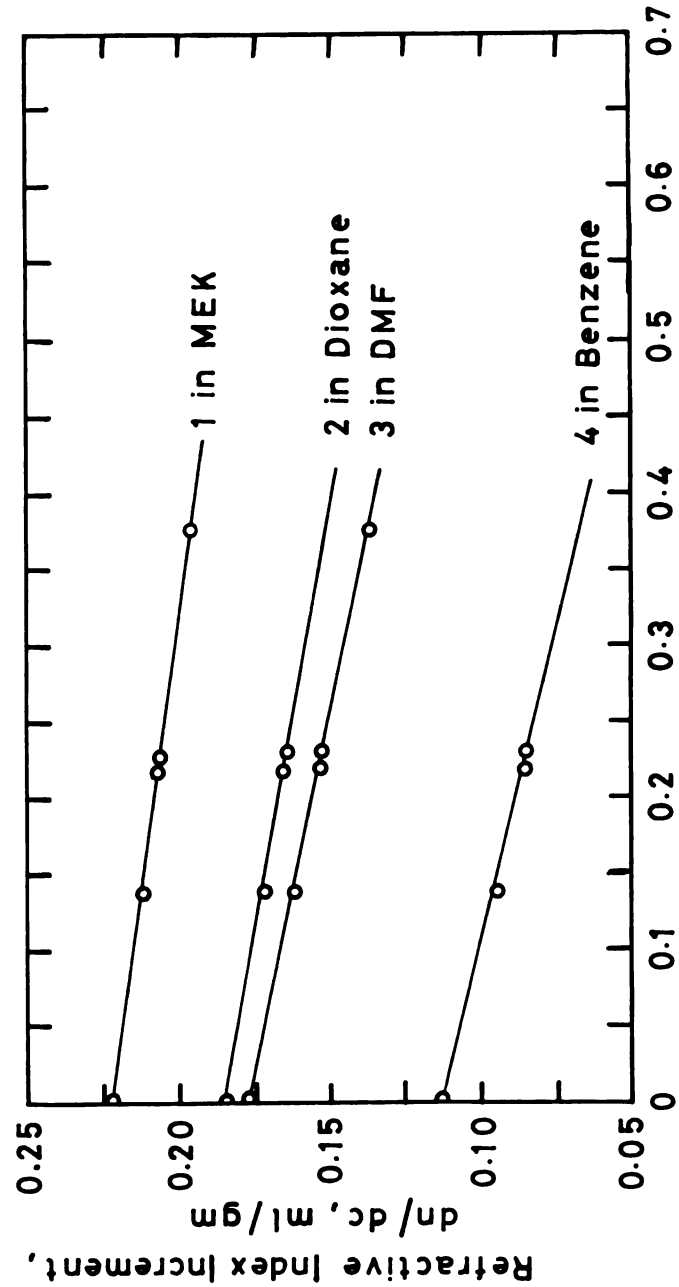

Figure 5.10.--Variation in Refractive Index Increment, dn/dc, of Copolymers in MEK, Dioxane, DMF and Benzene at 25°C as a Function of ACN Content.

shows such plots

and ϕ in differen

TABLE 5.4.--Value
Copol

Solve
Benze
Dioxa
MEK
DEF

om Fig. 5.2 and

an be easily cal

theoretical valu

ue" in DMF, are

in DMF is 0.08

Promotes value of

ers were was

Polystyren

ers were was

ue" in the ; val

ference the ; va

ers :

μ = -0.7

shows such plots in different solvents. Values of the constants b and d in different solvents are reported in Table 5.4.

TABLE 5.4.--Values of the Constants b and d (Eq. 5.2) for SAN Copolymers in Various Solvents at 25°C and 4358 Å.

Solvent	b	d
Benzene	-0.123	0.114
Dioxane	-0.0809	0.185
MEK	-0.0707	0.223
DEF	-0.0951	0.176

From Eq. 5.2 and Table 5.2, the values of ν_B in different solvents can be easily calculated for PAN by using x_B equal to 1. The hypothetical values of ν_B in benzene, dioxane and MEK, as well as that in DMF, are reported in Table 5.3. The extrapolated value of ν_B in DMF is 0.0809. This is in excellent agreement with the reported value of 0.08 (B-4a). The experimental value of ν_B in DMF in this work was found to be 0.083.

Polystyrene is not soluble in acetic anhydride and DMSO. Hence, ν_A values in these two solvents were obtained by interpolation. The ν_A values of PS in different solvents were plotted against the n_0 values of these solvents at 25°C and 4358 Å. Figure 5.11 is such a plot. The equation of the line in Fig. 5.11 is

$$\nu_A = -0.7996\ n_0 + 1.3291. \qquad (5.3)$$


o Experimental
x Interpolated
1 MEK

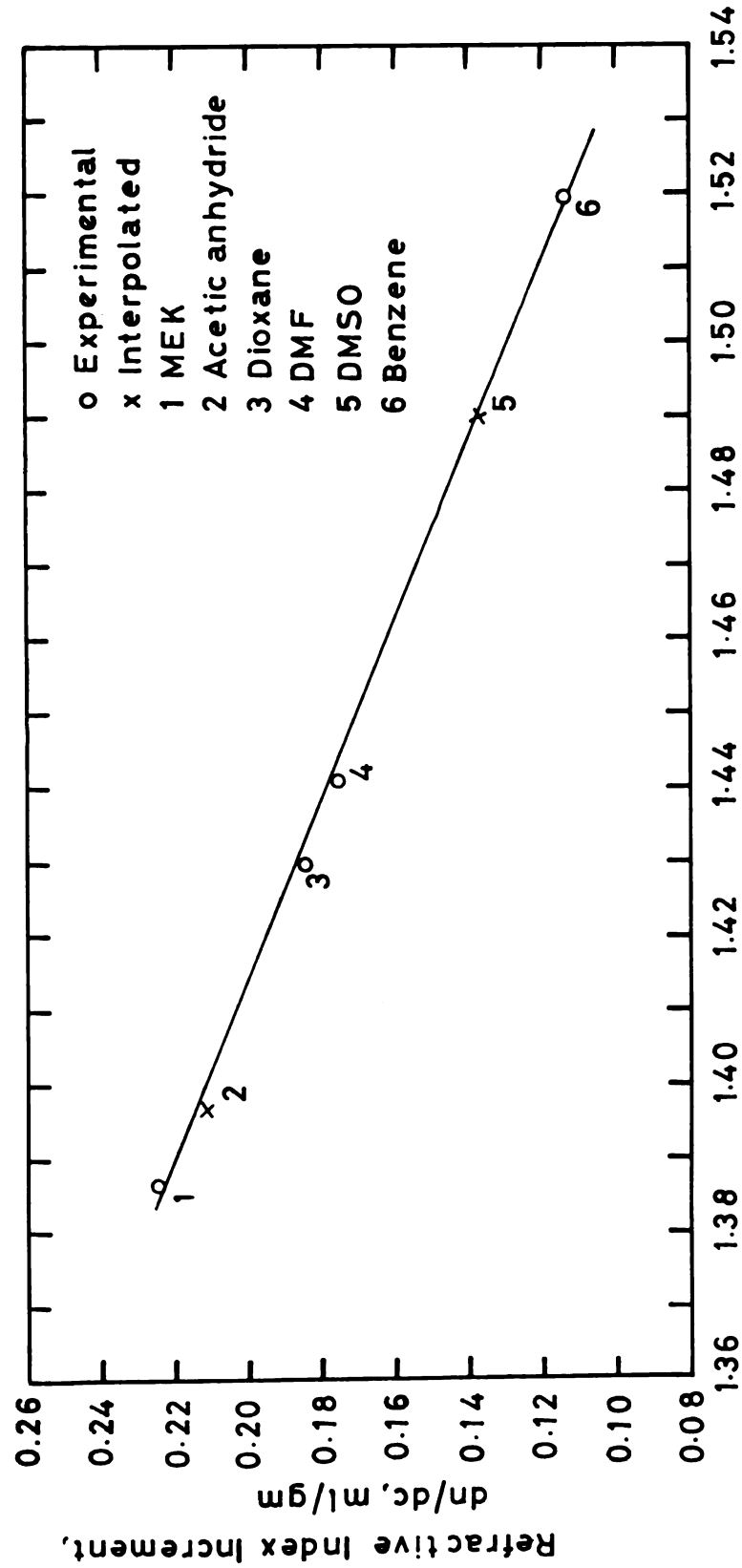

Figure 5.11.--Variation in Refractive Index Increment, dn/dc, of PS in Different Solvents at 25°C as a Function of Refractive Index, n_0, of Solvents.

from this equati

once the η_0 valu

the η_{sp} values in

for PS in acetic

of the copolymer

solvents can be

values are given

Figure 5.

the η_{sp} values.

a straight line.

[illegible] has shown t

[illegible] chloride ar

used by Kämmisch

[illegible] In thi

[illegible]

Figure 5.

[illegible] η_{sp} values

[illegible] the valu

[illegible] Cha

[illegible] and [illegible]

[illegible] number of va

[illegible]

[illegible] Mr.

[illegible]

[illegible] [illegible]

[illegible] [illegible]

[illegible] the scatter

From this equation, ν_A value in any other solvent can be calculated once the n_0 value of that solvent is known. Table 5.3 also lists the ν_A values in acetic anhydride and DMSO. Using the ν_A values for PS in acetic anhydride and DMSO and the experimental ν_0 values of the copolymer SAN C-3 in the same solvents, ν_B values in these solvents can be calculated by using Eq. 3.29 in Chapter III. These values are given in Table 5.3.

Figure 5.12 shows the ν_B values for PAN plotted against the n_0 values. It can be seen that the extrapolated values lie on a straight line. This renders confidence in the results. Klimisch (K-5) has shown the validity of this technique for copolymers of vinyl chloride and isobutylene. Some of the solvents that were used by Klimisch for the copolymers dissolved only one of the homopolymers. In this work also the interpolation technique was successful.

Figure 5.13 shows a plot similar to Figs. 5.11 and 5.12 where ν_0 values of different copolymers are plotted against n_0 values. The values plotted are for copolymers SAN C-1, SAN C-2 and SAN C-3. The values for SAN C-2' lie very close to those of SAN C-2, and hence are not plotted for clarity. These are all experimental values and they all lie on straight lines, as they should.

D. Molecular Weights and Second Virial Coefficients

The molecular weights and second virial coefficients of the polymers in different solvents were determined from Zimm plots of the light scattering data. The measurements were made at 25°C.


o Calculated from Eq. 5-2
x Experimental
□ From n.

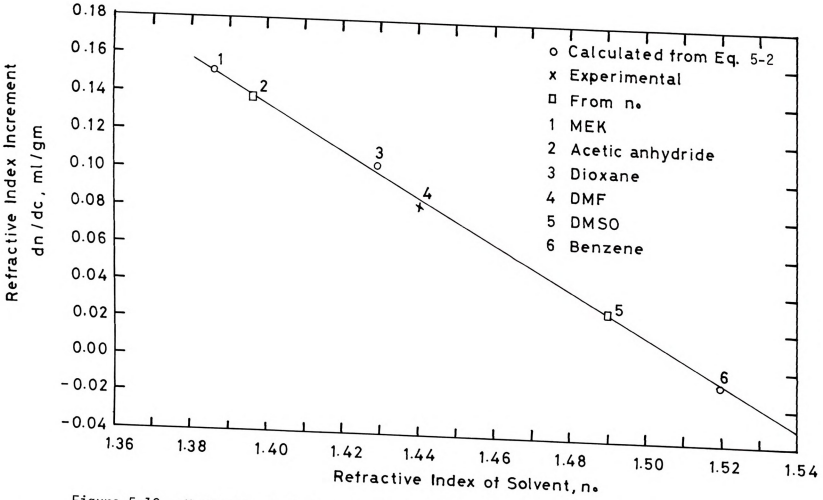

Figure 5.12.--Variation in Refractive Index Increment, dn/dc, of PAN in Different Solvents at 25°C as a Function of Refractive Index, n_0, of Solvents.


0.24
0.22
0.20
A SAN C-1
B SAN C-2
All experimental values
1 MEK

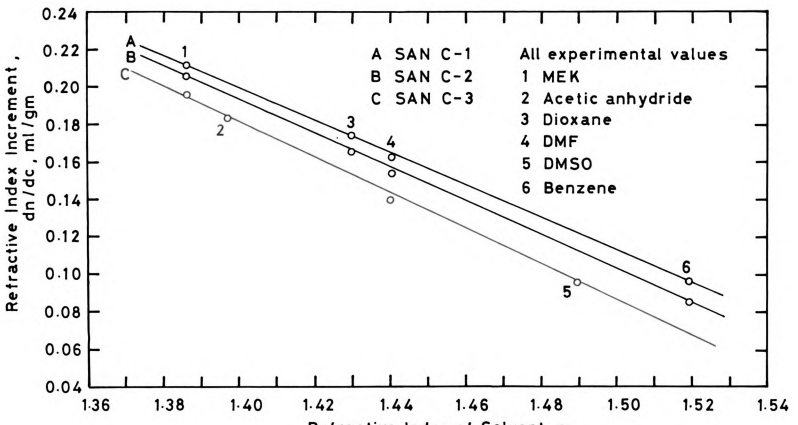

Figure 5.13.--Variation in Refractive Index Increment, dn/dc, of SAN C-1, SAN C-2 and SAN C-3 in Different Solvents at 25°C as a Function of Refractive Index, n_0, of Solvents.

The Zimm plots w

Reciproc

$(\sin^2(\theta/2) + Q_c$ a

were first drawn

extrapolated to

The points of co

best straight l

were drawn to a

which well repr

experimental err

The reciprocal o

average molecula

at weight, M_{app}

The slope

The coefficien

$B_2 = 2 \cdot$

The value of B_2,

Figure 5

From the Zi

The data

The zero

The

The

The Zimm plots were constructed according to the method of Zimm (Z-2). Reciprocal reduced intensities, Kc/R_θ, were plotted against $\sin^2(\theta/2) + q_c$ according to Eq. 3.24 in Chapter III. Straight lines were first drawn through the points of constant concentration and extrapolated to zero angle. Then straight lines were drawn through the points of constant angle and extrapolated to zero concentration. Next, straight lines through these two sets of extrapolated points were drawn to a common intercept on ordinate. All the data were fairly well represented by a linear extrapolation within the experimental error associated with the light scattering technique. The reciprocal of the intercept on the ordinate gives the weight average molecular weight, M_w, for homopolymers and apparent molecular weight, M_{app}, for copolymers. This is discussed in Chapter III.

The slope of the zero angle line is related to the second virial coefficient, A_2, by

$$A_2 = q \cdot (\text{Slope of the line } \theta = 0)/2. \qquad (5.4)$$

The unit of A_2, thus obtained, is $(\text{mole})(\text{cm}^3)/\text{gm}^2$.

Figures 5.14 to 5.17 show representative Zimm plots. Figure 5.16 shows the Zimm plot for the azeotropic copolymer, SAN C-2, in benzene. This plot is different from the others with respect to the order of the data points at different concentrations. Also, the slope of the zero angle line is negative, giving a negative value of A_2. This is due to the very nature of this copolymer-benzene interaction. This is discussed in Chapter VI. Also, for the azeotropic copolymer, SAN C-2', the Zimm plot for solutions in benzene

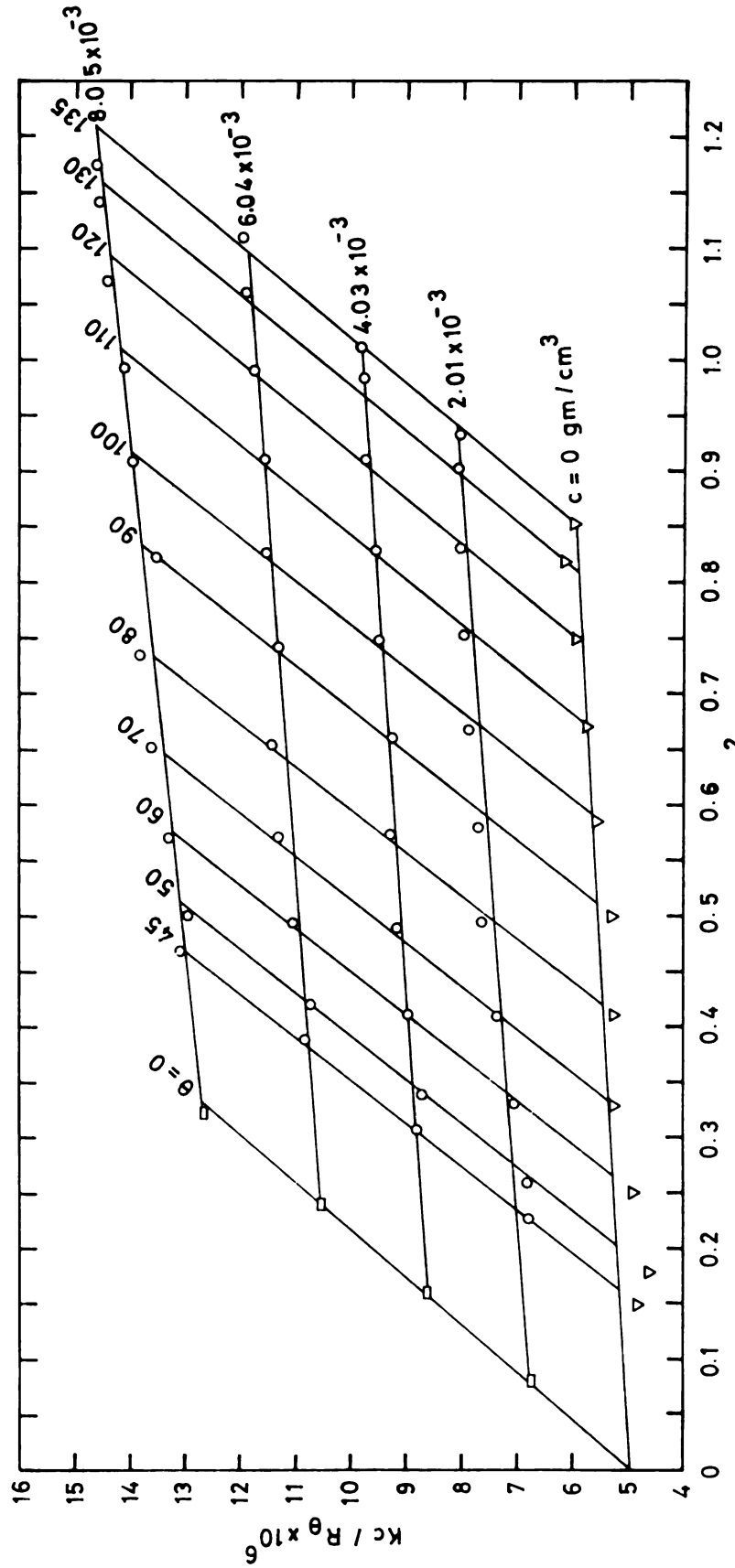

Figure 5.14.--Zimm Plot for PS-1 in Dioxane at 25°C.

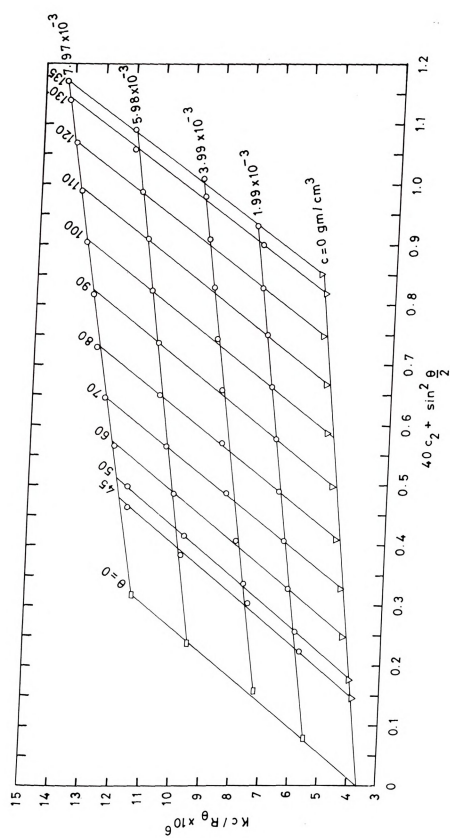

Figure 5.15.--Zimm Plot for SAN C-1 in DMF at 25°C.

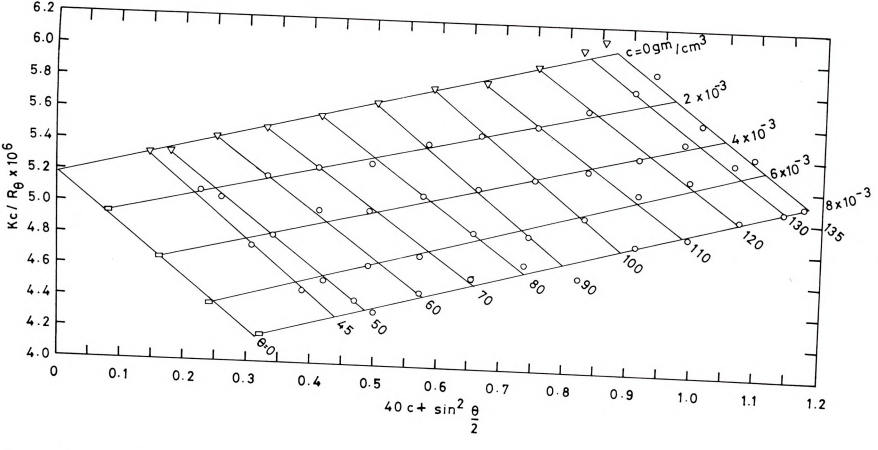

Figure 5.16.--Zimm Plot for SAN C-2 in Benzene at 25°C.

0.135
0.130
0.120
0.110
0.100
90
80

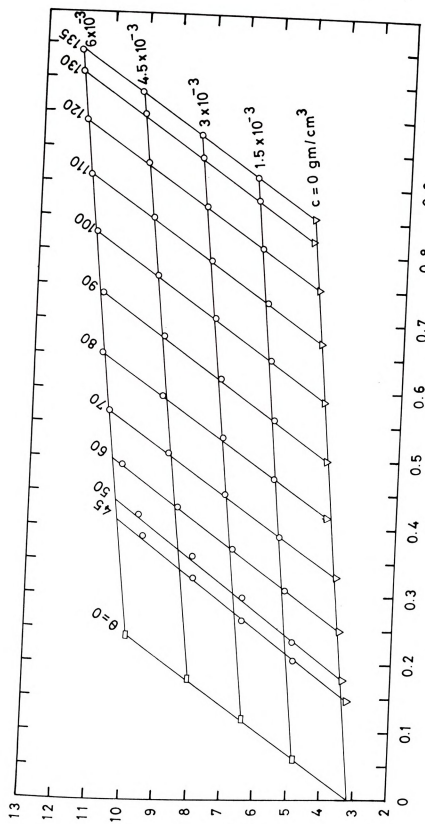

Figure 5.17.--Zimm Plot for SAN C-3 in MEK at 25°C.

similar. The Zi

solvents are "norma

solvent systems.

Table 5.5 g

solvents at 25°C.

TABLE 5.5.--Second V
Solvents

Polymer	
PC-1	
PC-2	
TAN C-1	
TAN C-2	
TAN C-2	
TAN C-3	
Film	
*Trom Pac	

is similar. The Zimm plots of azeotropic copolymers in other solvents are "normal" Zimm plots as in the cases of other polymer-solvent systems.

Table 5.5 gives the A_2 values of the polymers in different solvents at 25°C.

TABLE 5.5.--Second Virial Coefficient, A_2, of Polymers in Various Solvents at 25°C.

Polymer	Solvent	$A_2 \times 10^4$, (mole)(cc)/gm^2
PS-1	Benzene	5.64
	Dioxane	4.83
	MEK	1.73
PS-2	Benzene	5.71
SAN C-1	Dioxane	6.82
	Benzene	5.36
	DMF	4.80
	MEK	4.00
SAN C-2	DMF	6.92
	Dioxane	6.10
	MEK	5.70
	Benzene	-0.66
SAN C-2'	DMF	6.76
	Dioxane	6.00
	MEK	5.64
	Benzene	-0.68
SAN C-3	DMF	10.10
	MEK	5.66
PAN*	DMF	19.10

*From Ref. (K-10).

The values

ight scattering we

lists the value

ABLE 5.6.--Molecul
tering

Metho
GPC
L.S.
L.S.
L.S.
L.S.
Avera

The values of molecular weights, M_w, of PS obtained by light scattering were close to the values obtained by GPC. Table 5.6 lists the values of M_w of PS-1 obtained by the two methods.

TABLE 5.6.--Molecular Weight, M_w, of PS-1 from GPC and Light Scattering Measurements.

Method	$M_w \times 10^{-4}$
GPC	18.5
L.S. in Dioxane	20.0
L.S. in MEK	19.0
L.S. in Benzene	18.2
L.S. in DMF	19.1
Average by L.S.	19.1

Table 5.7 lists the values of M_{app} for the copolymers along with the values of refractive index increment, ν_0. For azeotropic copolymers, or more generally for low conversion copolymers of any composition, it is very likely that the composition variation with molecular weight or from molecule to molecule in a given polymer is negligibly small. This is true for the copolymers synthesized in this work and is clear from the M_{app} values in Table 5.7. The M_{app} values in different solvents for each copolymer are constant within the experimental accuracy. This leads to the assumption that

TABLE [illegible] Effects and of Molecular weights of Copolymers with Refractive Index Increments at 25°C.

TABLE 5.7.--Light Scattering and GPC Molecular Weights of Copolymers With Refractive Index Increments at 25°C.

Polymer	ν_0 = dn/dc						GPC	$M_{app} \times 10^{-4}$					
	Benzene	Dioxane	MEK	DMF	Acetic Anhydride	DMSO	$M_w \times 10^{-4}$	Benzene	Dioxane	MEK	DMF	Acetic Anhydride	DMSO
SAN C-1	0.0966	0.174	0.212	0.163	--	--	27.5	28.2	26.7	25	27.3	--	--
SAN C-2	0.0856	0.166	0.206	0.154	--	--	20.3	19.3	18	18	18.8	--	--
SAN C-2'	0.0866	0.167	0.207	0.155	--	--	63.4	62.0	66.6	66.6	65.8	--	--
SAN C-3	--	--	0.196	0.140	0.184	0.0967	33.2	--	--	31.8	36.3	33.3	30.2

$$P = 0$$

$$Q = M_w \sum_i f_i$$

$$x = \sum_i Y_i X_i$$

where x is the aver
of component 1, Y_i
molecular weight is
fraction of all the
the molecular wei
heterogeneity is ve
the experimental value
accuracy ($B-B_o$). Th
results are given in

Copolymer	

$$P = 0 \tag{5.6}$$

$$Q = M_w \sum_i f_i (x_i - x)^2 \tag{5.7}$$

$$x = \sum_i \gamma_i x_i \tag{5.8}$$

where x is the average composition of the sample in weight fraction of component 1, γ_i is the weight fraction of component i whose molecular weight is M_i and composition is x_i, and f_i is the weight fraction of all the components with composition x_i regardless of their molecular weights. Chapter III gives details. If composition heterogeneity is very small, measurements even in a single solvent with large ν_0 value would allow one to determine M_w with reasonable accuracy (B-8). The data were analyzed as mentioned above and the results are given in Table 5.8.

TABLE 5.8.--Light Scattering Molecular Weights, M_w, and Q/M_w of Copolymers.

Copolymer	$M_w \times 10^{-4}$	Q/M_w
SAN C-1	29	0.0003
SAN C-2	18	0
SAN C-2'	66.6	0
SAN C-3	33.2	0.00004

It can be s

tically zero for SA

copolymers these va

before, for small o

of azeotropic copol

with large v_0 value

ately (B-8). The

values obtained fro

The GPC values of M

values of M_{app} (see

E.

This section

ment: The estimate

values with the know

The viscosit

the viscometer

values reported in t

of intri

was ar

The viscosit

were fou

The reprodu

the shear

that the pe

It can be seen that the computed values of Q/M_w are practically zero for SAN C-1 and SAN C-3, while for the two azeotropic copolymers these values were assumed to be zero. As mentioned before, for small or no heterogeneity in composition as in the case of azeotropic copolymers, the measurements even in a single solvent with large ν_0 value would allow one to determine M_w quite accurately (B-8). The M_w values for the azeotropic copolymers are the values obtained from MEK solution since in MEK ν_0 is the highest. The GPC values of M_w are remarkably close to the light scattering values of M_{app} (see Table 5.7 for comparison).

E. Discussion of Experimental Accuracy

This section gives estimates of accuracy in different experiments. The estimates are based on the comparison of the experimental values with the known values of standards used in each experimental setup.

The viscosities of distilled water and benzene measured with capillary viscometers were found to be within 0.1 per cent of the values reported in the literature. The estimated error in the measurement of intrinsic viscosities is not more than 0.5 per cent. This estimate was arrived at by repeated measurements.

The viscosities of standard oils measured with the rheogoniometer were found to be within 6 per cent of the supplied values. The reproducibility of the η-$\dot{\gamma}$ curves when increasing or decreasing the shear rates was excellent and the deviations were not more than one per cent.

The error f

ncrement, dn/dc, w

d by repeated meas

benzene and compari

n us (F-12).

The error f

molecular weight of

ng and Zimm plot w

from the error invo

ncrement, dn/dc, s

equation (Eq. 3.20)

The error involved in the measurement of refractive index increment, dn/dc, was about 2 per cent. This estimate was arrived at by repeated measurements with standard polystyrene samples in benzene and comparing the experimental value with the I.U.P.A.C. value (F-12).

The error involved in the measurement of weight average molecular weight of standard polystyrene samples by light scattering and Zimm plot was about 8 per cent. Most of the error comes from the error involved in the measurement of refractive index increment, dn/dc, since this occurs as a squared term in the Debye equation (Eq. 3.20).

A

In this sec

nsion factor,

teraction parame

ent quality for th

ment of the poly

Intrinsic Visco
sion Factor

Intrinsic v

n determination o

ion of the its ca

ation might seem

measurements can

the property of

the property of

ion of a polym

ion of solvents

on is used by many

y many labs to evalu

of the same MS dep

CHAPTER VI

RESULTS AND DISCUSSION

A. Thermodynamics and Configuration of Polymer Chains

In this section a discussion of intrinsic viscosity, [η], expansion factor, α, second virial coefficient, A_2, and the Flory interaction parameter, χ_1, is given in order to establish the solvent quality for the polymers. Also, the effect of copolymer ACN content on the polymer chain stiffness is discussed.

1. Intrinsic Viscosity and Expansion Factor

Intrinsic viscosity measurements are most commonly made for the determination of the mass and the size of the polymer molecules in solution. It can also contribute thermodynamically significant data. It might seem strange at first that intrinsic viscosity measurements can give thermodynamic information of a system, which is the property of a system in equilibrium, while actually viscosity is the property of a system in flow, a non-equilibrium state. The viscosity of a polymer solution depends on the size of its molecules in dilute solutions and the size in turn depends on the nature of the solvent by way of its goodness for the polymer in question. The polymer chains expand or swell in solutions and the extent of expansion or swelling depends on the intermolecular polymer-solvent

hermodynamic forc

n Chapter III.

Table 5.1

ferent solvents at

olymer molecules

articular polymer

olymer. It can be

lected solvents,

cetone and MEK, in

olvent followed by

ylonitrile (SAN C-1 c

of the AcN units ha

mpared to the ord

non-solvent for p

decreases the goodn

ecipient or of an un

In acetone there is

presence of two sym

ranges, a through w

acetone molecules.

the chains is not sep

of the same. In

acetone from SAN C-1

the polymer. Again,

ones than MEK, a

acetone is an excel

thermodynamic forces. A discussion of intrinsic viscosity is given in Chapter III.

Table 5.1 lists the values of [η] of the polymers in different solvents at 30°C. Since [η] depends on the size of the polymer molecules in solution, the higher the value of [η] for a particular polymer in a solvent, the better is that solvent for that polymer. It can be seen from the values of [η] that among the selected solvents, benzene is the best solvent for PS followed by dioxane and MEK, in that order. For SAN C-1, dioxane is the best solvent followed by benzene, DMF and MEK, in that order. The copolymer SAN C-1 contains 14.2 per cent ACN by weight. The presence of the ACN units has brought about the change in solvent power as compared to the order of the solvent power for PS. Since benzene is a non-solvent for PAN, the presence of ACN units in this copolymer decreases the goodness of benzene despite the presence of a large proportion of ST units. Dioxane also is a non-solvent for PAN but in dioxane there is a localized separation of charges due to the presence of two symmetrical oxygen atoms. This separation of charges, although weak, creates polar forces between ACN and dioxane molecules. This effect is absent in benzene since in benzene there is no separation of charges. Methyl ethyl ketone is a polar solvent. In spite of this, it is poorer than dioxane or benzene for SAN C-1 due to the large amount of ST content in that copolymer. Again, for PS, benzene and dioxane are much better solvents than MEK, and also MEK is a non-solvent for PAN. Dimethylformamide is an excellent solvent for PAN. Thus, the presence of

ACN units in the co

but the amount of A

ORF a better solver

In the SAN

reversal in the deg

from the [+] values

is weight. Apparen

benzene the poorest

the solvents in ter

cetone, MEK and be

ame amount of ACN

ther MEK because of

cetone is a much b

ount or helps in

ater than benzene

ince ether

ter or ether contain

ethylene is large

e of the three, pro

of ether. The ethyl

ethers to a better

Let's 5.1 el

ter is consistent w

ne ether / large

Due to the

ethers of that beg

ACN units in the copolymer enhances the degree of goodness of DMF but the amount of ACN in this copolymer is not high enough to make DMF a better solvent than dioxane and benzene.

In the SAN C-2 and SAN C-2' copolymers, there is a big reversal in the degree of goodness of the solvents as can be seen from the [η] values. These polymers contain about 24 per cent ACN by weight. Apparently, this amount of ACN is high enough to render benzene the poorest solvent for these two copolymers. The order of the solvents in terms of decreasing degree of goodness is DMF, dioxane, MEK and benzene. Due to the presence of a relatively large amount of ACN, DMF is the best solvent. Dioxane is better than MEK because of the strong influence of the ST units (for PS, dioxane is a much better solvent than MEK). Also, its weak charge separation helps in making it a better solvent than MEK while MEK is better than benzene because of its strong polarity.

Copolymer SAN C-3 could be dissolved only in DMF and MEK. This polymer contains 38 per cent ACN by weight. Apparently, this ACN content is large enough to make benzene and dioxane non-solvents while the strong polarity of MEK helps keep it a solvent for this copolymer. Obviously, with increasing ACN content, DMF becomes increasingly a better solvent.

Table 5.1 also lists the values of Huggins constants. The Huggins constants for the copolymers SAN C-2 and SAN C-2' in benzene have unusually large values: 0.86 for SAN C-2 and 1.4 for SAN C-2'. This is due to the thermodynamically unfavorable environment in benzene. It has been known that while in a poor solvent a polymer

gives lower [η], it

it does in a good s

the following argum

tightly coiled and

spherical, structur

values discussed la

predicted the value

spheres. In benzen

long toward a spher

and [illegible] molecular

a longer chain, the

may be suggested th

least 40% by weight/

may also be close to 2

[illegible] ordered stru

As discusse

[illegible] solution

the [illegible] expan

[illegible] the expansion

[illegible] with an

[illegible] it would

[illegible] be more sver

[illegible] forms of

[illegible] of the

[illegible] attra

gives lower $[\eta]$, it leads to a higher value of Huggins constant than it does in a good solvent (F-7). This behavior is in accord with the following argument. In a poor solvent, the polymer molecule is tightly coiled and acts hydrodynamically like a compact, almost spherical, structure. This can be seen from the expansion factor values discussed later in the chapter. Frisch and Simha (F-7) have predicted the value of Huggins constant, k_1, to be about 2 for spheres. In benzene, the two copolymers are very tightly coiled and tend toward a spherical structure. The higher value of k_1 for SAN C-2' (molecular weight is 666,000) suggests that the larger a polymer chain, the larger will be the value of k_1 in benzene. It may be suggested that for a copolymer of this composition (24 per cent ACN by weight) and of infinitely large molecular weight, k_1 would be close to 2, since for a chain of infinite length the tightly coiled structure would tend to be spherical in shape.

As discussed in Chapter III, the dimensions of a polymer chain in a solution differ from the unperturbed dimensions due to the long-range effects. The two dimensions differ by a factor, α, called the expansion factor. If the free energy of a chain increases with an increase in the number of contacts between chain segments, as would be the case in good solvent media which favor polymer-solvent over polymer-polymer contacts, the bias against the contracted forms of the chain will be increased, leading to an expansion. On the other hand, in a thermodynamically poor solvent, chain segments attract one another, leading to a lower value of α.

At the θ-condition,

3.15 and 3.16 in Ch

$$[\eta] =$$

$$[\eta]_i =$$

and $[\eta]/[\eta]_i =$

we can make use of

structure informat

different solven

the coefficients of v

the A values

Table 6 ... values ... conds

...	...
...	...
...	...
...	...
...	...
...	...
...	...
...	...
...	...

... these values of

At the Θ-condition, α is equal to 1. Recapitulating Eqs. 3.13, 3.15 and 3.16 in Chapter III,

$$[\eta] = KM^{1/2}\alpha^3, \tag{3.13}$$

$$[\eta]_\Theta = KM^{1/2}, \tag{3.15}$$

and $$[\eta]/[\eta]_\Theta = \alpha^3, \tag{3.16}$$

we can make use of these equations, along with the experimental and literature information, to obtain the values of α for the polymers in different solvents. Shimura (S-7) obtained the K values for PS, SAN copolymers of various compositions and for PAN. Table 6.1 lists the K values of Shimura's polymers. From these K values, the

TABLE 6.1.--Values of Mark-Houwink Constant, K, of Polymers at Θ-Condition.

Polymer	Mole Fraction of ACN	$K \times 10^5$ $(dl)(mole^{1/2})/gm^{3/2}$
PS*	0	87
SAN CO-1*	0.383	124
SAN CO-2*	0.626	170
PAN*	1.0	227
SAN C-1	0.245	106
SAN C-2	0.371	122
SAN C-2'	0.36	121
SAN C-3	0.545	152

*These values are from Ref. (S-7).

K values for the copolymers synthesized in this work were obtained by interpolation. A smooth curve could be drawn through the points when the K values were plotted against mole fraction of ACN in the copolymers. (Shimura's SAN copolymers were also synthesized in bulk at 60°C by using AIBN initiator.) The K values thus obtained are also listed in Table 6.1. From these K values, $[\eta]_\Theta$ of each polymer-solvent system could be computed by using Eq. 3.15 and then the expansion factor, α, by using experimental $[\eta]$ and calculated $[\eta]_\Theta$ values in Eq. 3.16.

The α values are listed in Table 6.2. These values exhibit exactly the same trend in terms of goodness of solvent as the $[\eta]$ values since they were calculated from the $[\eta]$ and $[\eta]_\Theta$ values. An interesting feature is that the α values for the copolymers SAN C-2 and SAN C-2' in benzene are less than 1. Benzene is a very poor solvent so that the polymer chains coil up tightly to avoid the polymer-solvent contacts. In this poor solvent, the energy of interaction between the polymer and the solvent is unfavorable and hence smaller configurations, in which polymer-polymer contacts occur more frequently, are favored.

2. Stiffness Factor

It is known that the steric factor or stiffness factor, σ, which is a measure of the hindrance to internal rotation about the carbon-carbon single bonds of the backbone of a flexible chain molecule in the unperturbed state, generally increases with the molar volume of the substituent groups on the main chain of a linear polymer (K-2). The steric factor is defined as

TABLE 6.2.--Expans
30°C.

Polymer
PS-1
PS-2
SAN C-1
SAN C-2
SAN C-2'
SAN C-3

TABLE 6.2.--Expansion Factor, α, of Polymers in Various Solvents at 30°C.

Polymer	Solvent	α
PS-1	Benzene	1.278
	Dioxane	1.184
	MEK	1.050
PS-2	Benzene	1.380
	Dioxane	1.346
	MEK	1.084
SAN C-1	Dioxane	1.150
	Benzene	1.143
	DMF	1.094
	MEK	1.058
SAN C-2	DMF	1.185
	Dioxane	1.164
	MEK	1.128
	Benzene	0.952
SAN C-2'	DMF	1.287
	Dioxane	1.261
	MEK	1.215
	Benzene	0.901
SAN C-3	DMF	1.218
	MEK	1.107

$$\sigma = \langle L_0^2 \rangle^{1/2} / \langle L_0^2 \rangle_f^{1/2} \tag{6.1}$$

where $\langle L_0^2 \rangle^{1/2}$ is the root-mean-square end-to-end distance of the polymer chain in the unperturbed state and $\langle L_0^2 \rangle_f$ is the hypothetical root-mean-square end-to-end distance of a chain in which the internal rotation about the carbon-carbon bond of the main chain is completely free. The hindrance to internal rotation is called the short-range interaction.

In the abs

so-called "freely-

be easily computed

angles. The freel

one kind of bond f

$$\langle r^2 \rangle_f = n$$

where n is the numb

mean angle betwe

the lack of long-ra

rotational state. A

bond and the tetrah

parameter, σ, can b

the different polym

[illegible]

[illegible]

Polymer

[illegible]

[illegible]

[illegible]

[illegible]

[illegible]

From the

In the absence of any solvent or segment interaction, the so-called "freely-rotating chain" is obtained. Its dimension can be easily computed from the given data of bond lengths and bond angles. The freely rotating dimension of a chain consisting of only one kind of bond is given as (F-3e)

$$\langle L_0^2 \rangle_f = nl^2(1 + \cos\theta)/(1 - \cos\theta) \qquad (6.2)$$

where n is the number of bonds, l is the bond length, θ is the valence angle between successive bonds, and the subscript 0 denotes the lack of long-range interaction while f denotes the freely-rotating state. Assuming l equal to 1.54 Å for the carbon-carbon bond and the tetrahedral angle θ equal 109°-28', the stiffness parameter, σ, can be calculated. Table 6.3 lists the values of σ for different polymers. For PAN, reported value (K-2) of σ is 2.25 while for PS it is 2.22 (B-4a).

TABLE 6.3.--Stiffness Factor, σ, of Polymers.

	Polymer	ACN % Weight	ACN % Mole	σ
1.	PS-1	0	0	2.23
2.	SAN C-1	14.2	24.5	2.33
3.	SAN C-2	24	37.1	2.36
.	SAN C-3	38	54.5	2.40
.	PAN*	100	100	2.25

*From Ref. (B-4a).

The molar

about 89 ml and th

Despite this, the

and therefore the

such as hindrance

than the different

copolymers, it is

ion of ACN units

increases with the

shown in Table 6

Therefore, it can

ers are influence

the neighboring

the ratio of incr

ment of the copo

maximum value of

ers is significan

ers have the ma

maximum when 6 consta

ition where under

a greater value

ment state the co

ounce ers:

The molar volume of the substituent phenyl groups in PS is about 89 ml and that of the nitrile groups in PAN is about 38 ml. Despite this, the values of σ for the two homopolymers are similar and therefore the similarity in σ must be caused by other effects such as hindrance to rotation caused by system energetics rather than the different molar volumes of the side groups. For the SAN copolymers, it is statistically calculated (A-3) that the proportion of ACN units forming sequences of more than three units increases with the proportion of ACN in copolymer. The values of σ shown in Table 6.3 for different copolymers are not the same. Therefore, it can be said that the dimensions of the SAN copolymers are influenced by the fact that the electrostatic interactions of the neighboring nitrile groups are weakened by the phenyl groups. The value of σ increases very slowly along with the increase in ACN content in the copolymers. It is presumed that there would be a maximum value of σ between the two homopolymer values. The data here is insufficient to determine the value of ACN content where σ would have the maximum value. It seems from Table 6.3 that the maximum would probably occur at about 50 mole per cent ACN content in copolymer when the tendency for alternation is the maximum. The greater value of σ for the copolymers shows that in the unperturbed state the copolymers are more extended than the constituent homopolymers.

3. Second Virial Coefficient

The stiffness factor, σ, is a measure of short-range interactions. These interactions influence the dimensions of polymer

chains in bulk or

unperturbed. Aga

dimensions of poly

: what kind of

olutions? In oth

ain: interactions

compositions but n

the same solven

second virial coef

discussed late

ave measured in t

: thermodynam

ter 5 in chapt

The depend

chains in bulk or in a Θ-condition when the polymer molecules are unperturbed. Against this, long-range interactions influence the dimensions of polymer chains in solutions. The interesting question is: What kind of interactions can be observed for copolymers in solutions? In other words, what kind of polymer-solvent thermodynamic interactions can be observed from copolymers of different compositions but made out of the same two monomers and dissolved in the same solvents? These interactions may appear as a change of second virial coefficient, A_2, or of Flory thermodynamic parameter, χ_1 (discussed later in the chapter), from one polymer to another when measured in the same solvent. The second virial coefficient, A_2, is thermodynamic in nature and this is discussed in Chapter III. Table 5.5 in Chapter V presents the values of A_2.

The dependence of A_2 on molecular weight is negligibly small for both PS and SAN copolymers in the range of molecular weights considered in this work (B-4a). Therefore, we can examine the variation of A_2 with composition of polymers in different solvents. The higher the value of A_2 for a polymer in a solvent, the better is that solvent for that polymer. As the solvents for a polymer become poorer, the values of A_2 in those solvents become lower and finally, at the Θ-condition, A_2 becomes zero. Figure 6.1 shows the plots of A_2 of the polymers in different solvents versus ACN content. The points, though not many, are joined to demonstrate the trend in behavior. It is clear that the curve for the solutions of copolymers in MEK has a maximum in the neighborhood of 0.5 mole fraction of ACN. Thus, the intermolecular interaction of the SAN

Figu
Mole fractio

Figure 6.1.--Second Virial Coefficient, A_2, vs. Mole Fraction of ACN in Copolymers.

20
19
18
17
16
15
14
13
12
11
10
9
8
7
6
5
4
3
2
1

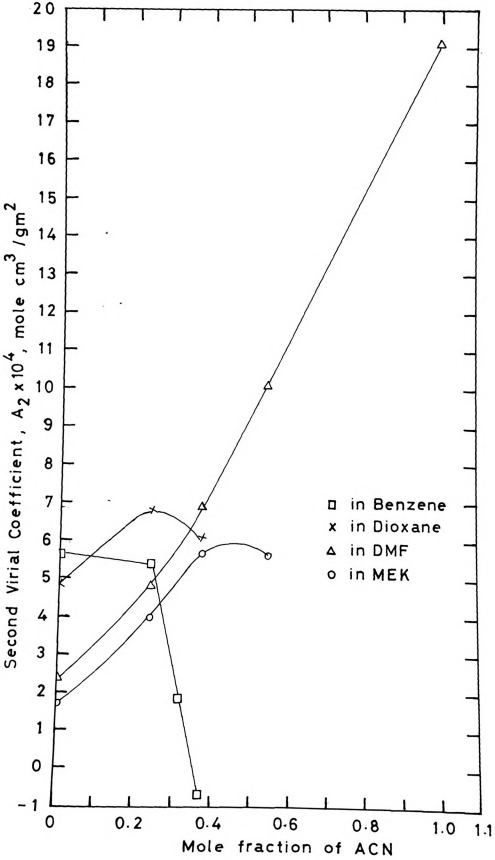
Second Virial Coefficient, $A_2 \times 10^4$, mole cm^3/gm^2
Mole fraction of ACN
in Benzene
in Dioxane
in DMF
in MEK
20
19
18
17
16
15
14
13
12
11
10
9
8
7
6
5
4
3
2
1
0
-1
0
0.2
0.4
0.6
0.8
1.0
1.1

copolymers in MEK shows a maximum at approximately equimolar composition where there exists the greatest tendency of alternation of copolymer units, ST and ACN. The behavior in dioxane shows a similar trend. The maximum in this case is at about 0.25 mole fraction of ACN. Both these solvents are non-solvents for PAN. With the ACN content higher than that in SAN C-3, MEK would be a non-solvent. It is not possible to predict this limiting concentration. Also, dioxane does not dissolve the copolymer SAN C-3 which has 0.54 mole fraction ACN content. Benzene is also a non-solvent for PAN. Benzene is non-polar and this makes it much poorer than other solvents for copolymers with ACN content higher than 0.24 mole fraction. This is evident from the deep plunge in the value of A_2 for SAN C-2. At the azeotropic composition (SAN C-2 and SAN C-2') the second virial coefficient is negative, indicating that the copolymer is in an extremely poor solvent, and the polymer molecules are tightly coiled. Since DMF is a good solvent for PAN and a comparatively poor one for PS (this can be seen from the A_2 or χ_1 values; see Table 6.4 for the χ_1 values), with increasing ACN content in the copolymer, A_2 increases continuously.

The negative value of A_2 for the azeotropic copolymers in benzene is entirely due to the very nature of the copolymer-benzene interaction. In an environment of benzene, the chains prefer polymer-polymer contacts rather than polymer-solvent contacts, since the presence of a large number of ACN units in the chains has a great influence on the polymer-solvent interactions. The tightly coiled nature of the chains is also indicated by the α value in

TABLE 6.4.--Flory
Vario

Polymer
PS-1
PS-2
SAN C-1
SAN C-2
SAN C-2'
SAN C-3

TABLE 6.4.--Flory Thermodynamic Parameter, χ_1, of Polymers in Various Solvents.

Polymer	Solvent	χ_1
PS-1	Benzene	0.426
	Dioxane	0.443
	MEK	0.481
PS-2	Benzene	0.424
SAN C-1	Dioxane	0.418
	Benzene	0.433
	DMF	0.450
	MEK	0.453
SAN C-2	DMF	0.426
	Dioxane	0.426
	MEK	0.429
	Benzene	0.507
SAN C-2'	DMF	0.420
	Dioxane	0.426
	MEK	0.430
	Benzene	0.507
SAN C-3	DMF	0.382
	MEK	0.428

benzene which is less than unity. It should be mentioned that at the same time benzene is not a theta solvent at 25°C. Also, it should be kept in mind that at the Θ-condition A_2 is equal to 0. Essentially, A_2 is a measure of the tendency of the solvent to interact with the segments of the polymer chain. The lower the value of A_2, the lower is the tendency for interaction and the poorer is the solvent until at A_2 equal to 0 the chain assumes its unperturbed dimensions governed only by the skeletal effects of the chain. Large values of A_2 indicate the tendency of polymer

segments to avoid

indicates a prefe

chains then have

It is int

solve either in d

of A_2 with respect

one would rather

the maximum for PS

This means that bo

copolymers with in

content. This may

of dioxan

with increasing v

Table 5.5

for a given molecul

compared to those

... to make

... scatter

... results

... weight

... range of mo

...

... and hence

... nearly

...

segments to avoid one another as a result of "excluded volume" and indicates a preference to interact with the solvent molecules. The chains then have a more expanded structure.

It is interesting to note that although PAN does not dissolve either in dioxane or in MEK, there is a maximum in the value of A_2 with respect to ACN content in the copolymers. Intuitively, one would rather expect the maximum at ACN content equal to 0; i.e., the maximum for PS homopolymer, as in the case of benzene solutions. This means that both dioxane and MEK become better solvents for copolymers with increased ACN content but only up to a certain ACN content. This may be due to the polarity of MEK and localized polarity of dioxane. The trend in DMF is normal, showing continuously increasing values of A_2 with ACN content.

Table 5.5 shows a slight decrease in the values of A_2 for the higher molecular weight azeotropic copolymer, SAN C-2', compared to those of the lower molecular weight, SAN C-2. It is difficult to make any conclusion regarding this trend with only two molecular weights available and considering the errors involved in the light scattering measurements. However, according to the literature results (B-4a), A_2 values decrease slightly with increasing molecular weight of polymer. Values of A_2 are rarely available over a range of molecular weights extending over two orders of magnitude. In this study, the variation in molecular weight is not large, either for the two PS samples or for the azeotropic copolymer samples, and hence for practical purposes the values of A_2 may be considered nearly constant in the range of molecular weights considered.

4. Flory Thermod

As explai

A_2 is a thermody

Flory parameter

from light scatte

ost quantity whi

of a given solven

virial coefficien

$$A_2 = (\bar{V}$$

where

$$\chi_1 = \chi'$$

4. Flory Thermodynamic Parameter

As explained in Chapter III, the second virial coefficient, A_2, is a thermodynamic quantity. This quantity is related to the Flory parameter χ_1 and hence χ_1 can be calculated from A_2 obtained from light scattering data (F-3a). The parameter χ_1 is a dimensionless quantity which includes the interaction energy characteristic of a given solvent-solute pair. According to the theory of second virial coefficient (F-3a),

$$A_2 = (\bar{v}_p^2/v_s)(1/2 - \chi_1)F(X) \tag{6.3}$$

where

$$F(X) = 1 - \frac{X}{2!\ 2^{3/2}} + \frac{X^2}{3!\ 3^{3/2}} - \frac{X^3}{4!\ 4^{3/2}} + \cdots \tag{6.4}$$

$$X = 2(\alpha^2 - 1) \tag{6.5}$$

$\bar{v}_p$ is the specific volume of polymer, v_s is the molar volume of solvent and α is the expansion factor for the polymer in the solvent used. The series given by Eq. 6.4 is an extremely rapidly converging series and hence only the first few terms need to be considered. The α values were obtained at 30°C while the A_2 values were obtained at 25°C. Since χ_1 is a weak function of temperature, the difference of 5°C was assumed not to introduce any significant error in the estimate of χ_1 values. The χ_1 values are listed in Table 6.4 given on page 145.

The parameter χ_1 may be used as a criterion for classifying solvents as good solvents, poor solvents or non-solvents. The

ower the value o

ies between 0

olvent for the p

rimarily indicate

uestion (B-16).

As the pr

alue of γ_1 in be

olvent for PAN w

hat DMF is incre

ncreasing Al

AN solution benzen

ore poor solvent

Thus, the

ue to for the so

lower the value of χ_1, the better is the solvent. If the value of χ_1 lies between 0.5 and 0.6 then the solvent may be poor or non-solvent for the polymer in question. Values of χ_1 larger than 0.6 probably indicate that the polymer is insoluble in the solvent in question (B-16).

As the proportion of ACN in the copolymer increases, the value of χ_1 in benzene also increases since benzene is a non-solvent for PAN while the value of χ_1 in DMF decreases, signifying that DMF is increasing in its degree of goodness for copolymers with increasing ACN content. The values of χ_1 for SAN C-2 and SAN C-2' in benzene are greater than 0.5, indicating that it is a very poor solvent.

Thus, the values of $[\eta]$, α, A_2 and χ_1 establish the solvent quality for the polymers.

B. Zero Shear Viscosities

1. The Influence of Solvent

Solvent effects have an important influence on the value of low shear specific viscosity, η_{sp}, of polymer solutions in both dilute and concentrated solutions. The importance of solvent effects has not been recognized widely in concentrated solutions. This influence on low shear viscosity will be demonstrated by considering semi-log plots of specific viscosity, η_{sp}, versus c in good and poor solvents and in the next section by log-log plots of relative viscosity, η_r, versus c.

At very low concentrations of polymer in solution, the polymer chains are believed to exist as isolated clouds of polymer

segments which do

model the very di

:ion of soft defo

ic ymer in soluti

overlap and the c

the shear viscosi

concentration. T

f gures 6.2

the SAA C-2 and S

the SAA C-3 in DM

cosities of di

normalized by

ed on:

At the dil

ter in water at

ents with the co

in DMF becomes

the gels MER

segments which do not interpenetrate with each other. With this model the very dilute polymer solution appears to flow as a suspension of soft deformable spheres in solvent. As the concentration of polymer in solution is increased, the polymer spheres begin to overlap and the chains become entangled. When this happens the low shear viscosity, η_{sp}, depends much more strongly on polymer concentration. The viscometric data are presented as log η_{sp} versus c in Figures 6.2 to 6.5 for copolymers SAN C-1 in DMF and MEK, for SAN C-2 and SAN C-2' in DMF AND MEK and in DMF and benzene and for SAN C-3 in DMF and MEK. To make a proper comparison between viscosities of different solutions, the zero shear viscosity should be normalized by the viscosity of the solvent, η_s, and then plotted against c.

As the proportion of ACN in the copolymers increases, starting with PS homopolymer, MEK and benzene become poorer solvents until the copolymers are no longer soluble in them. Progressively, DMF becomes a better solvent since PAN is soluble in DMF while it is not soluble in MEK and benzene. For SAN C-2 and SAN C-2' benzene is a very poor solvent as indicated by the expansion factor, α, given in Table 6.2. Copolymer SAN C-3 is not soluble in benzene and MEK. The solvents used in this study are good solvents for PS but their degree of goodness varies for copolymers.

The viscosity data make it clear that the solvent character can have a significant influence on viscosity in the whole range of concentrations. This reality differs from the oft-encountered belief that solvent effects are "neutralized" at high concentrations

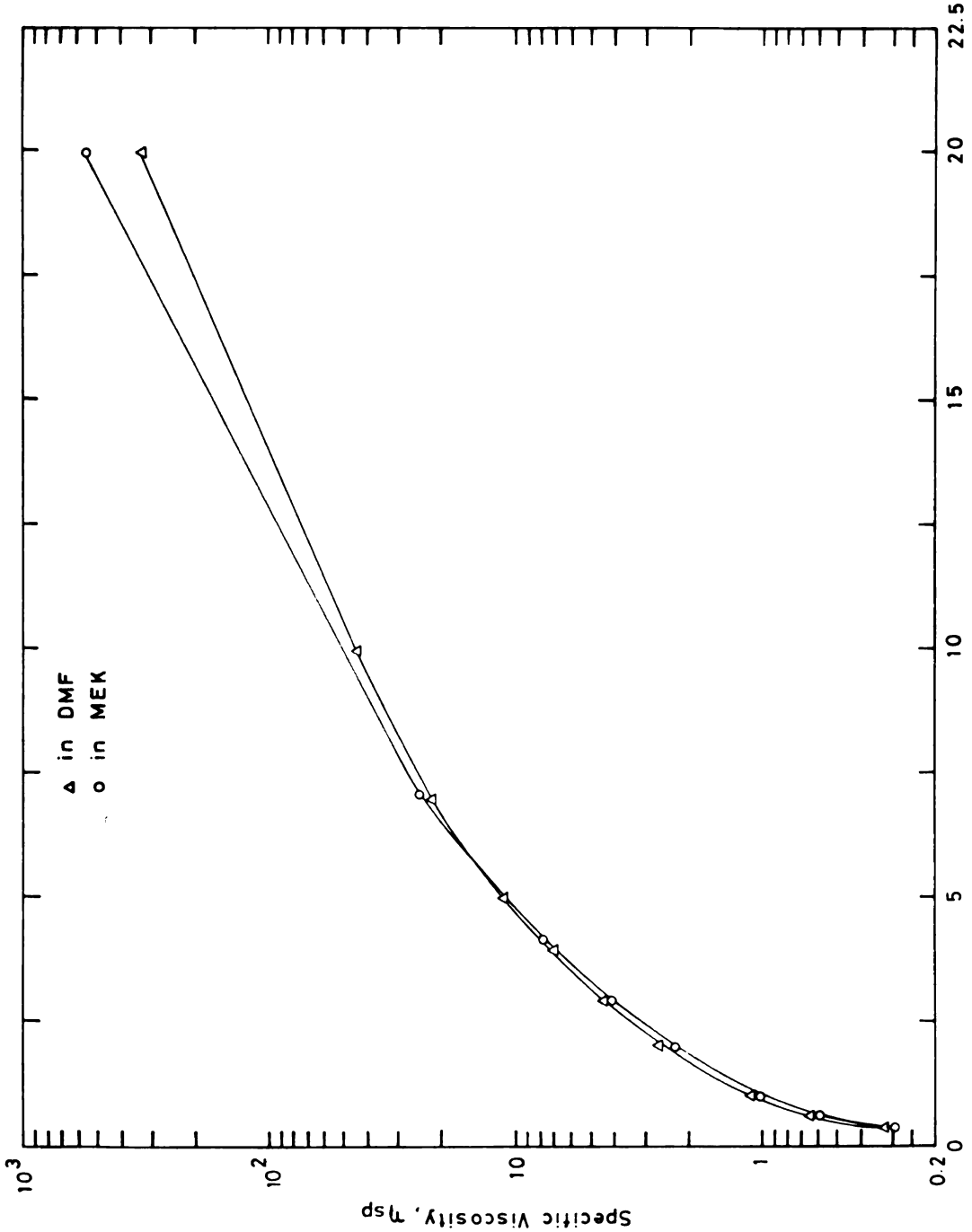

Figure 6.2.--Specific Viscosity, η_{sp}, vs. Concentration, c, of SAN C-1 in DMF and MEK at 30°C.

Figure 6.3.--Specific Viscosity, η_{sp}, vs. Concentration, c, of SAN C-2 and SAN C-2' in DMF and MEK at 30°C.

3x10^3
10^3

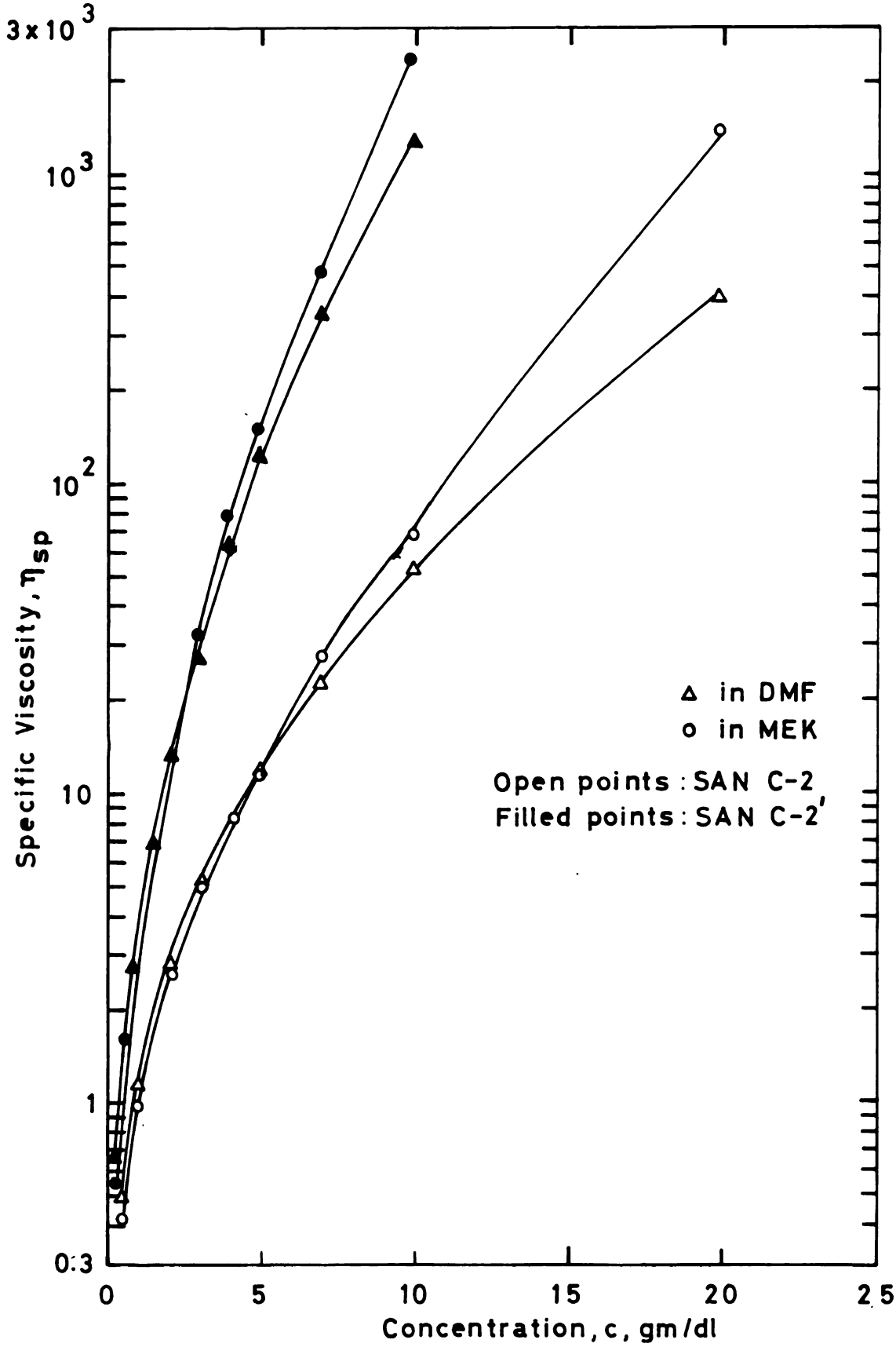
3x10^3
10^3
10^2
10
1
0·3
Specific Viscosity, η_{sp}
0
5
10
15
20
25
Concentration, c, gm/dl
△ in DMF
○ in MEK
Open points : SAN C-2
Filled points : SAN C-2'

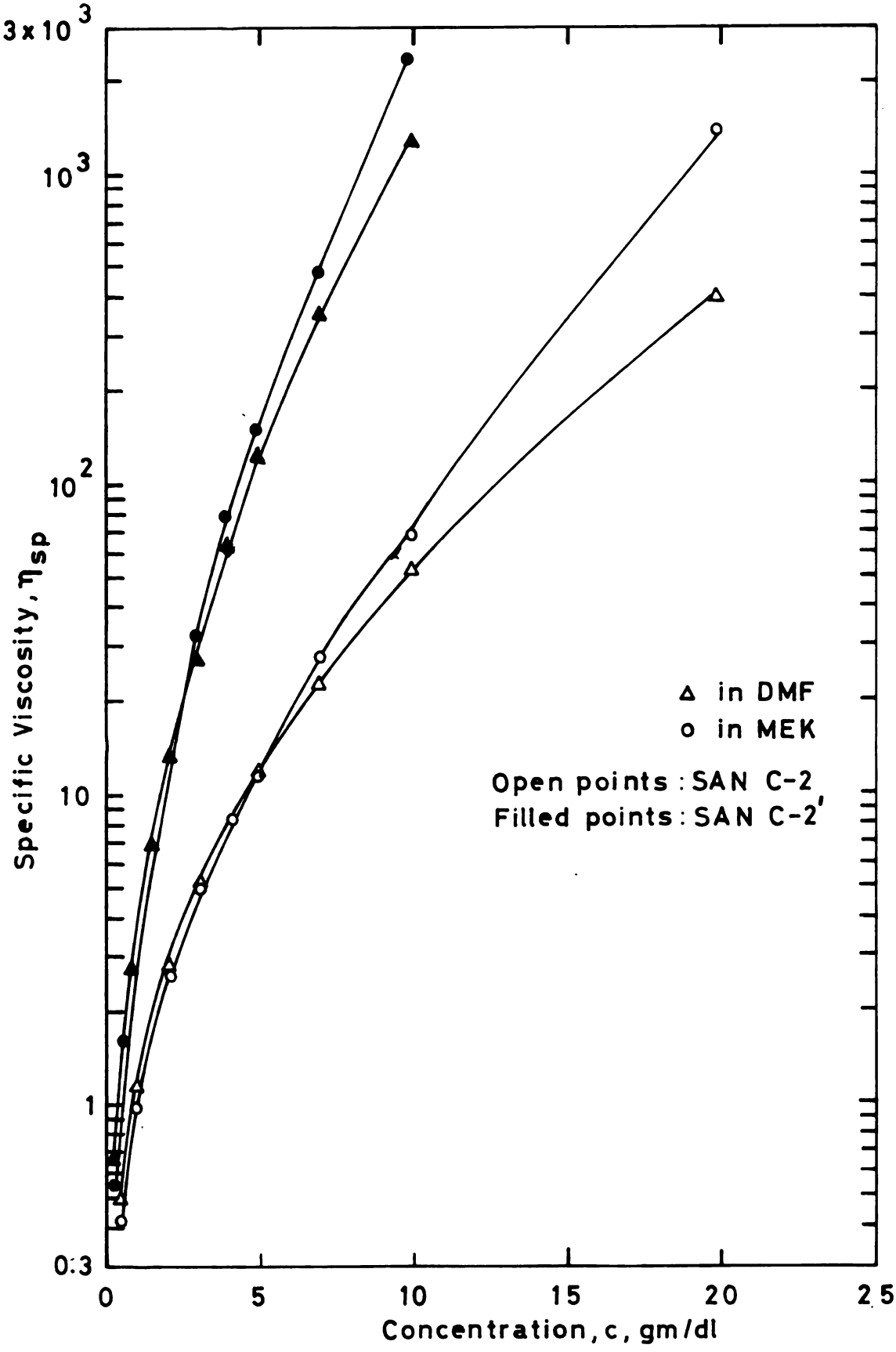
3x10 3
10 3
10 2
10
1
0:3
Specific Viscosity, ηsp
0
5
10
15
20
25
Concentration, c, gm/dl
△ in DMF
o in MEK
Open points : SAN C-2
Filled points : SAN C-2'


6×10^3
10^3

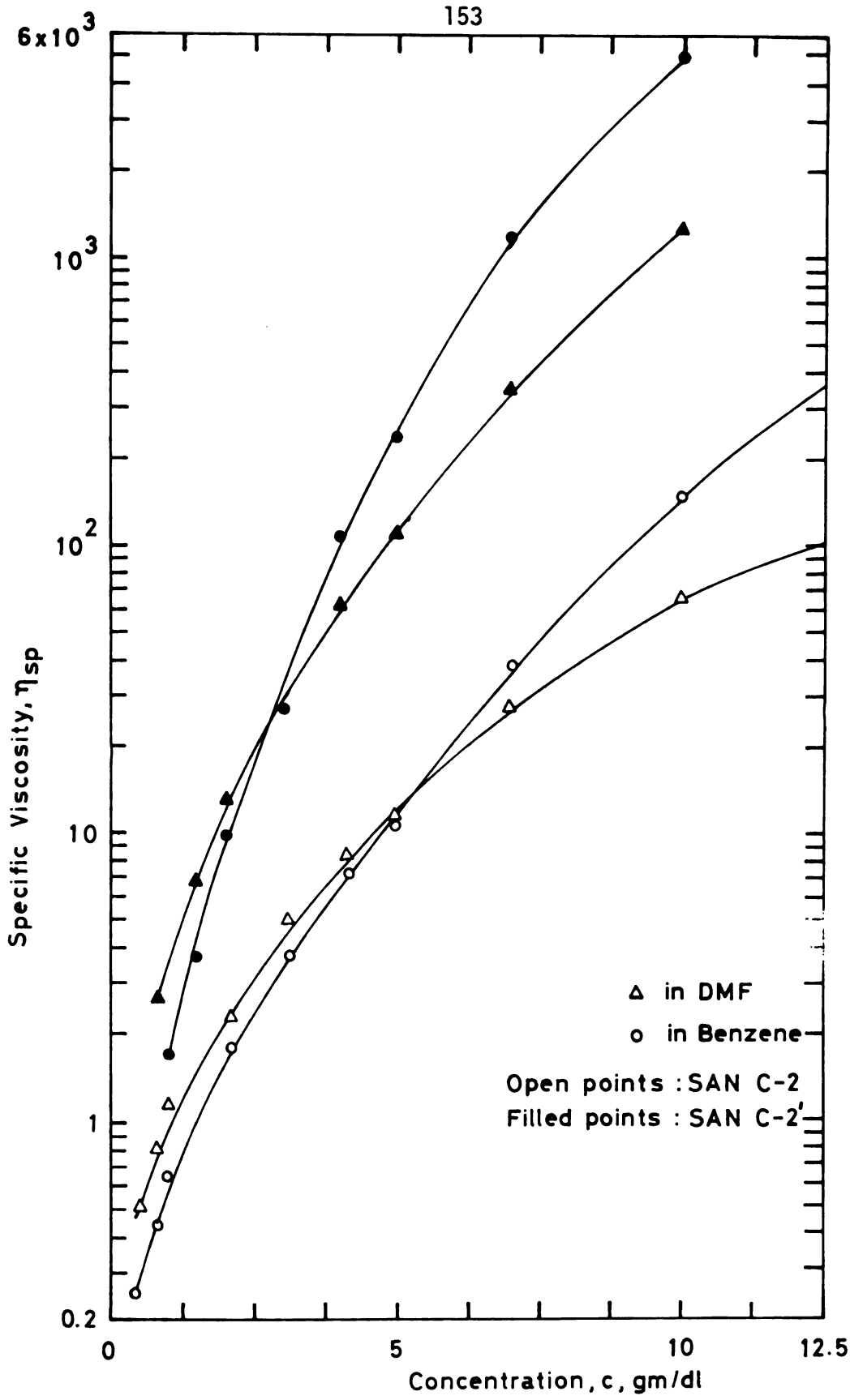

Figure 6-4.--Specific Viscosity, η_{sp}, vs. Concentration, c, of SAN C-2 and SAN C-2' in DMF and Benzene at 30°C.

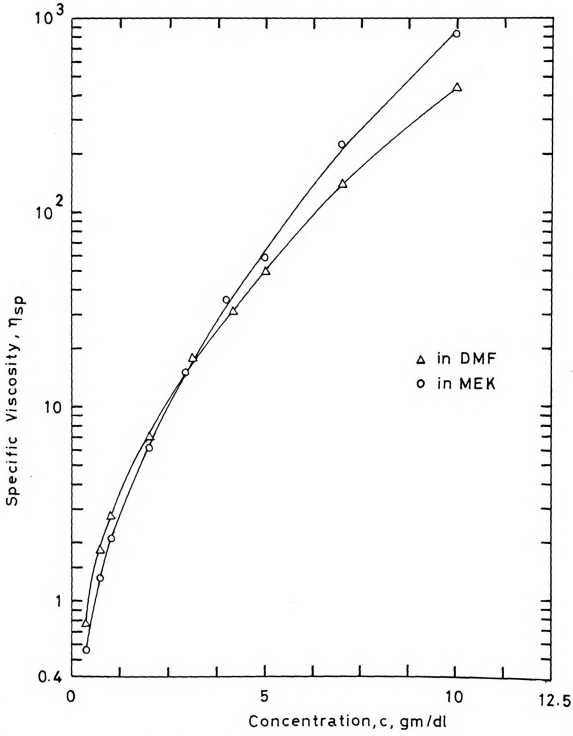

Figure 6.5.--Specific Viscosity, η_{sp}, vs. Concentration, c, of SAN C-3 in DMF and MEK at 30°C.

because they can

which depends o

it's fill up th

In this

arying ACN cont

's smaller i

entrations and

ncentration in

ge of viscosity

ts at low

ncentration in

n two domains.

ncentrations, w

s consisten

ntrations. At the

ngments per unit

ments per unit

ere is more, the

ticles that are

ments are betwe

ments are separ

ed end units ar

e more or equal

ments are separ

ed end units ar

because they can no longer influence the size of the polymer chains (which depends on the solvent in dilute solution) since the polymer coils fill up the space uniformly.

In this work the solvent effect is shown on copolymers of varying ACN content in the solvents, MEK and DMF. In all the cases, η_{sp} is smaller in poor solvents than in good solvents at low concentrations and it eventually becomes larger in poor solvents as concentration increases. This is a consequence of stronger dependence of viscosity in poor solvents on concentration at high concentrations. At low concentrations, viscosity increases rapidly with concentration in good solvents because of the larger size of the polymer domains. It can be seen in Figures 6.2 to 6.5 that at high concentrations, viscosity increases more rapidly in poor solvents. This is consistent with the following qualitative thermodynamic argument. As the concentration increases, the density of chain segments per unit volume of solution increases along with the entanglements between the polymer chains. In an environment of a poor solvent, the polymer segments prefer polymer-polymer contacts rather than polymer-solvent contacts. This enhances coiling-up of the polymer chain. The coiling-up of the polymer chains in effect enhances the entanglement or makes the entanglements "tighter." In a good solvent, solvent-polymer contacts are at least equally preferred and this deters direct inter-polymer chain interaction. Thus a polymer molecule in a good solvent finds it much easier to move freely among its neighbors while in a poor solvent freedom would be reduced and could eventually lead to aggregation.

In the d

r a poor one wh

ccupy a larger

olute solution

. The chain

concentration al

he effect of th

han the effect

g effect i

A close

he 'cross-over'

s are a good a

ook ymer solutio

r the copolymer

good solvent, a

P s for DAN

For P

her than

and DAN

DAN and

P s, respect

The observ

r ymer increas

r water or se

ore so weak. Wi

ore than ymer

In the dilute region, η_{sp} is higher in a good solvent than in a poor one which merely reflects the fact that polymer chains occupy a larger domain due to expansion in the good solvent. This dilute solution behavior is fully discussed in the literature (M-2, R-2). The chains are isolated in the dilute region. At higher concentration also the polymer chains expand in good solvents but the effect of this expansion on viscosity of solutions is much less than the effect of the entangled polymer chains enhanced by a coil-up effect in poor solvents.

A close examination of the data of this work indicates that the "cross-over" concentration (or the concentration at which η_{sp} values in good and poor solvents are equal) is much lower for the copolymer solutions than that for the PS homopolymer solutions. For the copolymers in this work, the cross-over concentration in DMF (good solvent) and MEK (poor solvent) is about 5 gm/dl for SAN C-1, 4 gm/dl for SAN C-2, 2.5 gm/dl for SAN C-2' and 3.5 gm/dl for SAN C-3. For PS in these solvents, the cross-over concentration will be much higher than the concentrations considered here. Also, for SAN C-2 and SAN C-2' in DMF and benzene (benzene is a poor solvent for SAN C-2 and SAN C-2', poorer than MEK), these values are 5 and 3 gm/dl, respectively.

The above result suggests that as the proportion of ACN in copolymer increases, starting with homopolymer PS, the cross-over concentration decreases. With increasing ACN content, an already poor solvent, MEK, becomes poorer and hence there is more preference for polymer-polymer contacts rather than polymer-solvent

contacts. This is also the case with benzene. This leads to more coiling up and so tighter entanglements and hence increased viscosity in a poor solvent, leading to a lower cross-over point with increased ACN content. These interactions may or may not be insensitive to molecular weight. Further evidence of this phenomenon comes from a study of PVC-acetate copolymer systems (J-1) in MEK (good solvent) and cyclohexanone (poor solvent). The cross-over concentration was about 2.5 gm/dl. These observations indicate that cross-over concentration becomes smaller as polymer-polymer interactions become progressively stronger. Further investigation is needed to study the molecular weight effects, and to quantitatively correlate this phenomenon with molecular variables. In this study, the variation in molecular weight between the two samples of azeotropic copolymers was about 3.7 fold. With the data of this work, it is difficult to arrive at a definite conclusion regarding the molecular weight dependence of the cross-over point. By eliminating the parameter of molecular weight,* one should be able to observe features which can be attributed directly to polymer-solvent interaction (due to different average polarity of copolymers as a result of different ACN content). The number of chain atoms may be a more proper variable to consider. However, the data of this work are still insufficient to show the influence of chain length or molecular weight on the cross-over concentration.

---

*For PS and different SAN copolymers, if molecular weights are the same, the number of chain atoms will be different because ST and ACN have different molecular weights; ST M.W. = 104, ACN M.W. = 53.

It must

oderately conce

igher concentra

he molecules of

olymer chains r

ute and moder

creases to 100

ained only by th

Entanglement

The feat

he optical plot

and 3 show

ecent wo

egree of

he curves show

ent

ic

he

own

It must be emphasized that this discussion pertains to moderately concentrated solutions (up to about 20 per cent). At higher concentrations the polymer-solvent mass exists as a gel and the molecules of the solvent would diffuse within the network of polymer chains rather than the polymer molecules diffusing as in dilute and moderately concentrated solutions. As the concentration increases to 100 per cent polymer, the two curves should be separated only by the ratio of solvent viscosities.

2. Entanglement Concentrations

The features of viscometric data can also be examined from the log-log plots of the viscosity-concentration curves. Figures 6.6 and 6.7 show such plots for PS-1 and PS-2 in benzene and MEK, respectively. These two solvents present the extreme cases in degree of goodness for PS among the solvents chosen in this work. The curves show an abrupt increase in relative viscosity when a certain concentration is reached which corresponds to the concentration characteristic of entanglement networks. Various methods have been proposed to calculate the value of the concentration at which such a pronounced increase should be expected (P-1, P-4).

The onset of entanglement in polymer solutions can be observed from sharp changes in the slopes of the plots of $\eta_r(c)$ versus c, $\eta_r(M)$ versus M or $\eta_r(c,M)$ versus cM^b. Plots of zero shear viscosity versus molecular weight for polymer melts show two distinct linear regions with a sharp break point (M-1a). The molecular weight of the polymer at the break point is referred to

10^4
10^3
10^2

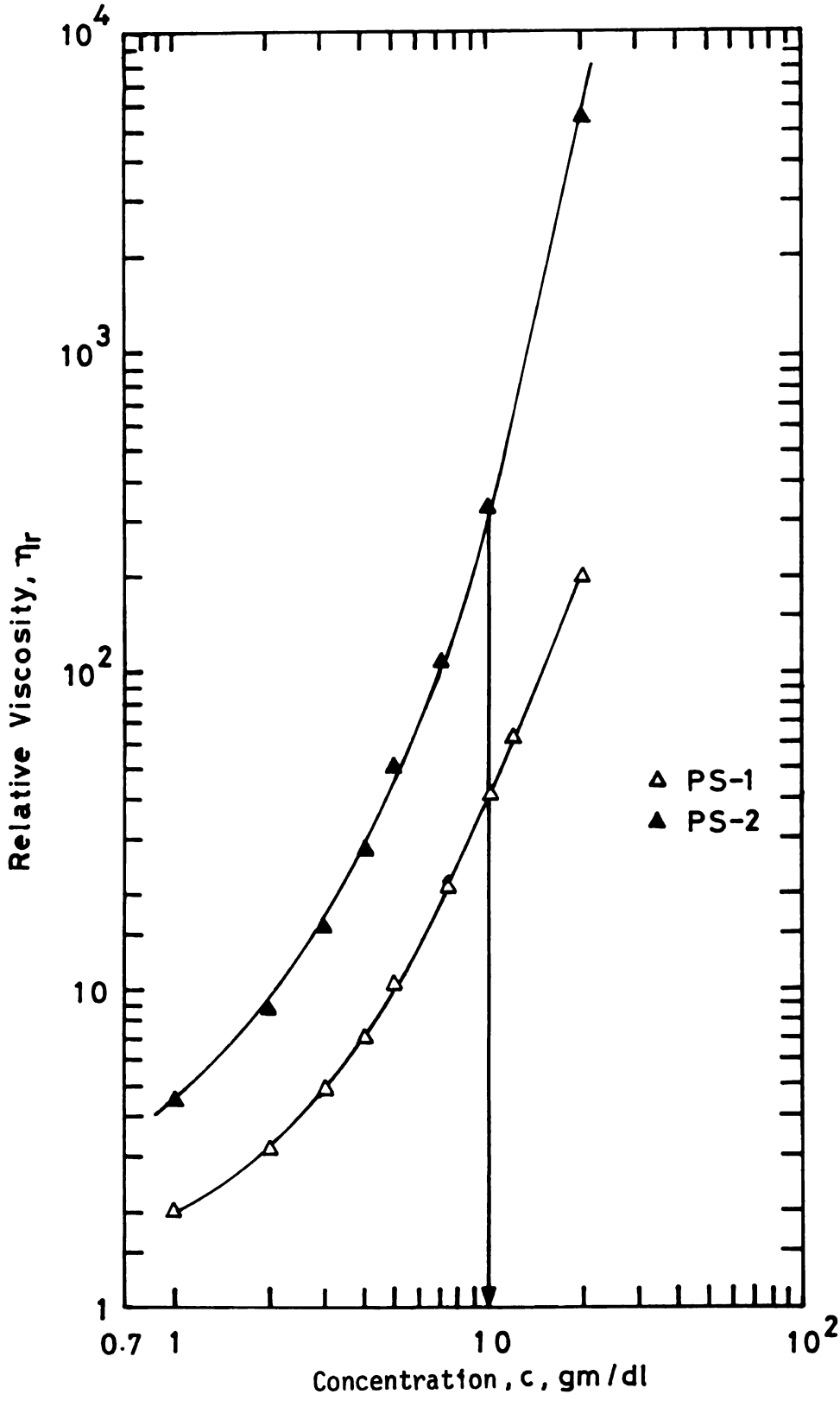

Figure 6.6.--Relative Viscosity, η_r, vs. Concentration, c, of PS in Benzene at 30°C.

10^4
10^3
10^2

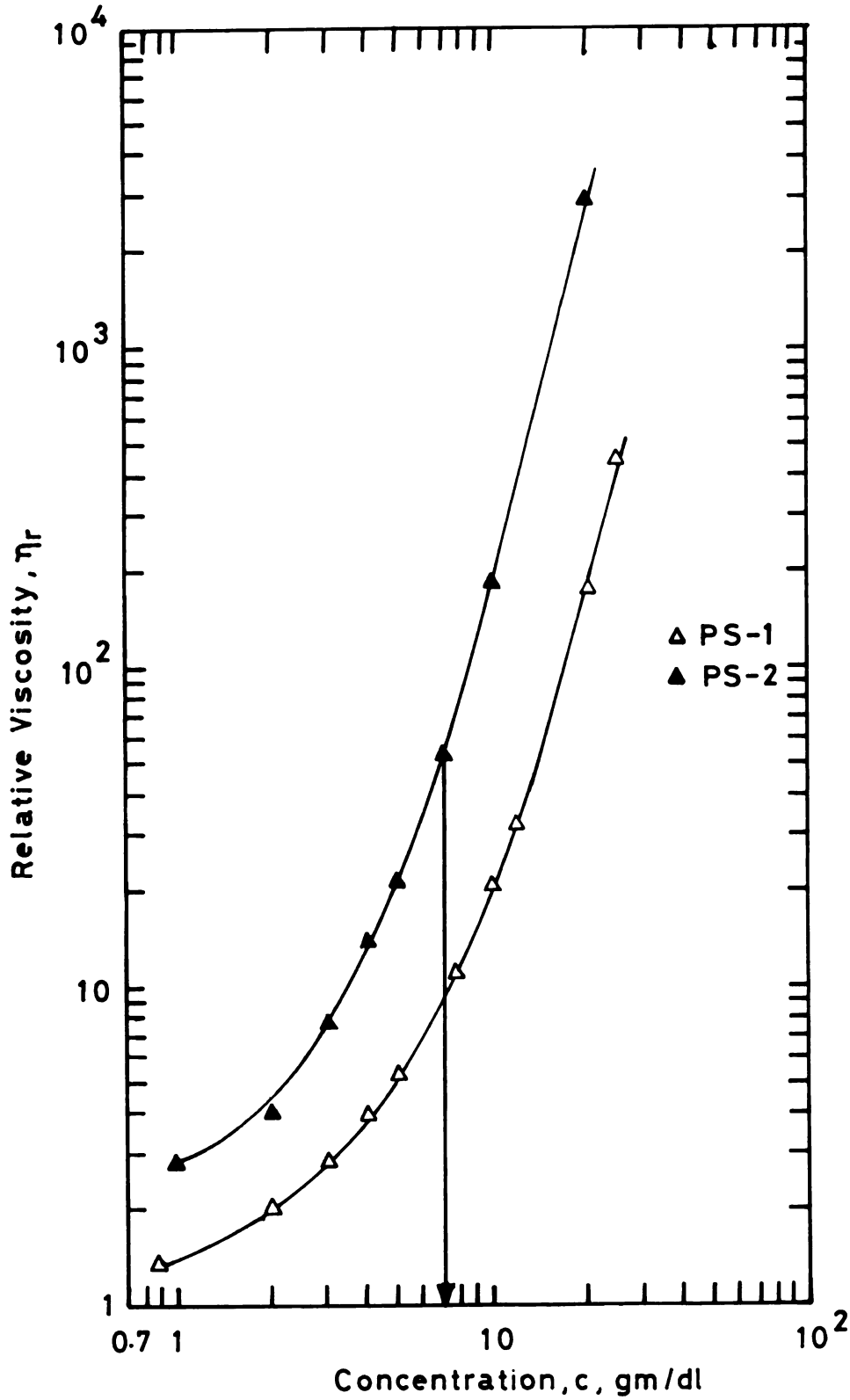

Figure 6.7.--Relative Viscosity, η_r, vs. Concentration, c, of PS in MEK at 30°C.

as the critical

weight curve wit

slope than that

'M^a). Porter

for a polymer ma

c_{ent} in solutio

$$c_{ent}M =$$

where , is the c

ment concentrati

'r : idea ignore

ic exact type of

Porter and Johns

at zero, all one

According

of M zero rotti

$$[\eta]_{zero} =$$

where the mean

is proportional

the is molecular

of zero,

$$[\eta]_{zero} = //$$

When the or re

as the critical molecular weight, M_c. The melt viscosoty-molecular weight curve with molecular weights higher than M_c has a greater slope than that of the curve with molecular weights less than M_c (M-1a). Porter and Johnson (P-1) recommended that this value of M_c for a polymer may be used to calculate entanglement concentration, c_{ent}, in solutions. Accordingly, they recommended that

$$c_{ent}M = \rho M_c \tag{6.6}$$

where ρ is the density of bulk polymer, and c_{ent} is the entanglement concentration in solution for a polymer of molecular weight M. This idea ignores solvent effects and essentially considers the solvent type of no importance to the onset of entanglement. With Porter and Johnson's approach to find the concentration c_{ent} for a polymer, all one needs is a tabulated value of ρM_c for that polymer.

According to Coronet (C-3) from a theory based on packing of polymer coils,

$$(c/M)_{ent} = 2.28 \times 10^{-23}/\langle L_0^2 \rangle^{3/2} \tag{6.7}$$

where the mean-square end-to-end distance, $\langle L_0^2 \rangle$, is evaluated at the unperturbed (theta) condition. However, since $\langle L_0^2 \rangle$ is proportional to molecular weight, the product $cM^{1/2}$ would be a constant, and hence,

$$c_{ent}M^{1/2} = c\, M_{ent}^{1/2} = \text{Constant}. \tag{6.8}$$

Other similar relations have also been proposed (O-6).

The prec

re presented fr

olecular weight

for the lower mo

namely differe

the abrupt incre

of about 10 gm/c

values are in fa

for PS-1, no sha

observed in the

While the slope is

The predicted values of c_{ent} for PS using various relations are presented in Table 6.5. The predicted values for the higher molecular weight, PS-2, are in fair agreement with each other but for the lower molecular weight, PS-1, the values predicted are markedly different from different relations. As shown in Fig. 6.6, the abrupt increase in the slope for PS-2 in benzene is probably at about 10 gm/dl and in MEK (Fig. 6.7), at about 7 gm/dl. These values are in fairly good agreement with the values in Table 6.5. For PS-1, no sharp increase in slope in either solvent can be observed in the range of concentrations considered, although in MEK the slope is much steeper at higher concentrations (about 20

TABLE 6.5.--Estimation of Entanglement Concentration, c_{ent}, for PS.

Relation*	c_{ent}, gm/dl		Reference
	M=501,000 PS-2	M=185,000 PS-1	
$(cM)_{ent} = 4.41 \times 10^6$	8.8	23.8	P-1
$(cM)_{ent} = 3.75 \times 10^6$	7.5	20.2	P-1
$(cM)_{ent} = 3.03 \times 10^6$	6.1	16.4	G-2
$(cM^{1/2})_{ent} = 4.65 \times 10^3$	6.6	10.8	Eq. 6.7 and Ref. (B-4a)†
$(cM^{1/2})_{ent} = 5.28 \times 10^3$	7.5	12.3	P-1

*$(cM)_{ent}$ stands for the value of cM beyond which entanglement networks prevail.

†Obtained by using Eq. 6.7 with $\langle L_0 \rangle^2/M = 757$ Å taken from Ref. (B-4a).

gm/dl) than in

SN_{ent} scheme

we relatively

benzene, it is

Figures

and SAN C-2

respectively.

about 6 gm/dl i

6 6. Fo

seems to be at

gm/dl. This

methane emmett co

a wet to SMS

gm/dl, re

ml 3 ml Sere

reference

are eva

Fig

values given

Fig. 6 - Ene

SAN

SAN

SAN

SAN

gm/dl) than in benzene. From this work a slight superiority of the $(cM)_{ent}$ scheme compared with $(cM^{1/2})_{ent}$ scheme is suggested for the two relatively good solvents involved, although MEK is poorer than benzene, it is not a Θ-solvent for PS.

Figures 6.8 to 6.11 show the plots for the copolymers SAN C-2 and SAN C-2' in DMF and benzene and SAN C-3 in DMF and MEK, respectively. For SAN C-2', the abrupt increase in slope is at about 6 gm/dl in DMF (Fig. 6.8) and at about 3 gm/dl in benzene (Fig. 6.9). For SAN C-2 in DMF (Fig. 6.8), the increase in slope seems to be at 20 gm/dl while in benzene (Fig. 6.9), it is about 5 gm/dl. This is a strong indication of the lower value of the entanelement concentration in poor solvents. For SAN C-3, the values in DMF (Fig. 6.10) and MEK (Fig. 6.11) are at about 10 gm/dl and 5 gm/dl, respectively. Thus, the influence of solvent on c_{ent} is evident from the data on copolymers.

Unfortunately, no relations for c_{ent} (as shown in Table 6.5 for PS) are available in the literature for SAN copolymers, except for Eq. 6.7. Equation 6.7 was used for prediction of c_{ent} for the SAN copolymers. These values are listed in Table 6.6.

TABLE 6.6.--Entanglement Concentrations, c_{ent}, from Eq. 6.7, for SAN Copolymers.

Copolymer	c_{ent}, gm/dl
SAN C-2	11
SAN C-2'	5.8
SAN C-3	9

Figure 6.8.--Relative Viscosity, η_r, vs. Concentration, c, of SAN C-2 and SAN C-2' in DMF at 30°C.

3x10^4
10^4
10^3
10^2

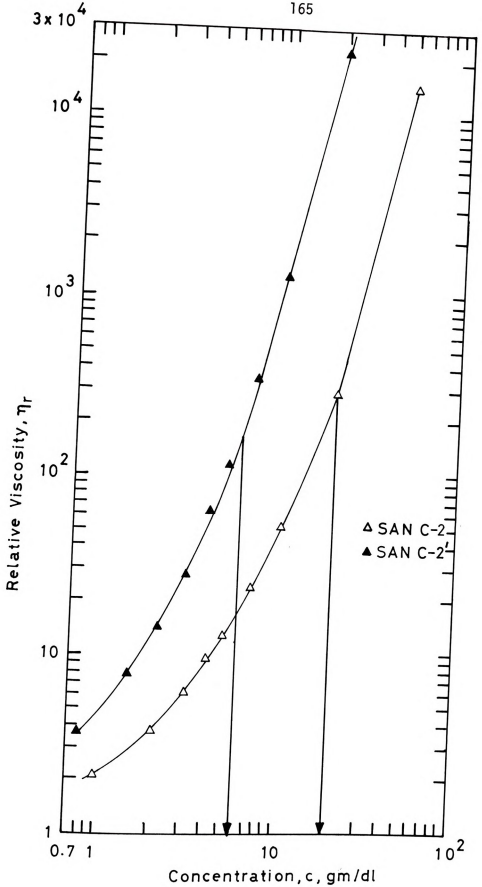
3x10^4
10^4
10^3
10^2
10
1
Relative Viscosity, η_r
△ SAN C-2
▲ SAN C-2'
0.7
1
10
10^2
Concentration, c, gm/dl

10^4
10^3
10^2

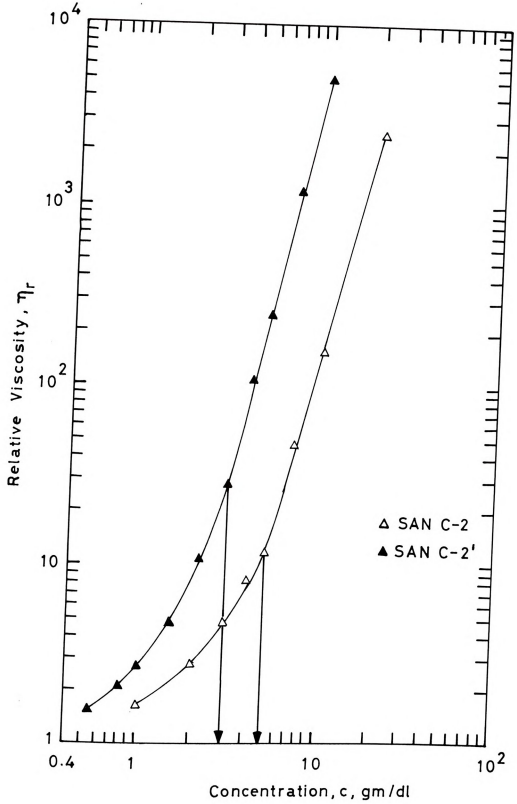

Figure 6.9.--Relative Viscosity, η_r, vs. Concentration, c, of SAN C-2 and SAN C-2' in Benzene at 30°C.

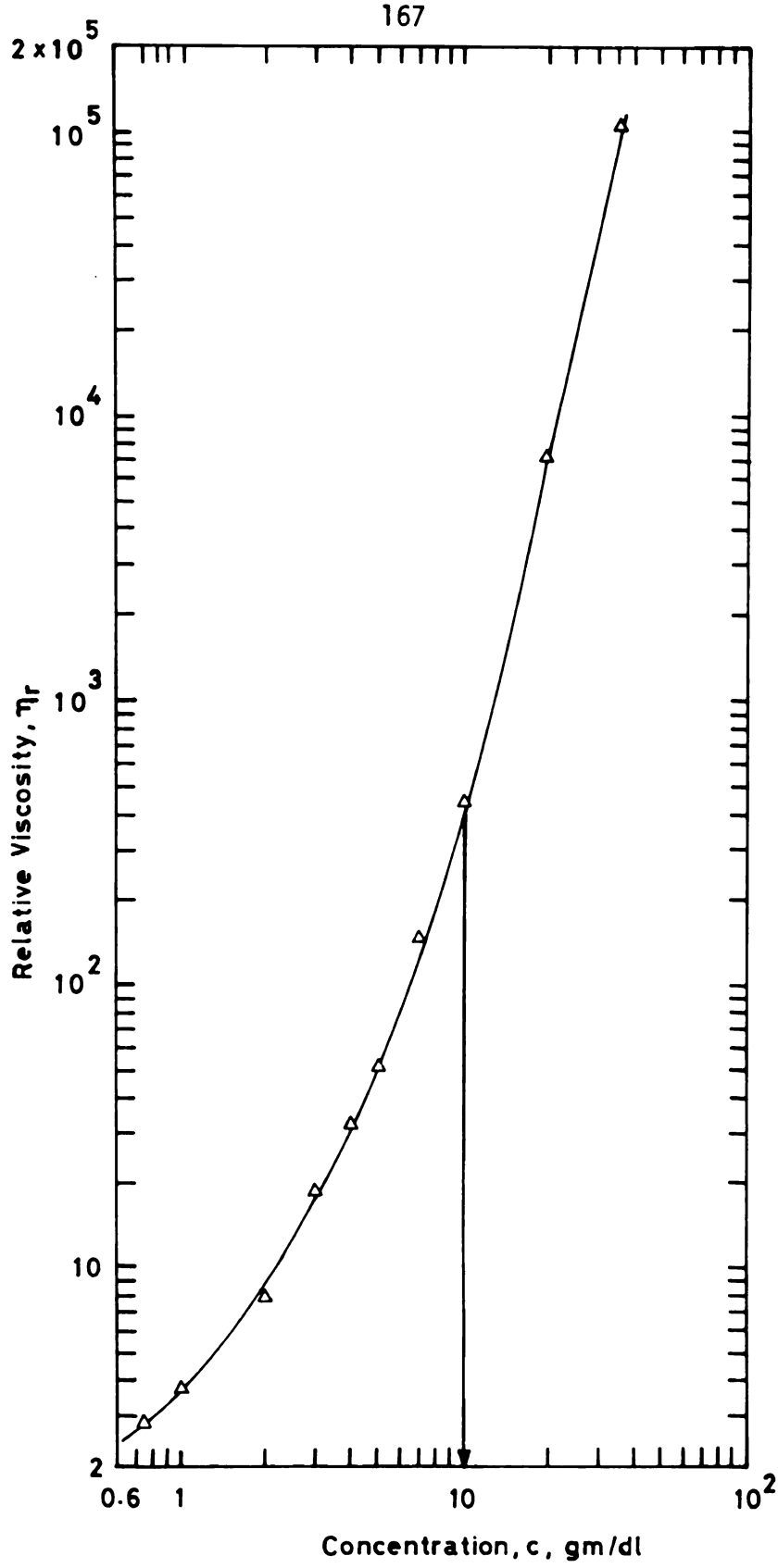

Figure 6.10.--Relative Viscosity, η_r, vs. Concentration, c, of SAN C-3 in DMF at 30°C.

Figure 6.11.--Relative Viscosity, η_r, vs. Concentration, c, of SAN C-3 in MEK at 30°C.

4x10^4
10^4
10^3
10^2
Relative Viscosity · η_r

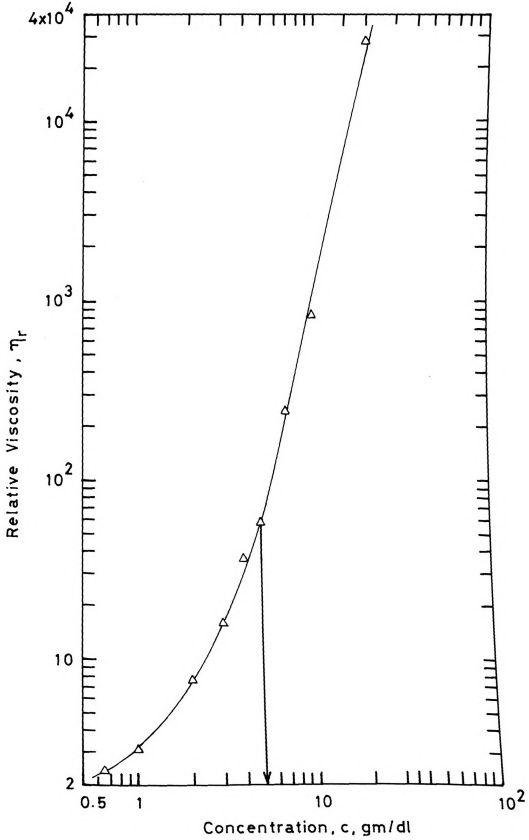
4x10^4
10^4
10^3
10^2
10
2
Relative Viscosity , η_r
0.5
1
10
10^2
Concentration, c, gm/dl

The val

obtained from E

value in good

SAA C-2 the val

since the exper

the range of co

predicted are v

ac events. In p

predicted since

experiment overl

is not with ti

expect that Eq.

for E 1 seems

the slope; of t

nature of the c

It is t

are based on ca

of the ... per y

... of ...

... the ...

... average ... o

... ...

... of ...

The value of c_{ent}, for the polymers, SAN C-2' and SAN C-3, obtained from Eq. 6.7 compares reasonably well with the observed value in good solvents for the respective polymers. For PS-1 and SAN C-2 the value of c_{ent} predicted by Eq. 6.7 seems to be too low since the experimental values are higher, perhaps even higher than the range of concentrations considered in this work. The values predicted are very different from the experimental values in poor solvents. In poor solvents the observed values are much less than predicted since Eq. 6.7 is based on the packing of polymer coils at incipient overlap, and in poor solvents, the polymer chains tend to coil up with tighter entanglements. It is therefore reasonable to expect that Eq. 6.7 may not hold for poor solvent solutions. Equation 6.7 seems to hold for solutions in better solvents where conditions of incipient overlap may exist due to the "unfolded" nature of the chains as opposed to coiled-up nature.

It is to be noted that most relations for predicting c_{ent} are based on observations in good solvents. This factor probably did not clearly bring out the influence of the nature of the solvent on c_{ent}. The observations in this work point out the necessity to use published relations for c_{ent} very carefully. Also, Porter and Johnson's approach cannot be applied to all the solvents. Unfortunately, more data must be obtained before the influence of solvent on c_{ent} may be theoretically explained in a quantitative manner.

C. Correlation Techniques

1. Power Law Correlation

The power law correlation is discussed in Chapter III. It has been commonly believed (F-2a, C-4, F-13, O-7) that η_r is independent of the solvent nature for values of $cM^{0.68}$ higher than the "critical" value. Thus, the equation

$$\eta_r \sim (cM^b)^\beta \tag{6.9}$$

with be equal to 0.68 or b equal to 0.625 and β equal to 5 contains no thermodynamic parameters.

In Figures 6.12 to 6.18, the power law correlation is used to correlate the data collected in this work. All the plots indicate that there is no sharp change in slope from 1 to 5 as the concentration increases from that typical of the equation for dilute solutions:

$$\eta_r = 1 + KcM^a \tag{6.10}$$

to that typical of concentrated solutions:

$$\eta_r \sim (cM^b)^\beta. \tag{6.11}.$$

Therefore, the evaluation of a "critical" entanglement point becomes either very subjective, or meaningless. The curves are smooth, indicative of a gradual change from one type of physical phenomenon to another. At very low concentrations of polymer in solvent, the chains exist as isolated clouds in a sea of solvent. The dependence

10^3
10^2
Relative Viscosity, η_r

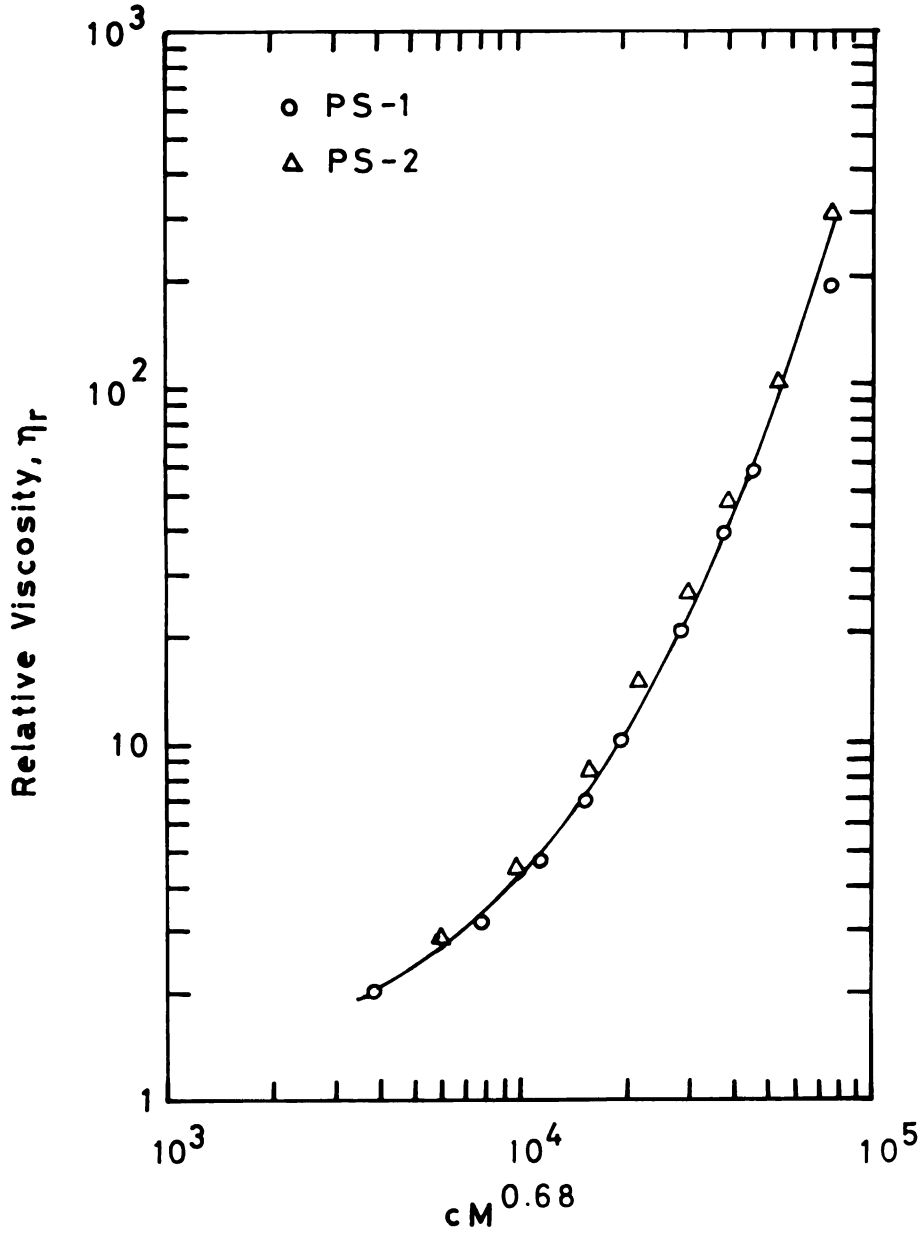

Figure 6.12.--Relative Viscosity, η_r, vs. $cM^{0.68}$ for PS in Benzene at 30°C.

4x10^3
10^3
10^2

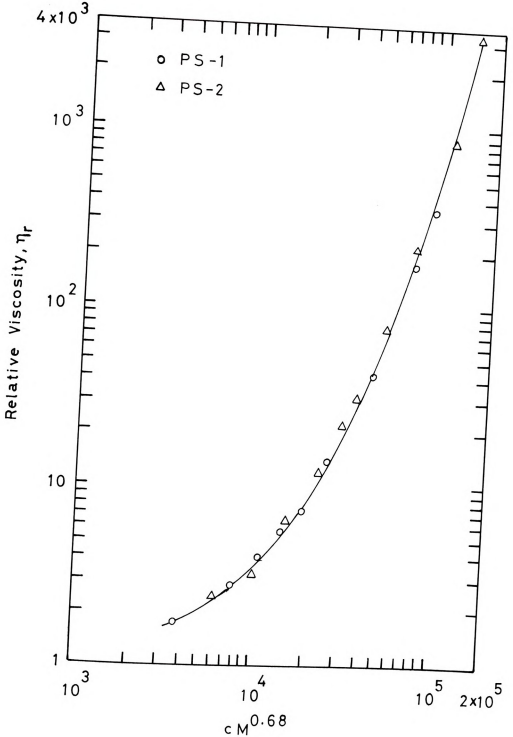

Figure 6.13.--Relative Viscosity, η_r, vs. $cM^{0.68}$ for PS in Dioxane at 30°C.

Relative Viscosity, η_r
10^3
10^2
10
1
10^{-3}

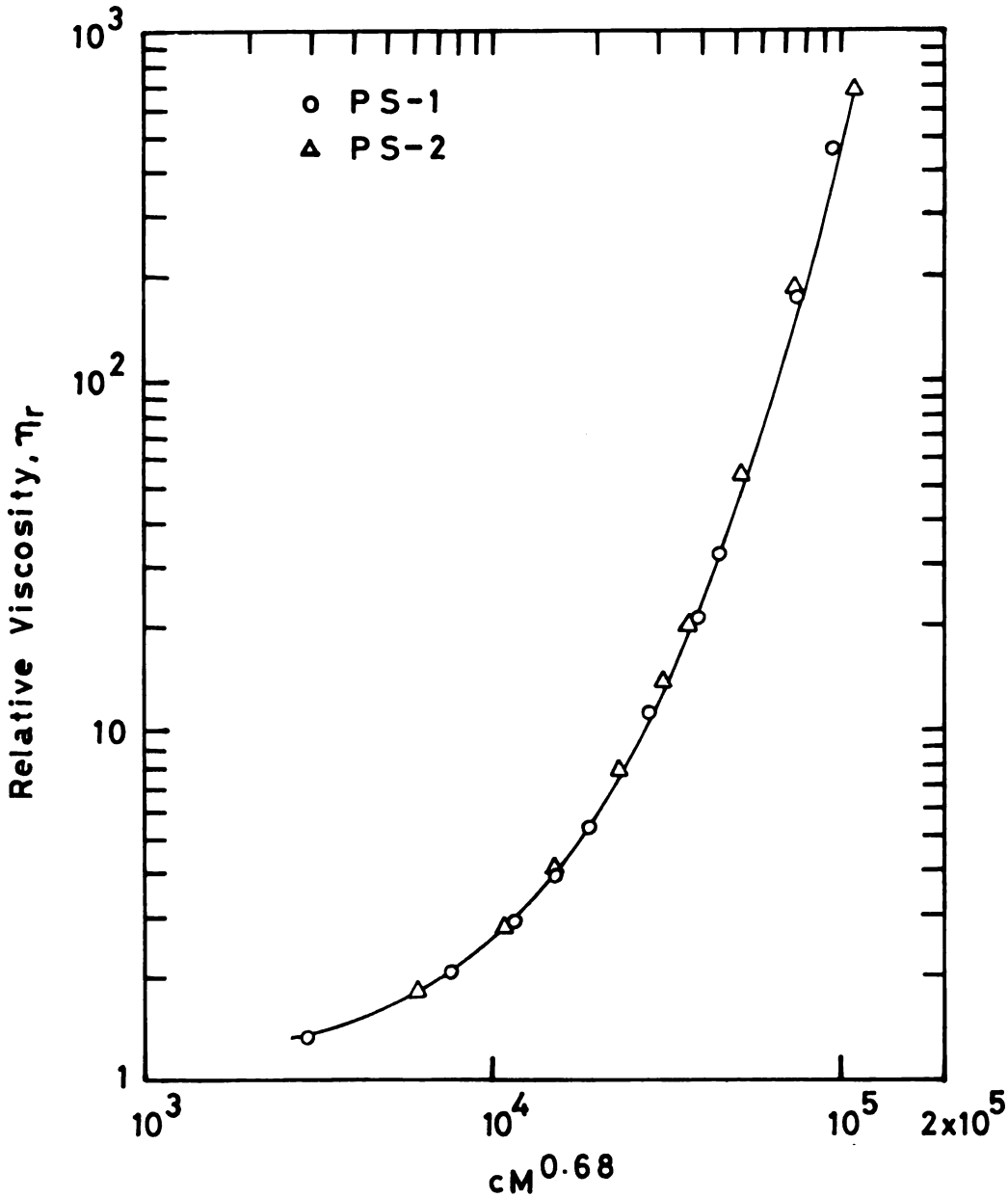

Figure 6.14.--Relative Viscosity, η_r, vs. $cM^{0.68}$ for PS in MEK at 30°C.

4x10^3
10^3
10^2
10
Relative Viscosity, η_r

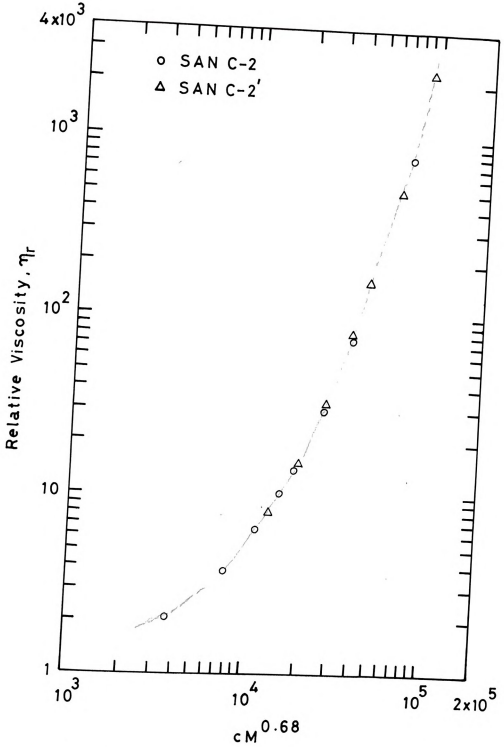

Figure 6.15.--Relative Viscosity, η_r, vs. $cM^{0.68}$ for SAN C-2 and SAN C-2' in Dioxane at 30°C.

4x10^3
10^3
10^2
10
Relative Viscosity, η_r

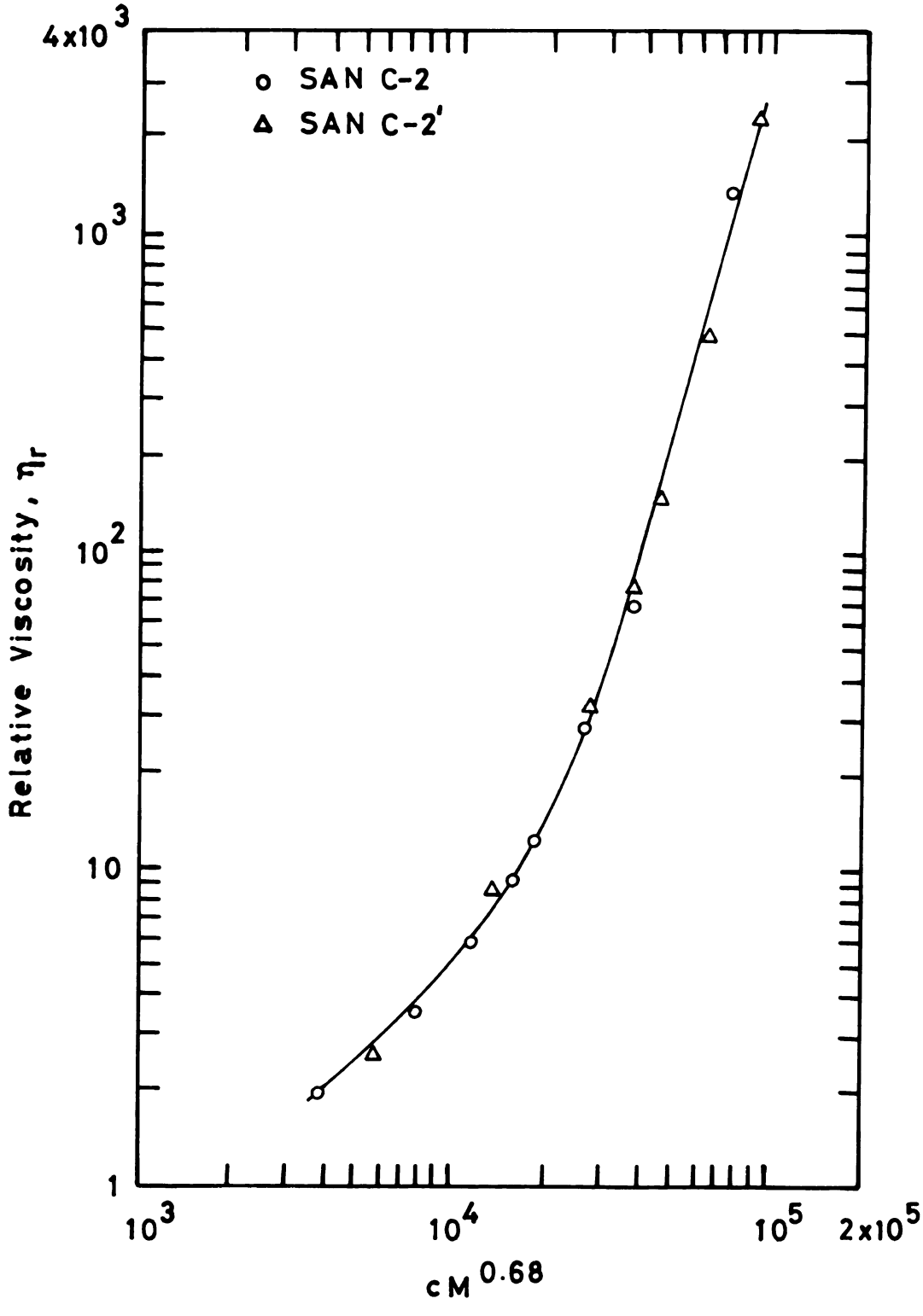

Figure 6.16.--Relative Viscosity, η_r, vs. $cM^{0.68}$ for SAN C-2 and SAN C-2' in MEK at 30°C.

Figure 6.17.--Relative Viscosity, η_r, vs. $cM^{0.68}$ for SAN C-2 and SAN C-2' in DMF at 30°C.

3x10^4
10^4
10^3
10^2
Relative Viscosity, η_r

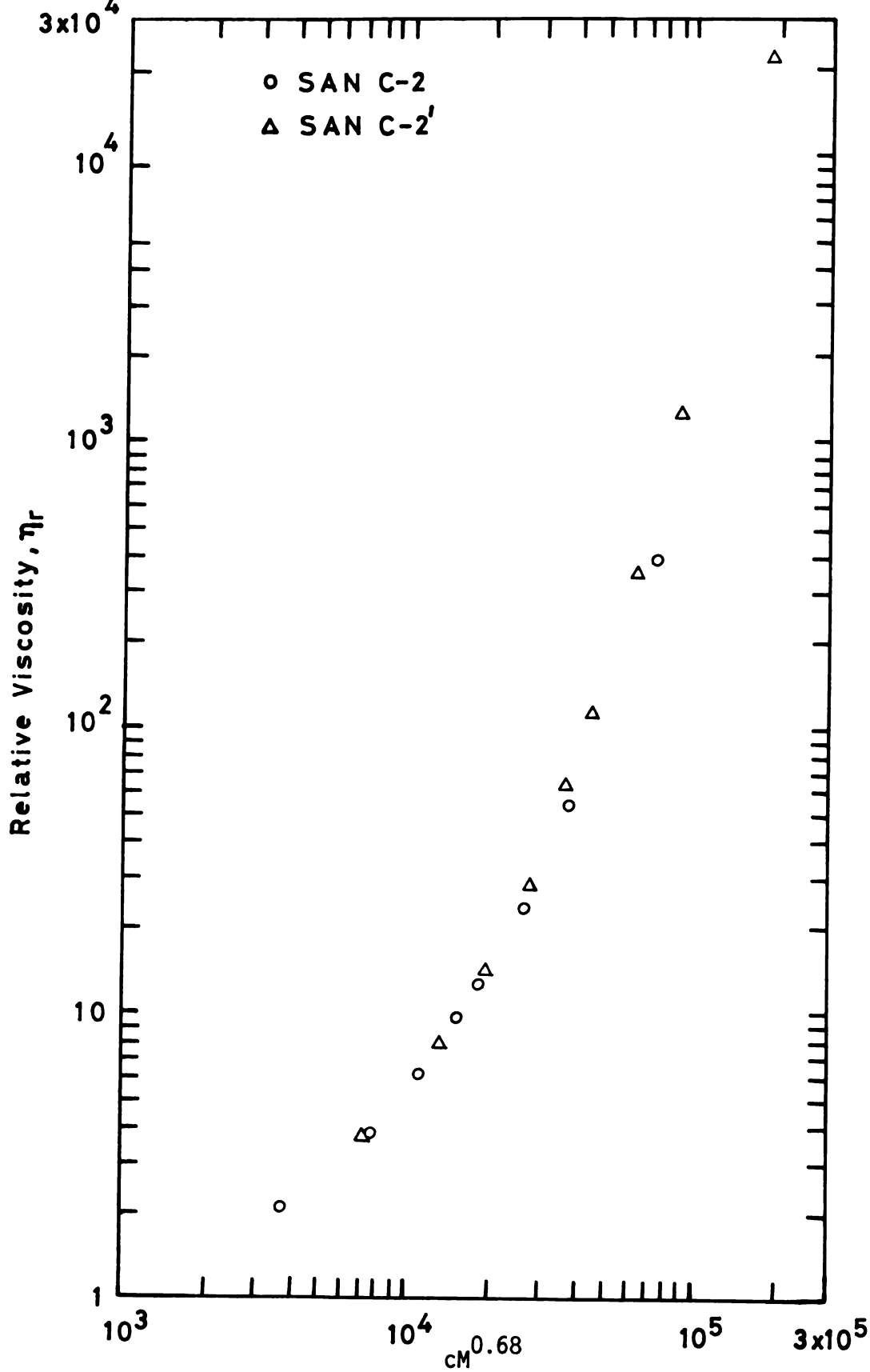
3x10^4
10^4
10^3
10^2
10
1
Relative Viscosity, η_r
o SAN C-2
Δ SAN C-2'
10^3
10^4
10^5
3x10^5
cM^0.68

8x10^3
10^3
10^2
Relative Viscosity, η_r

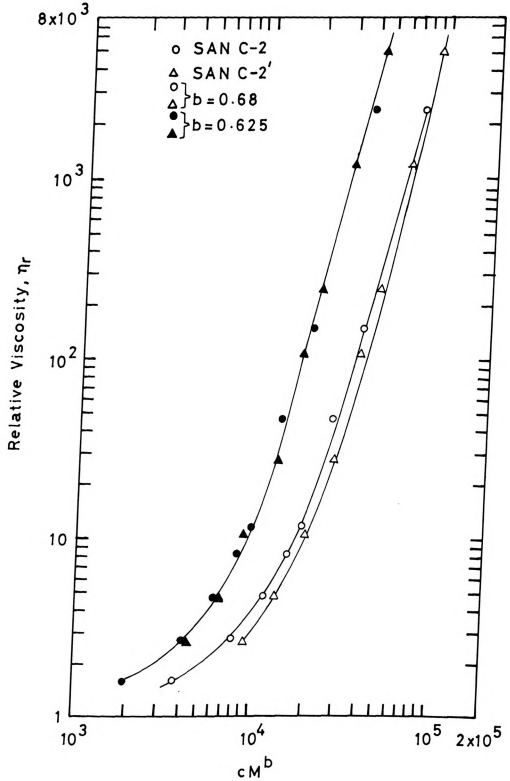

Figure 6.18.--Relative Viscosity, η_r, vs. cM^b for SAN C-2 and SAN C-2' in Benzene at 30°C.

of viscosity on concentration is linear and is indicated by Eq. 6.10. As the concentration increases, the polymer chains begin to overlap each other. At still higher concentration, they begin to penetrate each other and ultimately they become entangled. This gradual change from isolated clouds of polymer chains to entangled network is evident from the smooth curve. The curves indicate that the viscosity dependence increases gradually from $(cM^a)^1$ to $(cM^b)^5$.

Figures 6.12 to 6.14 show plots of η_r against $cM^{0.68}$ for PS-1 and PS-2 in benzene, dioxane and MEK, respectively. Figures 6.15 to 6.17 show plots for SAN C-2 and SAN C-2' in dioxane, MEK and DMF, respectively. The solvents may be labeled as good to fairly good. The data for the two molecular weights in each case are reasonably well correlated by the power law equation. The plots of η_r against $cM^{0.625}$ are not shown for these polymer-solvent systems; however, the exponent 0.625 also works well.

Figure 6.18 shows plots for SAN C-2 and SAN C-2' in benzene with both values of the exponent, b. Clearly, the correlation with the exponent 0.68 is not as effective as with the exponent 0.625. Two distinct curves are obtained for the two samples of azeotropic copolymers (SAN C-2 and SAN C-2') when using the 0.68 exponent, thus not correlating the data. Correlation with the power 0.625 shows a marked improvement in unifying the data for the azeotropic copolymers in benzene. Benzene is a poor solvent for this copolymer and it appears that for poor solvent-polymer systems a lower value of the exponent in this type of correlation produces an improvement. The data for SAN C-2 and SAN C-2' in benzene obtained in this work

lend support for lower exponents of M in the power correlations for poor solvent systems. As a result it may be suggested that a general correlation of the type

$$\eta_r \sim cM^a \qquad (6.12)$$

may be used where a may be related to the Mark-Houwink constant from intrinsic viscosity correlations (G-6). The exponent a depends upon the nature of the solvent and is usually found to lie between 0.5 and 0.8. For good solvents, a has high values (0.65-0.8) while for poor solvents a has low values (0.5-0.6), and for Θ-solvents a is equal to 0.5.

Figure 6.19 shows a plot of η_r against $cM^{0.5}$ for SAN C-2 and SAN C-2' in benzene. The correlation is not as good as the 0.625 correlation. This indicates that for this system, the value of the exponent lies between 0.5 and 0.625, probably closer to 0.625. This is due to the fact that benzene is not a Θ-solvent for azeotropic SAN copolymers at 30°C, but is quite a poor solvent which may have a Mark-Houwink exponent between 0.5 and 0.625, probably closer to 0.625.

The above data show that for one particular polymer in different solvents, a power law correlation, using a single value of exponent is not possible. In the past, most data have been obtained with good solvents and hence differences caused by polymer-solvent interactions were not observed. This led to the belief that the data in different solvents could be correlated by a single exponent.

7x10^3
10^3
10^2
10
1
2x1
Relative Viscosity, ηr

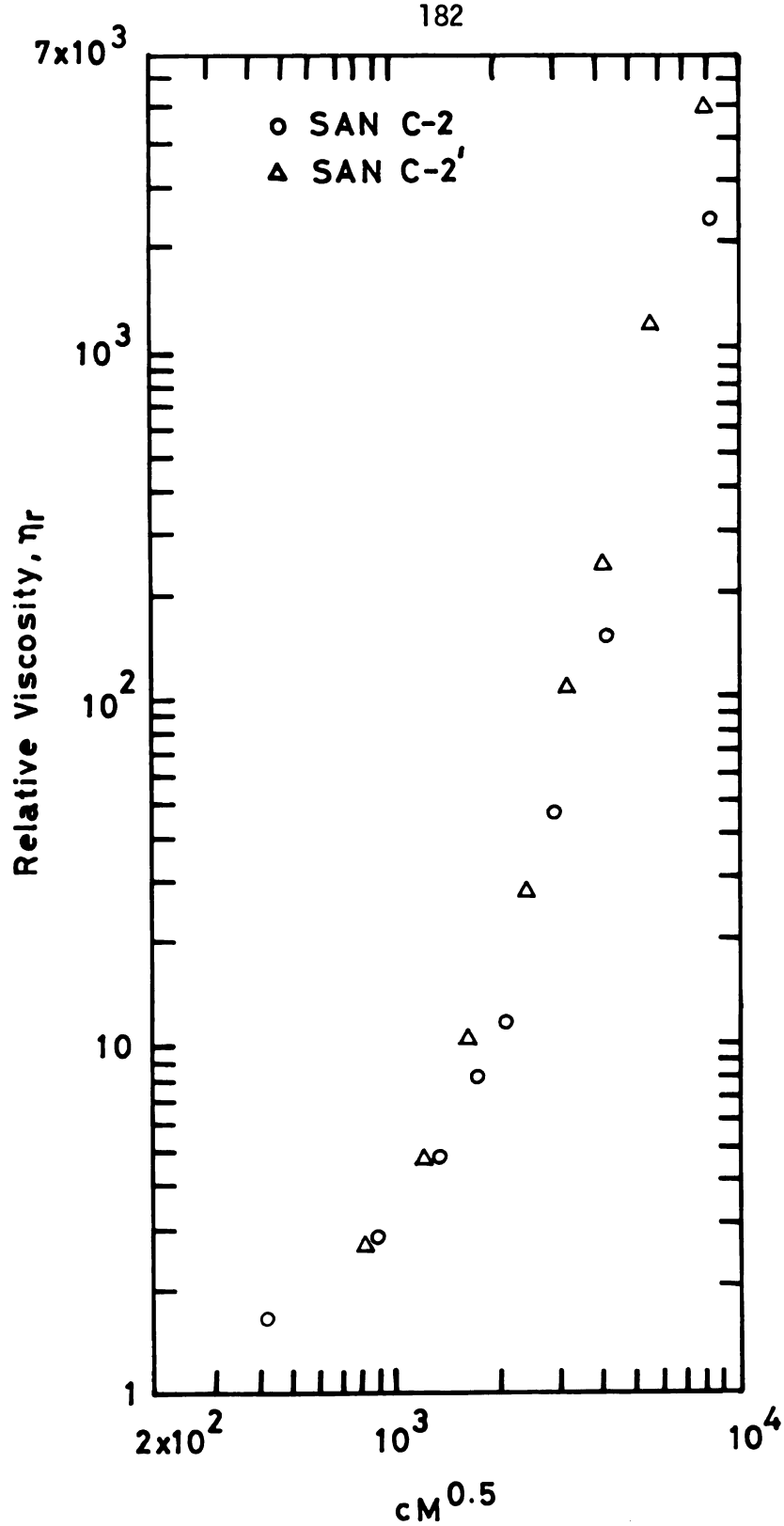

Figure 6.19.--Relative Viscosity, η_r, vs. $cM^{0.5}$ for SAN C-2 and SAN C-2' in Benzene at 30°C.

In summary

particular polymer

1. It cor
values
lower

2. The us
0.625
sider
and so

3 It giv
mer in
data i
the pa

4 The us
sliders
power
lead to

In summary it may be said for this correlation that for a particular polymer-solvent system:

1. It correlates c, M data in good solvents with higher values of exponent a and in poor solvents with lower values.

2. The use of the power b equal to 0.68 or b equal to 0.625 for all polymer-solvent systems does not consider thermodynamic interactions between polymers and solvents.

3. It gives different curves for one particular polymer in different solvents. Thus it does not unify data in different solvents as has been claimed in the past.

4. The use of the Mark-Houwink exponent directly considers these interactions since the value of the power depends on these interactions and hence may lead to a better correlation of data.

2. Simha Correlation

This correlation proposes that plots of $\eta_{sp}/c[\eta]$ versus c/γ should produce master curves independent of molecular weight of the polymer for a given polymer-solvent system. The parameter γ is a shift factor for each molecular weight. The details are given in Chapter III. Simha and Utracki (S-6) have tested the usefulness of this correlation for a variety of homopolymer-solvent systems. They used the solutions of relatively low concentration where extensive interpolymer contacts are not important. In this work this correlation is tested for azeotropic SAN copolymer (SAN C-2 and SAN C-2') in four solvents up to high concentrations.

To test this correlation for these copolymers, γ was chosen to be 1 for the low molecular weight sample. Then a suitable value of γ was found for the high molecular weight sample to produce

a superposed curve

which the plot for

become coincident

s the ratio of

is attain

correlation to be

values of ν_{sp}/

Table 6.7

ures Figures 6.7

ABLE 6.7.--Shift

Concen

Solven

Benzen	
	% 4(
	% 3(
	% 3(
	% 4(
	% 4(
	% 4(
	% 3(
	% 4(
	% 4(
	% 4(
	% 4(

a superposed curve. This value of γ represents the shift factor by which the plot for high molecular weight sample may be shifted to become coincident with the plot for lower M. Hence, the value of γ is the ratio of concentrations at which a specified value of $\eta_{sp}/c[\eta]$ is attained for both molecular weight samples. For the correlation to be successful, the value of γ should be the same at all values of $\eta_{sp}/c[\eta]$.

Table 6.7 lists the values of γ for all the systems considered. Figures 6.20 to 6.23 show plots of $\eta_{sp}/c[\eta]$ vs. c/γ with

TABLE 6.7.--Shift Factors, γ, for Superposition of Viscosity-Concentration Data of SAN C-2 and SAN C-2' in Various Solvents.

$\frac{\eta_{sp}}{c[\eta]}$	Benzene	MEK	Dioxane	DMF
2	--	0.34	0.42	
3	0.40	0.33	0.41	0.38
4	0.39	0.34	0.40	0.36
5	0.39	0.34	0.40	0.35
7	0.40	0.35	0.40	0.35
10	0.41	0.37	0.40	0.35
20	0.40	0.39	0.39	0.35
50	0.39	0.43	0.39	0.35
70	0.40	0.44	0.38	0.35
100	0.40	0.45	0.38	0.36
200	0.40	--	--	0.36
500	0.40	--	--	0.36

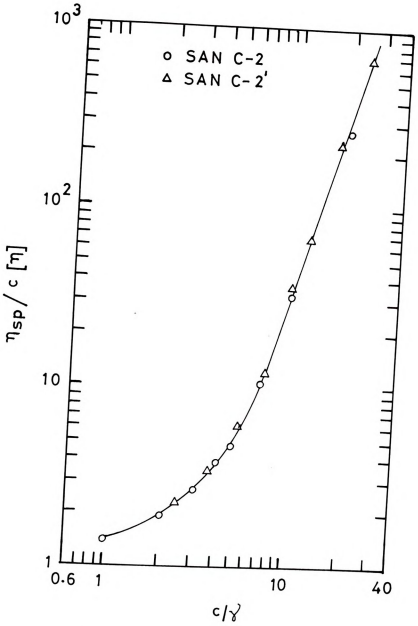

Figure 6.20.--Simha Plot for SAN C-2 and SAN C-2' in Benzene at 30°C.

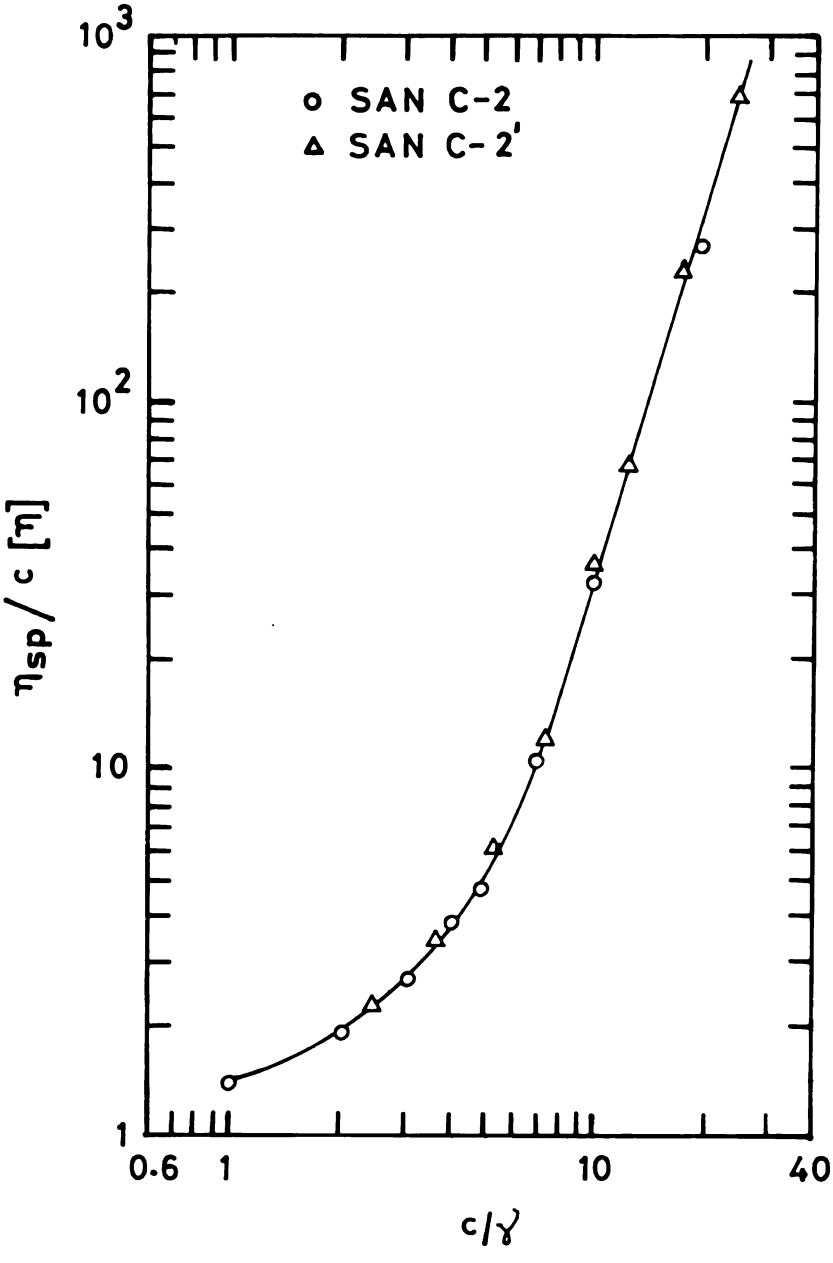

Figure 6.20.--Simha Plot for SAN C-2 and SAN C-2' in Benzene at 30°C.

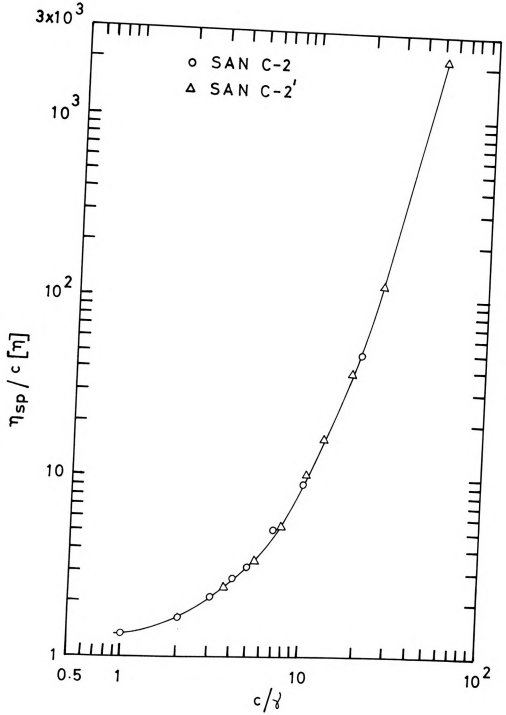

Figure 6.21.--Simha Plot for SAN C-2 and SAN C-2' in Dioxane at 30°C.

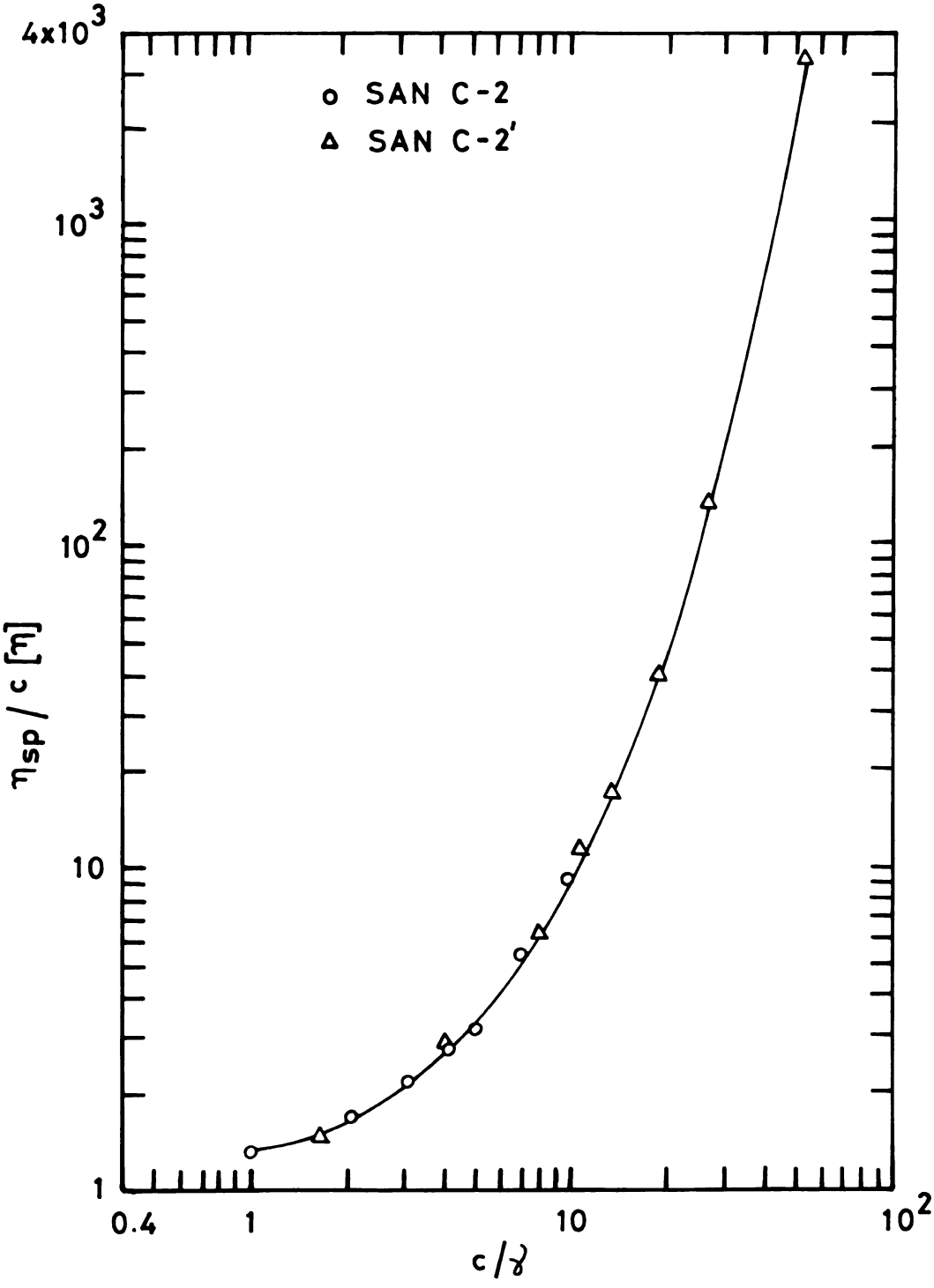

Figure 6.22.--Simha Plot for SAN C-2 and SAN C-2' in MEK at 30°C.

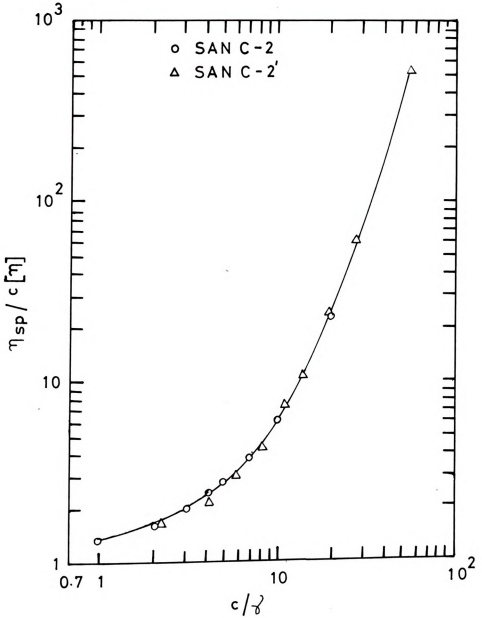

Figure 6.23.--Simha Plot for SAN C-2 and SAN C-2' in DMF at 30°C.

γ value of 0.4 in benzene, 0.4 in dioxane, 0.37 in MEK and 0.36 in DMF. As can be seen from Table 6.7, for benzene and DMF solutions, the correlation works well up to the highest values of $\eta_{sp}/c[\eta]$ attained in this work. For dioxane and MEK solutions there is a deviation in γ values at high concentrations, the deviation being higher in MEK. In these two cases, the correlation works well up to $\eta_{sp}/c[\eta]$ equal to 7 to 10. An interesting feature is that the values of γ for non-polar solvents (dipole moment being zero) benzene and dioxane, and for polar solvents, MEK and DMF, are similar; the values for non-polar solvents being slightly higher. The exact effect of deviations at higher concentrations cannot be evaluated unless the data on a larger number of samples with varying molecular weights are available. In spite of the variations at high concentrations in the two cases mentioned above, the data of this work support the applicability of Simha's correlation method to systems containing different thermodynamic interactions.

For this correlation it may be said that:

1. It unifies the c, M data quite well up to high concentrations, i.e., concentrations beyond which $\eta_{sp}/c[\eta] > 10$. (The data of Simha and Utraki (S-6) did not exceed concentrations beyond which $\eta_{sp}/c[\eta] > 10$.)

2. Different curves are obtained for different polymer-solvent systems. The data cannot be unified for the same polymer in different solvents with a single value of γ in each case. The shift factors are specific for particular polymer-solvent pairs.

3. In the absence of the values of intrinsic viscosity, $[\eta]$, this correlation is not useful.

D. Williams Model for Zero Shear Viscosity

The correlation techniques described previously are not useful in predicting the low shear viscosity, η_r, of a polymer solution of known concentration if the appropriate data are not available. A general equation for η_r in powers of c is

$$\eta_r = 1 + c[\eta] + k_1[\eta]^2c^2 + k_2[\eta]^3c^3 + k_3[\eta]^4c^4 + \cdots \quad (6.13)$$

This equation is discussed in Chapter III. To predict η_r of a polymer solution of known concentration, $[\eta]$, k_1, k_2, etc. must be known. Thus far attempts have been made to predict k_1 (I-2, P-5). The series can be truncated to the c^2 term at low concentration to give an equation of Huggins

$$\eta_{sp}/c = [\eta] + k_1[\eta]c \quad (6.14)$$

where k_1 is called Huggins constant.

Imai made an exact calculation of k_1 from the pearl necklace model. He evaluated Eq. 3.51 for the stress tensor, however, the procedure followed is rather tedious because of the mathematical complexity involved in attempting to obtain a rigorous solution that includes solvent effects. The solvent effects were included in terms of the coil expansion factor, α. A discussion on α is given in Chapter III. His result was

$$k_1 = k_\Theta/\alpha^4 + \bar{k}z/\alpha^5 \quad (6.15)$$

where k_Θ is the Huggins constant at Θ-condition, and $\bar{k}$ is a constant unspecified by Imai.

$$z = (3/2\pi)^{3/2} A_2 N^{1/2}/b^3 \tag{6.16}$$

where A_2 is the segment-solvent second virial coefficient, which is zero at Θ-condition, N is the number of segments per molecule and b is the segment dimension.

Another method of predicting k_1 is the one proposed by Peterson and Fixman (P-5). The polymer molecules in this model are considered as spheres penetrable by other polymer molecules when there is a contact between two polymer molecules, but impermeable to solvent. The solvent simply flows around the spheres. In this calculation they included hydrodynamic interactions to the perturbations in a flow field caused by different polymer "spheres." This led to the calculation of the Huggins constant for penetrable spheres. Since polymer molecules can penetrate each other, they were assumed to form temporary doublets and the doublets were assumed to behave like rigid dumbbells. In their calculation solvent effects were considered and the result obtained was

$$k_1 = 0.69 + 0.16\, f(A) \tag{6.17}$$

where

$$A = \frac{3\, N^2 A_2}{8\pi r^3}, \tag{6.18}$$

r is the radius of a single polymer sphere, f(A) is a graphical function presented in (P-5) and f(A) has a maximum which means the predicted k_1 has a maximum. Such a maximum has not been experimentally observed. Also, another serious objection to this treatment is that the polymer spheres are considered impenetrable to solvent instead of treating them as porous spheres.

Both of the above methods of calculation of k_1 have limited application to engineering or industrial purposes since Imai's parameters k_Θ and $\bar{k}$ are not defined and Peterson's function, f(A), does not agree with experimental observations.

Williams (W-1) proposed a model to apply specifically to moderately concentrated polymer solutions. The details of the derivation of the model are given in Chapter III. The equation for low shear viscosity, η_r, is

$$\eta_r = 1 + \left(\frac{cN_{AV}}{M}\right)^2 \frac{A}{kT} B^{3/2} C\xi. \tag{6.19}$$

All the terms are defined in Chapter III. One good feature of this model is that all the parameters involved can be estimated or measured directly. An inquiry of the dependence of η_0 on concentration, c, and molecular weight, M, warrants a closer examination of the parameters involved in the above equation. In Eq. 6.19, B is a measure of effective molecular size in terms of the end-to-end distance of the polymer molecules. The distortion of molecular configuration by intermolecular interaction is appreciable in dilute solutions (F-3e), but when the polymer concentration is large, the perturbation in dimensions tends to be less. Then the polymer end-to-end distance may be approximated by its Θ-value, L_0. Hence Williams proposed that

$$B = 3/2 \langle L_0^2 \rangle. \tag{6.20}$$

A discussion on L_0 is given in Chapter III. The value of $\langle L_0^2 \rangle$ for each polymer can be obtained from the knowledge of the Mark-Houwink constant, K, for each polymer at its Θ-condition by using

$$K = \Phi(\langle L_0^2 \rangle / M)^{3/2} \tag{6.21}$$

in which Φ is a constant and is equal to 2.5×10^{21} dl/[(mole)(cm^3)] for broad molecular weight polymers (B-4a). The values of K are listed in Table 6.1. From these K values, $\langle L_0^2 \rangle$ and hence B can be easily calculated using Eqs. 6.21 and 6.20, respectively.

The key parameter for polymer-solvent intermolecular forces is A.

$$A = V_p^2 \frac{d^2\varepsilon}{dv_p^2} \tag{6.22}$$

where V_p is the molecular volume of a polymer molecule, ε is the Gibbs free energy of mixing polymer segments with solvent and v_p is the volume fraction of polymer. Williams (W-1) chose the Flory-Huggins form for ε (F-3a), which is

$$\varepsilon = kT[n_s \ln (1 - v_p) + n_p \ln v_p + \chi_1 v_p n_s] \tag{6.23}$$

where n_s and n_p are, respectively, the number of solvent and polymer molecules per unit volume of solution and χ_1 is a dimensionless quantity that characterizes interaction between the solvent and the polymer; i.e., it is an enthalpy and entropy of mixing parameter.

The quantity, $kT\chi_1$, represents merely the difference in energy of a solvent molecule immersed in the pure polymer compared with one surrounded by molecules of its own kind, i.e., in the pure solvent (F-3a). The parameter χ_1 is called the Flory thermodynamic parameter.

As polymer molecular weight becomes very high, n_p becomes vanishingly small and then

$$\varepsilon = kT[n_s \ln (1 - v_p) + \chi_1 v_p n_s]. \tag{6.24}$$

If V_s is the molecular volume of solvent, then

$$n_s V_s = (1 - v_p) \tag{6.25}$$

whereby

$$\varepsilon = \frac{kT}{V_s} (1 - v_p)[\ln (1 - v_p) + \chi_1 v_p] \tag{6.26}$$

and

$$\frac{d^2\varepsilon}{dv_p^2} = \frac{1}{1 - v_p} - 2\chi_1 + 2(1 - 2v_p) \frac{d\chi_1}{dv_p}$$

$$+ v_p(1 - v_p) \frac{d^2\chi_1}{dv_p^2} . \tag{6.27}$$

As a first approximation, only the first two terms on the right-hand side of Eq. 6.27 will be considered, although for a few systems χ_1 has been found to be a function of v_p (H-7). Combining Eqs. 6.22 and 6.27,

$$\frac{A}{kT} = \frac{V_p^2}{V_s}\left[\frac{1}{1 - v_p} - 2\chi_1\right] . \qquad (6.28)$$

The volume fraction, v_p, was calculated from concentration c by assuming additivity of volumes. From the χ_1 values listed in Table 6.5 and Eq. 6.28, A/kT could be calculated.

The parameter C of Eq. 6.19 is given as a function of B, c, and A/kT as

$$C = \frac{1}{30\sqrt{2\pi}}\left[\frac{3.53}{\sqrt{2B \ln\left(\frac{N_{AV}c}{M}\frac{A}{kT}\right)}}\right]^5 . \qquad (6.29)$$

For evaluation of ξ, Williams (W-1) used Kirkwood's original theory of friction coefficient (K-11). Kirkwood derived an expression for ξ in terms of intermolecular potential energy between polymer molecules. This formulation has been used with fair success in calculating the viscosity of simple liquids such as argon (K-3). In a polymer solution, since the solvent is assumed to be present as a continuum, it exerts a frictional resistance to polymer molecules. However, Williams assumed that the frictional forces between overlapping and entangling polymer molecules are the dominant factor in comparison to the polymer-solvent friction. The evaluation of ξ was done in terms of A/kT and it was found to be weakly dependent on c. The original model gave values of η_r far too low for polymer-solvent systems considered in this work in comparison with the experimental values. The deficiency was believed to be caused by underestimates

of ξ. The values of ξ (of the order of 10^{-11}) obtained from the model were believed to be far too low in magnitude. From the values of diffusion coefficients at infinite dilution, an estimate of the order of magnitude of the friction coefficient can be made by using the equation (M-2a),

$$D = \frac{kT}{f} \tag{6.30}$$

where D is the diffusion coefficient at infinite dilution, f is the friction coefficient at infinite dilution, k is the Boltzmann constant and T is the absolute temperature. The parameter f is found to be of the order of 10^{-8} (B-4a).

The analogy of Williams between simple molecules like that of argon and complex polymer molecules in solution where interactions between like and unlike molecules are believed to be strong and complex is deficient in concept. Again in Williams formulation of ξ, the viscosity of solvent, η_s, is not involved at all. This is equivalent to the assumption that only interpolymer frictional forces are important and hydrodynamic frictional forces between polymer and solvent are unimportant. This deficiency has led to an alternative formulation for friction coefficient based on a model of concentrated suspension of spheres (G-6, F-11).

Frankel and Acrivos (F-11) used an asymptotic technique to derive the dependence of viscosity on concentration for a suspension of uniform solid spheres. Their result contains no empirical constants. The analysis of viscosity of a suspension of arbitrary concentration is an extremely difficult problem but their simple

approach to an asymptotic model for the viscosity of highly concentrated suspension of rigid spheres agrees well with the limited available data on suspensions. They assumed that the suspension behaved as a Newtonian continuum on a macroscopic scale. The adopted point of view was that the viscous dissipation of energy in highly concentrated suspensions arises mainly from the flow within the narrow gaps separating the solid spheres from one another. The relative motion of each sphere can be decomposed into two components, one along the axis joining the centers of the spheres and another normal to it. They indicated that the frictional force due to the motion of the spheres along the axis joining their centers is the dominant force. Then the frictional force from the rate of viscous dissipation is given by

$$F = 3\pi\eta_s U \frac{r^2}{h - 2r} = \xi' U \tag{6.31}$$

where U is the approach velocity of the fluid, ξ' is the friction coefficient, h is the gap width between two spheres, and r is the radius of the spheres. Thus,

$$\xi' = \frac{3\pi\eta_s r^2}{h - 2r} . \tag{6.32}$$

Assuming polymer coils to be spheres of radius of gyration $\langle S^2 \rangle^{1/2}$, we may write

$$\xi' = \frac{3\pi\eta_s \langle S^2 \rangle}{h - 2\langle S^2 \rangle^{1/2}} . \tag{6.33}$$

One serious drawback is that Eq. 6.31 is for hard spheres with undeformable boundaries while the equivalent polymer spheres are not so rigid. This means that when the concentration of polymer in solution is very high, leading to highly entangled chains, ξ' would not be applicable. Furthermore, when h is equal to $2\langle S^2\rangle^{1/2}$ or when the spheres are in contact with each other (which may occur at some high concentration before they are entangled), $\xi' \to \infty$. To alleviate this problem, Gandhi (G-6) made the following simplifications:

$$\xi' = 3\pi\eta_s \langle S^2\rangle / h \tag{6.34}$$

where

$$h = (M/cN_{AV})^{1/3}. \tag{6.35}$$

Equation 6.32 for ξ' represents purely hydrodynamic interactions between polymer and solvent and there is no accounting of polymer-solvent thermodynamic interaction. At sufficiently high concentrations, $\langle S^2\rangle^{1/2}$ can be taken at Θ-condition (F-3e). The predicted values of ξ' by Eq. 6.34 were found to be of the correct order of magnitude, 10^{-8}.

In the absence of data on friction coefficient at high concentrations, Eq. 6.34 can be used. It should also be mentioned that the use of $\langle S^2\rangle^{1/2}$ assumes the polymer sphere to be impermeable to solvent. This is not true in actual cases. Hence Eq. 6.34 gives an overestimation of friction. It must be kept in mind that both Williams equation and ξ' are applicable only in the absence of significant entanglements. These equations are not adequate

descriptions of phenomena observed beyond the onset of entanglement mechanisms.

Williams' model can be tested for predicting η_r using ξ' since all the parameters are known or can be calculated. The equation, after reinstating the linear term in c, may be rewritten as

$$\eta_r = 1 + [\eta]c + \frac{1}{\eta_s}\left[\frac{cN_AV}{M}\right]^2 \left(\frac{A}{kT}\right)(B)^{3/2}(C\xi'). \qquad (6.36)$$

This is the only available model for η_r where hydrodynamic and thermodynamic effects are accounted for with independently measurable properties.

Figures 6.24 to 6.26 show plots of experimental and predicted low shear relative viscosity, η_r, against concentration, c, for PS-1 in benzene, dioxane and MEK, respectively. The plots are made on semi-log papers to accommodate the complete range of η_r values. Figures 6.24 and 6.25 show that in good solvents the Williams equation over-predicts the values of η_r; that the two curves run parallel up to about c equal to 7.5 gm/dl; and that then the predicted values of η_r do not increase as fast as the experimental values. In the case of PS-MEK (Fig. 6.26), this deviation is observed at lower concentration. This is completely in agreement with Williams' model. The limitations and assumptions involved in the derivation of the model suggest that high concentration behavior could not be described within its framework. This means viscosity at high concentrations cannot be predicted.

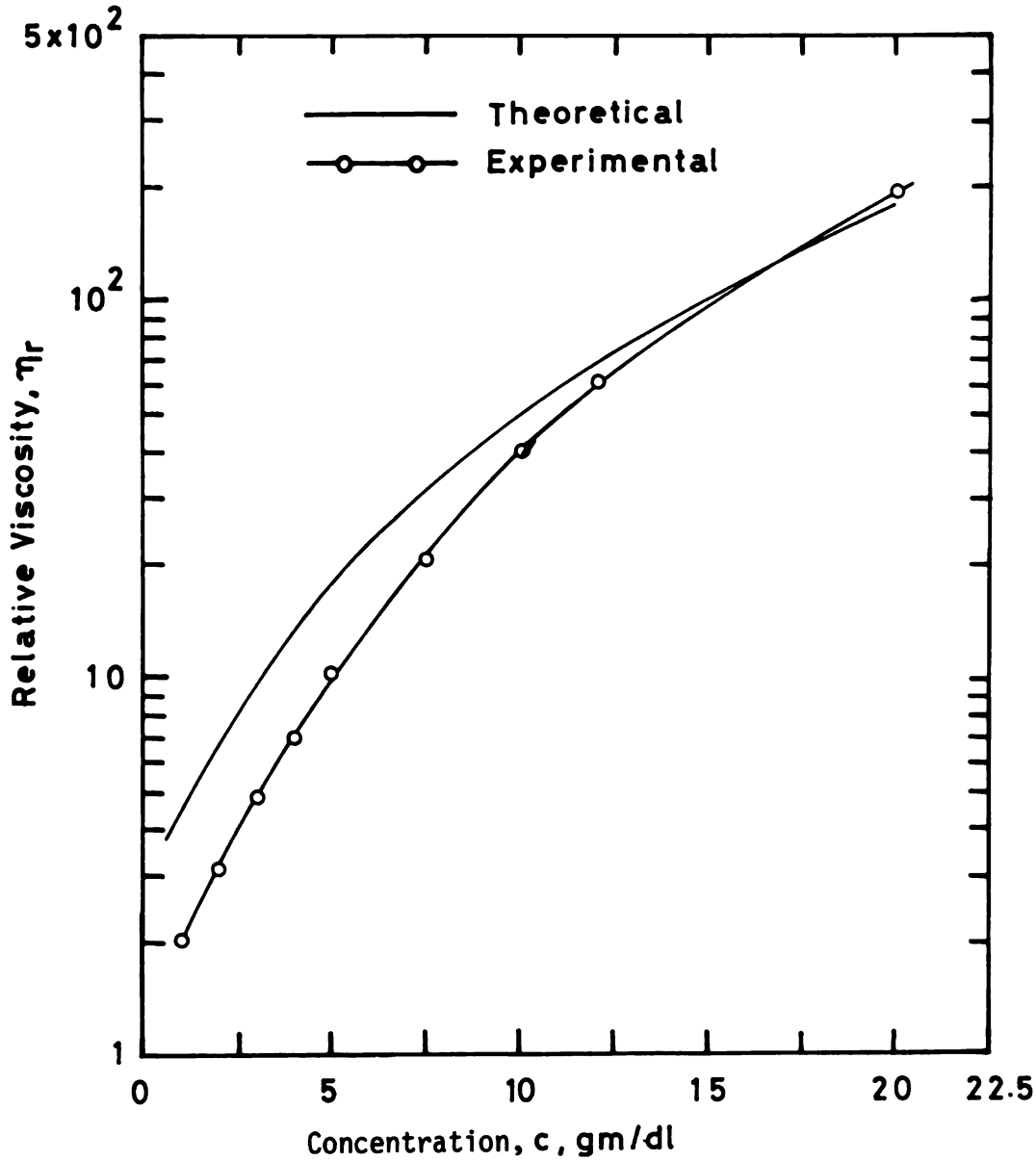

Figure 6.24.--Experimental and Calculated Relative Viscosity, η_r, vs. Concentration, c, of PS-1 in Benzene at 30°C.

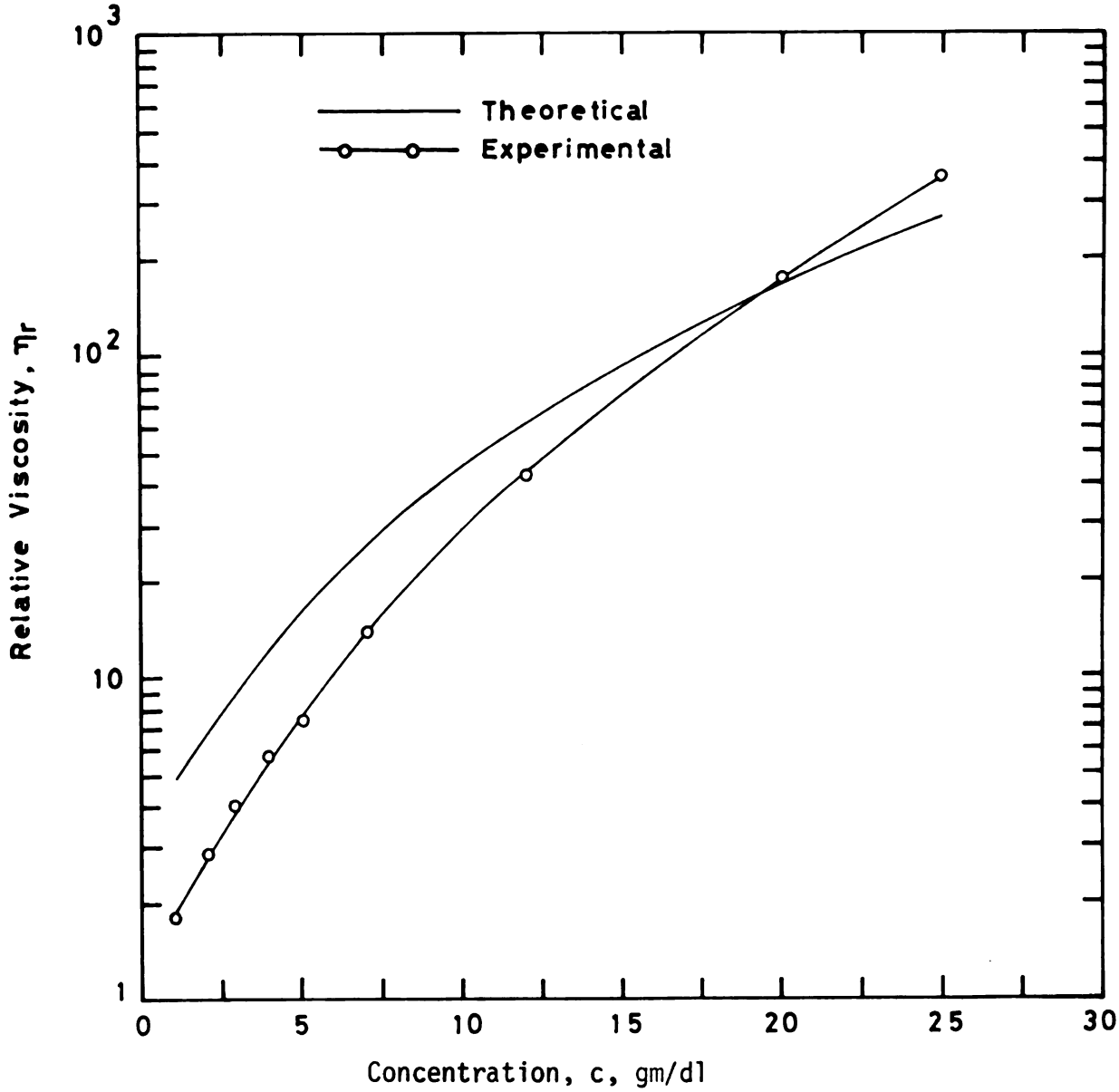

Figure 6.25.--Experimental and Calculated Relative Viscosity, η_r, vs. Concentration, c, of PS-1 in Dioxane at 30°C.

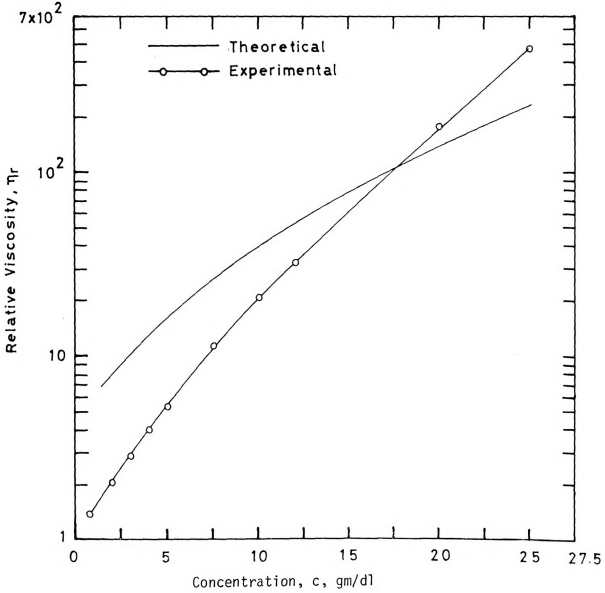

Figure 6.26.--Experimental and Calculated Relative Viscosity, η_r, vs. Concentration, c, of PS-1 in MEK at 30°C.

This is precisely shown in Figs. 6.24 to 6.26. The model is valid only for moderate concentrations. In MEK, the entanglements are enhanced at lower concentrations since it is a poor solvent for PS compared with benzene and dioxane and hence the deviation of predicted values from observed values is at lower concentration. Since Williams' model does not take into consideration the entanglements or aggregation it should be applicable to higher polymer concentrations in better solvents in comparison with poor solvents. The figures show qualitative success of the model. The difference between the predicted and experimental values differ by a fairly constant factor up to the concentrations when entanglements become important. Figures 6.27 and 6.28 show plots for PS-2 in dioxane and MEK, respectively. For this high molecular weight PS, entanglements become important at lower concentrations than for low molecular weight PS. The predicted values are much closer to experimental values in the good solvent, dioxane, than in the poor solvent, MEK.

Figures 6.29 to 6.32 show the same plots for SAN C-1 in all the four solvents. Here benzene and dioxane are fairly good solvents while MEK becomes relatively poorer, and DMF becomes a better solvent for this polymer than it was for PS. The effect of this change in degree of goodness is observed on the plots. Figure 6.31 (DMF solution) clearly shows that up to a relatively high concentration, 10 gm/dl, the two curves are parallel.

Figures 6.33 to 6.35 show plots for SAN C-2 in DMF, MEK and dioxane, respectively. For this polymer, DMF is the best solvent and this is obvious from the comparison of the three plots.

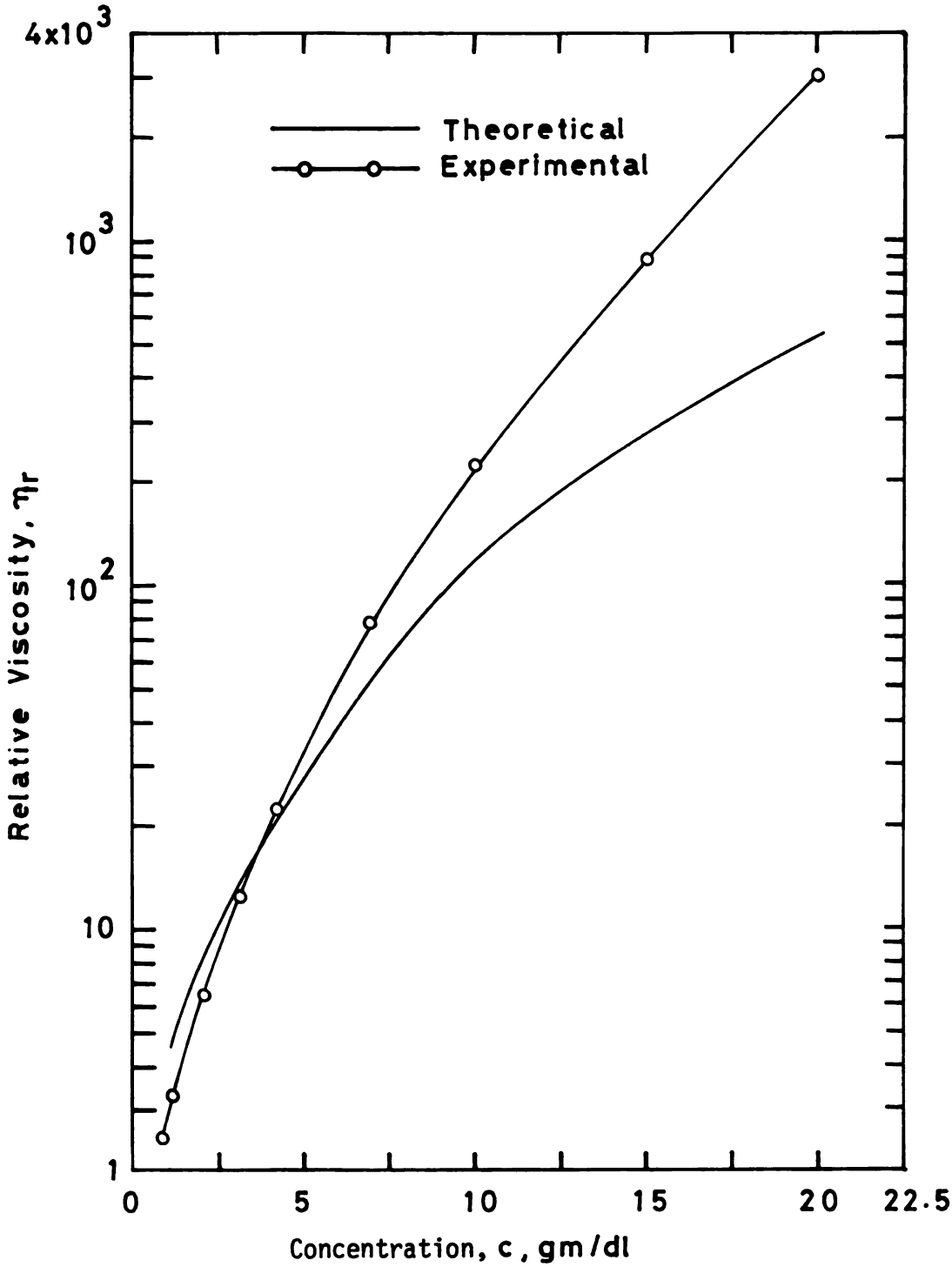

Figure 6.27.--Experimental and Calculated Relative Viscosity, η_r, vs. Concentration, c, of PS-2 in Dioxane at 30°C.

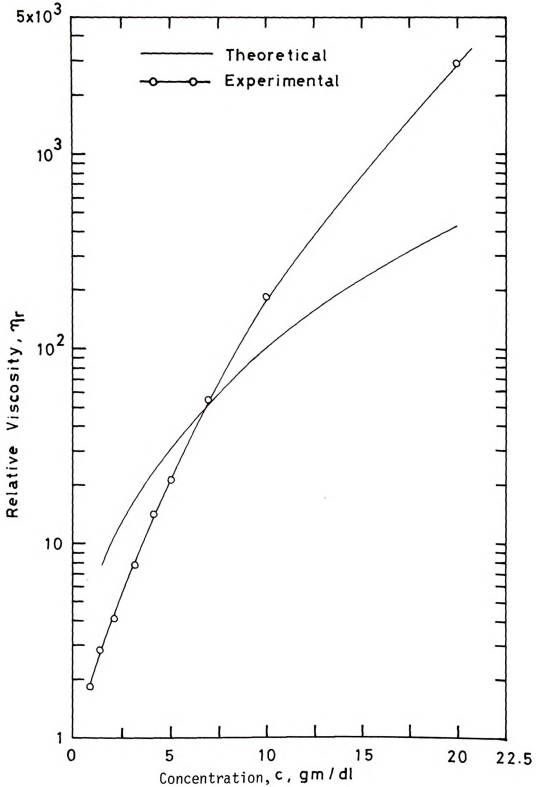

Figure 6.28.--Experimental and Calculated Relative Viscosity, η_r, vs. Concentration, c, of PS-2 in MEK at 30°C.

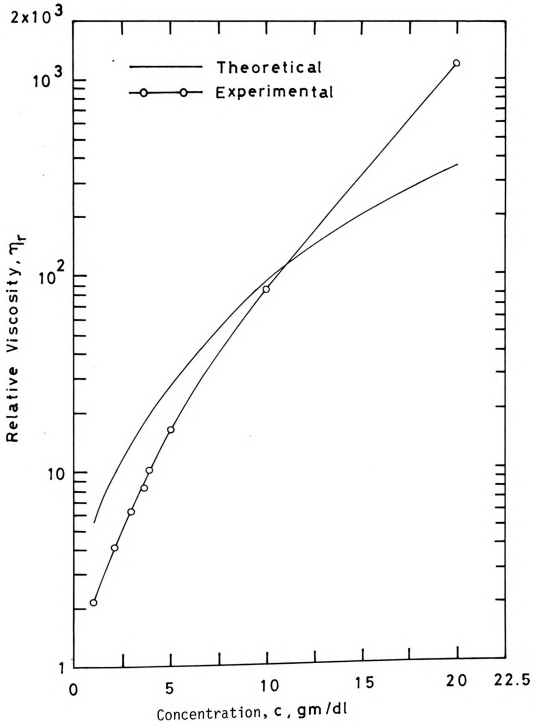

Figure 6.29.--Experimental and Calculated Relative Viscosity, η_r, vs. Concentration, c, of SAN C-1 in Benzene at 30°C.

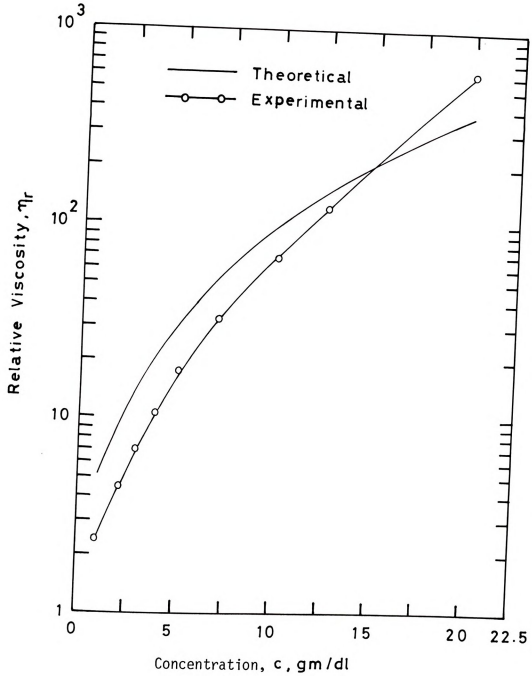

Figure 6.30.--Experimental and Calculated Relative Viscosity, η_r, vs. Concentration, c, of SAN C-1 in Dioxane at 30°C.

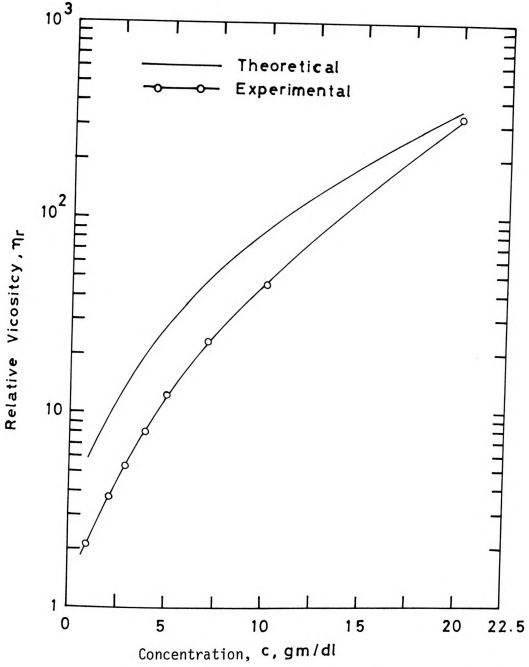

Figure 6.31.--Experimental and Calculated Relative Viscosity, η_r, vs. Concentration, c, of SAN C-1 in DMF at 30°C.

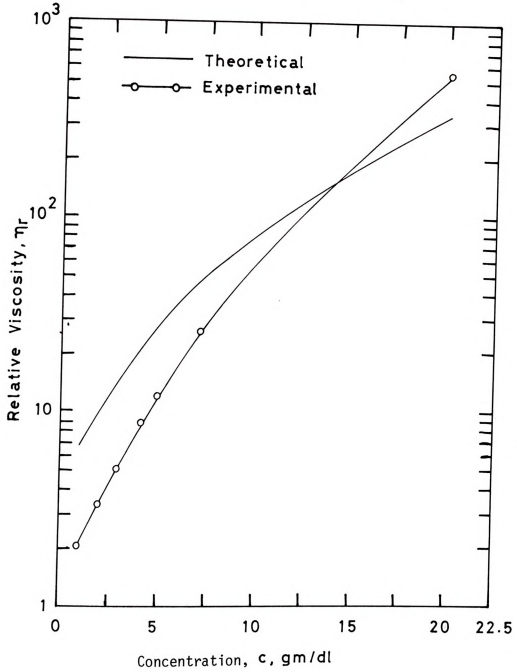

Figure 6.32.--Experimental and Calculated Relative Viscosity, η_r, vs. Concentration, c, of SAN C-1 in MEK at 30°C.

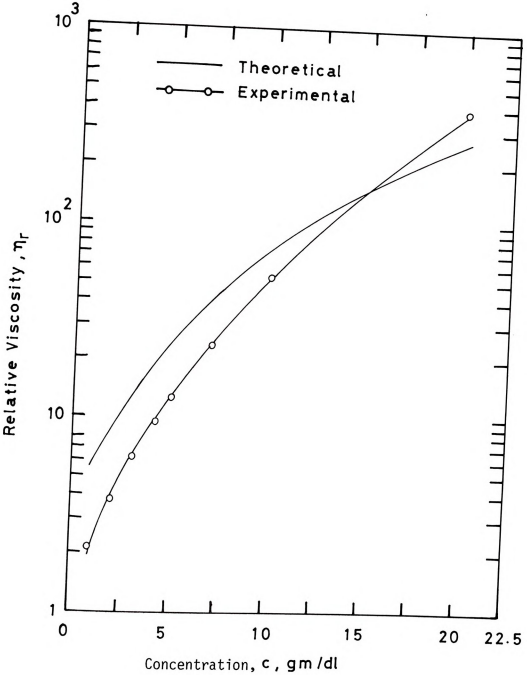

Figure 6.33.--Experimental and Calculated Relative Viscosity, η_r, vs. Concentration, c, of SAN C-2 in DMF at 30°C.

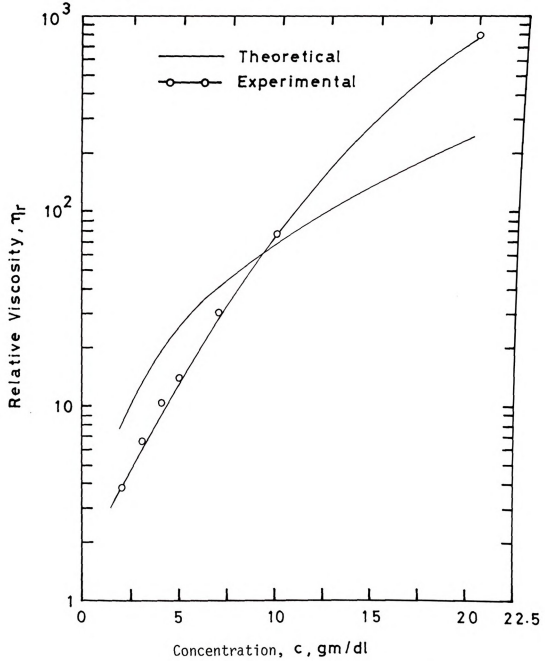

Figure 6.34.--Experimental and Calculated Relative Viscosity, η_r, vs. Concentration, c, of SAN C-2 in Dioxane at 30°C.

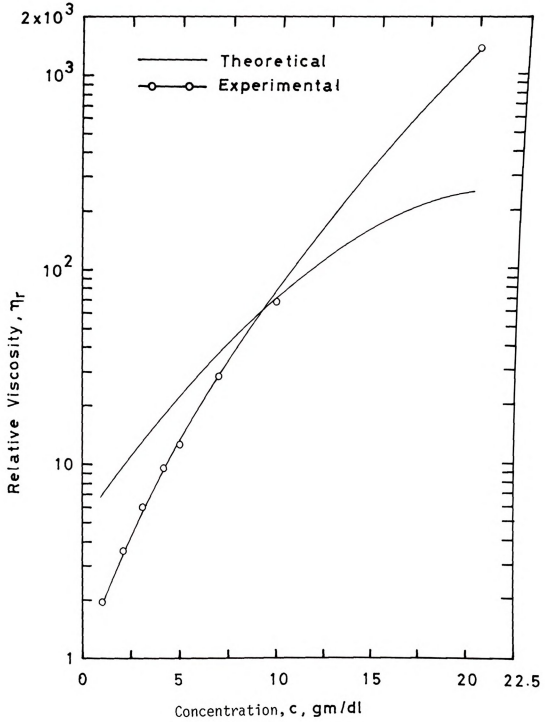

Figure 6.35.--Experimental and Calculated Relative Viscosity, η_r, vs. Concentration, c, of SAN C-2 in MEK at 30°C.

Figures 6.36 to 6.38 show the plots for SAN C-2' in DMF, dioxane and MEK. Since DMF is the best solvent, the deviation between the predicted and experimental values is the smallest. The experimental and predicted values of the viscosities of the solutions of SAN C-2 in benzene are not shown because of the computation difficulties involved due to the negative value of the thermodynamic parameter A_2. This leads to negative values of A/kT (see Eq. 6.28) for the lowest concentrations and small positive values for higher concentrations. This in turn gives negative value or fractional positive values of logarithmic term in C (see Eq. 6.29). For the highest concentrations, the computations could be made but the points were too few to plot them. For SAN C-2' in benzene the same difficulty occurred at the lowest concentrations. Figure 6.39 shows plot for the SAN C-2' copolymer in benzene. This system clearly shows the most discrepancy between the experimental and predicted values. Benzene is a very poor solvent for this copolymer and this is reflected by the A_2, χ_1 and α values. The polymer chains are very tightly coiled in benzene because of the unfavorable environment and this leads to tight entanglements even at low concentrations. This shows that Williams' model with the modified friction coefficient is not applicable in poor solvent environments.

Figures 6.40 and 6.41 show plots for SAN C-3 in DMF and MEK, respectively. Here also, the same trend as before is observed for the two curves involved for each solvent, DMF (good) and MEK (poor).

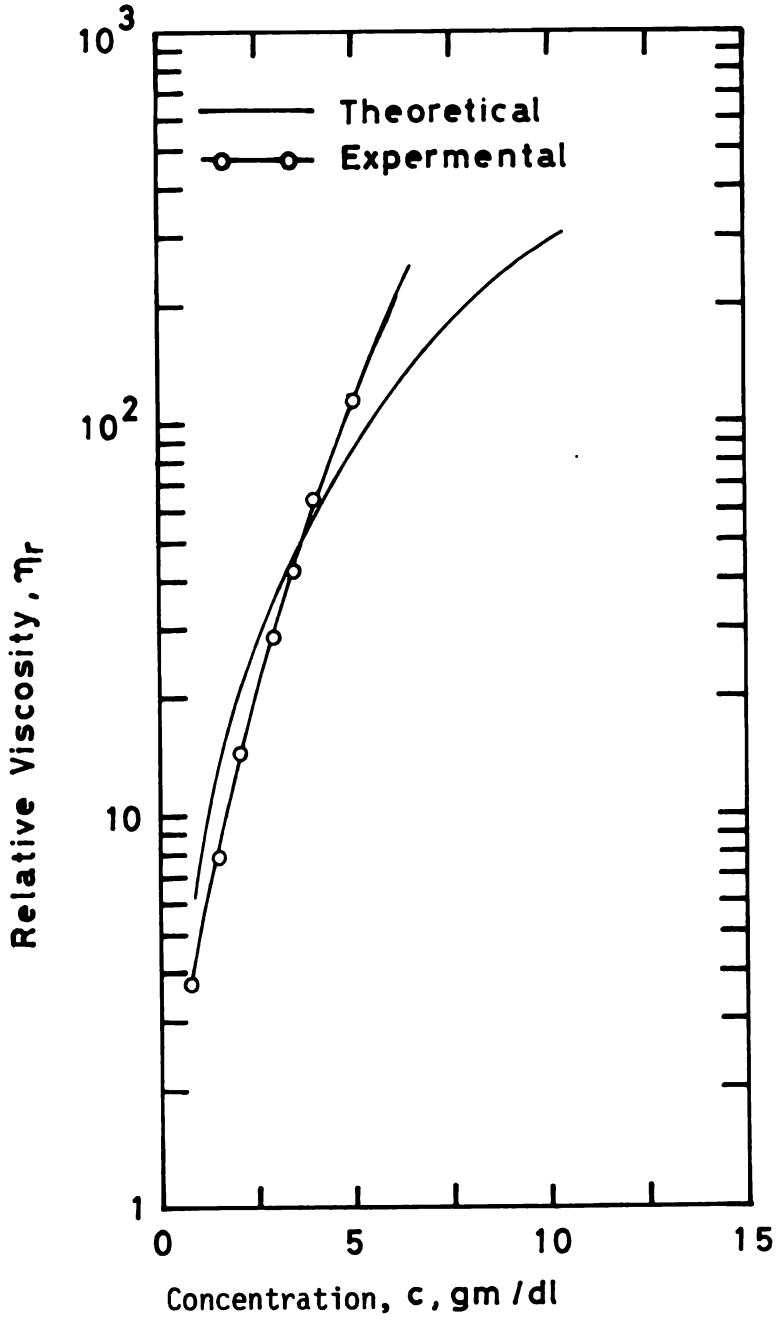

Figure 6.36--Experimental and Calculated Relative Viscosity, η_r, vs. Concentration, c, of SAN C-2' in DMF at 30°C.

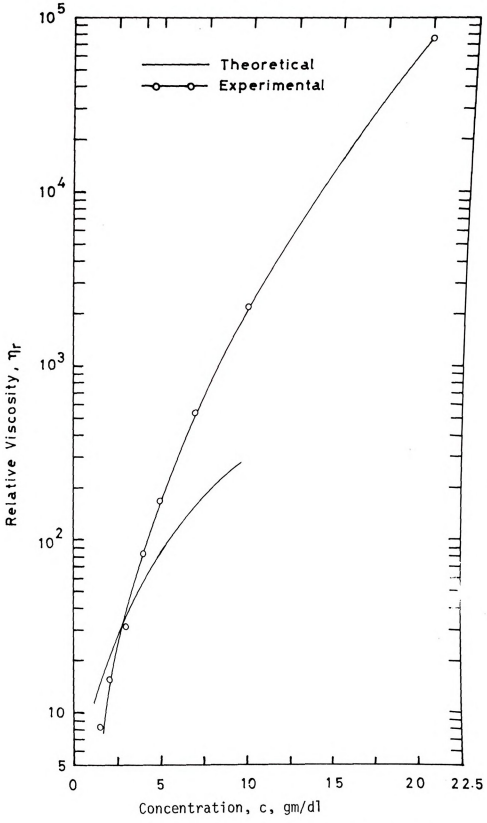

Figure 6.37.--Experimental and Calculated Relative Viscosity, η_{sp}, vs. Concentration, c, of SAN C-2' in Dioxane at 30°C.

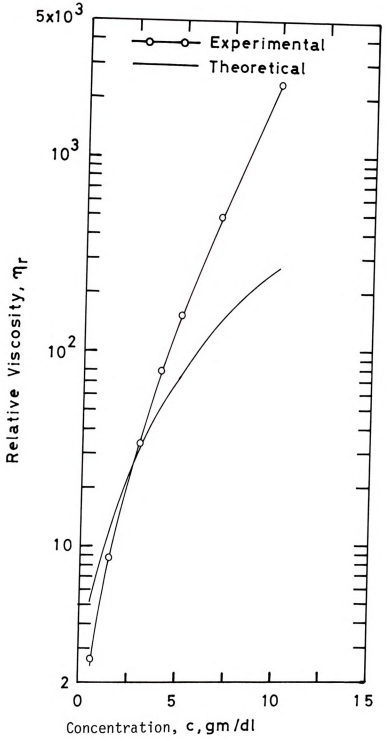

Figure 6.38.--Experimental and Calculated Relative Viscosity, η_r, vs. Concentration, c, of SAN C-2' in MEK at 30°C.

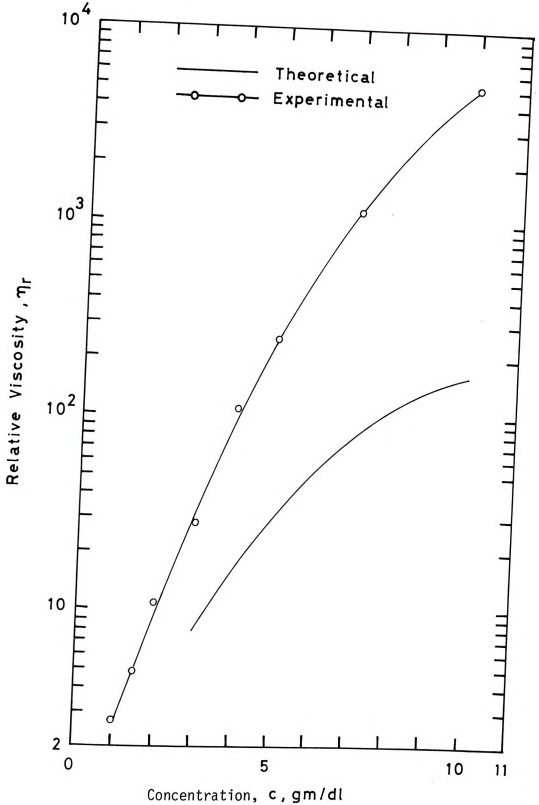

Figure 6.39.--Experimental and Calculated Relative Viscosity, η_r, vs. Concentration, c, of SAN C-2' in Benzene at 30°C.

Figure 6.40.--Experimental and Calculated Relative Viscosity, η_r, vs. Concentration, c, of SAN C-3 in DMF at 30°C.

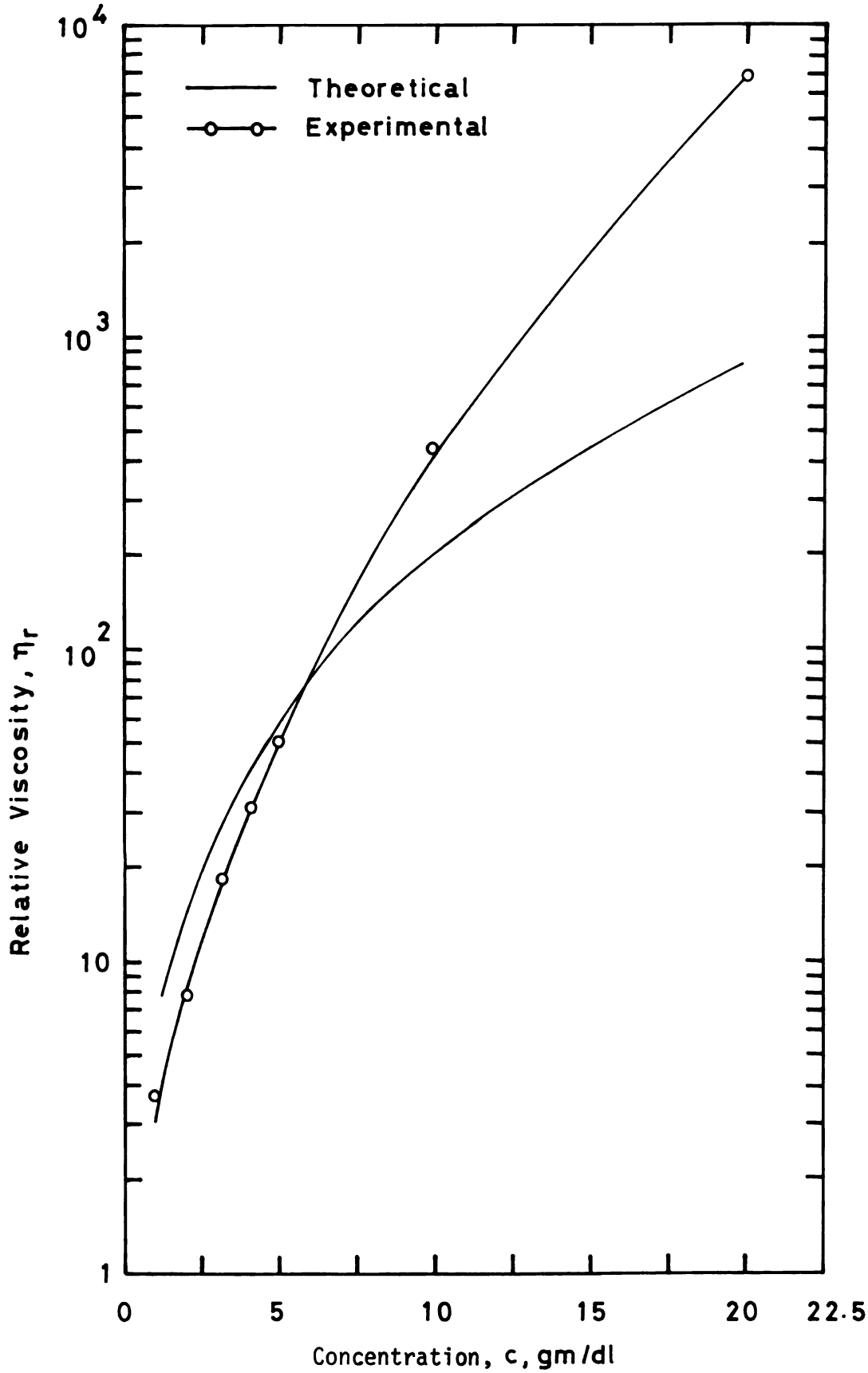
Theoretical
Experimental
Relative Viscosity, η_r
10^4
10^3
10^2
10
1
0
5
10
15
20
22.5
Concentration, c, gm/dl

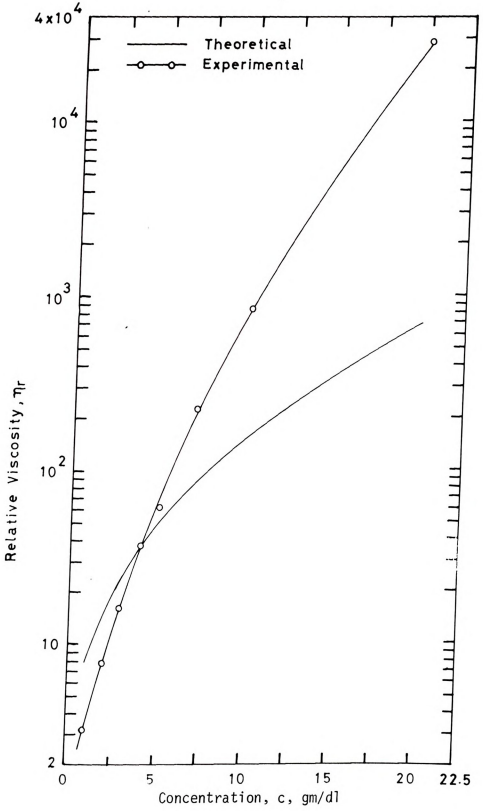

Figure 6.41.--Experimental and Calculated Relative Viscosity, η_r, vs. Concentration, c, of SAN C-3 in MEK at 30°C.

It should be noted that in all the cases the two curves run approximately parallel up to a certain concentration before crossing each other. Then the predicted values are much smaller than the experimental values. The model seems to be applicable for good solvents to higher concentrations than in poor solvents. The two curves can in turn be superposed by moving one onto the other by some constant factor. This demonstrates the need to check the model for the friction coefficient, and if possible obtain experimental values of ξ' from diffusion or ultracentrifugation data. Unfortunately, there is no data available on the friction coefficient for these systems at moderate concentrations. It is also not known how important a role the polymer-solvent hydrodynamics plays at high concentrations.

This is the only model available so far that takes polymer-solvent thermodynamics into consideration when predicting zero shear viscosity of moderately concentrated polymer solutions. It is qualitatively successful for polymer solutions of moderate concentrations in good solvents, and of dilute solutions in poor solvents. At higher concentrations, the predicted values are much less than the experimental values because of the aggregation due to entangled polymer chains. The friction coefficient, ξ', is proportional to $\langle S^2 \rangle$. Since aggregation increases the apparent size of the polymer domains, an effective value of $\langle S^2 \rangle$ for these "larger" molecules should increase ξ' and thus improve the model. Again with aggregation, enormous increases in friction are anticipated. This is not accounted for by the model and hence, at higher

concentrations, there is a large difference between the experimental and predicted values of viscosity.

E. Non-Newtonian Viscosity

The study of non-Newtonian behavior of macromolecular solutions and melts has attained an important status in the field of transport phenomena because of the industrial importance of such materials. These fluids differ from Newtonian fluids in that the viscosity of these fluids is dependent on the velocity gradient or shear rate being applied to them. It has been known for a long time that macromolecular fluids are generally shear-thinning; i.e., the viscosity drops dramatically from the zero shear or Newtonian viscosity as the shear rate increases. This behavior is very important for engineering considerations. Along with this behavior, there are many peculiar but interesting phenomena associated with non-Newtonian fluids which are described in Ref. (B-17).

Up to this point all the discussion in this work has been with regard to the viscosity at sufficiently low shear rate where it is independent of shear rate (Newtonian region of the viscosity-shear rate curve). This section is devoted to the discussion of non-Newtonian behavior. As the shear rate increases, at a certain value of the shear rate, the viscosity begins to decrease from its Newtonian value and continues to do so as the shear rate is increased to still higher levels. It is believed and also observed in some cases (T-3) where extremely high shear rates could be attained, that at some range of higher shear rates Newtonian behavior would again be observed. This is called the upper-Newtonian region.

1. Dependence of Relaxation Time on Concentration

The low shear Newtonian viscosity and the shear rate where the viscosity begins to decrease, which may be called the critical shear rate region, may change by many orders of magnitude from one system to another depending on the nature of the polymer, its molecular weight, the solvent and the concentration of the solution. The distribution of molecular weight or the degree of polydispersity is also important since the functional form of the viscosity-shear rate curve depends on it (M-1c, G-5).

Graessley (G-3) has developed a molecular model of polymer behavior which leads to the concept of a non-Newtonian viscosity. He envisions interaction between polymer molecules which he considers to be of an entanglement nature, leading to increased dissipation of energy with shear. This entanglement process is a kinetic phenomenon in which two molecules in a shear field entangle at a finite rate when they are sufficiently close. As the molecules pass each other in a flow field, disentanglement occurs. The detailed kinetics of this process is unknown. In Graessley's picture, two molecules must first be within a certain distance of each other, say, within a sphere of radius $\bar{R}$, for entanglement to occur. Then the molecules must remain within this sphere for a finite time, τ, or else no entanglement occurs. The greater the shear rate, the more rapidly the two molecules move relative to one another. Hence at high shear rates the entanglement density is reduced, thereby causing a reduction in viscosity. At zero rate

of shear the time constant for the formation of chain entanglements is τ_0. Rouse (R-1) has calculated the relaxation time for a bead-spring model and according to him,

$$\tau_R = (6/\pi^2)(\eta_0 M/cRT) \tag{6.37}$$

where η_0 is the zero shear viscosity, M is the molecular weight, c is the polymer concentration (gm/cm^3), R is the gas constant, and T is the absolute temperature. The physical significance of the relaxation time is that an imposed orientation of molecules reverts to random orientation with an exponential time decay proportional to $e^{-t/\tau}$. Graessley assumes that the two parameters, τ_R and τ_0, are related by

$$\tau_0 = K\tau_R \tag{6.38}$$

where K is a constant of the order of unity (G-3).

The viscosity-shear rate curves for several concentrations of a polymer in a solvent can be superposed to form a single master curve by appropriately shifting the curves horizontally at each concentration after plotting the normalized values of η/η_0 against $\dot{\gamma}$. It is also possible in turn to superpose the master curves for polymers of different molecular weights, again by appropriately shifting the curves horizontally. Later in this chapter a method of obtaining these shift factors is described.

Figures 6.42 to 6.44 show mater curves for azeotropic copolymers (SAN C-2 and SAN C-2') in benzene, dioxane and DMF, respectively, while Fig. 6.45 shows a master curve for SAN C-3

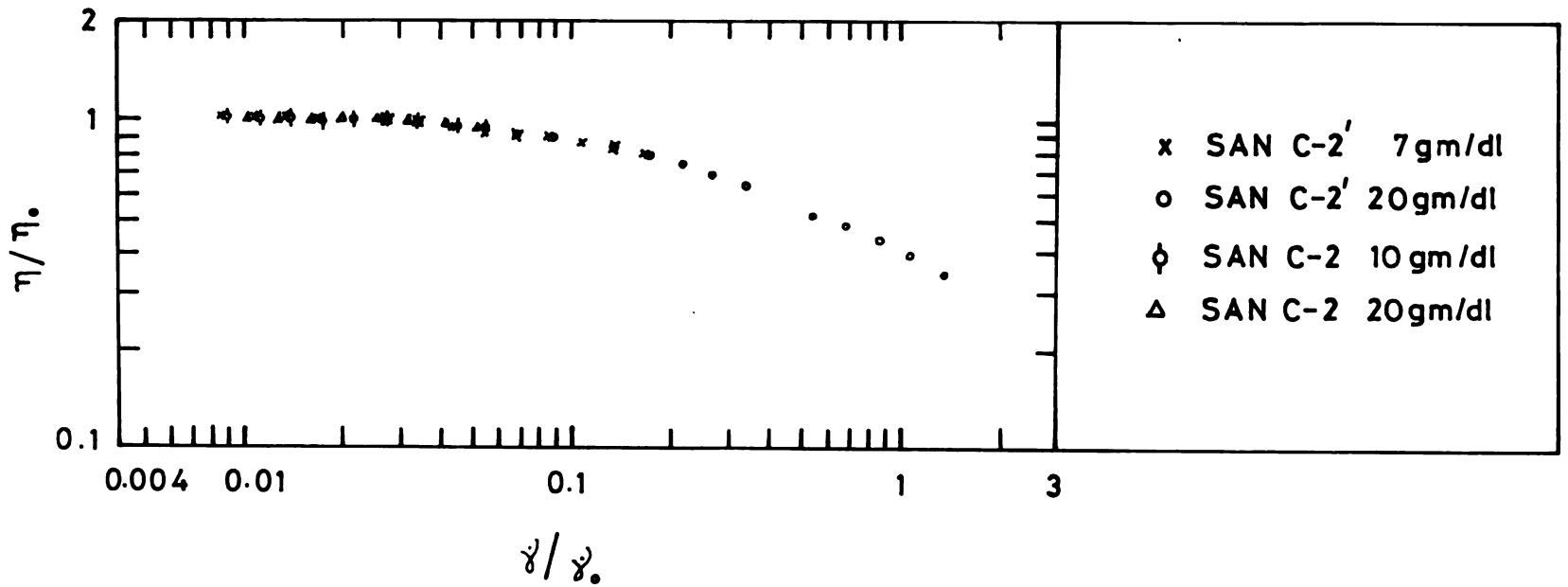

Figure 6.42.--Superposition of Viscosity-Shear Rate, $\eta - \dot{\gamma}$, Curves of SAN C-2 and SAN C-2' of Various Concentrations in Benzene at 30°C.

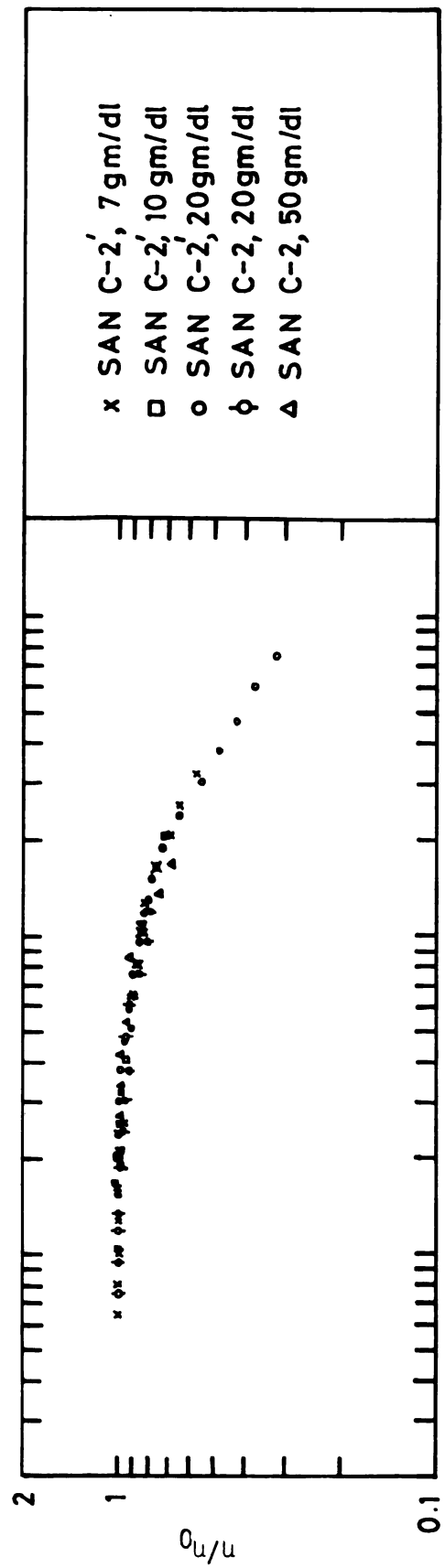

Figure 6.43.--Superposition of Viscosity - Shear Rate, η-$\dot{\gamma}$, Curves of SAN C-2 and SAN C-2' of Various Concentrations in Dioxane at 30°C.

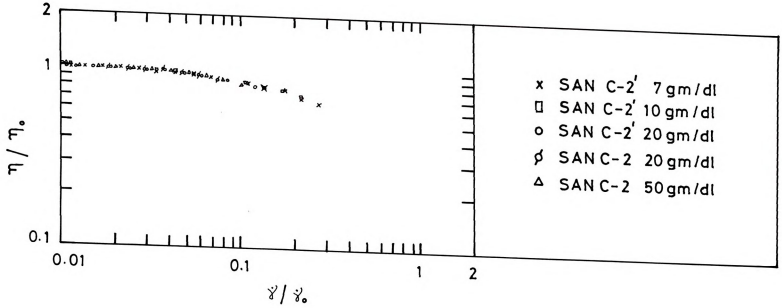

Figure 6.44.--Superposition of Viscosity-Shear Rate, η - $\dot{\gamma}$, Curves of SAN C-2 and SAN C-2' of Various Concentrations in DMF at 30°C.

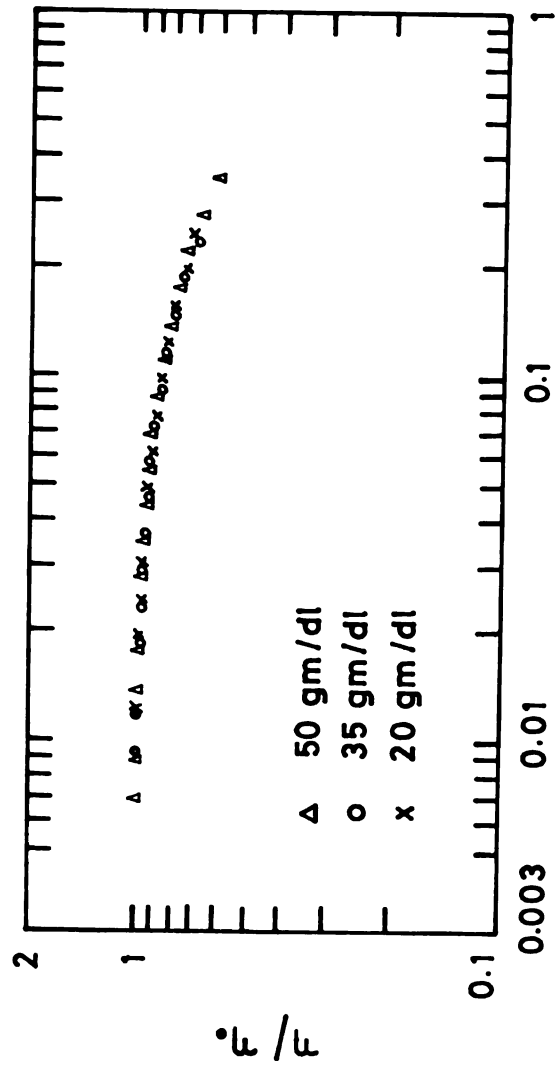

Figure 6.45.--Superposition of Viscosity-Shear Rate, $\eta - \dot{\gamma}$, Curves of SAN C-3 of Various Concentrations in DMF at 30°C.

in DMF. These curves are formed by finding appropriate shift factors at each concentration and molecular weight as mentioned before. The major differences in behavior between various solutions are reflected in two parameters. One is the zero shear viscosity, η_0, and the other is the characteristic shear rate which locates the critical shear rate which in turn is related to τ_0. Thus the slopes in the non-Newtonian region appear relatively insensitive to concentration and molecular weight.

There has been considerable success in correlating viscosity-shear rate relationships for polymer melts and solutions using reduced master plots. These master plots are of the form

$$\eta/\eta_0 = f(\tau_0\dot{\gamma}). \tag{6.39}$$

The parameter τ_0 also denotes the shift for each curve along the shear rate axis required to effect superposition on the master plots. The function $f(\tau_0\dot{\gamma})$ depends on the molecular weight distribution. Graessley (G-5) has predicted f $(\tau_0\dot{\gamma})$ from a theory based on the shear induced changes in the network of intermolecular entanglements. In his theory, τ_0 has a meaning of a characteristic time for formation or disruption of entanglements. The effect of molecular weight distribution on the function, $f(\tau_0\dot{\gamma})$, was also predicted by him. He (G-5) has given a table of values of η/η_0 and corresponding values of $\tau_0\dot{\gamma}/2$ for various molecular weight distributions. The polymers synthesized in this work have molecular weight distribution represented by polydisperity values close to 2 and hence theoretical master curve for

polydisperse entangling chains with polydispersity of 2 was used for superposing the experimental data. The experimental curves were shifted parallel to the shear rate axis to achieve the best fit with the theoretical curve. This allowed the determination of τ_0 from a direct comparison of the $\dot{\gamma}$ axis of the experimental curve with the $\tau_0\dot{\gamma}/2$ axis of the theoretical curve. The values of τ_0 thus obtained are listed in Table 6.8 along with the Rouse relaxation times, τ_R. It can be seen that τ_0 and τ_R are always of the same order of magnitude. Many forms of τ_0 have been suggested as a result of the attempts to correlate data for solutions and melts. Most of the suggested shift factors are of the form

$$\tau_0 \propto \frac{\eta_0 M^a}{T^b F(c)} . \tag{6.40}$$

TABLE 6.8.--Flow Parameters of Polymer Solutions at 30°C.

Polymer	M_w	Solvent	c, gm/dl	η_0, Poise	$\tau_0 \times 10^3$, sec.	$\tau_R \times 10^3$, sec.
PS-2	501,000	Dioxane	10	2.14	0.465	0.291
			15	9.56	1.15	0.771
			50	4493	136	109
SAN C-2'	666,000	Dioxane	7	5.83	1.38	1.34
			10	25.9	3.85	4.16
			20	806	50	64.8
SAN C-3	332,000	DMF	10	3.38	0.332	0.27
			20	52.6	2.33	2.11
			35	768	17.4	17.6

Table 6.9 summarizes many of the suggested forms. It is interesting to note that Graessley's form (G-4, G-1),

$$\tau_0 \propto \frac{\eta_0 M}{cT(1 + \beta cM)} , \tag{6.41}$$

includes other forms as special cases.

It is not possible to make a complete comparison of the forms of τ_0 given in Table 6.9 for the solutions studied since M and T were not varied. The ratio τ_0/τ_R is plotted against c in Fig. 6.46 for PS-2 in dioxane and SAN C-2' in dioxane, and in Fig. 6.47 for SAN C-3 in DMF. According to Eq. 6.40, τ_0/τ_R is inversely proportional to F(c)/c. Because of the limited concentration range, the exact form of F(c) cannot be decided but the curves in Figs. 6.46 and 6.47 indicate that the data can be described adequately by the Graessley form.

TABLE 6.9.--Suggested Forms of τ_0.

F (c)	a	b	Reference
c	1	1	B-18, B-19, B-20
c^2	0	0	M-6
c and c^2 (depending on concentration)		1	D-5
c^2	0	1	W-1

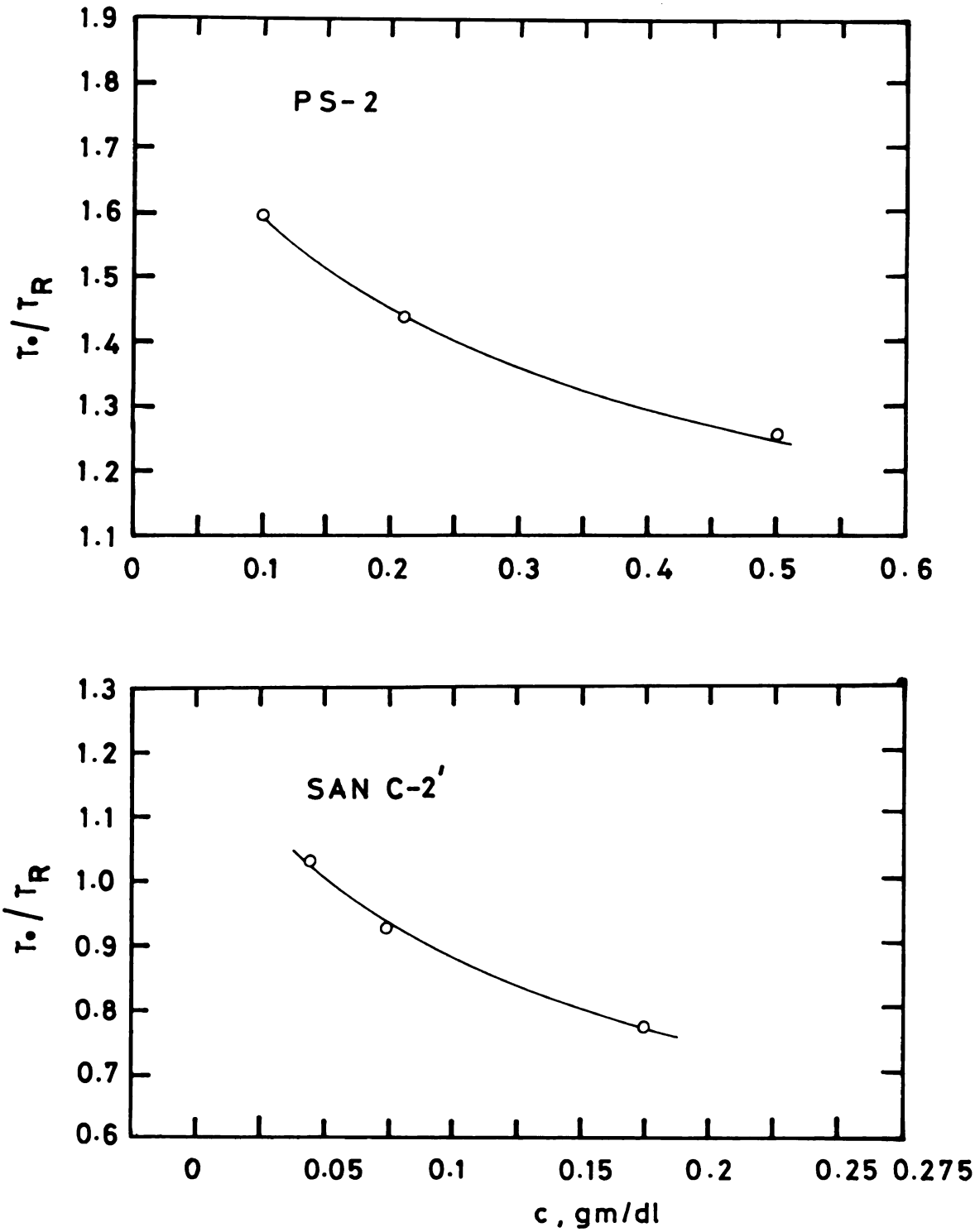

Figure 6.46.--Ratio of Experimental to Rouse Relaxation Time, τ_0/τ_R, vs. Concentration, c, of PS-2 and SAN C-2' in Dioxane at 30°C.

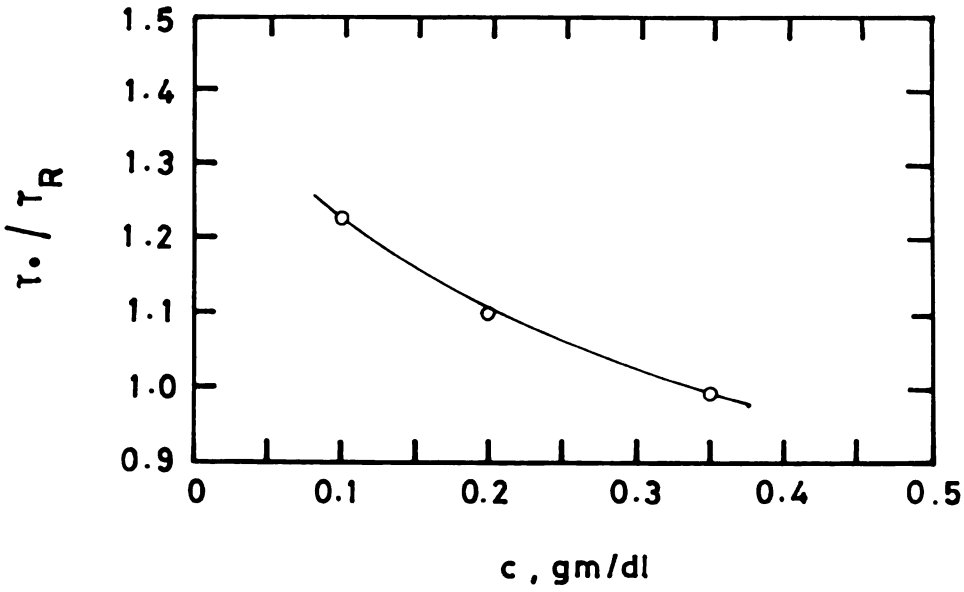

Figure 6.47.--Ratio of Experimental to Rouse Relaxation Time, τ_0/τ_R, vs. Concentration, c, of SAN C-3 in DMF at 30°C.

2. Dependence of Non-Newtonian Viscosity on Thermodynamic Quality of Solvent

Graessley argued that a decrease in viscosity with increasing shear rate in polymer solutions having concentration high enough to give rise to entanglements of molecules can be explained on the basis of the change in density of the chain entanglements. The ratio τ_R/τ_0 increases with the increase in the value of the product of concentration and molecular weight (see Figs. 6.46 and 6.47), i.e., a quantity expressing the density of chain entanglements. The interesting question is: What is the effect of the thermodynamic quality of the solvent on the density of chain entanglements which is reflected in the slope of the non-Newtonian curve or how are the mechanical formation and break-up of chain entanglements affected by the quality of the solvent? The effect should be evident from the plot of η/η_0 against $\tau_R\dot{\gamma}/2$ for one polymer in different solvents but of the same concentration in all the solvents so that the density of chain entanglements (expressed as cM) is the same in all the solutions. For this purpose, solutions of SAN C-2' in benzene, DMF, dioxane and MEK were used. In each solvent, concentrations of 7, 10 and 20 gm/dl were considered. Also, SAN C-3 in MEK and DMF at 35 gm/dl was considered. The solvents that were used have different viscosities and also they are of varying degree of goodness for the polymers as indicated by different values of the expansion factors, α (see Table 6.2).

The experimental results are plotted in Figs. 6.48 to 6.51. The figures indicate that correlations of η/η_0 with $\tau_R\dot{\gamma}/2$ in different solvents form master plots for each concentration. It

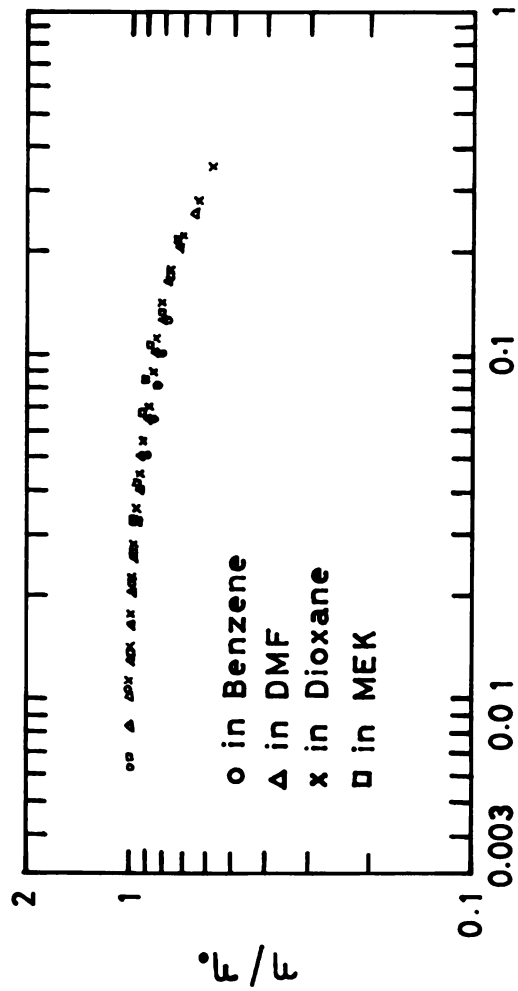

Figure 6.48.--Superposition of Viscosity-Shear Rate, $\eta - \dot{\gamma}$, Curves of SAN C-2' in Benzene, DMF, Dioxane and MEK at 7 gm/dl and 30°C.

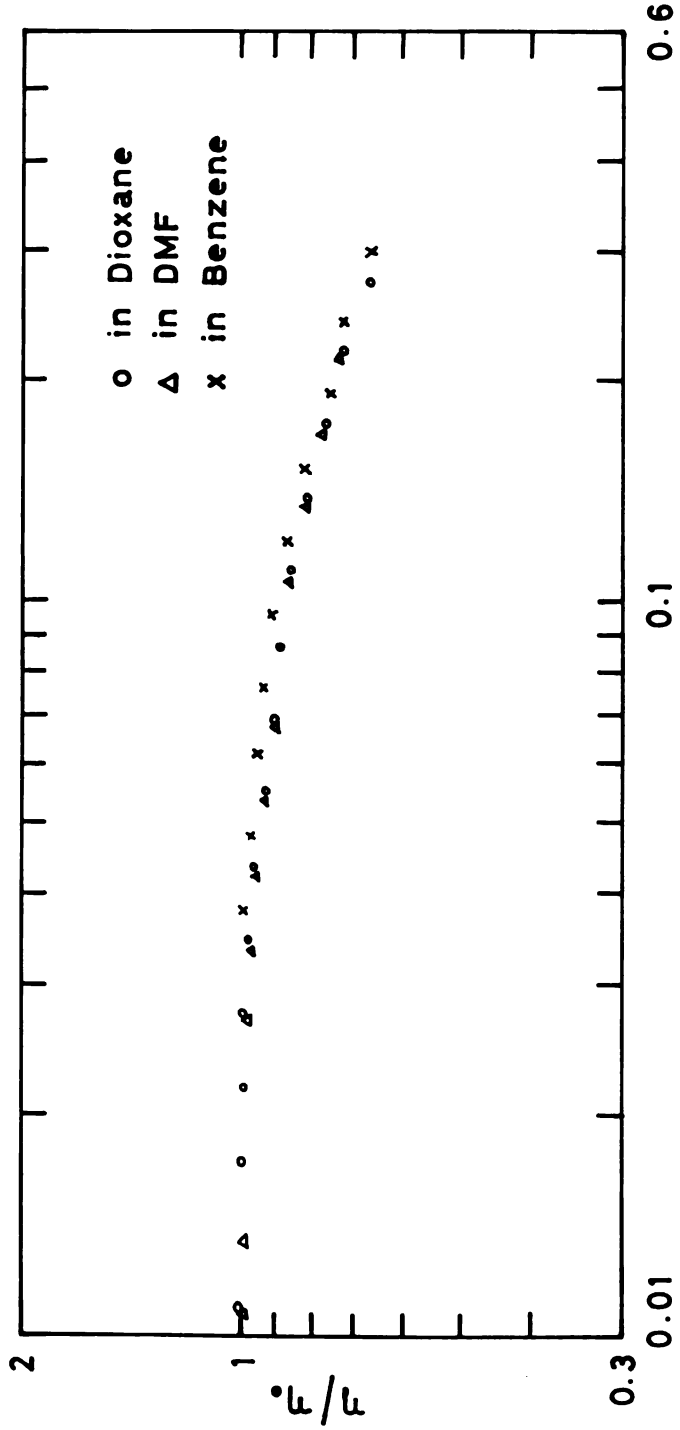

Figure 6.49.--Superposition of Viscosity-Shear Rate, $\eta - \dot{\gamma}$, Curves of SAN C-2' in Dioxane, DMF and Benzene at 10 gm/dl and 30°C.

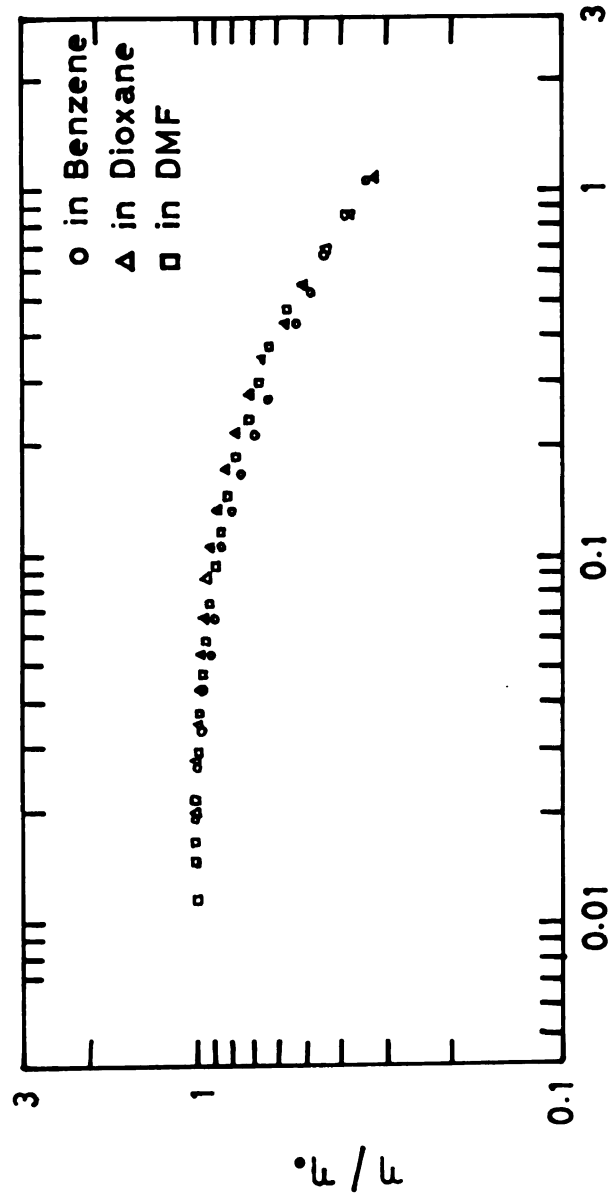

Figure 6.50.--Superposition of Viscosity-Shear Rate, $\eta - \dot{\gamma}$, Curves of SAN C-2' in Benzene, Dioxane and DMF at 20 gm/dl and 30°C.

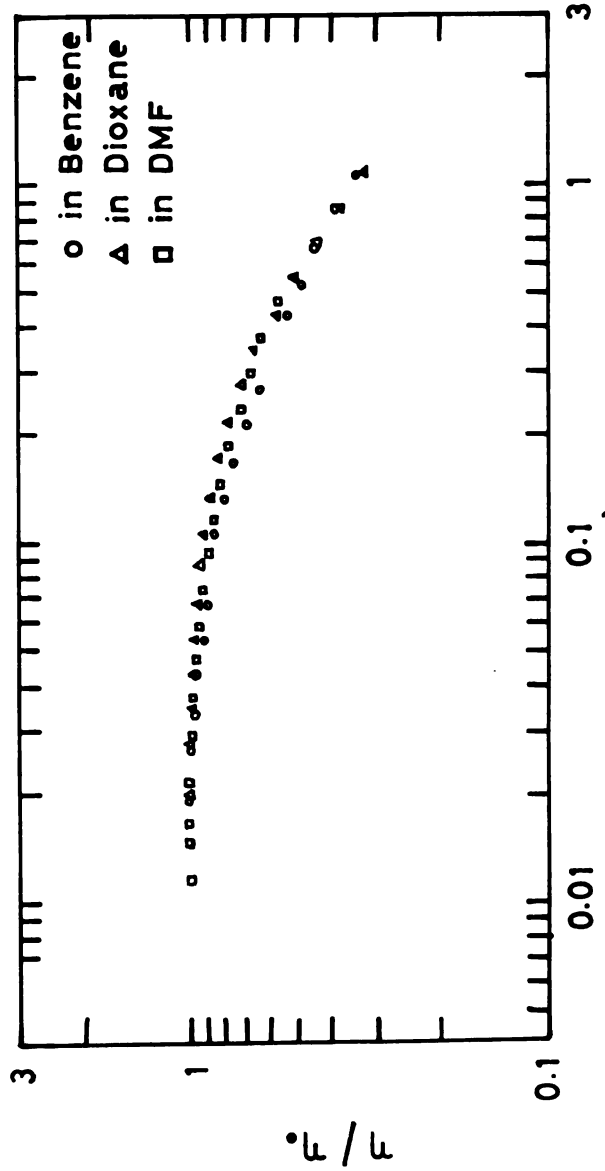

Figure 6.50.--Superposition of Viscosity-Shear Rate, $\eta - \dot{\gamma}$, Curves of SAN C-2' in Benzene, Dioxane and DMF at 20 gm/dl and 30°C.

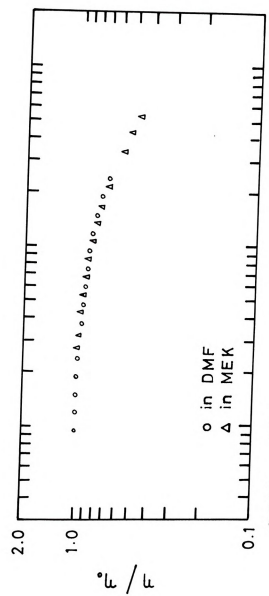

Figure 6.51.--Superposition of Viscosity-Shear Rate, $\eta - \dot{\gamma}$, Curves of SAN C-3 in DMF and MEK at 35 gm/dl and 30°C.

then follows that the magnitude (and hence the slope) of the non-Newtonian decrease in viscosity with the velocity gradient (or shear rate) at a constant polymer concentration does not depend on the thermodynamic quality of the solvent and the thermodynamic quality of the solvent appears to affect only η_0.

In the range of shear rates where polymer solutions display non-Newtonian behavior, the slope of the curve is independent of the nature of the solvent because in this range of shear rates, the mechanical force completely overcomes the thermodynamic forces between polymer and different solvents.

CHAPTER VII

CONCLUSIONS

The results of this investigation may be summarized as follows.

(1) Influence of Solvent on Zero Shear Viscosity: At low concentrations of polymer, viscosity in a good solvent is greater than that in a poor solvent. At higher concentrations, viscosity in a poor solvent is greater than that in a good solvent. The viscosity data show that the solvent character has a significant influence on viscosity in the whole range of concentrations. At low concentrations, η_{sp} increases more rapidly with concentration in a good solvent because of the larger size of polymer domains. At higher concentrations, η_{sp} increases more rapidly in a poor solvent. This is consistent with the thermodynamic argument that as the concentration increases, the density of chain segments increases along with the entanglements between the chains. It is much easier for a polymer coil to writhe freely in a good solvent than in a poor one. In a poor solvent, polymer-polymer contacts are preferred and so coiling-up takes place. The coiled-up polymer chains when entangled may tend to form aggregates. This aggregation enhances the viscosity. Then relative viscosity, η_r, in a poor solvent is several orders of magnitude larger than that in a good solvent.

The "cross-over" concentration--the concentration at which the relative viscosities of one polymer in good and poor solvents are the same--is much lower for copolymer solutions than that for the PS homopolymer solutions. As the proportion of ACN in copolymer increases, this "cross-over" concentration decreases. This is because of the enhanced coiling up in poor solvents like benzene, MEK and dioxane due to progressively stronger polymer-polymer polar interactions.

(2) Viscosity Correlation Techniques: The power law correlates viscosity with concentration and molecular weight of polymer with values of the exponent, b, close to 0.68 in good solvents and with lower values in poor solvents. Thus, the value of the exponent depends on the nature of the solvent. The use of a single value of the exponent, b, for all the solvents does not distinguish between different thermodynamic interactions between polymers and different solvents. The failure of the higher values of the exponent for the SAN C-2-benzene system clearly demonstrated this. The need for different values of the exponent for different solvents shows that the data for one particular polymer in different solvents cannot be correlated with the present type correlations. The power law exponent seems to be related to the Mark-Houwink exponent, a, since both exponents have lower values in poor solvents and higher values in good solvents, a being 0.5 in a Θ-solvent and 0.8 in a good solvent.

The Simha correlation unifies c, M data quite well up to high concentrations of polymer in solutions. The parameter, $\gamma(M)$,

seems to be dependent on the nature of the solvent. There is an indication that the values of $\gamma(M)$ for the non-polar solvents, benzene and dioxane, are similar to each other and the values of $\gamma(M)$ for the polar solvents, MEK and DMF, are similar to each other.

(3) Entanglement Concentrations: The estimate of onset-of-entanglement concentration, c_{ent}, by the method of Porter and Johnson, is applicable for polymer solutions in good solvents. For PS in good solvents the estimate of c_{ent} from the $(cM)_{ent}$ scheme is suggested. Their method ignores solvent effects. The data of this work clearly indicate that this can be very misleading. The onset-of-entanglement concentration is much lower in poor solvents than in good solvents: e.g., for PS-2 in benzene, c_{ent} is equal to 10 gm/dl while in MEK, c_{ent} is equal to 7 gm/dl; for SAN C-2' in DMF, c_{ent} is equal to 6 gm/dl while in benzene, c_{ent} is equal to 3 gm/dl. This result demonstrates the influence of polymer-solvent thermodynamics on viscosity. The common assumption that solvent effects in concentrated solutions are unimportant because of the dominance of chain entanglements is incorrect. The method of Porter and Johnson or that of Coronet based on packing of polymer coils does not take into account the nature of the solvent and hence cannot be applied universally. There is a direct relationship between the value of c_{ent} and the expansion factor, α, for a polymer in a solvent; the lower the value of α, the lower is the value of c_{ent}.

The results obtained indicate clearly that the transition from the rules governing the flow of dilute solutions to those governing the flow of concentrated solutions is determined by the nature of the polymer-solvent thermodynamic interactions.

(4) Williams Model: This model when used with the modified friction coefficient, ξ', gives better order of magnitude estimate of viscosity of moderately concentrated polymer solutions in good solvents than in poor solvents. The model fails at higher concentrations where entanglements of polymer chains are of significant density. Further work is required to refine Williams' model to improve the accuracy of viscosity predictions. At higher concentrations where entanglements are significant, terms in higher powers of c will be necessary to predict viscosity.

(5) Non-Newtonian Viscosity: The magnitude (and hence the slope) of the non-Newtonian decrease in viscosity with the increase in velocity gradient (or shear rate) at a constant polymer concentration in different solvents does not depend on the thermodynamic quality of the solvent but is a function of the density of chain entanglements only. The thermodynamic quality of solvent appears to affect only the zero shear viscosity.

The Graessley shift factor, τ_0, and the Rouse relaxation time, τ_R, are of the same order of magnitude; i.e., τ_0 is equal to $K\tau_R$ where K is of the order of unity for the systems studied. Of the many suggested forms, τ_0 follows the Graessley form of dependence on concentration, c; i.e., $\tau_0 \alpha \eta_0 M/cT(1 + \beta cM)$.

(6) Kinetic Models for the Rate of SAN Copolymerization: Neither of the two kinetic models, based on chemical controlled and diffusion controlled termination, alone describes the kinetics of copolymerization of styrene and acrylonitrile. For the copolymerizations studied in this work both termination mechanisms appear to be acting simultaneously and a single parameter kinetic expression is inadequate to describe the rate of copolymerization data.

(7) Short-Range Interaction: The values of the stiffness factor, σ, of the SAN copolymers are higher than those of the homopolymers, PS and PAN. This means that in the unperturbed state the SAN copolymers are more extended than the constituent homopolymers. The maximum in the value of σ is at about 50 mole per cent ACN content in an SAN copolymer where the tendency for alternation is the maximum.

NOMENCLATURE

NOMENCLATURE

Sometimes the same notation is used for different quantities in order to preserve the already established nomenclature in the literature.

a	Exponent in Eq. 2.27, defined by Eq. 2.29a.
a	Mark-Houwink exponent in the empirical relationship between intrinsic viscosity and molecular weight, Eq. 3.7.
a	Parameter depending on particle shape, Eq. 3.43.
a_1	Activity of solvent.
a_2, a_3	Constants in Eq. 3.47.
A	Thermodynamic constant that determines magnitude of intermolecular potential energy between polymers, $(gm)(cm^5)/sec^2$, Eq. 3.55.
$\mathring{A}$	Ångström unit, 10^{-8} cm.
A_2	Coefficient in the virial expansion, $(mole)(cm^3)/gm^2$, Eq. 3.20.
A_3	Third virial coefficient, Eq. 3.39.

b	Exponent in Eq. 2.27, defined by Eq. 2.29b.
b	Exponent in power law correlations.
b	Dimension of segment of a polymer molecule, Eq. 6.16.
B	Coefficient in the virial expansion, Eq. 3.20.
B	Factor related to molecular size, cm^{-2}, Eq. 3.62.
c	Exponent in Eq. 2.27, defined by Eq. 2.28c.
c	Concentration in gm/cm^3 in Ch. V, sections C and D, and in gm/dl in other chapters.
c_A, c_B	Weight concentration of species A and B in copolymer.
c_{ent}	Entanglement concentration, gm/dl.
c_i	Weight concentration of component i in copolymer, Eq. 3.26.
C	Parameter in the Williams equation, Eq. 3.61, defined by Eq. 3.63, cm^5.
C	Constant characteristic of given chain structure, Eq. 3.12.
d_1, d_2	Differential refractometer readings for solution at cell positions 1 and 2, respectively.

d_1^0, d_2^0	Corresponding readings for solvent.
f	Fraction of primary radicals, released by an initiator, which initiate polymer chains, Eq. 2.2.
f_1, f_2	Mole fractions of monomers 1 and 2, respectively, in monomer mixture.
f_{1W}	Weight fraction of monomer 1 in monomer mixture.
f_1^0	Initial mole fraction of monomer 1 in monomer mixture.
F_1, F_2	Mole fractions of monomer 1 and 2, respectively, in copolymer.
F_0, F_θ	Product of transmittance of neutral filters of light scattering photometer at angles 0 and θ, respectively.
ΔF_m	Free energy change on mixing.
F_{1W}	Weight fraction of monomer 1 in copolymer.
g	Pair correlation function.
g_0	Radial distribution function.
G_0, G_θ	Galvanometer readings in light scattering measurements at angles 0 and θ, respectively.
$\bar{G}_1$, $\bar{G}_1^0$	Partial molar Gibbs free energy at any and standard states, respectively.

h	Gap width between spheres, cm, Eq. 6.31.
H	Optical constant defined by Eq. 3.22.
ΔH_m	Heat of mixing.
$\Delta \bar{H}_1$	Partial molar heat of dilution.
i_θ	Intensity of light scattered at angle θ.
I_0	Incident intensity of light.
$[I]$	Concentration of initiator, mole/cm^3.
k	Differential refractomer constant, Eq. 4.1.
k	Boltzmann's constant.
$\bar{k}$	Unspecified constant in Eq. 6.15.
k_1	Huggins constant.
k_2, k_3	Constants in Eq. 3.49.
$\bar{k}_1$, $\bar{k}_2$	Constants in Eq. 3.48.
k_Θ	Huggins constant at Θ-condition.
k_d, k_p, k_t	Reaction rate constants for initiator decomposition, chain propagation, and chain termination, respectively.
k_{11}, k_{12}, k_{21}, k_{22}	Copolymerization propagation constants for a radical of the type indicated by the first subscript with a monomer indicated by the second.

i_{tc}, i_{td}	Reaction rate constants for termination by combination (coupling) and disproportionation, respectively.
k_{t11}, k_{t12}, k_{t22}	Termination constants for a radical of the type indicated by the first subscript with a radical of the type indicated by the second.
$k_{t(12)}$	Termination rate constant in diffusion-controlled copolymerization.
K, K'	Optical constants defined by Eqs. 3.20 and 3.27, respectively.
K	Mark-Houwink constant in the theoretical intrinsic viscosity-molecular weight relationship, Eq. 3.14.
K_m	Empirical constant in Eq. 3.9.
l	Bond length.
$\langle L^2 \rangle$, $\langle L_0^2 \rangle$	Mean-square end-to-end distance of a polymer chain in any and unperturbed states, respectively.
$\langle L_0^2 \rangle_f$	Mean-square end-to-end distance of a "freely rotating" polymer chain having no hindrance to internal rotation about carbon-carbon bond.
M	Amount of monomers, moles.
M, M_0	Molecular weights of polymer and monomer, respectively.

$[M]$	Monomer concentration.
M_1, M_2, $[M_1]$, $[M_2]$	Monomer 1 and 2, respectively, and their concentrations.
M_c	Critical molecular weight, Eq. 6.6.
M_i	Molecular weight of component i in a copolymer having weight fraction, γ_i, Eq. 3.31.
M_n, M_w	Number and weight average molecular weight, respectively.
M_{app}	Apparent molecular weight.
M^0	Initial amount of monomers.
M_1^*, M_2^*	Chain radicals of types 1 and 2, respectively.
M_x^*	Radical at the end of a growing chain.
n	Number of links in a polymer chain, Eq. 3.12.
n, n_0	Refractive index of solution and solvent, respectively.
n_1, n_2	Number of solvent and polymer molecules, respectively.
n_p, n_s	Number of polymer and solvent molecules, respectively, per volume of solution.
N	Number of segments per polymer molecule, Eq. 6.16.

N_{AV}	Avogadro's number.
P	Pressure.
P	Parameter representing heterogeneity in composition of copolymer, Eq. 3.31.
$P(\theta)$	Factor expressing reduction in scattered intensity at angle θ due to interparticle interference, Eq. 3.21a.
q	Arbitrary constant of Zimm plot.
Q	Parameter representing heterogeneity in composition of copolymer, Eq. 3.32.
r	Distance, Eq. 3.17.
r	Radius of sphere, Eqs. 6.18 and 6.31.
$\underline{r}$	Position vector between two molecular centers.
r_1, r_2	Monomer reactivity ratios in copolymerization.
R	The gas constant.
R_e	Effective radius of polymer chain, Eq. 3.8.
R_i, R_p	Rates of initiation and propagation, respectively, of polymerization.
R_{90}, R_θ	Rayleigh ratio at the angles 90° and θ, respectively.

S	Entropy.
$\Delta\bar{S}_1$	Partial molar entropy of dilution.
ΔS_m^{conf}	Configurational entropy of mixing.
$\langle S^2 \rangle$, $\langle S_0^2 \rangle$	Mean-square radius of gyration of a polymer molecule in any and in unperturbed states, respectively.
t	Time
T	Absolute temperature.
U	Velocity of spheres, Eq. 6.31.
U	Potential of mean force due to presence of all segments, $(Gm)(cm^2)/sec^2$.
v_p	Volume fraction of polymer.
$\bar{v}_p$	Specific volume of polymer.
v_s	Molar volume of solvent.
V	Intermolecular potential energy, $(gm)(cm^2)/sec^2$, Eq. 3.54.
$\bar{V}_1$	Partial molar volume of solvent.
V_{1s}	Volume fraction of solvent.
V_p, V_s	Molecular volume of polymer and solvent, respectively.

x	Fractional conversion of monomer to polymer, Eq. 2.3.
$\bar{x}$	Average composition of copolymer, Eq. 3.33.
x_1, x_2	Mole fractions of solvent and solute, respectively, Eqs., 3.34 and 3.36.
x_A, x_B	Weight fraction of monomers A and B, respectively, in copolymer.
$\bar{x}_A$, $\bar{x}_B$	Mole fraction of monomers A and B, respectively, in copolymer.
x_i	Composition of component i in a copolymer, Eqs. 3.31 and 3.32.
$\underline{x}_i$	Position of i^{th} segment of a polymer molecule, referred to arbitrary origin, Chapter III, Section D.
X	Parameter in Eq. 3.27, defined by Eq. 2.28.
α	Exponent in Eq. 2.16, defined by Eq. 2.17.
α	Polarizability of scattering particles, Eq. 3.17.
α	Factor expressing the linear deformation of a polymer molecule owing to solvent-polymer interaction.
β	Exponent in Eq. 2.16, defined by Eq. 2.17.

β	Power law correlation parameter, Eq. 3.41.
β	Constant in Eq. 6.41.
γ	Exponent in Eq. 2.16, defined by Eq. 2.17.
γ	Shift factor in Simha correlation, Chapter III, Section C, Part 2.
$\dot{\gamma}$	Shear rate, sec^{-1}.
γ_i	Weight fraction of component i in a copolymer, Eqs. 3.31, 3.32 and 3.33.
δ	Parameter in Eq. 2.16, defined by Eq. 2.17.
δ_1, δ_2	Parameters in Eq. 2.21, defined by Eqs. 2.23a and 2.23b.
ε	Number of isotropic scattering particles per unit volume having polarizability α, Eq. 3.17.
ε	Free energy of mixing polymer segments with solvent, $gm/(cm)(sec^2)$, Eq. 3.55.
ζ	Frictional coefficient for a bead of polymer chain, Eq. 3.8.
η	Viscosity.
η_0	Zero shear or low shear viscosity.
η_r	Relative viscosity, η/η_0.

η_s	Viscosity of solvent
η_{sp}	Specific viscosity, $\eta_r - 1$.
$[\eta]$, $[\eta]_\Theta$	Intrinsic viscosity at any and at Θ-temperature, respectively, in deciliters per gram.
θ	Angle between transmitted and scattered beam, Eq. 3.17.
Θ	"Ideal" or "Flory" temperature at which polymer chains in a solution assume unperturbed dimensions.
κ_1	Parameter expressing the energy, divided by kT, of interaction between a solvent molecule and polymer.
λ	Time constant for polymer chain response, Eqs. 3.50 and 3.60.
λ	Wave length of light, Eq. 3.17.
μ	Newtonian viscosity.
$\Delta\mu_1$	Chemical potential of solvent.
$\Delta\mu_1^{id}$	Ideal chemical potential of solvent.
$\Delta\mu_1^{ex}$	Excess chemical potential of solvent.
ν	Kinetic chain length.

ν, ν_0, ν_A, ν_B	Refractive index increment, its average value for a copolymer and its values for homopolymers A and B, respectively.
ξ, ξ'	Friction coefficient between polymer molecules, gm/sec.
π	3.14159 . . . . .
π	Osmotic pressure.
ρ	Density of bulk polymer.
σ	Stiffness or steric factor.
τ	Turbidity as determined by light scattering measurements, Eq. 3.18.
τ	Shear stress.
τ_0	Experimental relaxation time.
τ_R	Rouse relaxation time.
$\underline{\underline{\tau}}$	Total stress tensor, Eq. 3.51.
$\underline{\underline{\tau}}_0$	Stress tensor representing stress due to solvent and externally imposed isotropic pressure, Eq. 3.51.
ϕ	Parameter in chemical controlled termination, Eq. 2.21.
ϕ	Volume fraction of spheres, Eq. 3.42.

Φ	Flory's parameter relating intrinsic viscosity to molecular dimension $\langle L^2 \rangle$, Eq. 3.10.
χ_1	Flory's thermodynamic parameter expressing interaction between polymer and solvent.
χ_A, χ_B	Corresponding parameter for homopolymers A and B, respectively, Eq. 1.6.
χ_{AB}	Flory's thermodynamic parameter expressing interactions between homopolymers A and B, Eq. 1.6.
ψ	r-dependent factor in shear perturbation of g_0, Eq. 3.57a.
ψ_1	Parameter characterizing the entropy of dilution of polymer with solvent.
Ψ	Distribution function in coordinate space of all segments.

BIBLIOGRAPHY

BIBLIOGRAPHY

A-1. Alfrey, T., Jr., J. J. Bohrer, and H. Mark, "Copolymerization," Vol. 8 of High Polymer Series, Interscience, New York (1952).

A-2. Atherton, J. N., and A. M. North, Trans. Farad. Soc., 58, 2049 (1962).

A-3. Alfrey, T., Jr., and G. Goldfinger, J. Chem. Phys., 12, 205 (1944).

A-4. American Cyanamid Company,"Acrylonitrile," 2nd ed., New York (1959).

B-1. Boundy, R. H., and R. F. Boyer, eds., "Styrene," Reinhold, New York (1952).

B-2. Bird, R. B., W. E. Stewart, and E. N. Lightfoot, "Transport Phenomena," John Wiley and Sons, Inc., New York (1960), (a) Ch. 2.

B-3. Blanks, R. F., private communications.

B-4. Brandrup, J., and E. H. Immergut, eds., "Polymer Handbook," Interscience, New York (1966), (a) Ch. 4.

B-5. Baysal, B., and A. V. Tobolsky, J. Polym. Sci., 8, 529 (1952).

B-6. Barb, W. G., J. Polym. Sci., 11, 117 (1953).

B-7. Beatie, W. H., and C. Booth, J. Phys. Chem., 64, 696 (1960).

B-8. Bushuk, W., and H. Benoit, Canad. J. Chem., 36, 1616 (1958).

B-9. Blanks, R. F., and B. N. Shah, Polymer Preprints, 15, 147 (1974)

B-10. Brice Phoenix Light Scattering Photometer Operational Manual OM-2000, Phoenix Precision Instrument Co., Vir Tis, Gardiner, N.Y. 12525.

B-11. Bhagvantam, S., "Scattering of Light and Raman Effects," Andhra University, Waltair, India (1940), p. 84.

B-12. Brice, B. A., and M. Halwar, J. Opt. Soc. Am., 41, 1033 (1951).

B-13. Brice Phoenix Differential Refractometer Model BP-2000-V, Operational Manual, Phoenix Precision INstrument Co., Vir Tis, Gardiner, N.Y. 12525.

B-14. Bates, F. J., and Associates, "Polarimetry Saccharimetry and the Sugars," Circular C440, National Bureau of Standards, U.S. Govt. Printing Office, Washington, D.C. (1942), p. 652.

B-15. Blanks, R. F., H. C. Park, D. R. Patel, and M. C. Hawley, Polymer Eng. Sci., 14, 1, 16 (1974).

B-16. Blanks, R. F., Ph.D. dissertation, University of California, Berkeley, 1963.

B-17. Bird, R. B., O. Hassager, and S. I. Abdel-Khalik, A. I. Ch. E. J., 20, 1014 (1974).

B-18. Bueche, F., J. Chem. Phys., 27, 1210 (1957).

B-19. Bueche, F., and S. W. Harding, J. Polym. Sci., 32, 177 (1958).

B-20. Bueche, F., J. Appl. Phys., 30, 1114 (1959).

C-1. Carr, C. I., Jr., and B. H. Zimm, J. Chem. Phys., 18, 1616, 1624 (1950).

C-2. Casassa, E. F., and W. H. Stockmayer, Polymer, 3, 53 (1962).

C-3. Coronet, C. F., Polymer, 6, 373 (1965).

C-4. Chou, L., and J. L. Zakin, J. Coll. Interface Sci., 25, 547 (1967).

D-1. Das, S. K., S. R. Chatterjee, and S. R. Palit, Indian J. Chem., 6, 43 (1968).

D-2. Debye, P., J. Chem. Phys., 14, 636 (1946).

D-3. Debye, P., and F. Bueche, J. Chem. Phys., 16, 573 (1948).

D-4. Debye, P., J. Phys. Coll. Chem., 51, 18 (1947).

D-5. Dewitt, T. W., H. Markowitz, F. J. Padden, and L. J. Zapas, J. Coll. Sci., 10, 174 (1955).

E-1. Eringen, A. C., "Nonlinear Theory of Continuous Media," McGraw-Hill, New York (1962).

F-1. Fredrickson, A. G., "Principles and Applications of Rheology," Prentice Hall, Inc., Englewood Cliffs, N.J. (1964).

F-2. Ferry, J. D., "Viscoelastic Properties of Polymers," 2nd ed., John Wiley and Sons, Inc., New York (1970), (a) Ch. 17.

F-3. Flory, P. J., "Principles of Polymer Chemistry," Cornell University Press, Ithaca, N.Y. (1953), (a) Ch. 12, (b) Ch. 4, (c) Ch. 8, (d) Ch. 5, (e) Ch. 10, (f) Ch. 14.

F-4. Fischer, T. M., Jr., Ph.D. dissertation, Michigan State University, E. Lansing, Michigan (1968).

F-5. Fineman, M., and S. D. Ross, J. Polym. Sci., 5, 259 (1950).

F-6. Fox, T. G., S. Gratch, and S. Loshaek, "Rheology," ed., F. Eirich, Vol. 1, Academic Press, New York (1958), Ch. 12.

F-7. Frisch, H. L., and R. Simha, "Rheology," ed., F. Eirich, Vol. 1, Academic Press, New York (1956), Ch. 4.

F-8. Fixman, M., J. Chem. Phys., 42, 3831 (1965).

F-9. Fixman, M., Ann. N.Y. Acad. Sci., 89, 657 (1961).

F-10. Fixman, M., J. Polym. Sci., 41, 91 (1960).

F-11. Frankel, N. A., and A. Acrivos, Chem. Eng. Sci., 22, 847 (1967).

F-12. Frank, H. P., and H. F. Mark, J. Polym. Sci., 17, 1 (1955).

F-13. Fox, T. G., and G. D. Berry, Adv. Polym. Sci., 5, 261 (1968).

F-14. Flory, P. J., "Statistical Mechanics of Chain Molecules," Interscience, New York (1969).

G-1. Graessley, W. M., R. L. Hazelton, and L. R. Lindeman, Trans. Soc. Rheol., 11, 3, 267 (1967).

G-2. Gupta, D., and W. C. Forsman, Macromolecules, 2, 304 (1969).

G-3. Graessley, W. W., J. Chem. Phys., 43, 2696 (1965).

G-4. Graessley, W. W., and L. Segal, Macromolecules, 2, 49 (1969).

G-5. Graessley, W. W., J. Chem. Phys., 47, 1942 (1967).

G-6. Gandhi, K. S., and M. C. Williams, J. Polym. Sci., C, 35, 211 (1971).

H-1. Ham, G. E., "Kinetics and Mechanisms of Polymerization," Vol. 1, Part 1, M. Dekker, Inc., New York (1967), Chs. 1 and 3.

H-2. Hamielec, A. E., J. W. Hodgins, and K. Tebbens, A. I. Ch. E. J., 13, 1087 (1967).

H-3. Huggins, M. L., J. Am. Chem. Soc., 64, 2716 (1942).

H-4. Harris, R., and J. E. Hearst, J. Chem. Phys., 44, 2595 (1966).

H-5. Hirschfelder, J. O., C. F. Curtiss, and R. B. Bird, "Molecular Theory of Gases and Liquids," John Wiley and Sons, Inc., New York (1965), (a) Ch. 1.

H-6. Hutton, J. F., Nature, 200, 646 (1963).

H-7. Heil, J. F., and J. M. Prausnitz, A. I. Ch. E. J., 12, 678 (1966).

I-1. Instruction Manual--the Weissenberg Rheogoniometer Model R-16, Sangamo Controls Limited, North Bersted, Bognor Regis, Sussex, England.

I-2. Imai, S., Proc. Roy. Soc., A 308, 497 (1969).

J-1. Jansen, A. G., and B. P. Caldwell, Polymer Bull., 1, 120 (1945).

K-1. Kirkwood, J., and J. Riseman, J. Chem. Phys., 16, 565 (1948).

K-2. Kurata, M., and W. H. Stockmayer, Fortschr. Hochpolym. Forch., 3, 196 (1963).

K-3. Kirkwood, J. G., F. P. Buff, and M. S. Green, J. Chem. Phys., 17, 988 (1949).

K-4. Kinsinger, J. B., J. S. Bartlett, and W. H. Rauscher, J. Appl. Polym. Sci., 6, 529 (1962).

K-5. Klimisch, H. M., M.S. thesis, Michigan State University, E. Lansing, Michigan (1970).

K-6. Kratohvil, J. P., Gj. Dezelic, M. Kerker, and E. Matijevic, J. Polym. Sci., 57, 59 (1962).

K-7. Kratohvil, J. P., Anal. Chem., 36, 459 R (1964).

K-8. Kruis, A., Ziet. Phys. Chem., 34 B, 13 (1936).

K-9. King, R. G., Rheo. Acta., 5, 35 (1966).

K-10. Krigbaum, W. R., and A. M. Kotliar, J. Polym. Sci., 32, 323 (1958).

K-11. Kirkwood, J. G., J. Chem. Phys., 14, 180 (1946).

L-1. Lord Rayleigh, Phil. Mag., 41, 447 (1881).

L-2. Lodge, A. S., "Elastic Liquids," Academic Press, New York (1964).

M-1. Middleman, S., "The Flow of High Polymers," Interscience, New York (1968), (a) Ch. 5, (b) Ch. 3, (c) Ch. 4.

M-2. Morawetz, H., "Macromolecules in Solution," Interscience, New York (1966), (a) Ch. 6.

M-3. Meyer, V. E., and G. G. Lawry, J. Polym. Sci., A3, 2843 (1965).

M-4. Meyer, V. E., and R. K. S. Chan, Polymer Preprints, 8(1), 209 (1967).

M-5. Mead, D. J., and R. M. Fuoss, J. Am. Chem. Soc., 64, 277 (1942).

M-6. Markowitz, H., and D. R. Brown, Trans. Soc. Rheol., 7, 137 (1963).

N-1. North, A. M., Polymer, 4, 134 (1963).

O-1. Odian, G. "Principles of Polymerization," McGraw Hill, New York (1970).

O-2. O'Driscoll, K. F., W. Wertz, and A. Husar, Polymer Preprints, 8(1), 380 (1967).

O-3. O'Driscoll, K. F., and R. Knorr, Macromolecules, 1, No. 4, 367 (1968).

O-4. Outer, P., C. I. Carr, Jr., and B. H. Zimm, J. Chem. Phys., 18, 830 (1950).

O-5. Ovenall, D. M., and F. M. Peaker, Die Makromol. Chem., 33, 237 (1959).

O-6. Onogi, S., T. Kobayashi, Y. Kojima, and Y. Taniguchi, J. Appl. Polym. Sci., 7, 847 (1963).

O-7. Onogi, S., S. Kimura, T. Kato, T. Masuda, and N. Miyanaga, J. Polym. Sci., C, 15, 381 (1966).

P-1. Porter, R. S., and J. F. Johnson, Chem. Rev., 66, 1 (1966).

P-2. Park, H. C., Ph.D. dissertation, Michigan State University, E. Lansing, Michigan (1972).

P-3. Peyrot, P., Comptes Rendus, 203, 1512 (1936).

P-4. Porter, R. S., W. J. Macknight, and J. F. Johnson, Rubber Chem. Technol., 41, 1 (1968).

P-5. Peterson, J. M., and M. Fixman, J. Chem. Phys., 39, 2516 (1963).

R-1. Rouse, P. E., J. Chem. Phys., 21, 1272 (1953).

R-2. Rodriguez, F., "Principles of Polymer Systems," McGraw-Hill, New York (1970).

R-3. Riddick, J. A., and W. B. Bunger," Organic Solvents: Physical Properties and Methods of Purification," 3rd ed., John Wiley and Sons, Inc., New York (1970).

S-1. Skiest, I., J. Am. Chem. Soc., 68, 1781 (1946).

S-2. Staudinger, H., and W. Heuer, Ber., 63, 222 (1930). Staudinger, H., and R. Nodzu, Ber., 63, 721 (1930).

S-3. Stacey, K. A., "Light Scattering in Physical Chemistry," Butterworths, London (1956).

S-4. Stockmayer, W. H., L. D. Moore, Jr., M. Fixman, and B. N. Epstein, J. Polym. Sci., 16, 517 (1955).

S-5. Simha, R., J. Appl. Phys., 23, 1020 (1952).

S-6. Simha, R., and L. Utracki, J. Polym. Sci., Part A2, 5, 853 (1967).

S-7. Shimura, Y., J. Polym. Sci., Part A2, 4, 423 (1966).

T-1. Tomimatsu, Y., K. J. Palmer, J. Polymer Sci., 54, S21 (1961), ibid., 35, 549 (1959).

T-2. Tannahill, M., Ph.D. dissertation, Michigan State University, E. Lansing, Michigan (1973).

T-3. Tager, A. A., V. Ye. Dreval, M. S. Lutsky, and G. V. Vinogradov, J. Polym. Sci., Part C, 23, 181 (1968).

V-1. Van Hook, J. P., and A. V. Tobolsky, J. Am. Chem. Soc., 80, 779 (1958).

V-2. Van Wazer, J. R., J. W. Lyons, K. Y. Kim, and R. E. Colwell, "Viscosity and Flow Measurement," Interscience, New York (1963).

V-3. "Viscometers Bulletin 82," Cannon Instrument Co., State College, Pa. 16801.

V-4. "Viscosity Standards Bulletin 71," Cannon Instrument Co., State College, Pa. 16801.

W-1. Williams, M. C., A. I. Ch. E. J., 12, 1064 (1966), ibid., 13, 534 (1967), ibid., 13, 955 (1967).

W-2. Walling, C., J. Am. Chem. Soc., 71, 1930 (1949).

W-3. Walling, C., "Free Radicals in Solution," John Wiley and Sons, Inc., New York (1957), (a) Ch. 4, (b) Chs. 3-5.

W-4. Williams, M. C., J. Polym. Sci., Part C, 35, 211 (1971).

Y-1. Yamakawa, H., "Modern Theory of Polymer Solutions," Harper and Row, New York (1971).

Z-1. Zimm, B. H., J. Chem. Phys., 24, 269 (1956).

Z-2. Zimm, B. H., J. Chem. Phys., 16, 1093, 1099 (1948).

APPENDICES

APPENDIX A

MACHINE CONSTANTS OF WEISSENBERG RHEOGONIOMETER AND CANNON-UBBELOHDE FOUR-BULB SHEAR DILUTION CAPILLARY VISCOMETERS

APPENDIX A

MACHINE CONSTANTS OF WEISSENBERG RHEOGONIOMETER AND CANNON-UBBELOHDE FOUR-BULB SHEAR DILUTION CAPILLARY VISCOMETERS

The rheogoniometer was used in the constant shear configuration. Platen diameter and cone angle were not varied in any of the viscosity measurements. Three different torsion bars were available for different ranges of viscosity. The constants of the rheogoniometer are listed in Table A.1.

TABLE A.1.--Constants of Weissenberg Rheogoniometer.

Torsion Bar	Torsion Bar Constant, dyne cm/micron
ST/6	8.603
ST/7	0.091×10^3
ST/8	0.875×10^3
Platen diameter: 7.5 cm	Cone angle: 1°-37'

Two Cannon-Ubbelohde four-bulb shear dilution type capillary viscometers were used for measuring viscosities of dilute polymer solutions. The constants of the viscometers are listed in Table A-2.

TABLE A.2.--Constants of Capillary Viscometers.

Bulb	Constant, centistokes/sec	Shear Rate Constant
Viscometer 1, Capillary diameter: 0.0364 cm		
1	0.001984	672,000
2	0.002028	317,000
3	0.001874	146,000
4	0.001830	68,000
Viscometer 2, Capillary diameter: 0.0417 cm		
1	0.003609	411,000
2	0.003697	201,000
3	0.003826	92,000
4	0.003758	40,000

To obtain viscosity in centistokes, efflux time in seconds is multiplied by the viscometer constant.

To obtain shear rate at the wall of the capillary in sec^{-1}, shear rate constant is divided by the efflux time in seconds.

APPENDIX B

WEISSENBERG RHEOGONIOMETER

η-$\dot{\gamma}$ DATA

TABLE B.1.--Weissenberg Rheogoniometer η-$\dot{\gamma}$ Data for PS-1 in Benzene at 30°C.

Gear Box Setting	Shear Rate, $\dot{\gamma}$, sec^{-1}	Viscosity, η, Poise c = 20 gm/dl
2.4	6.67	1.082
2.3	8.4	1.087
2.2	10.55	1.082
2.1	13.26	1.089
2.0	16.74	1.107
1.9	21.01	1.087
1.8	26.51	1.102

TABLE B.2.--Weissenberg Rheogoniometer η-$\dot{\gamma}$ Data for PS-1 in MEK at 30°C.

Gear Box Setting	Shear Rate, $\dot{\gamma}$, sec^{-1}	Viscosity, η, Poise	
		c = 20 gm/dl	c = 25 gm/dl
2.7	3.34	0.61	--
2.5	5.28	0.61	--
2.3	8.40	0.63	--
2.1	13.26	0.62	--
1.8	26.51	0.63	1.68
1.7	33.39	--	1.70
1.6	42.02	0.63	1.70
1.5	52.77	--	1.69
1.4	66.67	0.63	1.63
1.3	84.03	--	1.61
1.2	105.54	0.63	1.55
1.1	132.55	--	1.53
1.0	167.43	0.63	--
0.8	265.10	0.63	--

TABLE B.3.--Weissenberg Rheogoniometer η-$\dot{\gamma}$ Data for PS-1 in Dioxane at 30°C.

Gear Box Setting	Shear Rate, $\dot{\gamma}$, sec^{-1}	Viscosity, η, Poise			
		c=12 gm/dl	c=20 gm/dl	c=25 gm/dl	c=50 gm/dl
2.0	16.74	--	--	3.85	--
1.9	21.01	--	--	3.88	51.6
1.8	26.51	0.456	--	3.90	52.4
1.7	33.39	0.440	--	3.90	52.0
1.6	42.02	0.456	1.94	3.95	51.3
1.5	52.77	0.461	1.93	3.89	50.6
1.4	66.67	0.448	1.95	3.80	48.7
1.3	84.03	0.451	1.96	3.72	47.7
1.2	105.54	0.456	1.97	3.60	46.0
1.1	132.55	0.455	1.95	3.40	42.0
1.0	167.43	0.461	1.90	--	38.8
0.9	210.1	0.451	1.89	--	36.5
0.8	265.1	--	1.87	--	33.9
0.7	333.9	--	1.85	--	--
0.6	420.2	--	1.77	--	--

TABLE B.4.--Weissenberg Rheogoniometer η-$\dot{\gamma}$ Data for PS-2 in Benzene at 30°C.

Gear Box Setting	Shear Rate, $\dot{\gamma}$, sec^{-1}	Viscosity, η, Poise	
		c = 10 gm/dl	c = 20 gm/dl
2.3	8.4	--	29.7
2.2	10.55	--	29.5
2.1	13.26	--	29.0
2.0	16.74	--	29.1
1.9	21.01	--	29.4
1.8	26.51	--	29.0
1.7	33.39	--	28.6
1.6	42.02	1.84	27.7
1.5	52.77	1.86	25.6
1.4	66.67	1.85	24.6
1.3	84.03	1.85	23.1
1.2	105.54	1.84	20.9
1.1	132.55	1.83	18.3
1.0	167.43	1.82	17.1
0.9	210.1	1.78	15.8
0.8	265.1	1.74	14.0
0.7	333.9	1.70	--
0.6	420.2	1.61	--
0.5	527.7	1.50	--

TABLE B.5.--Weissenberg Rheogoniometer η-$\dot{\gamma}$ Data for PS-2 in MEK at 30°C.

Gear Box Setting	Shear Rate, $\dot{\gamma}$, sec^{-1}	Viscosity, η, Poise		
		c = 10 gm/dl	c = 15 gm/dl	c = 20 gm/dl
1.9	21.01	--	--	10.9
1.8	26.51	--	--	10.8
1.7	33.39	0.68	2.56	10.8
1.6	42.02	0.67	2.55	10.8
1.5	52.77	0.69	2.54	10.7
1.4	66.67	0.69	2.54	10.9
1.3	84.03	0.69	2.53	10.7
1.2	105.54	0.69	2.51	10.9
1.1	132.55	0.68	2.50	10.7
1.0	167.43	0.67	2.49	10.5
0.9	210.1	0.67	2.44	9.83
0.8	265.1	0.67	2.42	8.95
0.7	333.9	0.67	2.40	8.10
0.6	420.2	--	2.30	6.96
0.5	527.7	--	2.18	6.30
0.4	--	--	2.10	--

TABLE B.6.--Weissenberg Rheogoniometer η-$\dot{\gamma}$ Data for PS-2 in Dioxane at 30°C.

Gear Box Setting	Shear Rate, $\dot{\gamma}$, sec^{-1}	Viscosity, η, Poise			
		c=7 gm/dl	c=10 gm/dl	c=15 gm/dl	c=20 gm/dl
2.3	8.4	--	--	9.56	--
2.2	10.55	--	--	--	31.0
2.1	13.26	--	--	--	31.0
2.0	16.74	--	--	9.59	30.9
1.9	21.01	0.85	--	--	29.8
1.8	26.51	0.83	--	--	29.4
1.7	33.39	0.83	--	9.52	28.7
1.6	42.02	0.83	--	9.48	28.1
1.5	52.77	0.83	2.41	9.42	27.5
1.4	66.67	0.85	2.41	9.28	26.4
1.3	84.03	0.83	2.40	9.20	25.4
1.2	105.54	0.84	2.41	8.93	23.9
1.1	132.55	0.85	2.37	8.58	22.4
1.0	167.43	0.84	2.34	8.27	21.0
0.9	210.1	0.85	2.33	7.89	19.4
0.8	265.1	0.85	2.27	--	17.4
0.7	333.9	0.84	2.15	--	--
0.6	420.2	--	2.08	--	--
0.5	527.7	--	1.97	--	--

TABLE B.7.--Weissenberg Rheogoniometer η-$\dot{\gamma}$ Data for PS-2 in Dioxane at 30°C.

Gear Box Setting	Shear Rate, $\dot{\gamma}$, sec^{-1}	Viscosity, η, Poise c = 50 gm/dl
3.6	0.42	4,562
3.5	0.53	4,438
3.4	0.67	4,480
3.3	0.84	4,380
3.2	1.06	4,200
3.1	1.33	4,057
2.9	2.10	3,674
2.8	2.65	3,431
2.7	3.34	3,144
2.6	4.20	2,890

TABLE B.8.--Weissenberg Rheogoniometer η-$\dot{\gamma}$ Data for SAN C-1 in Benzene at 30°C.

Gear Box Setting	Shear Rate, $\dot{\gamma}$, sec^{-1}	Viscosity, η, Poise	
		c = 10 gm/dl	c = 20 gm/dl
2.2	10.55	--	6.80
2.1	13.26	--	6.85
2.0	16.74	--	6.80
1.9	21.01	--	6.60
1.8	26.51	--	6.30
1.7	33.39	--	6.05
1.6	42.02	--	5.84
1.5	52.77	--	5.65
1.3	84.03	0.49	--
1.2	105.54	0.49	--
1.1	132.55	0.50	--
1.0	167.43	0.50	--
0.9	210.1	0.50	--
0.8	265.1	0.50	--
0.7	333.9	0.49	--

TABLE B.9.--Weissenberg Rheogoniometer η-$\dot{\gamma}$ Data for SAN C-1 in MEK at 30°C.

Gear Box Setting	Shear Rate, $\dot{\gamma}$, sec^{-1}	Viscosity, η, Poise	
		c = 20 gm/dl	c = 35 gm/dl
2.7	3.34	--	21.9
2.6	4.20	--	21.8
2.5	5.28	--	21.7
2.4	6.67	--	21.8
2.3	8.40	--	21.1
2.2	10.55	--	20.7
1.6	42.02	2.01	--
1.5	52.77	2.01	--
1.4	66.67	2.04	--
1.3	84.03	1.95	--
1.2	105.54	1.89	--

TABLE B.9.--Weissenberg Rheogoniometer η-$\dot{\gamma}$ Data for SAN C-1 in MEK at 30°C.

Gear Box Setting	Shear Rate, $\dot{\gamma}$, sec^{-1}	Viscosity, η, Poise	
		c = 20 gm/dl	c = 35 gm/dl
2.7	3.34	--	21.9
2.6	4.20	--	21.8
2.5	5.28	--	21.7
2.4	6.67	--	21.8
2.3	8.40	--	21.1
2.2	10.55	--	20.7
1.6	42.02	2.01	--
1.5	52.77	2.01	--
1.4	66.67	2.04	--
1.3	84.03	1.95	--
1.2	105.54	1.89	--

TABLE B.11.--Weissenberg Rheogoniometer η-$\dot{\gamma}$ Data for SAN C-1 in DMF at 30°C.

Gear Box Setting	Shear Rate, $\dot{\gamma}$, sec^{-1}	Viscosity, η, Poise		
		c = 10 gm/dl	c = 20 gm/dl	c = 50 gm/dl
2.7	3.34	--	--	235
2.6	4.20	--	--	233
2.5	5.28	--	--	234
2.4	6.67	--	--	234
2.3	8.4	--	--	231
2.2	10.55	--	--	230
2.1	13.26	--	--	229
2.0	16.74	--	--	223
1.9	21.01	0.34	--	220
1.8	26.51	0.34	2.44	216
1.7	33.39	0.34	2.45	212
1.6	42.02	0.34	2.42	208
1.5	52.77	0.34	2.42	201
1.4	66.67	0.34	2.43	192
1.3	84.03	0.33	2.44	--
1.2	105.54	0.34	2.40	--
1.1	132.55	0.34	2.39	--
1.0	167.43	0.35	2.37	--
0.9	210.1	0.34	2.36	--
0.8	265.1	0.34	2.30	--
0.7	333.9	0.34	2.23	--
0.6	420.2	--	2.18	--

TABLE B.11.--Weissenberg Rheogoniometer η-$\dot{\gamma}$ Data for SAN C-1 in DMF at 30°C.

Gear Box Setting	Shear Rate, $\dot{\gamma}$, sec^{-1}	Viscosity, η, Poise		
		c = 10 gm/dl	c = 20 gm/dl	c = 50 gm/dl
2.7	3.34	--	--	235
2.6	4.20	--	--	233
2.5	5.28	--	--	234
2.4	6.67	--	--	234
2.3	8.4	--	--	231
2.2	10.55	--	--	230
2.1	13.26	--	--	229
2.0	16.74	--	--	223
1.9	21.01	0.34	--	220
1.8	26.51	0.34	2.44	216
1.7	33.39	0.34	2.45	212
1.6	42.02	0.34	2.42	208
1.5	52.77	0.34	2.42	201
1.4	66.67	0.34	2.43	192
1.3	84.03	0.33	2.44	--
1.2	105.54	0.34	2.40	--
1.1	132.55	0.34	2.39	--
1.0	167.43	0.35	2.37	--
0.9	210.1	0.34	2.36	--
0.8	265.1	0.34	2.30	--
0.7	333.9	0.34	2.23	--
0.6	420.2	--	2.18	--

TABLE B.12.--Weissenberg Rheogoniometer η-$\dot{\gamma}$ Data for SAN C-2 in Benzene at 30°C.

Gear Box Setting	Shear Rate, $\dot{\gamma}$, sec^{-1}	Viscosity, η, Poise	
		c = 10 gm/dl	c = 20 gm/dl
1.5	52.77	--	11.9
1.4	66.67	--	11.9
1.3	84.03	--	11.8
1.2	105.54	0.716	11.9
1.1	132.55	0.715	11.9
1.0	167.43	0.719	11.8
0.9	210.1	0.711	11.7
0.8	265.1	0.717	11.4
0.7	333.9	0.720	--
0.6	420.2	0.711	--
0.5	527.7	0.690	--
0.4	666.7	0.670	--

TABLE B.13.--Weissenberg Rheogoniometer η-$\dot{\gamma}$ Data for SAN C-2 in MEK at 30°C.

Gear Box Setting	Shear Rate, $\dot{\gamma}$, sec^{-1}	Viscosity, η, Poise c = 20 gm/dl
1.7	33.9	5.09
1.6	42.02	5.11
1.5	52.77	5.10
1.4	66.67	5.03
1.3	84.03	5.08
1.2	105.54	5.08
1.1	132.55	4.99
1.0	167.43	4.97
0.9	210.1	4.77
0.8	265.1	4.59
0.7	333.9	4.20
0.6	420.2	3.83

TABLE B.14.--Weissenberg Rheogoniometer η-$\dot{\gamma}$ Data for SAN C-2 in Dioxane at 30°C.

Gear Box Setting	Shear Rate, $\dot{\gamma}$, sec^{-1}	Viscosity, η, Poise		
		c = 7 gm/dl	c = 10 gm/dl	c = 20 gm/dl
1.7	33.39	--	0.825	8.40
1.6	42.02	--	0.820	8.40
1.5	52.77	0.331	0.827	8.50
1.4	66.67	0.331	0.820	8.38
1.3	84.03	0.326	0.813	8.33
1.2	105.54	0.323	0.833	8.23
1.1	132.55	0.332	0.835	8.16
1.0	167.43	0.323	0.830	8.05
0.9	210.1	0.331	--	7.91
0.8	265.1	0.329	--	7.82
0.7	333.9	0.337	0.835	7.43
0.6	420.2	0.325	--	7.12
0.5	527.7	0.326	--	6.80
0.4	666.7	0.329	--	--
0.3	840.3	0.332	--	--

TABLE B.15.--Weissenberg Rheogoniometer η-$\dot{\gamma}$ Data for SAN C-2 in DMF at 30°C.

Gear Box Setting	Shear Rate, $\dot{\gamma}$, sec^{-1}	Viscosity, η, Poise	
		c = 20 gm/dl	c = 50 gm/dl
3.2	1.06	--	110
3.0	1.67	--	111
2.9	2.10	--	110
2.8	2.65	--	110
2.7	3.34	--	111
2.6	4.20	--	111
2.5	5.28	--	111
2.4	6.67	--	110
2.3	8.40	--	111
2.2	10.55	--	110
2.1	13.26	--	111
2.0	16.74	2.94	111
1.9	21.01	2.95	110
1.8	26.51	2.94	109
1.7	33.39	2.92	109
1.6	42.02	2.95	108
1.5	52.77	2.94	106
1.4	66.67	2.94	103
1.3	84.03	2.93	97.7
1.2	105.54	2.94	92
1.1	132.55	2.91	--
1.0	167.43	2.93	--
0.9	210.1	2.95	--
0.8	265.1	2.85	--
0.7	333.9	2.76	--
0.6	420.2	2.61	--

TABLE B.16.--Weissenberg Rheogoniometer η-$\dot{\gamma}$ Data for SAN C-2' in Benzene at 30°C.

Gear Box Setting	Shear Rate, $\dot{\gamma}$, sec^{-1}	Viscosity, η, Poise		
		c = 7 gm/dl	c = 10 gm/dl	c = 20 gm/dl
3.7	0.33	--	--	1,580
3.6	0.42	--	--	1,582
3.5	0.53	--	--	1,530
3.4	0.67	--	--	1,502
3.3	0.84	--	--	1,434
3.2	1.06	--	--	1,394
3.0	1.67	--	--	1,323
2.9	2.10	--	--	1,234
2.8	2.65	--	--	1,150
2.7	3.34	--	--	1,080
2.6	4.20	--	--	981
2.4	6.67	--	--	798
2.3	8.40	6.69	--	749
2.2	10.55	6.65	--	680
2.1	13.26	6.85	--	609
2.0	16.74	6.69	--	530
1.9	21.01	--	--	--
1.8	26.51	6.62	28.47	--
1.7	33.39	6.54	28.17	--
1.6	42.02	6.40	26.69	--
1.5	52.77	6.28	25.34	--
1.4	66.67	6.10	23.94	--
1.3	84.03	5.89	22.64	--
1.2	105.54	5.71	20.89	--
1.1	132.55	5.55	19.40	--
1.0	167.43	5.30	--	
0.9	210.1	--	--	--
0.8	265.1	--	--	--
0.7	333.9	--	--	--
0.6	420.2	--	--	--

TABLE B.17.--Weissenberg Rheogoniometer η-$\dot{\gamma}$ Data for SAN C-2' in MEK at 30°C.

Gear Box Setting	Shear Rate, $\dot{\gamma}$, sec^{-1}	Viscosity, η, Poise		
		c = 7 gm/dl	c = 10 gm/dl	c = 20 gm/dl
3.8	0.265	--	--	399
3.7	0.33	--	--	397
3.6	0.42	--	--	399
3.5	0.53	--	--	393
3.4	0.67	--	--	397
3.3	0.84	--	--	389
3.2	1.06	--	--	378
3.1	1.33	--	--	369
3.0	1.67	--	--	347
2.9	2.10	--	--	328
2.3	8.40	--	--	226
2.2	10.55	--	8.64	203
2.1	13.26	--	8.70	188
2.0	16.74	--	8.62	171
1.9	21.01	--	8.55	161
1.8	26.51	--	8.45	152
1.7	33.39	1.78	8.23	140
1.6	42.02	1.73	8.08	132
1.5	52.77	1.76	7.80	122
1.4	66.67	1.77	--	110
1.3	84.03	1.76	--	--
1.2	105.54	1.74	--	--
1.1	132.55	1.76	--	--
1.0	167.43	1.70	--	--
0.9	210.1	1.70	--	--
0.8	265.1	1.70	--	--
0.7	333.9	1.68	--	--
0.6	420.2	1.63	--	--
0.5	527.7	1.59	--	--
0.4	666.7	1.45	--	--
0.3	840.3	1.36	--	--
0.2	1,055.4	1.31	--	--

TABLE B.18.--Weissenberg Rheogoniometer η-$\dot{\gamma}$ Data for SAN C-2' in Dioxane at 30°C.

Gear Box Setting	Shear Rate, $\dot{\gamma}$, sec^{-1}	Viscosity, η, Poise		
		c = 7 gm/dl	c = 10 gm/dl	c = 20 gm/dl
4.1	0.133	--	--	806
3.4	0.67	--	--	802
3.3	0.84	--	--	810
3.2	1.06	--	--	802
3.1	1.33	--	--	805
3.0	1.67	--	--	792
2.9	2.10	--	--	780
2.8	2.65	--	--	755
2.7	3.34	--	--	733
2.6	4.20	--	--	705
2.5	5.28	--	25.8	671
2.4	6.67	5.87	--	634
2.3	8.40	5.67	26.0	578
2.2	10.55	5.84	26.1	523
2.1	13.26	5.89	25.8	450
2.0	16.74	5.79	24.9	394
1.9	21.01	5.82	24.6	348
1.8	26.51	5.89	24.2	306
1.7	33.39	5.79	23.5	261
1.6	42.02	5.74	23.1	--
1.5	52.77	5.68	22.4	--
1.4	66.67	5.54	21.1	--
1.3	84.03	5.42	20.0	--
1.2	105.54	5.32	19.1	--
1.1	132.55	5.12	17.3	--
1.0	167.43	5.04	--	--
0.9	210.1	4.80	--	--
0.8	265.1	4.47	--	--
0.7	333.9	4.18	--	--
0.6	420.2	3.79	--	--
0.5	527.7	3.40	--	--

TABLE B.19.--Weissenberg Rheogoniometer η-$\dot{\gamma}$ Data for SAN C-2' in DMF at 30°C.

Gear Box Setting	Shear Rate, $\dot{\gamma}$, sec^{-1}	Viscosity, η, Poise		
		c = 7 gm/dl	c = 10 gm/dl	c = 20 gm/dl
3.6	0.42	--	--	172
3.5	0.53	--	--	172
3.4	0.67	--	--	173
3.3	0.84	--	--	170
3.2	1.06	--	--	172
3.1	1.33	--	--	172
3.0	1.67	--	--	174
2.9	2.10	--	--	171
2.8	2.65	--	--	171
2.7	3.34	--	--	169
2.6	4.20	--	--	168
2.5	5.28	--	10.0	169
2.4	6.67	--	--	164
2.3	8.40	--	9.86	161
2.2	10.55	--	--	156
2.1	13.26	--	10.1	153
2.0	16.74	--	9.95	144
1.9	21.01	--	--	139
1.8	26.51	2.68	--	131
1.7	33.39	2.69	9.79	122
1.6	42.02	2.72	9.73	116
1.5	52.77	2.66	9.50	106
1.4	66.67	2.68	9.40	96.6
1.3	84.03	2.64	9.03	--
1.2	105.54	2.59	--	--
1.1	132.55	2.55	8.62	--
1.0	167.43	2.53	8.25	--
0.9	210.1	2.46	7.82	--
0.8	265.1	--	7.40	--
0.7	333.9	2.32	--	--
0.6	420.2	2.20	--	--
0.5	527.7	2.12	--	--
0.4	666.7	1.96	--	--
0.3	840.3	1.80	--	--

TABLE B.20.--Weissenberg Rheogoniometer η-$\dot{\gamma}$ Data for SAN C-3 in MEK at 30°C.

Gear Box Setting	Shear Rate, $\dot{\gamma}$, sec^{-1}	Viscosity, η, Poise	
		c = 20 gm/dl	c = 35 gm/dl
3.4	0.67	--	3,500
3.3	0.84	--	3,533
3.2	1.06	--	3,435
3.1	1.33	--	3,350
3.0	1.67	--	3,225
2.9	2.10	--	3,150
2.8	2.65	--	2,950
2.7	3.34	--	2,796
2.6	4.20	--	2,654
2.5	5.28	103	2,456
2.4	6.67	104	2,071
2.3	8.40	106	1,847
2.2	10.55	105	1,628
2.1	13.26	105	--
2.0	16.74	106	--
1.9	21.01	106	--
1.8	26.51	100	--
1.7	33.39	94	--
1.6	42.02	86	--

TABLE B.21.--Weissenberg Rheogoniometer η-$\dot{\gamma}$ Data for SAN C-3 in DMF at 30°C.

Gear Box Setting	Shear Rate, $\dot{\gamma}$, sec^{-1}	Viscosity, η, Poise	
		c = 10 gm/dl	c = 20 gm/dl
2.3	8.40	--	52.5
2.2	10.55	--	52.5
2.1	13.26	--	52.8
2.0	16.74	--	52.4
1.9	21.01	--	51.9
1.8	26.51	--	51.1
1.7	33.39	--	51.0
1.6	42.02	3.38	50.0
1.5	52.77	3.37	47.9
1.4	66.67	3.40	46.9
1.3	84.03	3.38	45.4
1.2	105.54	3.33	44.3
1.1	132.55	3.34	42.3
1.0	167.43	3.33	40.2
0.9	210.1	3.32	38.0
0.8	265.1	3.21	--
0.7	333.9	3.16	--
0.6	420.2	3.05	--
0.5	527.7	2.91	--
0.4	666.7	2.81	--

TABLE B.22.--Weissenberg Rheogoniometer η-$\dot{\gamma}$ Data for SAN C-3 in DMF at 30°C.

Gear Box Setting	Shear Rate, $\dot{\gamma}$, sec^{-1}	Viscosity, η, Poise	
		c = 35 gm/dl	c = 50 gm/dl
4.0	0.167	--	4,990
3.9	0.21	--	5,010
3.8	0.265	--	4,975
3.7	0.33	--	4,978
3.6	0.42	--	5,003
3.5	0.53	--	4,937
3.4	0.67	--	4,851
3.3	0.84	--	4,811
3.2	1.06	769	4,767
3.1	1.33	779	4,700
3.0	1.67	770	4,668
2.9	2.10	765	4,490
2.8	2.65	758	4,366
2.7	3.34	740	4,144
2.6	4.20	735	3,934
2.5	5.28	723	3,728
2.4	6.67	718	3,409
2.3	8.40	704	3,120
2.2	10.55	686	--
2.1	13.26	653	--
2.0	16.74	617	--
1.9	21.01	588	--
1.8	26.51	536	--

APPENDIX C

CALIBRATION OF REFRACTOMETER

APPENDIX C

CALIBRATION OF REFRACTOMETER

The Brice-Phoenix refractometer was calibrated according to the procedure recommended in the manual (B-13).

Table C-1 lists the refractive index differences, Δn, between potassium chloride solutions and distilled water (B-13). For all calibration purposes, potassium chloride solutions were used. Table C-1 is taken from Ref. (B-13).

TABLE C-1. Refractive Index Differences, Δn, Between Potassium Chloride Solutions and Distilled Water.

Solution	Concentration in Water		$\Delta n \times 10^6$ at 25°C and 4358 Å
	(1) gm/100 ml	(2) gm/100 gm	
1	0.0696	0.0699	100
2	0.1067	0.1070	153
3	0.2799	0.2812	399
4	0.5964	0.5994	845
5	1.0794	1.0869	1,521
6	1.4911	1.5037	2,093
7	2.9821	3.0250	4,135
8	3.9969	4.0703	5,500
9	4.4732	4.5647	6,136
10	5.9642	6.1217	8,105
11	6.4680	6.6526	8,763

Concentration: (1) gm of salt/100 ml of distilled water at 25°C.
(2) gm of salt/100 gm of distilled water.

When concentration, c, is plotted against refractive index difference, Δn, a straight is obtained whose equation is $c = 732.4379\ \Delta n$ where c is in gm/100 cm^3. From this equation, values of Δn for other concentrations can be calculated.

Table C-2 presents the results of calibration of the differential refractometer cell using potassium chloride solutions at 25° ± 1°C. and 4358 Å.

TABLE C.2.--Calibration Constant of Differential Refractometer.

Concentration gm/100 cm^3 water	$\Delta n \times 10^6$	Δd	$k = \Delta n/\Delta d \times 10^3$
1.113	1,519.583	1.4828	1.0248
0.5518	753.374	0.7359	1.0237
0.3223	440.037	0.4298	1.0239
0.1004	137.076	0.1341	1.0221

Average k = 1.0236.

APPENDIX D

RAYLEIGH RATIO FROM LIGHT SCATTERING DATA AND PHOTOMETER CONSTANTS

APPENDIX D

RAYLEIGH RATIO FROM LIGHT SCATTERING

DATA AND PHOTOMETER CONSTANTS

For the measurements at different angles, cylindrical cell C-101 was used with narrow diaphragms as described in the manual B-10). The scattering ratios, $(G_\theta/F_\theta)/(G_0/F_0)$, at various angles, θ, both for the solutions and the solvents were measured to obtain net scattering due to the presence of polymer.

The Rayleigh ratio, R_θ, can then be calculated from the observed scattering ratios by means of the following equation which is given in the manual:

$$R_\theta = \frac{TDan^2(R_w/R_c)}{1.049\ \pi h}\left(\frac{r}{r'}\right)\left(\frac{\sin\theta}{1+\cos^2\theta}\right)\left[\frac{1}{(1-R)^2(1-4R^2)}\right]$$

$$\cdot\left\{\left[\left(\frac{G_\theta/F_\theta}{G_0/F_0}\right)_{\text{solution}} - \left(\frac{G_\theta/F_\theta}{G_0/F_0}\right)_{\text{solvent}}\right]\right.$$

$$\left. - 2R\left[\left(\frac{G_{180-\theta}/F_{180-\theta}}{G_0/F_0}\right)_{\text{solution}} - \left(\frac{G_{180-\theta}/F_{180-\theta}}{G_0/F_0}\right)_{\text{solvent}}\right]\right\} \qquad (D.1)$$

where (G_θ/F_θ) is the scattering ratio, or average observed ratio of galvanometer deflection for the light scattered by the solution at angle θ to that of the transmitted light at zero angle position; F_θ and F_0 are the products of transmittances of the neutral filters used in determining the scattering ratio at angles θ and zero, respectively; a is the constant that relates the working standard to the opal glass reference standard; TD is the experimentally determined product of the diffuse transmittance of the opal glass reference standard; h is the width of the diaphragm; n is the refractive index of the solution which for dilute solutions can be replaced by the refractive index of the solvent; R_w/R_c is an experimentally determined correction factor for incomplete compensation for reflection effects. The latter correction is not large and does not differ appreciably from instrument to instrument; however, its value does depend on the refractive index of the solvent and cell size.

Average values of R_w/R_c for the wave lengths of 436 mμ and 546 mμ for 40 x 40 mm and 30 x 30 mm cells are given in the manual along with n values of some common solvents. Values for other solvents, or for more concentrated solutions with refractive index differing appreciably from that of the solvent, can be estimated with sufficient accuracy from a plot of R_w/R_c against n, or by simple interpolation in the given values of R_w/R_c. In general, for dilute solutions in common solvents, R_w/R_c values are very close to unity.

The factor (r/r') is the calibration relating the narrow beam geometry and cylindrical cell to the standard beam geometry and standard cell. It is dependent on the refractive index of the solution and hence must be determined for each solute-solvent system. This correction is quite large in comparison with R_w/R_c. Complete details of its determination are given in the manual.

The factor sin θ corrects for the volume change on viewing the solution at different angles, $(1 + \cos^2\theta)$ accounts for the state of polarization of the scattered light, and the factor R is defined as

$$R = \left(\frac{\bar{n} - 1}{\bar{n} + 1}\right)^2 \qquad (D.2)$$

where $\bar{n}$ is the refractive index of the glass. For λ equal to 436 mμ, the value of R is equal to 0.046 for the sinter-fused cells and equal to 0.039 for Pyrex cells.

Equation D.1 takes into account the change of the scattering envelope due to the scattering of the reflected fraction, R, of the primary beam, the attenuation of scattered light at an angle θ by reflection at the air-glass interface at the point of measurement, and the contribution of reflection, in the -θ direction, of the light scattered in the +(180-θ) direction.

Table D.1 lists the calibration constants of the light scattering photometer used in this work.

TABLE D.1.--Constants of Photometer for 436 mμ Wavelength.

Diffuse transmittance times diffusor correction factor	TD	0.263
Width of primary beam, cm	h	1.20
Working standard constant	a	0.0423
Transmittance of neutral filter		
No. 1	F_1	0.477
No. 2	F_2	0.219
No. 3	F_3	0.109
No. 4	F_4	0.0349

A computer program in FORTRAN IV was written to carry out the calculations of Rayleigh ratios and Zimm plots were made by plotting Kc/R_θ against $qc + \sin^2 (\theta/2)$ where the terms are defined in Chapter III.